In Vitro and In Vivo Study of Pyrrolizidine Alkaloids-Induced Hepatotoxicity

LI, Yanhong

A Thesis Submitted in Partial Fulfillment

of the Requirements for the Degree of

Doctor of Philosophy

in

Pharmacology

The Chinese University of Hong Kong

August 2011

UMI Number: 3504720

UMI

Dissertation Publishing

UMI 3504720

ProQuest

Thesis/Assessment Committee

Professor Yu Huang (Chair)

Professor Ge Lin (Thesis Supervisor)

Professor Zhong Zuo (Committee Member)

Professor Zhongzhen Zhao (External Examiner)

Abstract of thesis entitled:

In Vitro and In Vivo Study of Pyrrolizidine Alkaloids-Induced Hepatotoxicity

Submitted by Li Yanhong

For the degree of Doctor of Philosophy in Pharmacology

at The Chinese University of Hong Kong

Abstract

Pyrrolizidine alkaloids (PAs) are hepatotoxic and present in a wide variety of plant species. The consumption of PAs through the intake of either PA-containing natural products or PA-contaminated food stuffs leads to serious health problems in human. However, the severity of hepatotoxicity of different PAs varies significantly, and thus makes it difficult to set up the regulation for a universal threshold of toxic dose of individual PAs. In addition, the detailed mechanisms underlying PA-induced hepatotoxicity and the resultant hepatic sinusoid occlusion syndrome (HSOS) remain largely unknown, which results in the lack of specific methods for its diagnosis. Therefore, the aims of the present study included two aspects: the first is to develop a convenient *in vitro* model for the rapid assessment of the hepatotoxicity of different PAs; the second is to identify potential biomarkers for the diagnosis of PA intoxication in rats.

The results demonstrated that the developed *in vitro* model using MTT and BrdU assays under optimal incubation conditions was able to discriminate the cytotoxicity of three types of PAs. Among different PAs tested, clivorine, an otonecine-type PA representative, was significantly more toxic than retrorsine, a retronecine-type one, while platyphylline, a platyphylline-type one, was not toxic. Moreover, the cytotoxicity of alkaloid extract of *Gynura segetum*, a senecionine and

seneciphylline-containing herb, was comparable to that of these two PAs tested individually, demonstrating that the developed model was also suitable for the assessment of PA-containing herb-induced cytotoxicity.

In the *in vivo* study, administration of retrorsine to rats produced hepatotoxicity in a dose-dependent manner: low dose induced a slight liver injury with an elevation of ALT, GSSG/GSH, MPO, and slight loss of SECs; medium dose caused a mild injury with enhanced elevation of ALT, MPO, RLW, GSH and GR, and pronounced damages in SECs and CVECs; whereas high dose resulted in severe damage evidenced by all aforementioned markers plus 1) significant increase in TB and LDH, 2) significant increase in GSH but no change in GSSG/GSH indicating the initiation of GSH depletion, 3) severe damages in SECs and CVECs, and 4) extensive sinusoid hemorrhage and lobular disarray. Using this developed rat model, a proteomic study was conducted to identify the modulations of hepatic proteins with a general trend of down-regulation at low dose and up-regulation at high dose, while remarkable variations were found at medium dose of retrorsine treatment. These proteins were found to belong to six clusters according to their functions, including proteins responsible for metabolism, related to cell organization, cell proliferation, and stress response, involved in thrombosis, as well as proteins related to several other functions. Among these modulated proteins, regulations of Cps1 and Atp5b were consistently observed at three dosage regimens, and were verified by immunostaining and Western blot analysis.

In conclusion, for the first time, a convenient *in vitro* model for the assessment of the severity of cytotoxicity of different type of PAs has been developed. This method has a potential to be used for the quick screening the toxicity of PA-containing natural products. Furthermore, Cps1 and Atp5b were found to have a potential to be developed as specific biomarkers for the diagnosis of PA intoxication in rats.

論文摘要

吡咯裏西啶生物鹼（PAs）作為一種天然產物，廣泛分佈於植物界，被用作草药和保健茶，或通过污染农作物，引起肝毒性损害而影响公众健康。由于PA种类繁多，毒性强弱不一，目前仍缺乏快速简便的方法统一评价PA的毒性。此外，PA引起毒性的机制也不甚清晰，目前仍无特定的手段判定PA中毒及其所导致的特异性临床症状-肝血窦阻塞症（HSOS）。因此，本研究旨在建立一种简便的体外模型来评价不同PA对肝细胞的毒性，并鉴定出与其毒性机制相关的体内生物标志物来判定PA中毒。

结果表明：MTT及BrdU在优化培养条件的HepG2细胞模型中联合应用，可区分出不同类型PA的毒性，其中clivorin（otonecine型）毒性强于retrorsine（retronecine型），而platyphylline（platyphylline型）未显示毒性。此外，菊三七总生物碱提取物的毒性与其所含的两种PA：senecionine及seneciphylline毒性相当，表明该模型也适合评价含PA天然产物的毒性。体内研究表明，retrorsine所致的大鼠肝毒性呈剂量依赖性。低剂量仅引起ALT、GSSG/GSH及MPO升高，肝窦内皮细胞（SECs）轻度受损丢失。中剂量时以上损伤程度加重，并累及中央静脉内皮细胞 (CVECs)。高剂量则导致显著性的血ALT、TB及LDH增加，SECs及CVECs严重丢失，及广泛性的肝窦出血和肝小叶结构破坏。在该模型上进行的蛋白质组学研究表明：低剂量retrorsine即导致数十种蛋白表达下调，这些蛋白与体内物质及能量代谢，细胞构成与增殖，氧化损伤及凝血等功能相关。中高剂量也累及以上几类蛋白，但其中一些蛋白表达出现上调，在高剂量时全部表现为上调。其中Cps1、Atp5b及Hspa9在三个剂量中连续出现表达变化。验证研究发现：Cps1及Atp5b在低、高剂量中的变化趋势与蛋白质组学结果一致。

综上所述，我们首次建立了一个快速简单的细胞模型来检测不同类型PA肝细胞毒性的差异，并能区分出有毒和无毒的PA。该方法有可能用于快速筛选含

PA的天然产物的毒性。另外，Cps1及Atp5b参与不同剂量retrorsine所致的肝毒性进展，具潜力进一步开发为生物标志物，用于检测PA引起的特异性肝损害。

Acknowledgments

I would like to express my great gratitude to my supervisor, Prof. Ge Lin, whose expertise, understanding, and patience, added considerably to my graduate experience. I appreciate her vast knowledge in many areas (e.g., biology, toxicology and chemistry), her skills on presentation and her guidance in writing reports (i.e., this thesis). I also thank her for giving me chance to attend international conference, which definitely widen my knowledge and experience.

I would like to thank the other members of my committee, Prof. Yu Huang, Prof. Zhong Zuo and Prof. Zhongzhen Zhao for the assistance they provided at all levels of the research project. I gratefully acknowledge the collaborators of my project, Prof. Wood Yee Chan and Prof. Wen Luan Wendy Hsiao for their advices, crucial suggestions and discussion on my project.

I must acknowledge Dr. Na Li for her persistent support, invaluable suggestions and selfless help throughout the duration of my study. Many thanks go in particular to Ms. Typhoon Wan for her great technical assistance and help. Appreciation also goes to Dr. William Chi Shing Tai, for his assistance in proteomic study. I also would like to thank all my lab mates, especially Dr Winnie Lai Ting Kan and Dr Bin Ma, for their invaluable helps and supports along the way.

Thanks also go out to Mrs. Joresa Ng and Miss Becky Kwan for the kind help they provided at times of critical need.

Very special thanks go out to my family, without whose love, encouragement and support, I would not even have completed this thesis.

Publications

1. **Li YH**, Li N, Lin G. Development of an *In Vitro* Model for the Assessment of Pyrrolizidine Alkaloids-Induced Hepatotoxicity (in preparation).

2. **Li YH**, Wan TF, Li N, Chan WY, Lin G. Investigation of the Progress of Hepatotoxicity Induced by Retrorsine, a Representative Pyrrolizidine Alkaloid, in Rats (in preparation).

3. **Li YH**, Tai WCS, Li N, Hsiao WLW, Lin G. Proteomic Study of Hepatotoxicity Induced by Retrorsine, a Representative Pyrrolizidine Alkaloid (in preparation).

4. **Li YH**, Tai WCS, Hsiao WLW, Lin G. Validation of Cps1, Atp5b and Hspa9 as Potential Biomarkers for Pyrrolizidine Alkaloid-Induced Hepatotoxicity in Rats (in preparation).

5. **Li YH**, Tai WCS, Li N, Hsiao WLW, Lin G. Proteomic Study of the Acute Hepatotoxicity Induced by Cyclophosphomide (in preparation).

Conference Abstract and Presentations

1. **Li YH**, Tai WCS, Wan TF, Li N, Chan WY, Hsiao WLW, Lin G. Proteomic approach for the identification of biomarkers for pyrrolizidine alkaloid hepatotoxicity. *The 13th Scientific meeting of Hong Kong Pharmacology Society*, Hong Kong, P.R.China. 17 December, 2010 (Oral presentation).

2. **Li YH**, Tai WCS, Li N, Wan TF, Chan WY, Hsiao WLW, Lin G. *In vivo* study the hepatotoxicity of retrorsine, a representative pyrrolizidine alkaloid. *2010 Hong Kong-Macau Postgraduate Symposium on Chinese Medicine*. Hong Kong, P. R. China. 12 August, 2010 (Oral presentation).

3. **Li YH**, Li N, Lin G. Development of an *in vitro* model for the investigation of pyrrolizidine alkaloid-induced hepatotoxicity. *WorldPharma2010-16th World Congress of Basic Clinical Pharmacology*. Copenhagen, Denmark. 17-23 July, 2010 (Oral presentation).

4. **Li YH**, Tai WCS, Li N, Wan TF, Chan WY, Hsiao WLW, Lin G. Proteomic study of hepatotoxicity induced by retrorsine, a representative pyrrolizidine alkaloid. *WorldPharma2010-16th World Congress of Basic Clinical Pharmacology*. Copenhagen, Denmark. 17-23 July, 2010 (Poster presentation).

5. **Li YH**, Li N, Lin G. Development of an *in vitro* model for the investigation of pyrrolizidine alkaloid induced hepatotoxicity. *Postgraduate Symposium on Chinese Medicine*. Hong Kong, P. R. China. 13 August, 2009 (Poster presentation).

List of Tables

List of Figures

List of Abbreviations

2-D	two-dimensional
7-GSH-DHP	7-glutathionyldehydroretronecine
ALT	alanine aminotransferase
ANOVA	analysis of variance
Atp5b	ATP synthases subunit beta
BW	body weight
BrdU	bromodeoxyuridine
CHAPS	3-(3-cholamidopropyl)-dimethyl- ammonio)-1-propane sulfonate
Cps1	carbamoyl phosphate synthases
CVECs	central venular endothelial cells
Cyc	cyclophophomide
CYP450	cytochrome P450 monooxygenase
DAB	diaminobenzidine
DHP	dehydropyrrolizidine
DMEM	dulbecco's modified Eagle's medium
DMSO	dimethyl sulfoxide
DNP	2,4-dinitrophenylhydrazine
DNTB	5,5'-dithiobis-2-nitrobenzoic acid
DTT	dithiothreitol
ECs	endothelial cells
ECGS	endothelial cell growth supplement
ECM	endothelial cell medium
EDTA	ethylediaminetetracetic acid
FBS	fetal bovine serum
Gapdh	glyceraldehyde-3-phosphate dehydrogenase
GR	GSH reductase
G. segetum	*Gynura segetum*
GSH	glutathione (reduced form)
GSSG	oxidized glutathione
GSSG/GSH	ratio of GSSG to reduced GSH
h	hour
HepG2	human hepatocellular carcinoma
H_2O_2	hydrogen peroxide
HCl	hydrochloric acid
H&E	haematoxylin and eosin

Hspa9	heat shock protein 70kDa protein 9
HSOS	hepatic sinusoidal occlusion syndrome
HVOD	hepatic veno-occlusive disease
IEF	isoelectric focusing
IHC	immunohistochemical
IPG	immobilized pH gradient
LDH	lactate dehydrogenase
MALDI-TOF-MS	matrix-assisted laser desorption/ionization-time of flight mass spectrometry
Min	minute
MPO	myeloperoxidase
MTT	3- (4, 5-Dimethylthiazol-2-yl)-2, 5-diphenyl- tetrazolium bromide
NaOH	sodium hydroxide
PAs	pyrrolizidine alkaloids
PBS	phosphate buffer solution
PFA	paraformaldehyde
PLL	poly-L-Lysine
PS	penicillin/streptomycin
RECA-1	anti-rat endothelial cell antigen-1
RLW	relative liver weight
SCT	stem cell transplantation
SD	standard deviation
SDS	sodium dodecyl sulphate
SECs	sinusoidal endothelial cells
SEM	standard error of mean
SOS	sinusoidal obstruction syndrome
SRB	sulforhodamine B
TB	total bilirubin
TCA	trichloroacetic acids
T/E	trypsin/EDTA solution
TEMED	N, N, N', N''-Tetramethylethylenediamine
HVOD	hepatic veno-occlusive disease

Table of Contents

Chapter 1 Introduction

1.1 Pyrrolizidine Alkaloids

Pyrrolizidine alkaloids (PAs) are heterocyclic compounds that form a large group of plant-secondary chemicals occurring in an estimated 3% of the world flowering plants (Smith and Culvenor, 1981). They are made of two parts: a basic amino alcohol, referred to as a necine base, and one or more acids (necic acid) that esterify the alcohol groups of the necines (Mattocks et al., 1986). Based on the necine bases as shown in Fig.1.1, PAs are generally divided into three types, namely otonecine-, retronecine- and platyphylline-type (Fu et al., 2004). Fig.1.2 shows the names and structures of the representatives of three type PAs as well as a retrorsine N-oxide. Usually, hepatotoxic PAs have a saturated necine base with a C_1-C_2 double bound as indicated in Fig.1.1 and are belonging to either retronecine- or otonecine-type (Mattocks, 1986; IPCS, 1988). More than 660 PAs and their N-oxides have been identified in over 6000 plants, and about half of them exhibit hepatotoxic activity (Roeder, 2000; Stegelmeier et al., 1999).

Fig.1.1. Common necine bases of PAs.
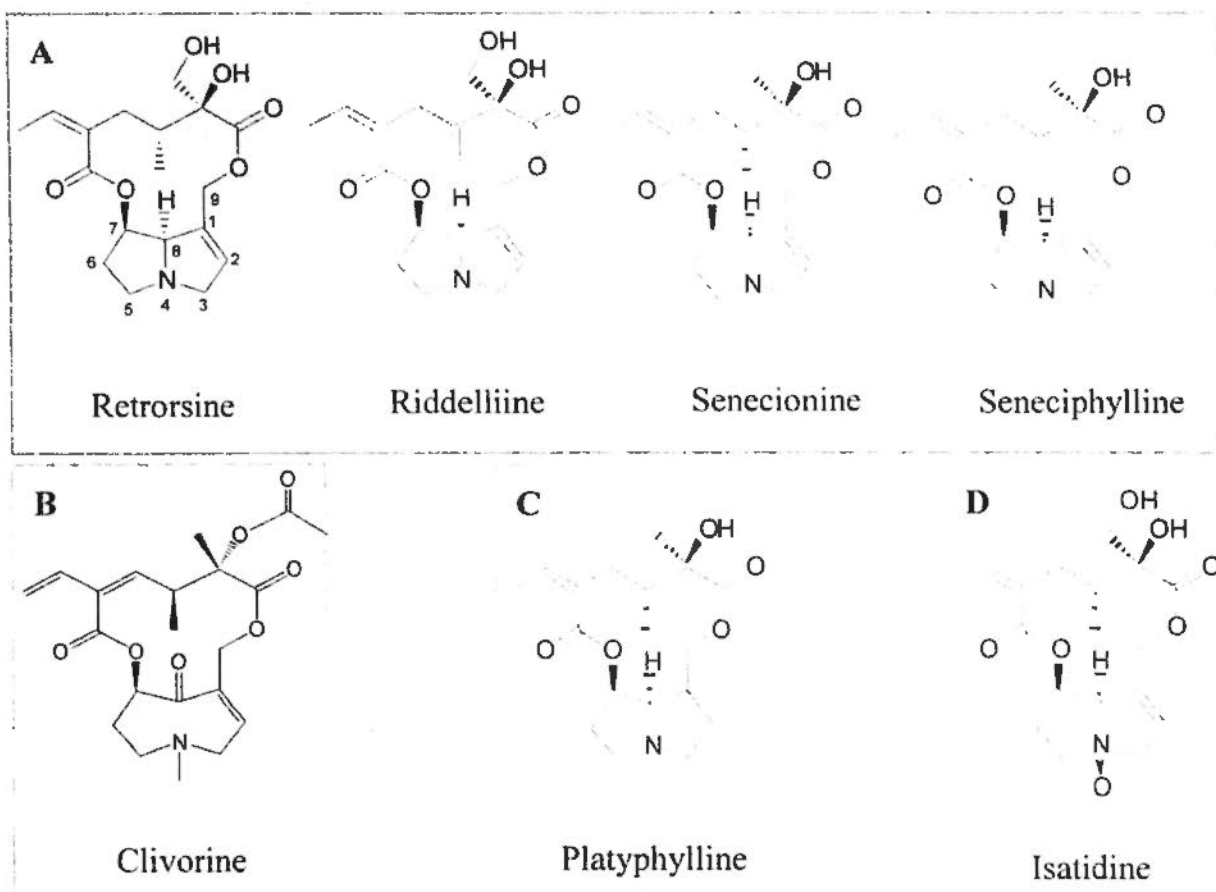
Fig.1.2. Representative retronecine- (A), otonecine- (B) and platyphylline (C) type PAs as well as retrorsine N-oxide (D).

1.1.1 Metabolism

In general, there are three principal metabolic pathways for the metabolism of retronecine-type PAs as summarized in Fig.1.3 (Fu et al., 2004; Yang et al., 2001b). The first pathway is hydrolysis of the ester functional groups to form corresponding necine bases and necic acids. The second pathway is N-oxidation of the necine bases to form corresponding PA N-oxides. The third metabolic pathway is oxidation via two steps, hydroxylation of the necine base at the C_3 or C_8 position to form the corresponding 3- or 8-hydroxynecine derivatives followed by spontaneous dehydration to produce the corresponding dehydropyrrolizidine derivatives—pyrrolic esters (Lin et al., 2002; Yang et al., 2001b). Both the first and second pathways are believed to be detoxification mechanisms. The third pathway leads to the formation

of toxic metabolites and appears to be the major activation mechanism (Fu et al, 2004).

Otonecine-type PAs have a necine base structurally different from retronecine-type (Fig.1.1 and 1.2). As such, there are only two general principal metabolic pathways, hydrolysis and oxidation, for this type of PAs as summarized in Fig.1.4 (Lin et al., 2000a; Lin et al., 2003; Lin et al., 2002; Lin et al., 2000b; Lin et al., 2007). The formation of the corresponding pyrrolic esters is through oxidative N-demethylation of the necine base followed by ring closure and dehydration. The C_7 position of the otonecine-type PAs possesses an R absolute configuration. Consequently, the resulting pyrrolic esters have a necine base identical to that of retronecine-type PAs.

The main metabolic route of PA N-oxides metabolism is to be reduced to corresponding PAs, which are be further metabolized as already described (Chu et al., 1993; Yan et al., 2008). This reduction has been shown to mainly occur in the gut which may be brought about by intestinal bacteria or gut enzymes and also, to some extent, occurs in the liver (Powis et al., 1979a, b).
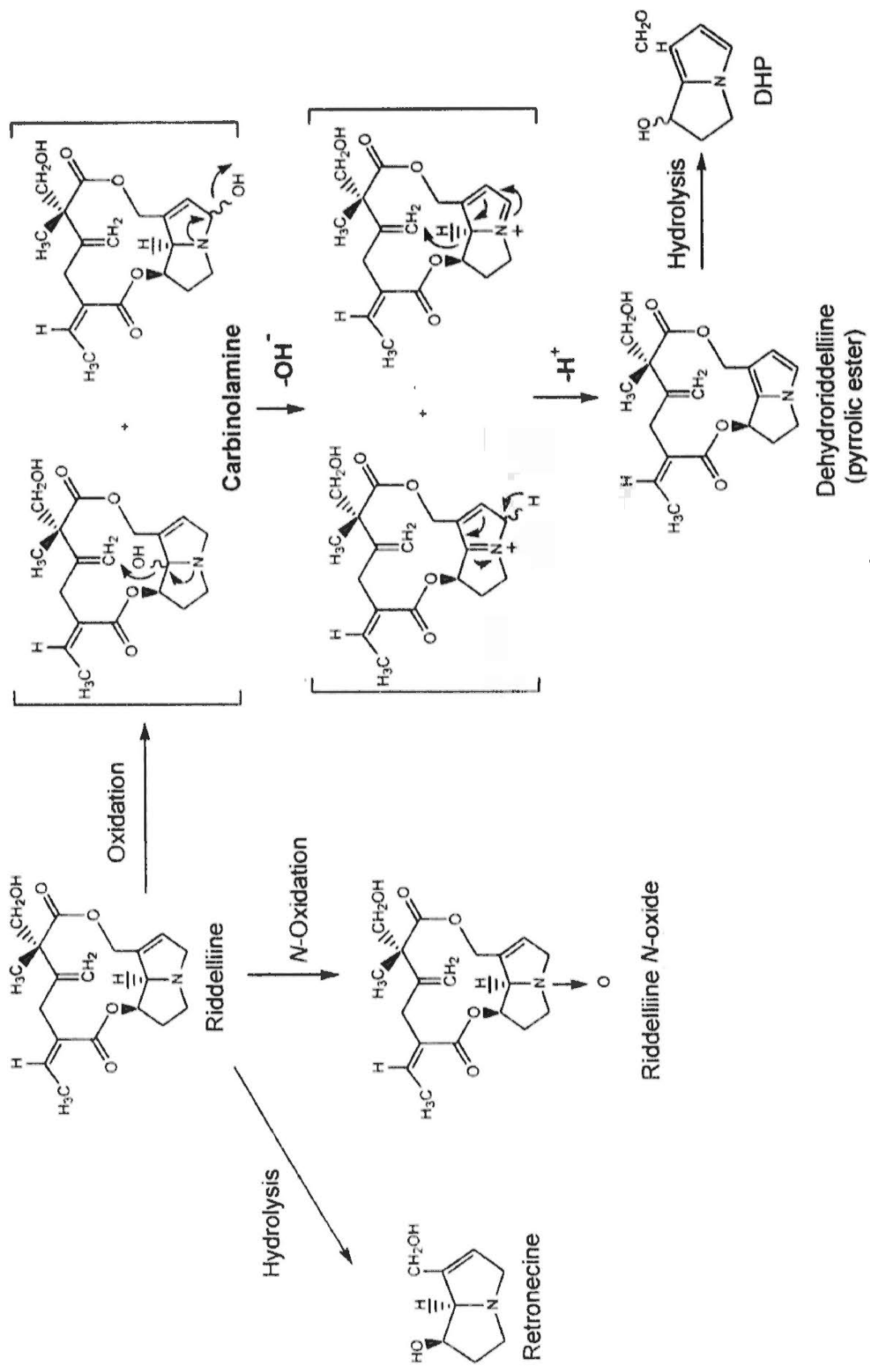
Fig.1.3. Phase I metabolism pathways of riddelliine, a retronecine-type PA (Fu et al, 2004).
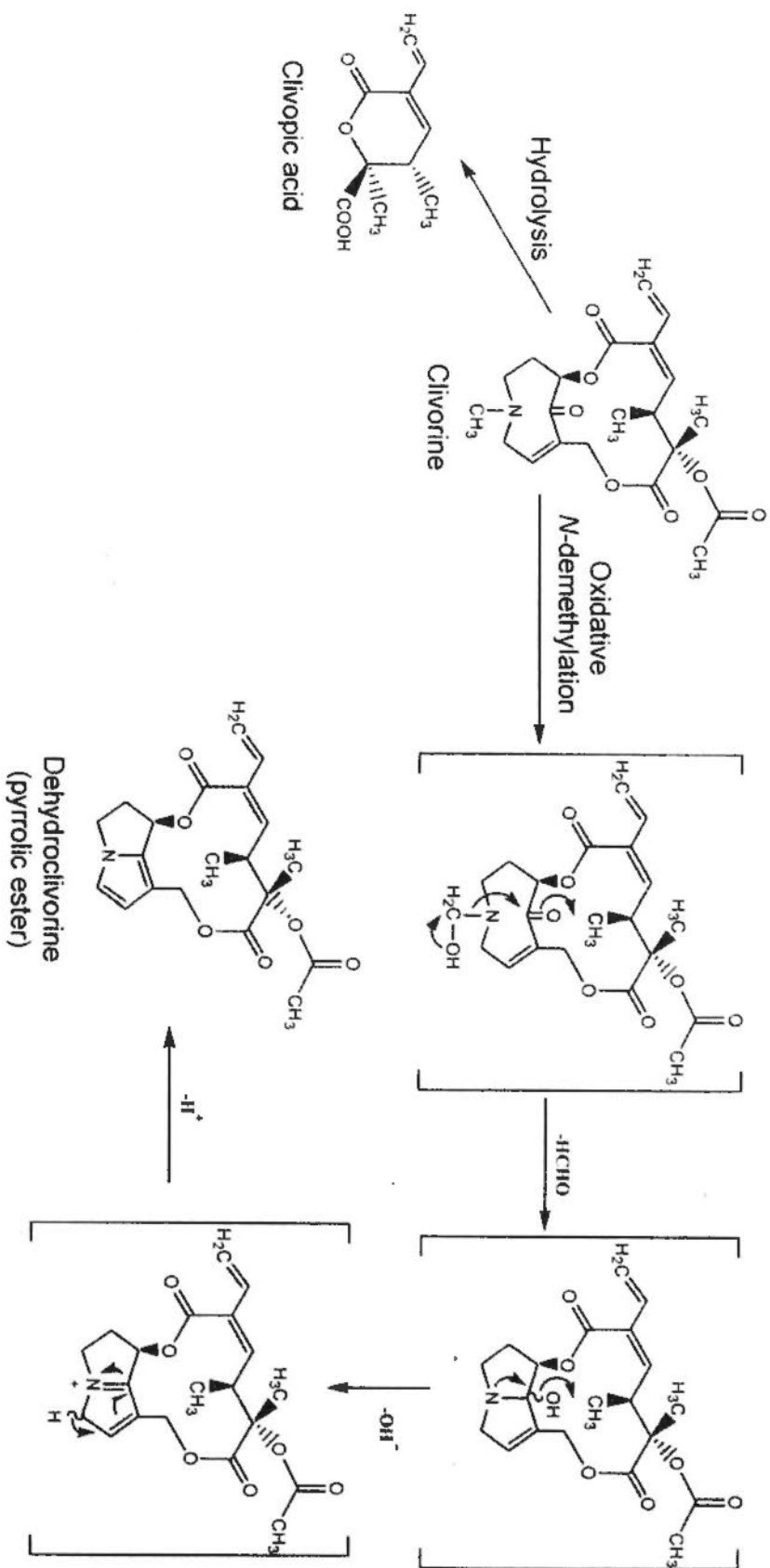
Fig. 1.4. Phase I metabolism pathways of clivorine, an otonecine-type PA (Fu et al, 2004).

1.1.2 Toxicity

The metabolic formation of pyrroles of PA is catalyzed by hepatic cytochrome P450 monooxygenase (CYP), mainly CYP3A and CYP2B isoforms in humans (Omiecinski et al., 1999; Yang et al., 2001a). These metabolites, pyrroles, are highly reactive and can react readily with water and other endogenous constituents, such as glutathione (GSH), to form the detoxified products. As shown in Fig.1.5, pyrroles may bind with one or two molecules of GSH to form 7-glutathionyl-6, 7-dihydro-1-hydroxymethyl-5H-pyrrolizine (7-GSH-DHP) or 7, 9-diglutathionyl-6, 7-dihydro-1-hydroxymethyl-5H-pyrrolizine (7, 9-diGSH-DHP), respectively (Fu et al., 2004; Lin et al., 2000a; Yan and Huxtable, 1995a, b). On the other hand, the pyrroles can also rapidly react with proteins and nucleic acids of the tissues, leading to DNA cross-linking, DNA-protein cross-linking, and DNA adduct formation (Yang et al., 2001b). Thus the reactions of pyrroles with components of the liver cell, thereby, affecting their structure and function are the main causes of liver cell necrosis (Fu et al., 2004; Guo et al., 2002; Yang et al., 2001b).

Sufficiently large dose of toxic PAs can cause rapid death between a few minutes and a few hours after intake. This type of toxicity, referred to as peracute, is not related to cytotoxic action. It is associated with pharmacological actions of the compounds and death may be preceded by convulsions or coma (Mattocks, 1986). Acute cytotoxicity may result in deaths between 2 day and about a week after the ingestion of PAs and mainly refer to liver cells (Mattocks, 1986). Animals surviving a sublethal dose of cytotoxic PA often show delayed (chronic) toxic effects in the liver and sometimes the lungs and elsewhere; such effects may also result from multiple (chronic) intake of smaller amounts of PAs, such as when PAs contaminate the diet. The mechanism of PA toxicity are believed to relate to DNA binding, DNA

cross-linking, DNA-protein cross-linking caused by the reactive pyrroles (Yang et al., 2001b; Kim et al., 1999).

There is a good correlation between the degree of hepatotoxicity and the quantity of pyrrole derivatives from PA detected in the liver (Mattocks AR. 1968). Rats receiving an oral administration of monocrotaline, a retronecine-type PA, develop progressive injury in the sinusoidal wall (loss of sinusoidal cells and sinusoidal hemorrhage) as well as the terminal hepatic vein endothelium (DeLeve et al., 1999). A week after treatment, following severe coagulative necrosis at zone 3 and inflammation with monocytes and macrophages, there is progressive fibrosis of the terminal hepatic veins and of the parenchyma (DeLeve et al., 1999). Increased portal pressure is the main consequence of the structural changes, resulting in increased resistance to portal blood flow in the sinusoids and terminal hepatic venules (DeLeve et al., 1999). Decreased production of the vasodilator 16 keto-Prostaglandin F1a by endothelial and Kupffer liver cells may contribute to the development of portal hypertension by increasing the resistance to portal blood flow (DeLeve et al., 1999).
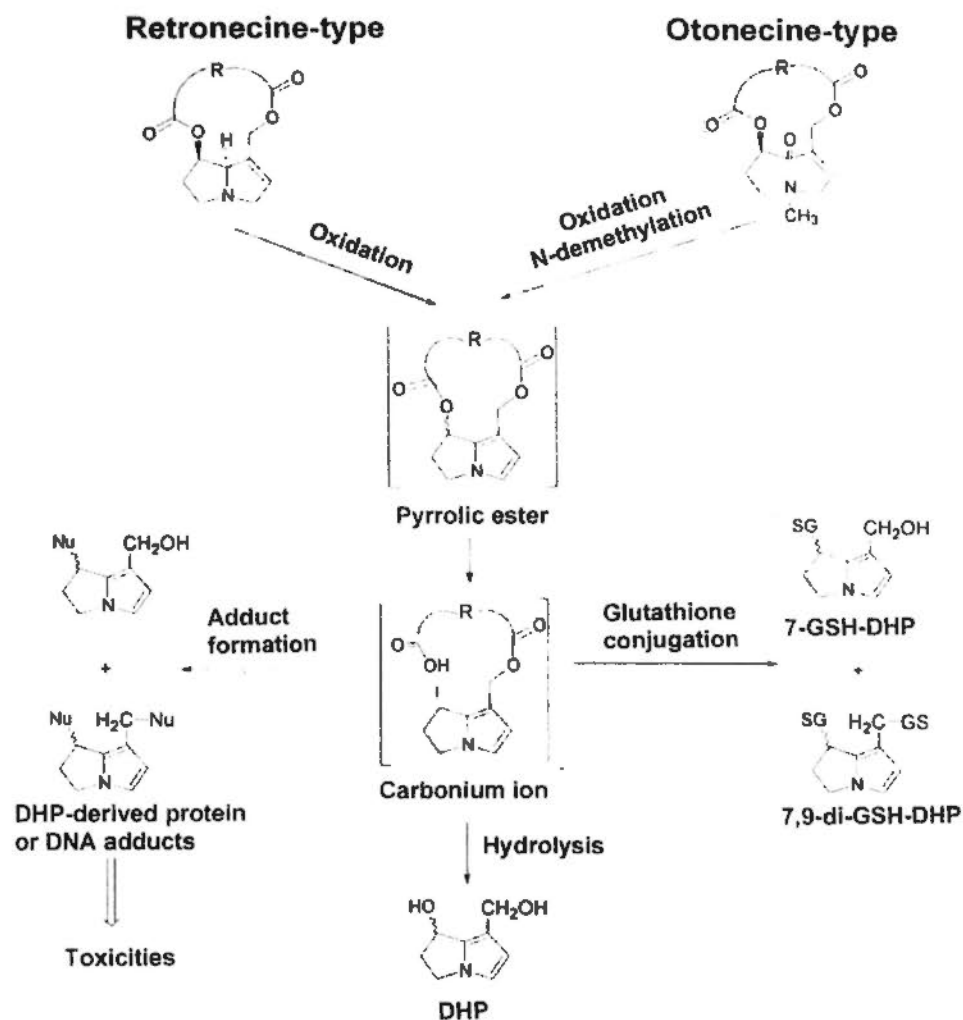
Fig.1.5. Detoxification and toxicity mechanism of pyrrolic ester of two toxic types of PAs after phase I metabolism (Fu et al, 2004).

1.1.3 PAs and Human Health

Hepatic sinusoid occlusion syndrome (HSOS) caused by the consumption of plants containing PAs has been recognized independently as an endemic disease in certain parts of the world (Mattocks, 1986; IPCS, 1988). The outbreaks of HSOS have affected significant segments of populations or large numbers of people in geographically confined areas in Afghanistan, India, and Uzbekistan (Mattocks, 1986; IPCS, 1989). These outbreaks are caused by contamination of the staple food crops with the seeds of plants containing PAs, growing among the crops; such plants

are likely to thrive following periods of drought (Roeder, 2000; Stegelmeier et al., 1999).

1.1.3.1 Source of Hepatotoxic PAs

Plants constitute the only natural source of PAs that cause toxic reactions in man and animals. The most important genera of PA-containing toxic plants are Crotalaria, Senecio, Heliotropium, Trichodesma, Amsinckia, Echium, and Symphytum (Mattocks, 1986; IPCS, 1989). The recorded cases of human toxicity have mainly been caused by at least 12 different PAs, mostly derived from Heliotropium, Senecio, and Crotalaria genera (Culvenor et al., 1980). There is a possibility that, upon further examination, hepatotoxic PAs may be found, as minor constituents, in strains or parts of these plants not yet investigated or under specific conditions of growth. Therefore, the species that have been investigated should be fewer when compared with the total number of species in each genera.

1.1.3.2 Pathway of Exposure

Plants containing PAs are found in most parts of the world and they are readily eaten by some animal species. The two main sources of PA poisoning reported in human beings are the consumption of cereal grain contaminated by weeds containing PAs and the use of PA-containing herbs for either medicinal or dietary purpose. A third form of exposure, with the potential to affect large populations is the possible low-level contamination of some foodstuffs, such as honey and milk (Coulombe, 2003).

1.1.3.2.1 Contamination of Staple Food Crops

Epidemics of PA poisoning have typically occurred when large numbers of people eat foods made from seeds contaminated by either the seeds or dusts of

PA-containing plants (IPCS, 1988). To reduce risk posed by PAs, reduction of exposure should be the best strategy. While the routinely used grain cleaning methods in industrial countries may reduce PA contamination to below the level causing acute poisoning by removing the foreign seeds, they do not remove the dust component. Thus there are concerns that poisoning could in some instance result from chronic exposure to low levels of PAs in products such as cereal grains even in the industrialized world (Edgar et al., 2011). However, this exposure is generally not recognized by the public. In addition, it is likely that drought, famine and political instability will also conspire to produce another large-scale outbreak of human poisonings.

1.1.3.2.2 Herbal Medicines

Plants have been traditionally used for medicinal purposes all over the world and have been the mainstay of the indigenous systems of medicine, especially in China, Greece, and India, since ancient times (Roeder, 1995, 2000; Roeder and Wiedenfeld, 2009). Recognition of this mode of human PA intoxication followed investigations into herbal teas and their connection with liver disease in Jamaica and other parts of the West Indies in the 1950s (Mattocks, 1986). The use of herbal teas made from PA-containing plants in treating minor illness is also recognized as a cause of liver disease in parts of Africa and other tropical and subtropical countries (IPCS, 1989). PA poisoning is more common in developing countries, while industrial countries, including the USA, UK, Germany, Switzerland and Austria, have also reported PA intoxications resulting from consumption of herbal medicines (Molyneux et al., 2011). Some of the suspected or known teas that contain PAs have been used as herbal medicines as well as home remedies and may be freely available in herbal shops in many countries.

1.1.3.2.3 Contaminated Honey

Honey derived from the flowers of PA-containing plants, has been shown to greatly exceed the levels of PAs deemed tolerable by some health authorities (Beales et al., 2004; Crews et al., 1997; Edgar et al., 2002; Kempf et al., 2010). Honey made from the flower of several PA-containing plants belonging to the genera *Senecio*, *Echium and Heliotropium* contains PAs (Beales et al., 2004). Both *E. plantagineum* and *E. vulgare* yield popular, mild-tasting, widely traded honeys. For example, the highest concentration of PAs reported in honey is originating from *Senecio jacobaea* in 3900 mg/kg (Culvenor, 1983). *Echium plantagineum* honey is said to contain up to 2300 mg/kg (Beales, Betteridge, 2004) and *E. vulgare* honey contain 500 – 2800 mg/kg of PAs (Betteridge et al., 2005). These levels of PAs in honey compare very unfavorably with the maximum tolerable level of 1 mg of PAs per kg of food allowed by law in the Netherlands (Boppre et al., 2008; Molyneux et al., 2011). They may also exceed the maximum of 1 µg of PAs allowed per daily dose of herbal medicines in Germany (Edgar et al., 2002). Although significant volumes of commercial honey from *Echium* species are produced in several countries, there is no monitoring of retail honeys for PA-containing plants.

1.1.3.2.4 Contaminated Pollen

It has been suggested that the PAs found in honey may come primarily from pollen, a natural contaminant of honey introduced by bees and also by apiarists during harvesting of the honey. For example, pollen from *Echium Vulgare* was shown to contain between 8000 and 14000 mg of PAs/kg (Boppre et al., 2008). However, pollen are believed to have many health benefits and are being widely sold as a health food supplement, thus pollen may contribute to an unrecognized dietary exposure to PAs (Boppre et al., 2008).

1.1.3.2.5 Milk Containing PAs

Milk has been proved to be a source of PAs exposure experimentally in animals (Mattocks, 1986; Molyneux and James, 1990). No human cases of PA poisoning via milk have been reported but Huxtable (1989) refers to several instances where HSOS occurred in sucking babies where there was no history of direct herbal administration to the infants.

1.1.3.2.6 Eggs Containing PAs

There have been a number of reports of poultry being poisoned by PA (Hill et al., 1997). In one incident involving commercial chickens, wheat containing seeds of *Heliotropium europaeum* was shown to be the principle cause and alkaloids characteristic of this plant were found in eggs laid by the chickens (Stegelmeier et al., 1999). The levels of PAs in the eggs ranged up to 9.7 mg per egg, considerably in excess of the maximum tolerable level specified for human exposure in Dutch and German regulations (Edgar et al., 2002).

1.1.3.2.7 Meats as a Possible Source of PAs

Many millions of meat-producing livestock are exposed to plants containing PAs and PAs poisoning is considered to be the most common poisoning disease of livestock worldwide (Prakash et al., 1999). It is however not yet been established whether hazardous residues of PAs remain in meat entering the human food chain.

1.1.3.3 Levels of Intake

Reliable estimates of levels of intake of PAs are extremely difficult to make because sampling of the contaminated grain may not be strictly representative since the extent of the contamination may vary in different sites and households (Mattocks, 1986; IPCS, 1989). The estimated lengths of exposure, and hence the amount of total

intake, are also approximate. In an outbreak in India, the estimated daily intake by the population was 0.66 mg/kg body weight. In a larger outbreak in Afghanistan, the estimated daily intake was 0.033 mg/kg body weight. These intakes, sustained for periods of approximate 2 and 6 months, respectively, resulted in typical acute HSOS (Mattocks, 1986; IPCS, 1989). A lowest intake rate has been associated with the use or misuse of medicinal herbs, which led to an estimated daily intake of 0.015 mg/kg body weight after a 4- to 6-month period (Stegelmeier et al., 1999). The dose estimates indicate that the effects of PAs in human beings are cumulative at very low intake rates. These lower rates of intake may lead to chronic forms of intoxication. However, the available information on dose-response relationships is very limited, thus at present, there is no evidence on which the degree of risk in these circumstances can be evaluated. But more importantly, it is definite that even low rates of intake of PAs over a period of time may present a health risk and that exposure should be minimized wherever possible (Stegelmeier, 2011; Stegelmeier et al., 1999).

1.1.3.4 Toxic Effect on Human

There are relatively few reports of human intoxication by PAs comparing to its extensive distribution, although some of the incidents described involve large numbers of people. It is possible that the recorded cases may represent the tip of an 'iceberg' of people affected by PAs because medical practitioners are unfamiliar with such poisoning, and thus some occasional PA-poisoning cases may be attributed to other causes.

Acute dosing with large amounts of PAs produces primarily liver disease in humans, but gastroenteritis may also be seen. Patients may present with vomiting and severe abdominal pain. Hepatomegaly, splenomegaly, right upper quadrant

abdominal pain, ascites formation and jaundice are seen inconsistently. Toxicity may also result from both subacute and chronic exposures. Plant PAs are among the first identified toxins which cause sporadic or epidemic intoxication for HSOS (Chen and Huo, 2010).

1.1.3.5 Diagnosis of PA-Induced Hepatotoxicity

Diagnosis of PA-poisoning is often difficult because the symptoms seldom appear until the condition is in its advanced stages, while PAs are usually excreted within 24 h after intake (Mendel et al., 1988; Winter et al., 1993). Thus it is seldom that a physician can see a patient who has, within the last hour or two, ingested a known quantity of PAs (Winter et al., 1994). Diagnosis is only made by the symptoms, pathological changes in the liver structure and histology, and analysis of available herbal material. A clear distinction between the acute and chronic effects of exposure is impossible since the history of onset of disease with intake of the toxic substance is not generally available. Therefore, precise dose or temporal relationships between PA exposure and the degree of toxicity is difficult to establish (Winter et al., 1993).

1.1.3.6 Precaution of PA-Induced Hepatotoxicity

At present, prevention of PA poisoning can be achieved only by reducing or eliminating ingestion of PAs through the following procedures (Mattocks, 1986)

1.1.3.6.1 Control of PA-Containing Plants

The control of plant populations for this purpose has been carried out only in Uzbekistan, USSR, following the epidemics of human disease due to contamination of grain by seeds of *Heliotropium lasiocarpum* and *Trichodesma incanum*. The following measures were thus introduced and supposed to be effective in preventing further outbreaks: 1) setting a state standard for the seed grain and quality of grain

14

stored for food; 2) monitoring levels of contamination of flour, bread, and similar products; 3) promotion of weed control by governmental authorities and provision of legislation to enforce the control measures.

1.1.3.6.2 Public Education

Several publications of educational booklets have described the biological, environmental, and morphological characteristics of the toxic weeds, their pathways of distribution and the causes of the toxicoses experienced (IPCS, 1988; 1989).

1.1.3.6.3 Prevention of Absorption

Prevention of absorption is only useful as ingestion has just occurred. There is no known way to prevent the liver damage, once a hepatotoxic dose of a PA has been ingested. A number of dietary regimes have been found to partially protect animals from the acute effects of subsequent alkaloids ingestion (IPCS, 1989).

1.1.3.7 Treatment of PA-Induced Hepatotoxicity

No specific treatment options are available and thus treatment is always supportive, especially for those cases that have progressed to liver failure (IPCS, 1989). Hemodialysis may be effective in treating the patient with liver failure but the attempts to remove PAs by hemodialysis have not been reported. Possible treatment may include blocking metabolism or adding reactive substrate may be able to protect the liver. However, it is only useful if the patients are seen early in intoxication (Mattocks, 1986).

1.1.4 Summary

PA poisonings in people have been referred to as an "iceberg disease" because reported cases of PA poisoning are probably only a small percentage of the true

incidence. The many poisoning cases resulting from consumption of "safe" and "natural" supplements emphasize the urgent need for greater awareness of the potential adverse effects of herbal produces. Nevertheless, the best strategy of reduction of risk posed by PAs should be reduction of its exposure. For this reason, several countries have enunciated regulations to restrict PA exposure (Roeder, 2000). However, these regulations are based on case studies; they cannot be used as general rules and applied universally for all PA-containing herbal products. Thus, the deficiency of an effective regulation results in several new reports of PAs poisoning (Bensaude et al., 1998; Rasenack et al., 2003).

1.2 HSOS

HSOS has long been known as a human and animal disease related to the ingestion or administration of certain toxins (DeLeve et al., 2002; Wadleigh et al., 2003). Although it was first described in Jamaicans who had consumed large amounts of bush tea containing PA, HSOS is now best recognized as a complication most commonly associated with high-dose chemotherapy after stem cell transplantation (SCT) (Helmy, 2006). For example, cyclophosphamide (Cyc)-containing regimens are one of the long identified risk factors (Poreddy and DeLeve, 2002).

HSOS generally has an acute onset, characterized by rapidly developing and progressing symptoms of upper abdominal discomfort, dragging pain in right hypochondrium, ascites, and sometimes oliguria and edema of the feet (Helmy, 2006). The onset of the disease may be sudden (acute) or insidious (subacute or chronic). The acute disease may recover completely or result in death. A few patients may go on to the subacute phase, with almost none or very few symptoms, but a persistent hepatomegaly. The patient may subsequently recover completely, or may,

after or without apparent clinical improvement, go on to the chronic phase of disease, mostly ending up in cirrhosis.

1.2.1 Pathogenesis of HSOS

Unlike most hepatic disorders, HSOS usually presents firstly as portal hypertension and then followed by the parenchymal dysfunction. This indicates a primary vascular nature of the disease. Pathologically, occlusion of the central venules by subendothelial oedema, haemorrhage or fibrosis can easily be detected, hence the original name, hepatic veno-occlusive disease (HVOD) (Helmy et al., 2005, Helmy, 2006). An animal model of HSOS using monocrotaline, a retronecine-type PA, has promoted clarification of the pathogenesis of the disease (DeLeve, 2007). A major step forward is to show that sinusoidal, not venous endothelial cells (ECs) are the toxic target of PAs (Chen et al., 2008b; Deleve et al., 2003). Thus, HSOS has been proposed to replace the previously used term HVOD (DeLeve et al., 2002). In the liver, PA produces ECs damage, dilation of sinusoids, sinusoids hemorrhage, and parenchymal cell injury (Wang et al., 2000). Studies *in vitro* prove that PAs directly damage sinusoidal endothelial cells (SECs), directly suggesting that these cells, but not parenchymal cells, should be the target of toxicity in the liver (DeLeve et al, 1999; Chen et al, 2008). Toxicity to these ECs is progressive, beginning with defenestration and gap formation in the SECs and central vein endothelia cells (CVECs) lining. The culminating complete loss of ECs from the sinusoid and central vein and may progress to complete disruption of vascular intima, then result in the ischemic parenchymal cell injury (DeLeve et al., 1999). Mechanism studies suggest that besides EC injury, other process such as GSH disturbance is also involved in the pathogenesis of PA-induced HSOS (Yan et al, 1995a, b; Valla, 2008).

1.2.1.1 GSH Depletion

The role of GSH depletion in the pathogenesis of HSOS is evidenced by *in vitro* and and *in vivo* monocrotaline model studies (Ji et al., 2008; Taylor et al., 1997; Yan and Huxtable, 1996). These include: (i) marked depletion of GSH in SECs before cell death, which is the most common biochemical change that is induced by drugs and toxins implicated in HSOS; (ii) maintenance of GSH in the presence of such toxins prevents cell death; (iii) continuous infusion of GSH or N-acetylcysteine prevents the development of HSOS in the monocrotaline model; (iv) infusion of GSH 24 h after monocrotaline only reduces the degree of hepatic sinusoidal injury, but to a lesser extent than prophylactic treatment with GSH.

1.2.1.2 Nitric Oxide (NO) Depletion

In parallel with the decline in hepatic blood flow, NO levels in the hepatic vein were shown to decrease. Indeed, inhibition of NO synthesis in the rat model of HSOS caused by sub-toxic doses of monocrotaline aggravated the disease (Copple et al., 2006). In addition, infusion of a specific liver NO precursor prevents the morphological changes of liver and the clinical features of HSOS (Cheng et al., 2005). This change suggests an involvement of NO depletion in the development of HSOS.

1.2.1.3 Oxidative Stress

Oxidative stress plays an important role in HSOS, since administration of GSH or its precursor N-acetyl-L-cysteine confers protection against HSOS (Ji et al., 2009; Ji et al., 2010). Biliary excretion of GSH and cysteinyl-glycineconjugates of monocrotaline pyrrole support the role of thiol compounds in the detoxification of PA (Lame et al., 1995). As reactive oxygen species (ROS) have a critical role in

monocrotaline induced pulmonary hypertension, it is supposed to be a possible underlying mechanism of HSOS (Chen et al., 2001).

1.2.1.4 Role of Clotting Factors

The role of clotting disorders in the pathogenesis of HSOS is debatable. Electron microscopic study of liver samples obtained from individuals revealed no evidence of clotting abnormalities in HSOS (Putzke and Persaud, 1976). In addition, immunohistochemical (IHC) studies of autopsy livers did not detect platelets, although fibrinogen and factor VIII were detected in the hepatic veins (Copple et al., 2002).

1.2.1.5 Increased Matrix Metalloproteins (MMPs)

In the monocrotaline-induced rat model of HSOS, there was an early increase of matrix metalloproteinase-9 (MMP-9) and a later, lower-magnitude increase of matrix metalloproteinase-2 (MMP-2) in the liver (Deleve et al., 2003; Hanumegowda et al., 2003). *In vitro* studies showed that SECs are the major source of both basal and monocrotaline-induced increase of MMP-9/MMP-2 activity (Hanumegowda et al., 2003). Monocrotaline caused depolymerization of F-actin in SECs, and blocking of F-actin depolymerization prevented the increase in MMP activity (Deleve et al., 2003). Administration of MMP inhibitors prevented the signs and histological changes associated with HSOS, and may be a therapeutically viable strategy for prevention (Deleve et al., 2003).

1.2.1.6 Apoptosis

Apoptosis has been described in the livers of animals exposed to several PAs and in a human patient who consumed an herbal concoction containing PAs, suggesting that PAs produce mixed lesions consisting of oncotic and apoptotic cell damage

(Copple et al., 2004; Ji et al., 2005). An intracellular signal transduction pathway, mitogen-activated protein kinases (MAPKs) has been proved to be involved in the clivorine-, an otonecine type of PA, induced toxic effects *in vitro* (Nyska et al., 2002). The PA-damaged hepatocytes have a decreased level of antiapoptotic protein Bcl-x, and an increased expression of the proapoptotic protein Bax, resulting in the release of cytochrome c from the mitochondria and induction of the intrinsic apoptotic pathway (Gordon et al., 2000a; Gordon et al., 2000b).

1.2.1.7 Endothelial Injury

Marked elevation in markers of endothelial injury and adhesion molecules occur in patients with HSOS, including plasma thrombomodulin, P-selectin, and plasminogen activator inhibitor (PAI-1) (Wadleigh et al., 2003). Studies have subsequently confirmed elevation of PAI-1 levels in SCT associated HSOS and shown elevation of tissue factor pathway inhibitor, soluble tissue factor, thrombomodulin, and P- and E-selectin (Wadleigh et al., 2003). Elevation of plasma levels of C-reactive protein in allo-SCT patients with severe HSOS, compared with those without, also supports the role of IL-6 in the disease process.

1.2.2 Diagnosis of HSOS

1.2.2.1 Clinical

Clinical criteria for the diagnosis of HSOS have been published by several investigators from Seattle and Baltimore (Table 1.1) (Ho et al., 2004; Wadleigh et al., 2003; Helmy, 2006). The course of HSOS is protracted, and symptoms persist for a long period if caused by chronic ingestion of teas or foods containing PAs. However, HSOS secondary to SCT has a more rapidly evolving course.

Table 1.1 Diagnostic criteria for HSOS (Helmy, 2006)

Seattle criteria

At least two of the three following criteria, within the first month after SCT:

1. Jaundice

2. Hepatomegaly and right upper quadrant pain

3. Ascites and/or unexplained weight gain

Baltimore criteria

Elevated total serum bilirubin (≥2 mg/dL) before day 21 after SCT and two of the three following criteria:

1. Tender hepatomegaly

2. weight gain >5% from baseline

3. Ascites

Modified Seattle criteria

Occurrence of two of the following events within 20 days of SCT:

1. Hyperbilirubinaemia (total serum bilirubin ≥2 mg/dL)

2. Hepatomegaly or right upper quadrant pain of liver origin

3. Unexplained weight gain (>2% of baseline body weight) because of fluid accumulation

1.2.2.2 Laboratory

Laboratory markers are usually required for early diagnosis, to assess severity, to predict disease outcome, to assess response to therapy, or to detect recurrence (Helmy, 2006). Many studies have observed that patients with HSOS have: (i) an increase in serum bilirubin, aspartate aminotransferase (AST) and alanine aminotransferase (ALT) (McCaughan et al., 1995), (ii) an increase in levels of EC markers such as hyaluronic acid, von Willebrand factor, plasminogen activator inhibitor-1 (PAI-1) and tissue plasminogen activator (t-PA) (Pihusch et al., 2005), (iii) an increase of coagulation activation markers, such as thrombin - antithrombin

complexes (Ibrahim et al., 2004); (iv) a decrease in the concentrations of natural anticoagulants, such as protein C and antithrombin III (Ibrahim et al., 2004); (v) an increase in procoagulants such as factor VIII and fibrinogen (Lee et al., 1998); (vi) an increase in thrombopoietin, cytokines, and procollagen peptides (Rio et al., 1993; Yasutomo and Himeno, 1993). In addition, low serum protein C levels can discriminate between patients with and those without HSOS (Bazarbachi et al., 1993).

1.2.2.3 Imaging

The common ultrasonographic findings reported in patients with HSOS include ascites, hepatomegaly, attenuated hepatic flow, hepatic veins or biliary dilatation (Matsumoto et al., 2009). Pulsed Doppler ultrasound usually shows a decreased or inverted portal blood flow, which is a relatively late finding in patients with HSOS (Deeg et al., 1993). Magnetic resonance imaging (MRI) can be used as a complementary technique following the non-conclusive ultrasound examination with the ability to show hepatomegaly, hepatic vein narrowing, periportal cuffing, gall-bladder wall thickening, ascites and pleural effusion (Mortele et al., 2002).

1.2.2.4 Histopathology

The most distinctive histolopathological feature of HSOS is a thickening of the subintimal zone of central and sublobular venules. This produces concentric or eccentric luminal narrowing (Shirai et al., 1987). In early stages of the disease, thrombosis does not occur and inflammatory cells are few or absent, but biopsies show marked widening of the subendothelial zone by the fragmented red cells, oedema and fibrinogen that can be identified by immunochemistry or Mallory's stain (Cesaro et al., 2011). In later stages, the non-specific change of chronic venous

outflow obstruction predominates leading to perivenular fibrosis, pericellular fibrosis, central-central fibrous bridges and eventually cirrhosis.

1.2.3 Treatment of HSOS

The limited advance in the knowledge about the pathophysiology of HSOS restricts the development of treatment strategy. Thus the way of therapeutic measures are mainly supportive care, defibrotide, and liver transplantation (Bearman, 2000; Chen et al., 2008a; Helmy, 2006).

Ascites is treated with sodium restriction, diuretics and therapeutic paracentesis for discomfort or shortness of breath. Other supportive measures, such as haemodialysis and mechanical ventilation, were used in patients with HSOS associated with multiorgan failure, while without any improvement in the outcome. Heparin plus t-PA showed improvement in <30% of patients with severe HSOS (Gruss et al., 1995; Hahn et al., 2003).

Defibrotide, a single-stranded polydeoxyribonucleotide that has specific binding sites on vascular endothelium, may have antithrombotic, anti-ischemic and thrombolytic effects and reduces leucocyte rolling and adherence to endothelium. Therefore, it shows to be a promising treatment of HSOS (Richardson et al., 1998). The suggested mechanisms of action of DT on HSOS include: (i) stimulation of EC release of tissue t-PA; (ii) up-regulation of the release of NO, prostacyclin I2, prostaglandin E2 (PGE2), thrombomodulin and t-PA both *in vitro* and *in vivo*; (iii) decreased release of PAI-1; and (iv) stimulation of the adenosine receptor. Moreover, defibrotide has been shown to decrease thrombin generation, tissue factor expression and endothelin activity (Richardson et al., 1998).

Liver transplantation should be considered only in patients with severe liver failure who are expected to have a good outcome in the absence of liver disease, and

those who have undergone bone marrow transplantation for benign disease (Shulman and Hinterberger, 1992). Liver transplantation is usually contra-indicated when malignancy is present because of the high rates of recurrence.

1.2.4 Summary

The etiology of HSOS is now definitely ascribed to two main causes, PA intoxication and chemotherapy after SCT. However, the pathogenesis of HSOS remains largely unknown; therefore no effective methods have been established for its diagnosis and treatment. Thus, HSOS remains a major barrier to successful auto-SCT. Hence, treatment for severe HSOS has been ineffective, prevention of this formidable transplant complication or PA exposure is tantamount. However, as illustrated earlier, it is impossible to thoroughly stop PA exposure, as well as SCT in most cases. Thus, a thoroughly investigation of underlying mechanism of HSOS would warrant a solution for this issue.

1.3 Objective of the Present Study

As discussed previously, chronic ingestion of PAs can cause HSOS leading to death in rodents and human (Chen and Huo, 2010). Due to its extensive distribution in large amount of plants, PAs represent a serious public health problem by means of PA-contaminated food and/or PA-contained natural products (Edgar et al., 2002). However, till now, no strategy has been established for an effective prevention, diagnosis and treatment of PA poisoning. The avoidance of consumption of PAs is the only known method to control PA-induced toxicity. However, the severity of hepatotoxicity of different PAs varies significantly (Mattocks, 1986), which makes it difficult to set up a regulation for a universal threshold of toxic dose of individual PAs. Thus an understanding of the diversity of PA-induced toxicity would be a critical step in its prevention.

In addition, despite extensive research efforts made in the past decades to understand the process leading to hepatotoxicity after PA exposure, the events that trigger the toxic response remain largely unknown, which result in the lack of a available method for the specific diagnosis of PA-induced HSOS (Boppre et al, 2011). Thus all the reported PA poisonings were based on clinical observations and conventional histopathological and biochemical indicators of liver injury, such as ALT, which are non-specific and do not distinguish PA poisoning from other causes. Afterwards, the cases were retrospectively suspected to be associated with PA exposures if the materials digested before and/or during disease progression were available and are determined to contain PAs. However, many new PAs poisoning cases are still reported (Bensaude et al, 1998; Rasenack et al, 2003; Ka et al, 2006), which urge the need for some selective and specific methods for the diagnosis and assessment of PA-induced hepatotoxicity. The limited understanding of the full mechanism, especially downstream biochemical events after formation of pyrrole-DNA or pyrrole-protein adduct, in PA-induced HSOS restrict the identification of any specific biomarkers.

Thus, the objectives of the present study are to:

1. Develop a simple *in vitro* model for the rapid assessment of the hepatocytotoxicity of PAs.

2. Assess the hepatocytotoxicity of three types of PAs using developed *in vitro* model.

3. Develop a reliable animal model of PA-induced acute hepatotoxicity to form a solid foundation for the further proteomic study.

4. Identify the protein signatures and potential biomarkers for PA-induced hepatotoxicty using proteomic study.

5. Find the common pathway and biomarkers involved in HSOS by the comparable proteomic study on Cyc-induced hepatotoxiity.

Chapter 2 Development of an *in vitro* Model for the Assessment of PA-Induced Hepatotoxicity

2.1 HepG2 Cell Model

2.1.1 Introduction

PA-induced hepatotoxicity represents a major clinical reason accounting for many cases of HSOS, most of which are due to unintentional misuse by consumption of PA-contaminated food or PA-contained natural products (Lin et al., 2011). Till now, there are over 8000 PA-poisoning cases have been reported throughout the world including Afghanistan, Britain, China, Germany, Hong Kong, India, Jamaica, South Africa, Switzerland, and the United States (Dai et al., 2007). It has been suggested that PAs are responsible for livestock loss and may lead to many public health problem (Edgar et al., 2002).

To have the PA-induced toxicity under control, several countries have established regulations for the restriction of exposure to PA-containing medicinal herbs (Roeder, 2000). Unfortunately, all these regulations are based on case studies and they cannot be applied universally. Therefore, it is necessary to set up a regulation for a universal threshold of toxic dose of individual PAs. However, there are a large number of PAs which are divided into different types according to their structures (Fu et al., 2004). Based on the structure-toxicity relationship reported (Mattoks, 1986; Wiedenfeld et al, 2008), the severity of hepatotoxicity of different PAs varies significantly. Thus a better prediction of the diversity of PA-induced toxicity by a systematic assessment is important for setting up an appropriate regulation for the restriction of PA-exposure.

In vitro system, an acceptable alternative to the whole animal model for toxicity screening, is generally recognized to be valuable for minimizing the numbers of animal sacrificed and amount of compound used. It has now been commonly used in the toxicological assessment of chemicals and chemical mixtures. A high concordance of drug-induced hepatotoxicity with *in vitro* cytotoxicity has been demonstrated by a cell-based model (O'Brien et al., 2006). As such, it is understandable that the use of *in vitro* systems is now becoming common in investigative toxicology (Dambach et al., 2005). In the present study, we aim to develop a convenient *in vitro* model to rapidly assess the hepatocytotoxicity of PAs.

In vitro systems such as primary cell cultures, immortalized cell lines, liver slices and whole perfused liver are well-established models used for investigative work on hepatology (Groneberg et al., 2002; Guillouzo et al., 1997). The primary cell culture system consists of confluent cultures of freshly isolated hepatocytes from humans or animal and has the full complement of metabolizing enzymes, albeit with inherent donor-to-donor variability (Groneberg et al., 2002; Guillouzo et al., 1997). Thus as compared to immortalized cells, they may represent an assay system that is more representative of hepatocytes *in vivo* and have proven valuable as a screening modality (Guillouzo et al., 1993; Li and Kedderis, 1997; Riley et al., 2004).

However, an immortalized cell line is generally more desirable in terms of the ease of culture and relevance to the diseases. Among the human hepatic cell lines, the use of HepG2 cell line to assess potential cytotoxicity is promoted by several commercial laboratories. The HepG2 cells have been extensively studied as a more feasible substitute for primary hepatocytes (El Golli Bennour et al., 2009; Hall et al., 1993; O'Brien et al., 2006; Rudzok et al., 2011; Tuschl and Schwab, 2004). In addition, the results obtained from HepG2 cells are more predictive than that from other human cancer cell line, such as HeLa, ECC-1 and CHO-k1 cells (Schoonen et

al., 2005a; Schoonen et al., 2005b). Both phase I and II metabolizing enzymes have been found in HepG2 cells and the activities of CYP1A2, CYP2C9, CYP2D6, CYP2E1 and CYP3A are proved to be present at levels similar to that in human hepatocytes (Hewitt and Hewitt, 2004). Actually, HepG2 cells have been used in the study of the hepatocytotoxicity induced by the drugs which only produce toxicity after metabolic activation, for example, acetaminophen and even PA-containing herb (Neuman et al., 2007; Roe et al., 1993). In the present study, a HepG2 cell model was used to elicit the cytotoxicity of PAs and to investigate whether it was applicable for the assessment of PA intoxication.

In cell culture system, it is most unlikely that any single test is able to mimic the complexity of a living body; a series of complementary assays should therefore be developed. In the present study, four assays measuring different endpoints were used: 3-(4,5-Dimethylthiazol-2-yl)-2,5-diphenyltetrazolium bromide (MTT) evaluates cell viability or cell number by evaluating the activity of mitochondrial dehydrogenases, alkaline transaminase (ALT) and lactate dehydrogenase (LDH) evaluate cell death by evaluating ALT and LDH leakage respectively through destructive cell membrane, glutathione (GSH) investigates a possible GSH depletion involved upon PA intoxication in liver cells. These four assays were selected because they are classic biochemical parameters for assessing hepatotoxicity and examining different mechanisms.

In addition, the toxic effects of PA are due to the metabolic activation of PA mediated by mainly CYP3A4 to form pyrroles in the liver. These pyrroles are detoxified by forming conjugation with GSH. Thus a high rate of pyrrole production induced by CYP3A4 induction and a low rate of GSH conjugation by GSH reduction are supposed to be able to enhance the cytotoxicity of PAs. In this study, GSH

reduction and CYP3A4 induction were thus used to improve the sensitivity of the cell model.

2.1.2 Materials and Methods

2.1.2.1 Materials

HepG2 cells were acquired from the American Type Culture Collection (Rockville, MD, USA). Dulbecco's modified Eagle's medium (DMEM) and fetal bovine serum (FBS) were obtained from Gibco Corporation (Grand Island, NY, USA). Penicillin G, streptomycin, dimethylsulfoxide (DMSO), MTT, DL-alanine, α-ketoglutaric acid, 2, 4-dimitrophenylhydrazine (DNP), 4-(2-hydroxyethyl)-1-piperazineethanesulfonic acid (HEPES), sodium pyruvate, GSH, 5, 5-dithio-bis-2-nitrobenzonic acid (DTNB), monocrotaline, retrorsine, cisplatin, rifampin and buthionine sulfoximine (BSO) were purchased from Sigma-Aldrich Corporation (St. Louis, MO, USA). LDH assay kit was purchased from Roche Applied Science (Catalog No, 04744926001, Roche Diagnostics Ltd, H.K). All other drugs and chemicals were acquired from Sigma-Aldrich unless stated otherwise, and were of analytical grade and commercially available.

2.1.2.2 Cell Culture

HepG2 cells (passages 10–25) were cultured in DMEM, supplemented with 10% heat-inactivated FBS, 2.2 g/L sodium bicarbonate, 0.1 g/L streptomycin sulfate, 0.06 g/L penicillin G and 5.958 g/L HEPES. The cells were maintained in a standard cell culture incubator at 37°C in a humidified atmosphere with 5% CO_2. Cells were washed twice in phosphate buffered saline (PBS) before incubation with trypsin-EDTA (5 ml) for 3 min. The detached cells were suspended in supplemented DMEM. Cell counts were determined by hemocytometry for the addition of cells to

96-well plates at a density of 5000 cells/well. The cells were incubated overnight in the CO_2 incubator to ensure the attachment of the cells to the bottom of the plate before drug treatment.

2.1.2.3 Cell Morphology

To make sure that the cultured HepG2 cells were healthy prior to use, the cells were observed and taken images under the microscope equipped with a digital camera (Nikon DS-5Mc) prior to PA treatment.

2.1.2.4 PA Treatment

Two retronecine-type PAs, monocrotaline and retrorsine, were initially dissolved in DMSO and further diluted with culture medium to final concentrations (0.015, 0.03, 0.14 and 0.28 mM or 0.125, 0.25, 0.5, 1, 2 and 4 mM). Cisplatin, a common used anti-cancer drug, was used as a positive control to make sure that the cell model and cytotoxicity assay worked well. Cells in 96-well plate were incubated for 24 h with different concentrations of two PAs prior to cytotoxicity assay.

2.1.2.5 MTT Assay

After compound incubation, medium was aspirated from the plates and 100 μl MTT solutions (0.5 mg MTT/ml in PBS) were added to each well. Cells were incubated for another 3 h at 37°C in a humidified 5% CO_2/95% air atmosphere to allow MTT oxidation by mitochondrial dehydrogenase in the viable cells. Then the MTT solution was aspirated and 200 μl DMSO was added to dissolve the resultant blue formazan crystals. Plates were shaken vigorously for 30 min. The absorbance was measured at 570 nm with 620 nm as reference wavelength using a Bio-rad Benchmark Plus Microplate Reader Spectrophotometer (Bio-rad Laboratories, Inc.,

Hercules, CA, USA). DMSO was used as a blank control. Cell viability was calculated as the percentage of vehicle control.

2.1.2.6 ALT Assay

ALT activity in medium or cells was measured by standard spectrophotometric method (Reitman and Frankel, 1957). The samples for generating standard curve for ALT activity were prepared according to Table 2.1. For ALT assay, 100 µl of freshly collected cell medium or supernatants of cell lysate were added to 0.5 ml ALT substrate solution and left in a water bath at 37°C for 30 min. Then 0.5 ml of 1 mM DNP color reagent was added to the reaction system and incubated for 20 min. Then 5 ml of 0.4 M sodium hydroxide (NaOH) solution was added to stop the reaction. The absorbency of the mixture was detected at 505 nm and was used to calculated the ALT activity of each sample based on the standard curve (R^2 = 0.9666).

Table 2.1 Sample preparation for ALT activity standard curve

ALT substrate solution (µl)	0.1 M PBS (µl)	1.5 mM standard pyruvate solution (µl)	ALT activity (SF unit/ml)
400	200	0	0
400	150	50	23
400	100	100	50
400	50	150	83
400	0	200	125

ALT substrate sulution: the mixture of 0.2 M L-alanine and 1.8 mM α-ketoglutaric acid.

2.1.2.7 LDH Assay

The release of cytoplasmic LDH into extracellular environment only occurs in dead cells (for example, liver parenchyma cells) or cells that have lost their membrane integrity such as hemolysis and thus indicates cell damage (Abraham,

2006). LDH activity can be determined by a coupled enzymatic reaction: LDH oxidizes lactate to pyruvate which then reacts with tetrazolium salt INT (2-[4-iodophenyl]-3-[4-nitropheny-1]-5-phenyltetrazolium chloride) to form formazan. The increase in the amount of formazan produced directly correlates to the increase in the LDH activity (Abraham, 2006). The assay was performed according to the protocol of the commercially available kit. Briefly, 100 µl of the reaction mixture (provided in the kit) was added to 50 µl freshly collected culture medium and incubated for 30 min at room temperature. The absorbance of the solution was measured at 490 nm, with background subtraction at 620 nm. The LDH activity in the medium was expressed as a percentage of the total activity (activity in the medium plus activity in cell lysates). The percentage of LDH activity in the medium of untreated HepG2 cells (vehicle control) was then subtracted from the percentage of LDH activity in the medium of all treatment groups. The resulting value was defined as the percent LDH release.

2.1.2.8 GSH Assay

The toxic metabolites of PA, pyrroles, conjugate with cellular GSH to form the non-toxic GSH conjugate. Thus, cellular GSH level is vital for the detoxification of PA and can influence the cytotoxicity of PA. Intracellular GSH content was measured following the method as previously reported (Tietze, 1969; Wang et al., 2006) and protein content in the cell lysates was measured by the method of Lowry et al (1951). Briefly, 6×10^5 cells were seeded on each well of six-well culture plates and incubated overnight before PA treatment. At the end of the designated treatment, cells were washed with PBS, harvested and lysed by three cycles of freezing and thawing in 10 mM HCl. The cell lysates were centrifuged at 10,000 g for 15 min in a Sigma 2K15 laboratorium centrifuge with temperature being controlled at 4 °C and

clear supernatant was obtained. The samples for constructing standard curve for GSH concentration were prepared according to Table 2.2. Then 48 μl supernatant was mixed with 15 μl of 1.5 mg/ml DTNB and 237 μl of 0.1 M phosphate buffer. The tube was shaken and left at room temperature for 20 min and then measured at 412 nm. The GSH concentration of each sample was calculated according to the standard curve ($R^2 = 0.9949$) and GSH level in drug treatment groups was expressed as a percentage of the vehicle control.

Table 2.2 Sample preparation for GSH concentration standard curve

20 μM GSH (μl)	DTNB solution (μl)	0.1 M PBS (μl)	GSH concentration (μM)
0	15	285	0
6	15	279	0.4
12	15	273	0.8
24	15	261	1.6
48	15	237	3.2
96	15	189	6.4

2.1.2.9 GSH Reduction

GSH reduction was hypothesized to be able to enhance the cytotoxicity of PAs through reducing the rate of toxic pyrroles conjugating to GSH. BSO, a chemical that inhibits the biosynthesis of GSH, switches the total GSH pool towards its oxidized form GSSG (Khamaisi et al., 2000), and was applied here to potentiate the cytotoxicity of PA. To reduce GSH, the cells were incubated with 4 mM BSO for 3 h prior to PA incubation. Then MTT and GSH assays were performed to assess the cell viability and GSH reduction, respectively.

2.1.2.10 CYP3A4 Induction

The hepatotoxicity of PAs is from the toxic metabolites mainly produced by CYP3A4 (Mattocks, 1968). Accordingly, induction of CYP3A4 should be able to increase the cytotoxicity of PAs by enhancing the rate of pyrroles formation. Numerous examples have proved that the induction of CYP3A4 could lead to an increased production of toxic metabolites of some chemicals (Fuhr, 2000; Li and Jurima-Romet, 1997). The methods of CYP3A4 induction used in primary hepatocyte cultures have been described previously (Guillouzo et al., 1993; LeCluyse, 2001; Venkatakrishnan et al., 2001a; Venkatakrishnan et al., 2001b). Similarly, this method was developed in the present HepG2 cell model. To achieve this, HepG2 cells were incubated with 50 μM rifampin, a drug with known CYP3A4-inducing activity (Matsuda et al., 2002), for 24 h prior to PA incubation.

2.1.2.11 Combination of GSH Reduction and CYP3A4 Induction

A high CYP3A4 activity in combination with the low rate of GSH conjugation were supposed to be able to bring about more toxic pyrroles from PAs and maintain them in the liver. Thus, the combinational pre-incubation with 4 mM BSO and 50 μM rifampin for 3 h prior to PA treatment was used to promote the cytotoxicity of PA through simultaneously increasing the formation of toxic metabolite and reducing the detoxified conjugation.

2.1.2.12 Statistical Analysis

All data are represented as mean values ± SD and the mean values were obtained from 9 data points from triplicate wells in triplicate cultures unless otherwise stated. For the comparison of different treatments in two or more than two groups, the data were analyzed by student's *t*-test or one-way analysis of variance (ANOVA)

followed by Bonferroni's multiple comparison post hoc test using GraphPad Prism 5.0, respectively. Differences were considered statistically significant at $P < 0.05$.

2.1.3 Results and Discussion

2.1.3.1 Cell Morphology

Prior to PA treatment, HepG2 cells were observed and their photomicrographs are shown in Fig.2.1. The culture of HepG2 cells were about 90% confluent (Fig.2.1A) and healthy with a spindle shaped morphology and granular cytoplasm (Fig.2.1B), indicating that the cells were suitable for further cytotoxicity study.
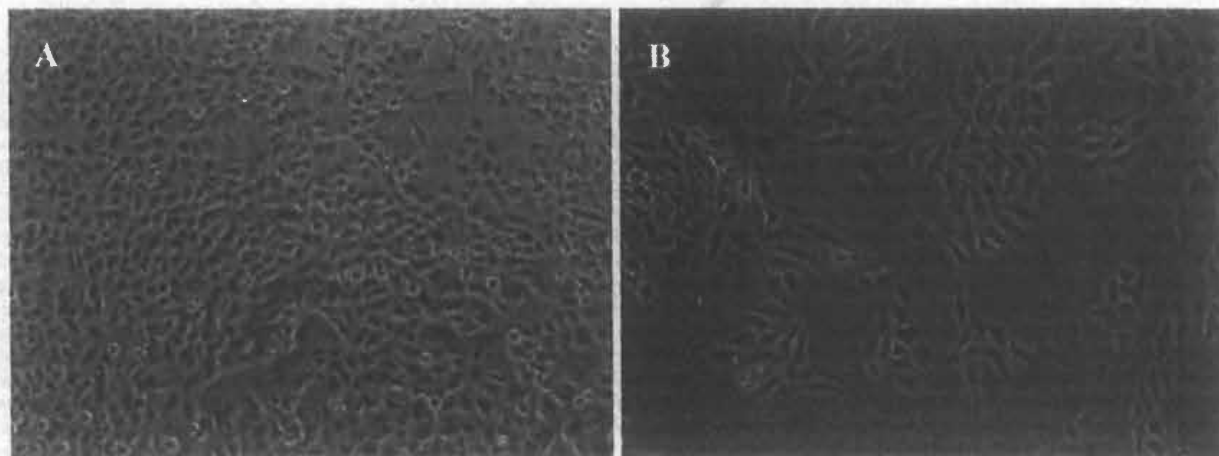
Fig.2.1. Photomicrographs of HepG2 cells under low (A: 100×) and high (B: 200×) magnification.

2.1.3.2 Effect of PAs on Cell Viability

As shown in Fig 2.2A, a relative low concentration range of PAs (0.015, 0.03, 0.14 and 0.28 mM) did not exhibit cytotoxic effects on HepG2 cells. Then a higher concentration range (0.25, 0.5, 1.0, 2.0 and 4.0 mM) was used to induce a detectable cytotoxicity. Cisplatin (16 µM), an anti-cancer drug with known toxic effects on HepG 2 cells (Schoonen et al, 2005), was used as the positive control. As shown in

Fig.2.2B, 16 µM cisplatin exhibited about 40% reduction of cell viability ($P < 0.01$ comparing with vehicle control), suggesting that the cell model and MTT assay work well for detecting its cytotoxicity. However, the degree of this cytotoxicity was lower than that demonstrated in a previous study (over 50% reduction) (Schoonen et al., 2005a; Schoonen et al., 2005b). As the cellular sensitivity to cisplatin-induced cell death could be determined by the mitochondrial and corresponding cell density (Qian et al., 2005), an optimal cell density was presumed to be able to induce a greater cytotoxicity of cisplatin. Accordingly, in several high concentrations of two PAs tested, only 1 mM retrorsine and 4 mM monocrotaline exhibited significant cytotoxicity. An about 25% decrease of cell viability induced by 1 mM retrorsine found in the present model is comparable to the toxic effect of monocrotaline, another retronecine-type PA, on primarily cultured hepatic SECs and hepatocytes reported previously (DeLeve et al., 1996). Based on the assumption regarding cisplatin, the toxicity degree of these two PAs may also be enhanced by exhibiting on an optimal cell density. As loss of cell viability is the late event of cytotoxicity, some early stage of pathogenesis of hepatotoxicity might be regulated by PA exposure. Thus, three conventional biochemical parameters, ALT, LDH and GSH assays, were performed to determine PA-induced cytotoxicity.
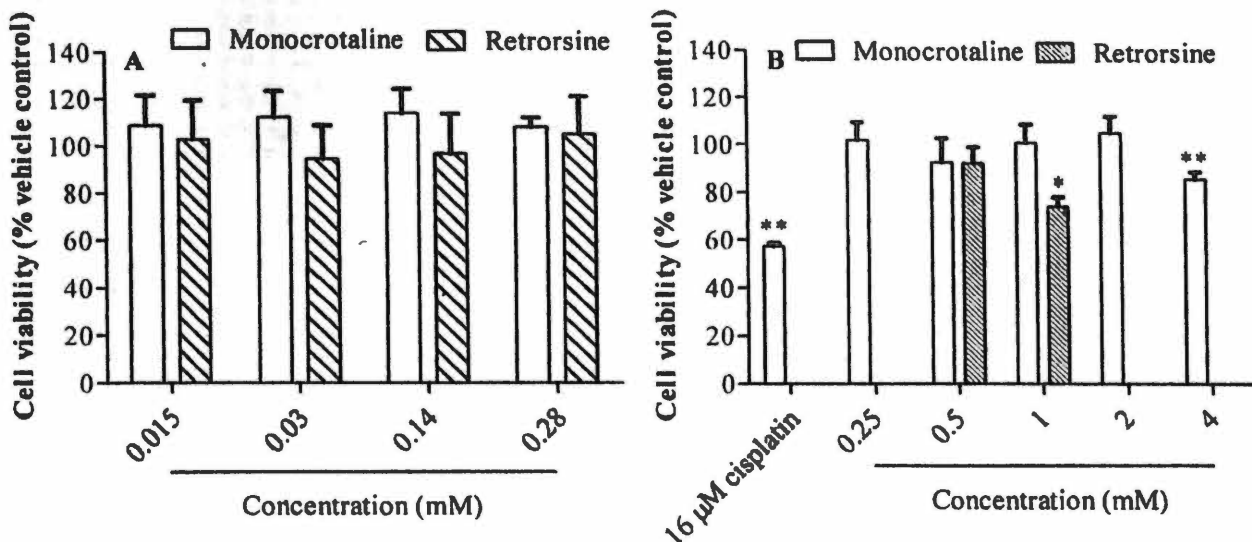
Fig.2.2. Effects of PAs at the low (A) and high (B) concentration range on cell viability. *$P < 0.05$ and **$P < 0.01$ comparing with vehicle control.

2.1.3.3 Effect of PAs on ALT Release and Cellular ALT Activity

ALT concentrations in the medium and cells were measured to assess the plasma membrane integrity and biosynthetic capacity of cells respectively. As shown in Fig.2.3A, the measured ALT activities in the collected medium were low with a large variation. Two PAs at the tested concentrations (0.0625, 0.125, 0.25, 0.5 and 1 mM) elicited slight elevation on it, indicating that some ALT was released from the injured cells. However, the elevating effects of all tested concentrations of PAs were insignificant, suggesting no obvious cell death occurred after PA exposure. Similarly, cellular ALT activity was not significantly regulated by any concentrations of PA exposure (Fig.2.3B), which on one hand, suggested that no obvious increase of biosynthetic ALT occurred, on the other hand, confirmed the default effect of PA on inducing ALT release. These results indicated that that the losses of cell viability induced by 1 mM retrorsien were not caused by direct cytotoxicity to the cells, but may be by inhibiting cell proliferation.
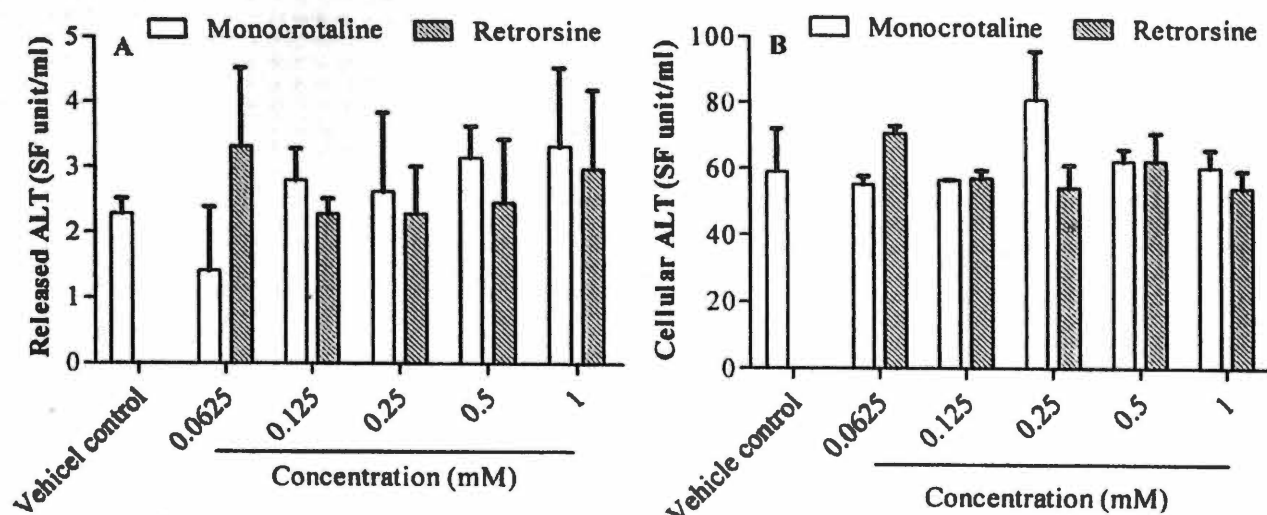
Fig.2.3. Effects of PAs on (A) ALT release and (B) cellular ALT activity.

2.1.3.4 Effect of PAs on LDH Release

Like ALT assay, LDH release into medium was also used as a measurement of cell death by determining whether cell destruction occurred after PA treatment. As shown in Fig.2.4, two PAs at the concentration of 0.5 and 1 mM did not induce a significant increase of LDH release. This result was in agreement with that obtained from above ALT assay, which confirmed that not direct destruction of cell structure contributed to the loss of cell viability after the tested PA exposure.
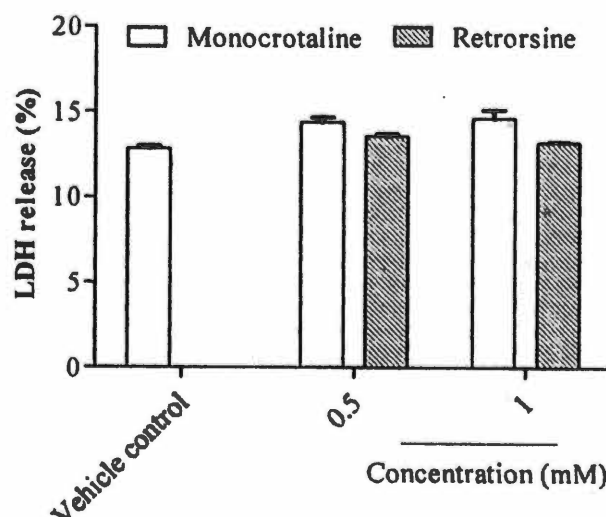
Fig.2.4. Effects of PAs on LDH release. Data are represented as mean values ± SEM ($n = 3$). **$P < 0.01$ comparing with vehicle control.

2.1.3.5 Effect of PAs on Cellular GSH Concentration

The toxicity of PA is due to the hepatic formation of a toxic pyrrole that is detoxified by conjugation with GSH (Yan and Huxtable, 1994). A previous study has established a correlation between hepatic GSH concentration and bile GSDHP formation, a compound with much lower toxicity, in the isolated perfused liver, indicating that the level of hepatic GSH influences PA metabolism and its toxicity (Yan and Huxtable, 1995a). In addition, exposure to PAs leading to an increase in hepatic GSH concentration has been proved to be via the stimulation of overall GSH synthesis (Yan and Huxtable, 1995b). Thus, the GSH level should be changed upon PA exposure in the present study. Total GSH level of cells is determined by cellular GSH concentration and cell number. Thus in order to investigate whether GSH depletion occurred in retrorsine-treated cells, both total GSH level as well as cellular GSH concentration were assessed.

As shown in Fig.2.5, no significant decreases in these two kinds of GSH level were detected after two PAs treatments, suggesting that these two PAs at the concentrations tested did not induce GSH depletion. This result obtained from the HepG2 cells was not in agreement with the that obtained from perfused liver as previously reported (Yan and Huxtable, 1995a), which may be caused by a lower metabolism capacity of the cells than that of perfused liver to produce enough toxic pyrroles to elicit GSH depletion.
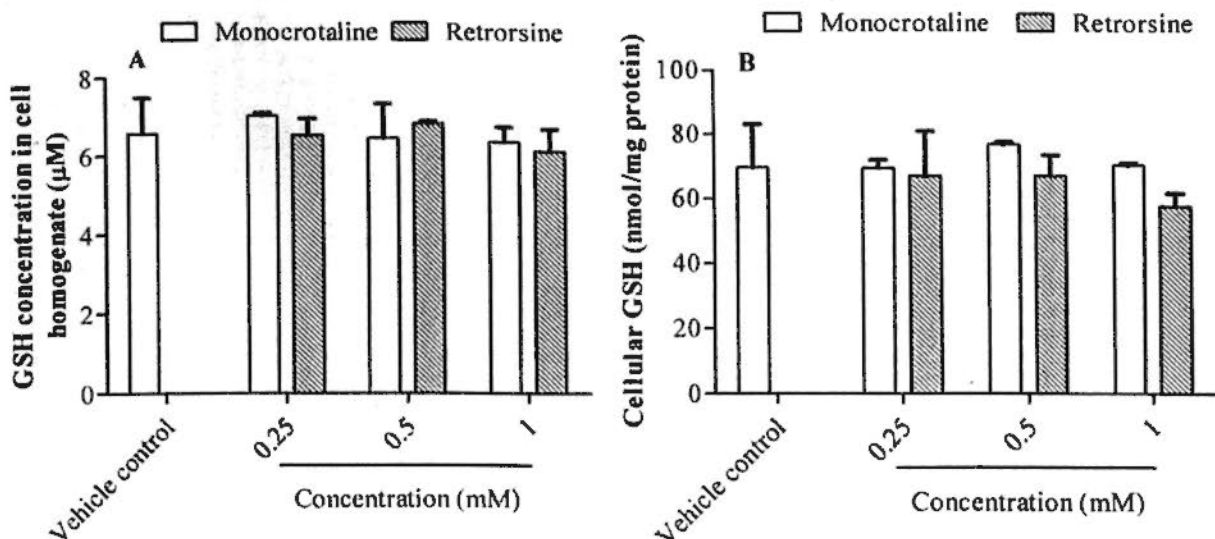
Fig.2.5. Effects of PAs on (A) total GSH level in cell and (B) cellular GSH.

2.1.3.6 Effect of GSH Reduction on the Cytotoxicity of PAs

GSH depletion should be able to potentiate the cytotoxicity of PAs by reducing the detoxification of toxic pyrroles of PAs (Yan and Huxtable, 1994). Several previous studies have proved that depletion of cellular GSH with BSO makes cells more sensitive to some toxic chemicals (Gomez-Quiroz et al., 2008; Hristova et al., 2007). In addition, the effects of GSH depletion on the cytotoxicty of PAs have been proved in two *in vitro* models (Chen et al., 2008; DeLeve et al., 1996). Thus, a same condition, 24 h of 4 mM BSO pre-incubation, was used to induce GSH depletion in the present HepG2 cell model.

As shown in Fig.2.6A, without BSO pre-incubation, only 1 mM retrorsine exhibited a significantly cytotoxic effect on HepG2 cells with a significant decrease of cell viability. After pretreatment with BSO, the cytotoxic effects of two PAs at tested concentrations were all augmented with a significant decrease of cell viability ($P < 0.05$ comparing with the corresponding vehicle control). However, the extent of the decreased cell viability induced by BSO pre-incubation was similar in both PA treated and vehicle control, indicating that the enhanced cytotoxicity of PAs by BSO

pre-incubation was due to the toxic effect of BSO itself. This phenomenon was also observed in a previous study for the investigation of whether GSH depletion induced by BSO could augment the cytotoxicity of PAs on L-02 cells (Ji et al., 2008).

The effect of BSO on GSH reduction was confirmed by GSH assay showing a 20% decrease of cellular GSH concentration (Fig.2.6B). This result was comparable to that of cell viability reduced by BSO incubation, suggesting that cellular GSH is important for maintaining the life of cell. However, when compared to a previous study also performed on HepG2 cells (Wang et al, 2006), the degree of GSH reduction elicited by BSO in our study was insufficient. In that study, a 12 h of 100 μM BSO incubation reduced cellular GSH concentration to less than 40% of control without toxic effect on cell viability (Ji et al, 2008). Moreover, to elicit a GSH depletion effect on different cell types, the concentrations of BSO used are found to be largely different (from 10 μM to 10 mM) (DeLeve et al, 1996; Khamaisi et al, 2000; Chen et al, 2009). These two findings suggest that the action of BSO should be determined by the cell status and is different among different cell types. Furthermore, as BSO is an irreversible inhibitor of intracellular GSH synthesis (Griffith, 1999), an inherent low GSH synthesis rate of the cells may also hamper BSO to exert its depleting effect on GSH. The concentration of BSO used and its toxic effect on the present HepG2 cells are comparable to those reported in a previous study performing on primary hepatocyte cultures, confirming that BSO itself was toxic to cells (DeLeve et al, 1999). Therefore, a higher concentration of BSO could not be used for further study to induce a greater GSH reduction.
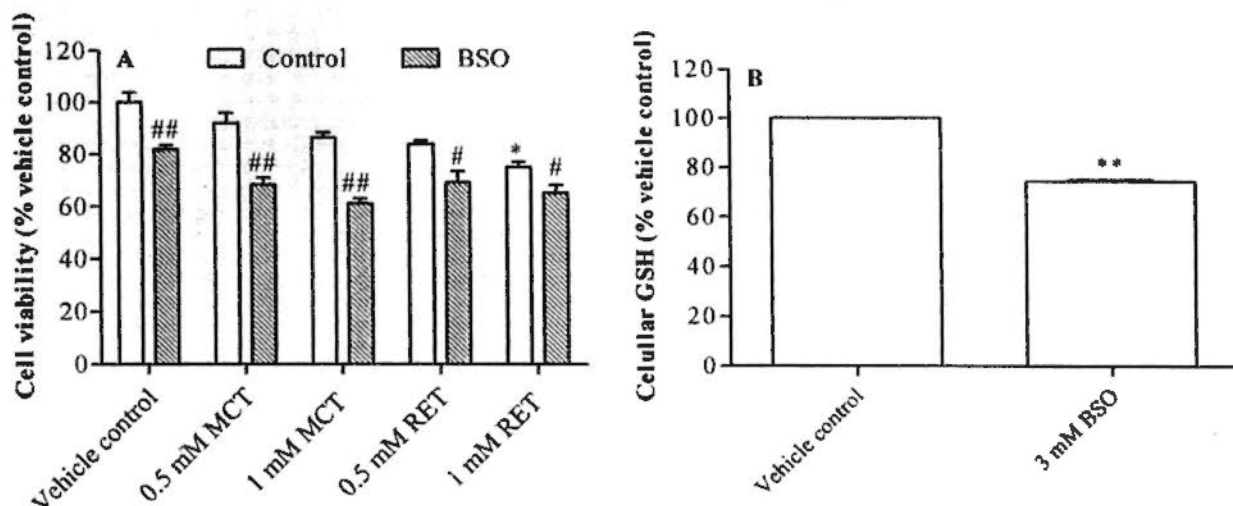
Fig.2.6. Effects of GSH reduction on cytotoxicity of PAs. A: Cytotoxicity of PAs in HepG2 cells pretreated with BSO for 3 h. B: Decrease in cellular GSH concentration in HepG2 cells pretreated with BSO for 3 h. Data are represented as mean values ± SEM ($n = 2$). *$P < 0.05$ and **$P < 0.01$ comparing with vehicle control; [#]$P < 0.05$ and [##]$P < 0.01$ comparing with the corresponding control. MCT: monocrotaline; RET: retrorsine.

2.1.3.7 Effect of CYP3A4 Induction on the Cytotoxicity of PAs

Rifampin incubation was used to potentiate the cytotoxicity of PAs by enhancing the formation of toxic metabolite of PAs through induction of CYP3A4. As shown in Fig.2.7, the cytotoxicity of 0.5 mM monocrotaline was increased by rifampin incubation evidenced by the significant decrease of cell viability ($P < 0.05$ comparing to corresponding control). However, in the corresponding vehicle control, cell viability was decreased in a similar degree by the only rifampin incubation when compared with that by the incubation with rafampin plus monocrotaline, indicating that rafampin itself was toxic to the cells.

One possible reason for the deficiency of a potentiating effect of CYP3A4 induction was that the levels of metabolic enzymes in the cells were low, and thus, the induction effect might be not adequate. Another explanation was that the weight

of contribution of different metabolism enzyme in the metabolism of different PAs. As discussed previously, in addition to CYP3A4, CYP2E is also responsible for the metabolism of PA. Thus, induction of only CYP3A4 may be not enough to produce enough toxic metabolite to exert a higher toxicity. Of course, with regard to the endpoint measurements, evaluation of a combination of changes in CYP3A4 mRNA and protein levels and enzyme activity will provide more useful information for interpretation of the present results (Rodriguez et al., 2001; Perez et al., 2003). Thus a further study on investigating whether CYP3A4 was successfully induced was recommended by measuring the protein express of CYP3A4 and its activity.
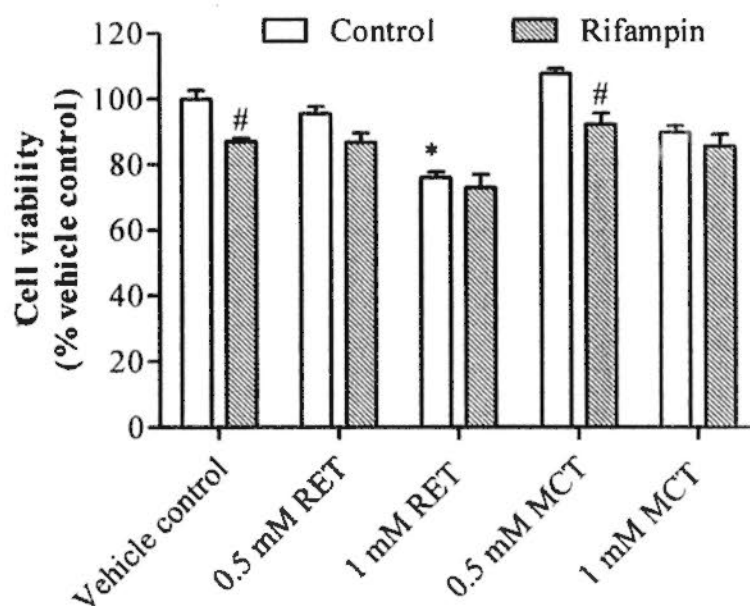
Fig.2.7. Effects of rifampin on cytotoxicity of PAs. Data are represented as mean values ± SEM ($n = 3$). *$P < 0.05$ and **$P < 0.01$ comparing with vehicle control; [#]$P < 0.05$ comparing with the corresponding control. MCT: monocrotaline; RET: retrorsine.

2.1.3.8 Effect of Combination of GSH Reduction and CYP3A4 Induction on Cytotoxicity of PAs

The combinational use of GSH reduction plus CYP3A4 induction should enhance the toxic response of PA by simultaneously reducing the detoxification and enhancing the formation of toxic metabolite. This combinational approach may allow the increased toxic pyrroles to directly act on cells with depleted GSH level. As shown in Fig.2.8, the cytotoxicity of two PAs at concentrations tested was not augmented by this combinational incubation. A possibility is due to the failure of either GSH reduction or CYP3A4 induction as demonstrated earlier or both. The other possible reason is that even the toxic metabolite was successfully increased by CYP3A4 induction (not proved yet) accompanied with 20% GSH reduction, whereas HepG2 cells might not sensitive enough to display the toxic effect of PA as hepatic SECs should be the specific target cell of PAs.
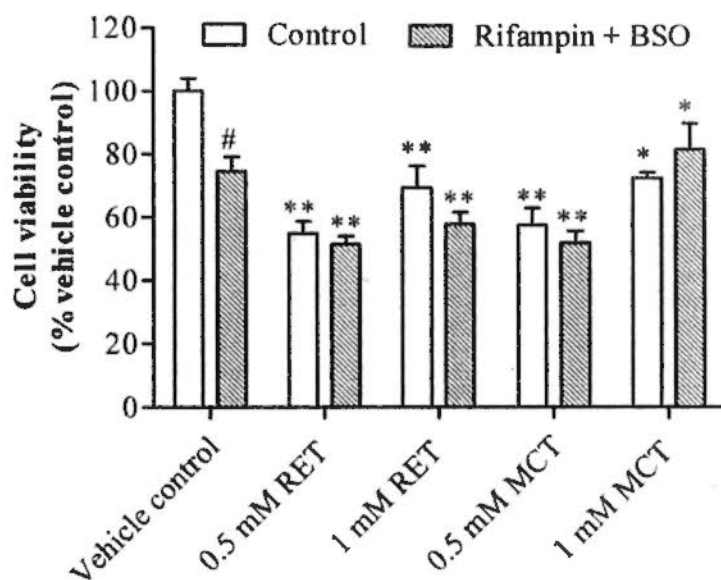
Fig.2.8. Effects of the combinational pre-incubation of BSO and rifampin on cytotoxicity of PAs. Data are represented as mean values $\pm$ SEM ($n = 3$). $*P < 0.05$ and $**P < 0.01$ comparing with vehicle control; $^{\#}P < 0.05$ comparing with the corresponding control. MCT: monocrotaline; RET: retrorsine.

2.1.4 Summary

The comparable toxic potency of PA on the present HepG2 cell model and on previously reported primary cultures of liver cells (DeLeve et al, 1996) suggests that these two types of cell models have similar sensitivity in detection of PA-induced cytotoxicity. Thus, it is suitable to use HepG2 cells for the development of an *in vitro* model for the screening of PAs-induced cytotoxicity. However, the sensitivity of this model is not idea for screening the cytotoxicity of more PAs when the concentration is lower than 1 mM. In addition, three conventional hepatotoxicity assays, ALT, LDH and GSH assays failed to present a greater cytotoxicity of PA than MTT assay, which imply that the decrease of cell viability should not come from the destruction of cells as measured by above three assays.

In order to increase the sensitivity of the model, two approaches, GSH reduction and CYP3A4 induction were used to enhance the cytotoxicity of PA. However, both each and the combinational usage of two approaches are found unsuccessful in potentiating the cytotoxicity of PAs, which may be due to the insufficiency of GSH reduction and metabolizing enzyme induction. However, the drugs for eliciting GSH reduction or CYP3A4 induction used at the present concentration had a toxic effect on HepG2 cells, which indicates that a higher concentration of drugs for inducing a greater degree of GSH reduction or CYP3A4 induction are not appropriate in the present HepG2 cell model.

In addition, as discussed earlier, hepatic SECs are the toxic target cells of PA intoxication. The toxic metabolite was successfully increased by CYP3A4 induction and HepG2 cells may not display the toxic effect of PAs due to its insensitivity to PA intoxication. Therefore, a culture of hepatic SECs, the supposed initial toxic target of PAs, should be investigated for its application and sensitivity in the assessment of PA-induced cytotoxicity.

2.2 Co-Culture Model

2.2.1 Introduction

In previous part of the study, a simple HepG2 cell model using three conventional hepatotoxicity assays was proved to be not ideal for screening the cytotoxicity of PAs. Moreover, two approaches aiming to enhance the sensitivity of the model by potentiating the cytotoxicity of PAs was found ineffective. The above findings urge us to find a more suitable cell model for further study.

As discussed in chapter 1, it is the sinusoidal, not venous endothelial cells (ECs) or parenchymal cells that are the toxic target of PAs (DeLeve et al, 1999; Chen et al, 2008). Thus, it is rational to assume that a cell model using SECs culture could elicit a greater cytotoxicity of PAs. Hepatic SECs are a morphologically distinct population of cells that form the lining of liver sinusoids (Perri and Shah, 2000). Features that distinguish hepatic SECs from ECs in other organs and in large vessels of liver are the presence of multiple fenestrae throughout the cells and the lack of an underlying basement membrane (Braet et al, 1995; Arii and Imamura M, 2000). The sinusoids are positioned between hepatocyte plates and initiate at the portal tract and terminate at the central vein (CV). Sinusoids carry blood that converges in the liver from the portal venous and the hepatic artery (Wake, 1997). The liver is exposed to numerous foreign antigens such as toxins that pass through the bowel mucosa and enter the portal circulation, thereby gaining access to the liver via the hepatic sinusoids (Lalor and Adams, 1999). Due to their position, SECs are the first cells in contact with blood flow into the sinusoids (Vidal-Vanaclocha, 1997; Shah, 2004), which means that they are also the first cells in contact with toxins included in blood circulation.

In addition, an *in vitro* model maintaining the cell-cell communication and biochemical cross-talk should be essential for an accurate prediction of the toxicity of a drug. As discussed in chapter 1, the hepatotoxicity of PAs *in vivo* is believed to involve two aspects: an initial damage to SECs and an ensuing injury to hepatocytes. Furthermore, the metabolic capacities of hepatocytes are supposed to be vital for the formation of toxic pyrroles of PA to exert their toxicity. However, current limitations of single-cell type culture hinder the progress in understanding the features and dynamics of heterotypic cell communication pathways critical to developing more sophisticated and effective alternative to an *in vivo* system (Yamato et al, 2002). In liver lobules, layers of hepatocytes and SECs are interconnected to form a continuous three-dimensional tissue lattice. Although cell-cell communication between SECs and hepatocyte *in vivo* seems to be essential for interpretation of PA-induced hepatotoxicity, efficient cell co-culture methods for mimicking such pathogenesis have not been developed (Harimoto et al, 2001).

In this part of study, the cell-cell communications between hepatocytes and SECs were achieved by patterning a co-culture of HepG2 cells and human hepatic sinusoid endothelial cells (HHSECs). Mechanism studies of PA-induced HSOS suggest that GSH disturbance is involved in the pathogenesis of EC injury (Yan et al, 1995a, b), thus GSH reduction was investigated for their action on potentiating the toxic effect of PAs on HHSECs.

2.2.2 Materials and Methods

2.2.2.1 Materials

Giemsa's staining solution and aacetaminophen (APAP) were purchased from Sigma-Aldrich. Clivorine (purity > 98%) was isolated from *Ligularia hodgsonii* in our laboratory using the previously established isolation method (Lin et al, 2000).

HHSECs (Catalog Number: 5000) from ScienCell Research Laboratories (CA, USA) are isolated from human liver and cryopreserved immediately after purification and delivered frozen. Each vial contains > 5×105 cells in 1 ml volume. HHSECs are characterized by immunofluorescent method with antibodies to vWF/Factor VIII and CD31 and guaranteed to further expand for 15 population doublings in the conditions provided by ScienCell Research Laboratories.

Endothelial cell medium (ECM, Catalog number: 1001) consisting of 500 ml of basal medium, 25 ml of FBS (Catalog number: 0025), 5 ml of endothelial cell growth supplement (ECGS, Catalog number: 1052) and 5 ml of penicillin/streptomycin solution (P/S, Catalog number: 0503) were purchased from ScienCell Research Laboratories and was protected from light and it is a medium designed for optimal growth of normal human microvascular ECs *in vitro*. Poly-L-Lysine (PLL, Catalog number: 0403), trypsin/EDTA solution (T/E solution, Catalog number: 0103), trypsin neutralization solution (TN solution, Catalog number: 0113), and Dulbecco's phosphate-buffered saline (DPBS, Catalog number: 0303) were also purchased from ScienCell Research Laboratories.

2.2.2.2 Cell Culture

2.2.2.2.1 HepG2 cells

The procedures are same as that described in section 2.1.2.2.

2.2.2.2.2 Human Hepatic Sinusoid Endothelial Cells (HHSECs)

To set up the culture, the bottom of a 5 ml flask was coated by the incubation of 10 µl PLL and 5 ml sterile distilled water in it at the incubator overnight. After the PLL solution was removed, the flask was rinsed twice with sterile water and 10 ml of ECM was then added into the flask prior to use. The vial with cryopreserved cells was placed and gently rotated in a 37°C waterbath until the contents were completely thawed. Then the vial was immediately removed from the waterbath and the cells were gently re-suspended and dispensed into the equilibrated, PLL-coated flask. The flask was gently shaken to make sure that the cells were evenly distributed and then put into the incubator. The culture was not disturbed for at least 16 h after the culture was initiated.

To maintain the culture, the growth medium was changed next day to remove the unattached cells and residual DMSO included in the cropreserved cells, then every other day thereafter. For subsequent subcultures, medium was changed 48 h after establishing the subculture. Thereafter the medium was changed every other day until the culture was approximately 50% confluent. Once the culture reached 50% confluence, the medium was changed every day until the culture was approximately 90% confluent.

The cells were sub-cultured when the culture was more than 90% confluent. A PLL-coated flask was prepared one day before subculture. The medium, TE solution, TN solution, and DPBS were warmed to room temperature prior to use. The cells were rinsed with DPBS and then incubate with 3 ml of TE solution until 80% of cells were rounded up (monitored with microscope, about 2-3 min). Three ml of TN solution were added to the digestion immediately and the flask was gently rocked. The released cells were harvested and transferred into a 15 ml centrifuge tube. The

flask was rinsed with another 3 ml of growth medium to collect the residue cells and was examined under microscope to make sure that less than 5% cells were left behind. The harvested cell suspension was centrifuged at 200 g for 5 min. Cells were then suspended in growth medium and were then counted and plated in a new PLL-coated flask.

2.2.2.2.3 Co-Culture of HepG2 cells and HHSECs

For co-culture, passage 10–20 of HepG2 cells and passage 2–10 of HHSECs were used. Briefly, 16000 dispensed HepG2 cells in 2.5 ml DMEM were seeded onto the lower bottom of a 6-well transwell plate. The inserts of the transwell plate were put in another 6-well plate and pre-coated with PLL overnight. Then 64000 dispensed HHSECs in 1.6 ml ECM were seeded in the PLL-coated inserts. After both cells were established, the inserts holding HHSECs were put into the 6-well transwell plate which held HepG2 cells prior to PA treatment. The medium used for the co-culture during the process of PA treatment was ECM.

2.2.2.3 Cell Morphology

The protocol is described in detail in section 2.1.2.3.

2.2.2.4 PA Treatment

Retrorsine were initially dissolved in DMSO. APAP was dissolved in saline and was used as a positive control since an overdose of APAP could also induce hepatotoxicity mediating by its toxic metabolites (Gibson et al., 1996) which are formed through CYP3A4-mediated hepatic metabolism (Cheng et al., 2009). Like PAs, the specific toxic target of APAP has also been proved to be the SECs (DeLeve et al., 1997). Retrorsine and APAP stock solutions were further diluted with culture medium to final concentrations. Cells in 6-well transwell plate (for co-culture) or in

96-well plate with 4000 cells/well (for separated culture) were incubated for 24 h with different concentrations of retrorsine or APAP before cytotoxicity assay.

2.2.2.5 MTT Assay

For 96-well plate, the procedure is same as that described in section 2.1.2.5. For six-well transewell plate, the inserts holding HHSECs were taken out from the stack of the transwell plate and put in another six-well plate. Then medium in the transwell was aspirated from the HepG2 cells it holding and 600 μl MTT solutions (0.5 mg MTT/ml in PBS) were added to each well for both the transwell and inserts. After 3 h of incubation, the MTT solution was removed and cell were observed and taken images under the digital camera-equipped light microscope, thereafter dissolved in DMSO for absorbance measurement.

2.2.2.6 Giemsa's Staining

After PA incubation, the cells were fixed with 10% formalin for 30 min and then rinsed twice with PBS. Giemsa's solution was added into cells. After 15 min staining, the Giemsa's solution was removed. The cells were observed and taken images under the digital camera-equipped light microscope.

2.2.2.7 Acridine Orange Staining

Acridine orange is a lysosomotropic agent emitting bright red fluorescence in acidic vesicles including lysosomes but fluoresced green in cytoplasm and nucleus (Paglin et al., 2001). It is commonly used to observe the formation of acidic vesicular organelles, suggesting macroautophagy (Klionsky et al., 2008). To investigate whether the medium affected the function of both type cells, the formation of acidic vesicular organelles in cells cultured with two kinds of mediums, DMEM and ECM was determined by acridine orange staining. To further investigate

the toxic effect of PAs on autophagy, acridine orange was added at a final concentration of 1 µg/ml for 15 min after 24 h of PA exposure. Images of the cells were obtained with a fluorescence microscope (Nikon TS100-F) equipped with a 50-W mercury lamp, a 450-490-nm band-pass blue excitation filters, a 505-nm dichroic mirror, a 520-nm long pass-barrier filter, and a digital camera (Nikon DS-5Mc).

2.2.2.8 GSH Depletion on Separately Cultured HHSECs

GSH depletion was supposed to potentiate the cytotoxicity of PA through reducing the available GSH for conjugating the toxic pyrroles. To induce enough GSH depletion and make sure that the cells were not severely damaged, 4 mM BSO was pre-incubated with cell for 24, 36, 48 and 72 h respectively prior to MTT and GSH assays. Then the incubation time was fixed and different concentrations of BSO were tried to find out an optimal concentration with minimal cytotoxicity. After that, a fixed incubation time and BSO concentration were determined and they were used to induce GSH depletion prior to 0.125-1 mM retrorsine treatment.

2.2.2.9 Statistical Analysis

The methods are same as that described in section 2.1.2.12.

2.2.3 Results and Discussion

2.2.3.1 Morphology of Cells Prior to Drug Treatment

As shown in Fig.2.9A, prior to co-culture with HepG2 cells for PA treatment, the culture of HHSECs was about 90% confluent. The cells were healthy with a spindle shaped morphology, long fiber and nongranular cytoplasm (Fig.2.9B), indicating the culture of HHSECs was ready for further study. The morphology of well established

HepG2 cells prior to co-culture and PA treatment was demonstrated as that described in section 2.1.3.1.
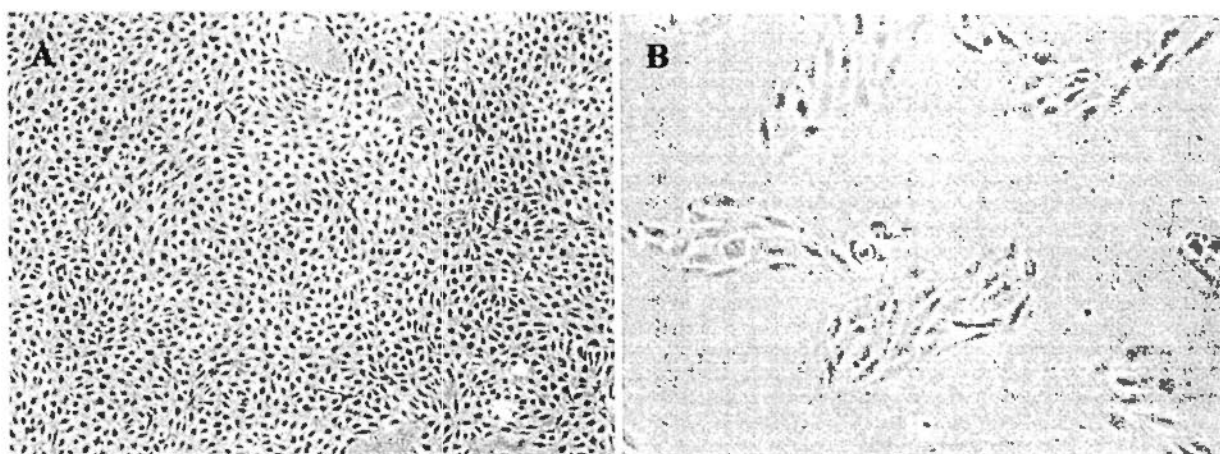
Fig.2.9. Photomicrographs of HHSECs under low (A: 100×) and high (B: 200×) magnification.

2.2.3.2 Cytotoxicity of Retrorsine on Co-cultured HepG2 cells and HHSECs

As shown in Table 2.3, the toxicities of 1 mM retrorsine and 10 mM APAP on HHSECs were obviously greater than that on HepG2 cells in the co-culture system. This result was confirmed by the morphology observation shown in Fig.2.10, in which retrorsine and APAP induced a greater decrease of cell number on HHSECs than on HepG2 cells. However, the morphology of co-cultured HepG2 cells was changed with the formation of some long threads as shown in Fig.2.10A.

Table 2.3 Effect of PA on cell viability of co-cultured HHSECs and HepG2 cells

Cell	Reduction of cell viability (%)		
	Vehicle control	1 mM RET	10 mM APAP
HHSEC	0	24.8	54.7
HepG2	0	14.1	24.8

RET: retrorsine. APAP: acetaminophen. $n = 2$.
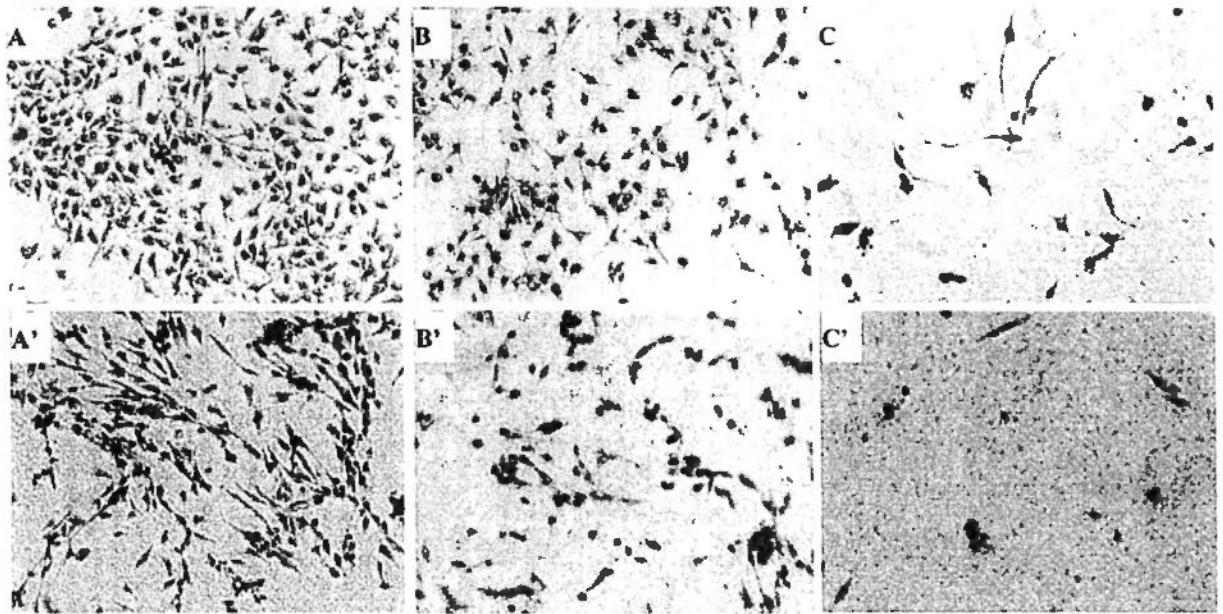
Fig.2.10. Toxic effects of retrorsine on co-cultured HepG2 cells (A-C) and HHSECs (A'-C') determined by MTT staining. A and A': Vehicle control. B and B': 1 mM retrorsine treatment and C and C': 10 mM acetaminophen treatment. (200 × magnification)

2.2.3.3 Morphology of Co-cultured HepG2 Cells and HHSECs

To confirm above observation obtained from MTT assay, co-cultured HepG2 cells and HHSECs were stained with Giemsa's solution and then observed under light microscope. As shown in Fig.2.11A, HepG2 cells exhibited a morphological change with long fiber formation. Furthermore, 1 mM retrorsine or 10 APAP elicited a decrease of cell numbers of both types of cells (Fig.2.11B and B' and Fig.2.11C and C'). The loss of cells induced by both compounds was more severe on HHSECs than that on HepG2 cells, which were in agreement with the results obtained from MTT assay.
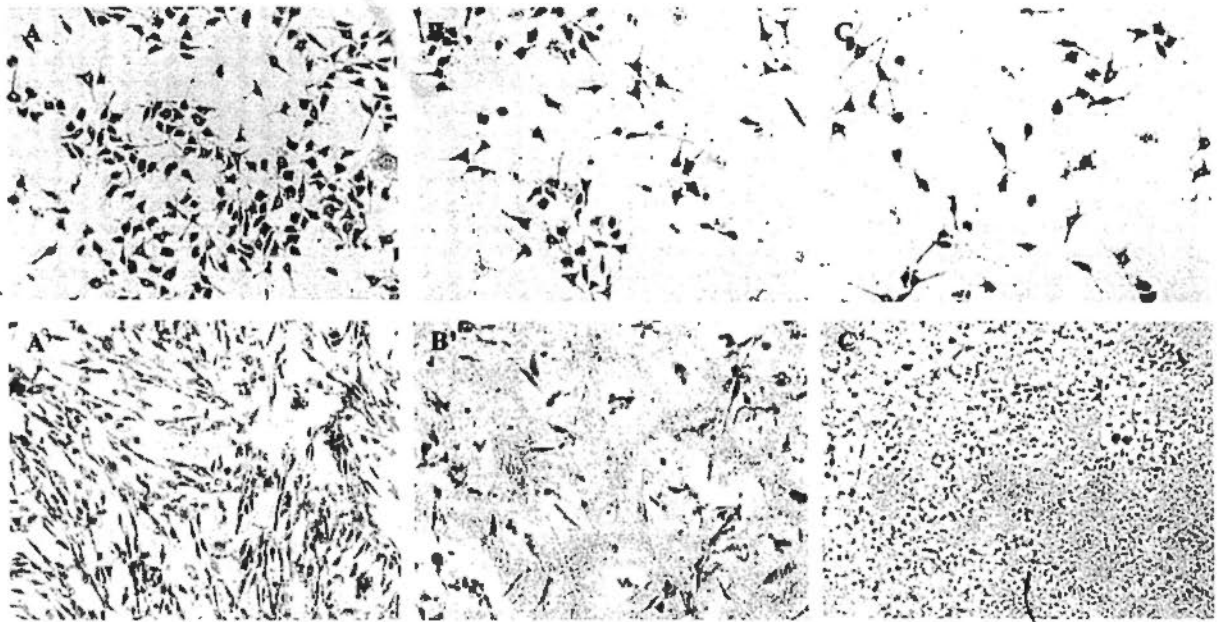
Fig.2.11. Toxic effects of retrorsine on co-cultured HepG2 cells (A-C) and HHSEC (A'-C') determined by Giemsa's staining. A and A': Vehicle control. B and B': 1 mM retrorsine and C and C': 10 mM acetaminophen treatment. (200 × magnification)

2.2.3.4 Autophagy of HepG2 Cells and HHSECs

The term *autophagy* (Greek, "to eat oneself") does not refer to a death process; it denotes an evolutionarily conserved catabolic process by which the cell degrades its cellular content through the lysosomal system. Autophagy is the major regulated mechanism of cell for degrading long-lived proteins and the only known pathway for degrading organelles. During autophagy, an isolated membrane forms, presumably arising from a vesicular compartment known as the preautophagosomal structure, invaginates, and sequesters cytoplasmic constituents including mitochondria, endoplasmic reticulum, and ribosomes. The edges of the membrane fuse to form a double or multimembranous structure, known as the autophagosome or autophagic vacuole. The outer membrane of the autophagosome fuses with the lysosome (in mammalian cells) to deliver the inner membranous vesicle to the lumen of the degradative compartment. Degradation of the sequestered material generates

nucleotides, amino acids, and free fatty acids that are recycled for macromolecular synthesis and ATP generation (Levine and Yuan, 2005). Autophagy occurs at low basal levels in all cells to perform homeostatic functions (e.g., cytoplasmic and organelle turnover) but is rapidly up-regulated when cells need to generate intracellular nutrients and energy (e.g., during starvation or trophic factor withdrawal), undergo architectural remodeling (e.g., during developmental transitions), or rid themselves of damaging cytoplasmic components (e.g., during oxidative stress, infection, and accumulation of protein aggregates). Nutritional status, hormonal factors, temperature, oxygen concentrations, and cell density are important factors in the control of autophagy (Levine and Yuan, 2005). Therefore, autophagy functions across a diverse range of species as a pro-survival pathway during nutrient deprivation and other forms of cellular stress. Paradoxically, in cells that cannot die by apoptosis and, more speculatively, in cells that cannot be removed by engulfment of cells, the autophagic machinery may also be used for self-destruction.

To determine whether the morphological change of HepG2 cells was induced by the medium used in co-culture system and explore the possible mechanism of PA intoxication, acridine orange staining was performed on HepG2 cells. When cells were cultured in ECM, the medium used for co-culture system, HepG2 cells showed morphological changes with long fiber formation as indicated in Fig.2.12A'. When HepG2 cells were separately cultured in DMEM, both 1 mM retrorsine and 10 mM APAP induced an obvious decrease of cell numbers as well as increase of autophagic vesicular organelles formation (Fig.2.12B and C), which was also observed in retrorsine treatment when cells were cultured in ECM (Fig.2.12B'). After 10 mM APAP treatment, cells were severely disrupted and no such increase of autophagy was observed. This result suggested that the damage induced by 1 mM retrorsine in

HepG2 cells was mainly through autophagy which leads the cells to rid themselves of damaged cytoplasmic components due to oxidative stress caused by retrorsine treatment.

Interestingly, when HHSECs were co-cultured in ECM together with HepG2 cells, they showed a normal morphology but with lots of autophagic vacuole formation as indicated in Fig.2.13C, implying that the function of HHSECs underwent changes which might be caused by cell communication with HepG2 cells. Then an alternative of culture medium, DMEM, was investigated for its effect on HHSECs culture. As indicated in Fig.2.13A'-C', the morphology of HHSECs was changed by DMEM with some loss of long fiber. However, different from that observed in HepG2 cells, except for resulting in a decrease of cell numbers, both 1 mM retrorsine and 10 mM APAP did not elicit an obvious increase of autophagic vacuole formation. This result indicated that the toxic mechanism of retrorsine on two cell types might be different.

The above results regarding the effects of two different culture mediums on the morphology and function of two cell types suggested that due to the medium incompatibility and possible cell communication, co-culture system using HepG2 cells and HHSECs was not recommended for further investigation.
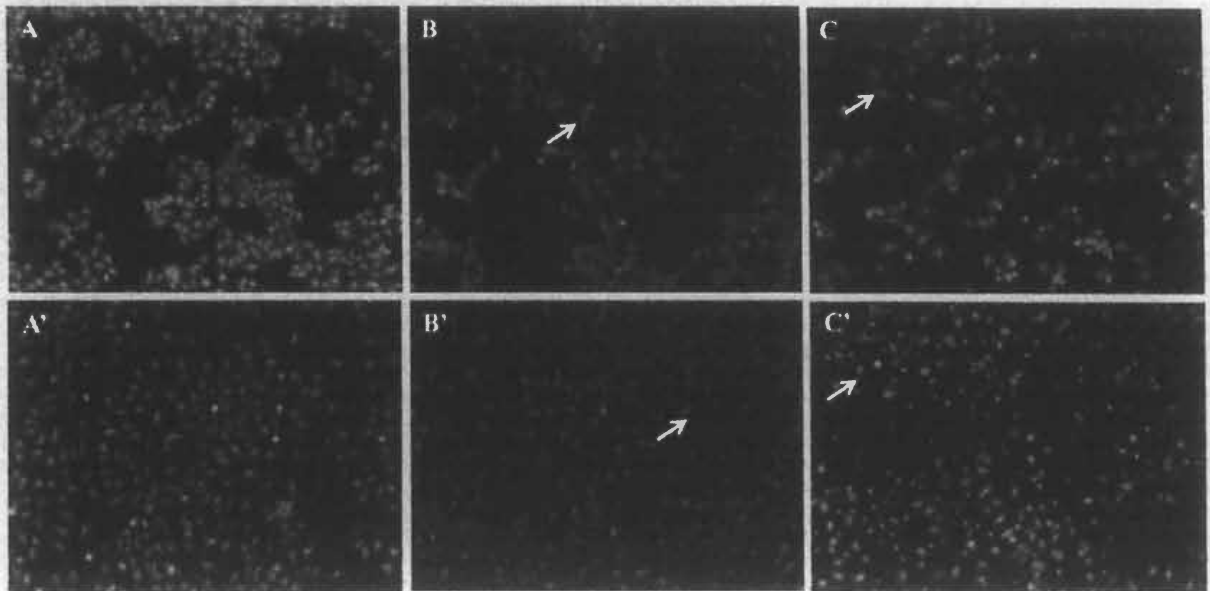
Fig.2.12. Toxic effects of retrorsine on HepG2 cells cultured in DMEM (A-C) or ECM (A'-C') determined by acridine orange staining. A and A': Vehicle control. B and B': 1 mM retrorsine. C and C': 10 mM acetaminophen treatment. (200 × magnification)
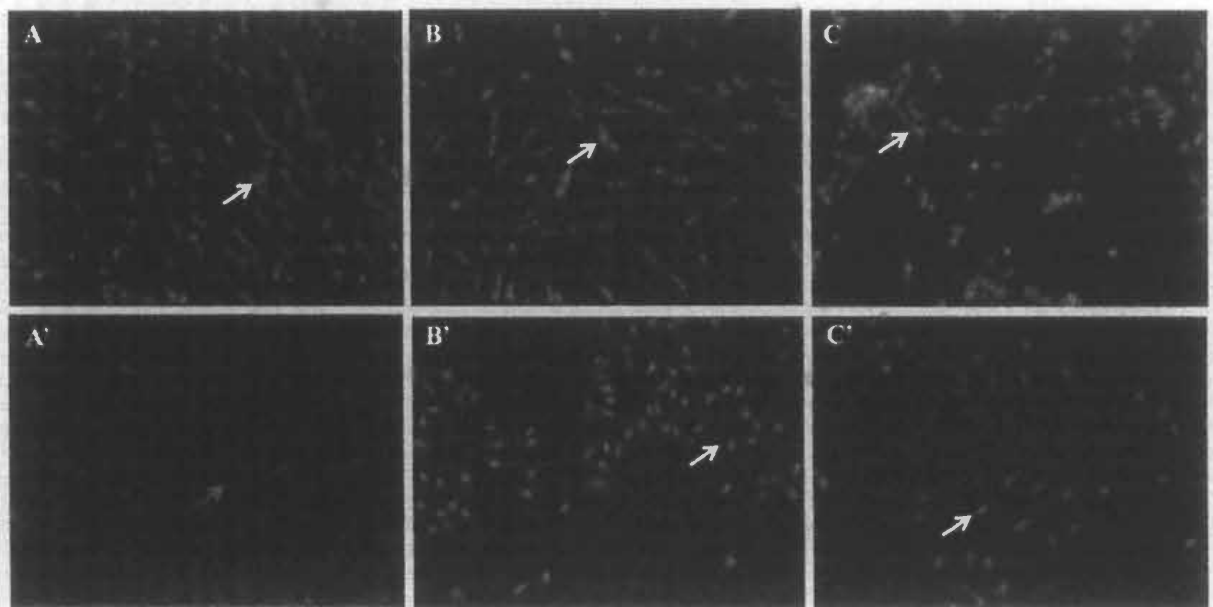
Fig.2.13.Toxic effects of retrorsine on co-cultured HHSEC in ECM (A-C) or separately cultured HHSEC in DMEM (A'-C') determined by acridine orange staining. A and A': Vehicle control. B and B': 1 mM retrorsine treatment. C and C': 10 mM acetaminophen treatment. (200 × magnification)

2.2.3.5 Cytotoxicity of Retrorsine on Separated Cultured HepG2 cells and HHSECs

The sensitivity of the two cell models, HepG2 cells and HHSECs, for the detection of PA cytotoxicity under separately cultured conditions was compared. As shown in Fig.2.14, the cytotoxicity of different concentrations of retrorsine was similar in both cells, indicating that these two cell models had similar sensitivity for the detection of PA cytotoxicity.
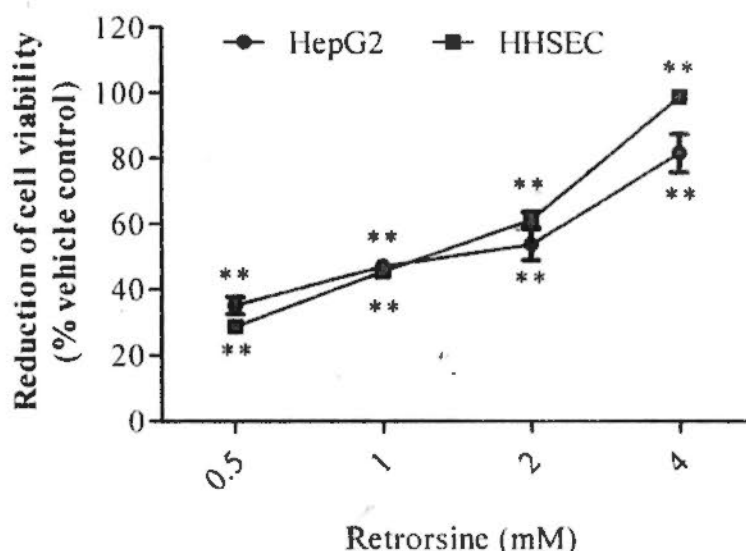
Fig.2.14. Cytotoxicity of retrorsine on separately cultured HepG2 cells and HHSECs. Data are represented as mean values ± SEM ($n = 4$). **$P < 0.01$ comparing with the corresponding vehicle control.

2.2.3.6 Effect of GSH Reduction on Cytotoxicity of PA in Separated Cultured HHSECs

As discussed earlier, HHSEC should be the toxic target of PA. Thus, GSH reduction is thought to be effective for promoting the sensitivity of the separately cultured HHSEC model. Firstly, the effects of 4 mM BSO on GSH reduction and cell viability of HHSECs were investigated. As shown in Table 2.4, 4 mM BSO induced a decrease of cellular GSH level and cell viability in a time-dependent

manner. The cell viability was significantly decreased since 36 h incubation. To avoid a more excessive cell loss prior to PA treatment, 36 h of incubation was selected for further study. Table 2.5 shows the effect of 36 h incubation of BSO at different concentrations on cell viability of HHSECs. BSO induced the decrease of cell viability in a concentration-dependent manner, which was significant at 1 mM and higher concentrations. Then, the concentration of 2 mM was selected since among the three concentrations (1, 2 and 4 mM) having similar cytotoxicity to HHSECs, this concentration showed a relatively lower variation. When the cells were pre-incubated with 2 mM BSO for 36 h, the cell viability of HHSECs was significantly decreased ($P < 0.05$ comparing with vehicle control). The cell viability of HHSECs treated with different concentrations of retrorsine in the presence of BSO was lower than that in the absence of BSO ($P < 0.05$ or $P > 0.05$ comparing with corresponding vehicle control) (Table 2.6). However, the reduced cell viability induced by retrorsine was comparable to that induced by vehicle control, suggesting that the decrease of cell viability was due to the toxic effect of BSO itself.

Table 2.4 Effect of 4 mM BSO on GSH reduction and cell viability in HHSECs

BSO incubation time (h)	GSH level (% vehicle control)	Cell viability (% vehicle control)
24	71.7 ± 13.7*	92.4 ± 2.4
36	57.9 ± 9.1**	79.5 ± 4.9*
48	46.2 ± 12.4**	65.8 ± 9.7*
72	23.6 ± 5.1**	35.7 ± 4.2**

*$P < 0.05$ and **$P < 0.01$ comparing with the corresponding vehicle control.

Table 2.5 Effect of 36 h BSO incubation on cell viability in HHSECs

BSO (mM)	Cell viability (% vehicle control)
0.25	93.2 ± 3.5
0.5	89.4 ± 2.1
1	82.0 ± 6.5*
2	80.0 ± 2.5*
4	79.5 ± 4.9*

*$P < 0.05$ comparing with vehicle control.

Table.2.6 Effect of 36 h of 2 mM BSO incubation on cytotoxicity of retrorsine in HHSECs

Retrorsine (mM)	Cell viability (% vehicle control)	
	Control	BSO
0	100.3 ± 4.5	80.0 ± 2.5#
0.125	77.1 ± 9.3*	75.7 ± 11.1*
0.25	76.4 ± 5.4*	70.9 ± 4.4**
0.5	73.9 ± 11.4*	61.5 ± 3.0***#
1	65.4 ± 4.2**	61.8 ± 5.2**

*$P < 0.05$ and **$P < 0.01$ comparing with the corresponding vehicle control; #$P < 0.05$ comparing with control.

2.2.4 Summary

When compared with on co-cultured HepG2 cells, the cytoxicity of PA on co-cultured HHSECs was enhanced to some extent. However, the toxic concentration was still around mM level, suggesting that the co-culture model was also not sensitive enough for an accurate prediction of PA intoxication in cells. In

addition, the morphology and function of both HepG2 cells and HHSECs were changed in the co-culture system. The incompatibility of the medium for two cell types has been proved to be the main reason and there was no alternative medium available at present which could be simultaneously suitable for both cells. Therefore, separately cultured HHSEC model was then investigated. The results indicated that the extent of cytotoxicity of PA on HHSECs was similar to that on HepG2 cells. GSH depletion was also not effective for potentiating the toxicity of retrorsine on HHSECs. As discussed earlier, the cell-cell communication between hepatocytes and SECs are complex and this complexity may contribute to the lack of a well established pathogenesis of PA-poisoning, resulting in difficulties in developing an effective *in vitro* system for the demonstration of PA intoxication. In addition, HHSEC is a newly developed human cell line, its value of application in expressing the real function of hepatic SEC await further investigation. Thus, considering the expense and simplicity, HepG2 cell model was investigated again for further development of the model.

2.3 Optimized HepG2 Cell Model

2.3.1 Introduction

As discussed earlier, a 25% decrease of cell viability induced by 1 mM retrorsine found in our HepG2 cell model is comparable to the inhibitory effect of monocrotaline, another retronecine-type PA, on primary cultured hepatic SECs and hepatocytes (DeLeve et al., 1996). This result suggests that the HepG2 cell line is an effective cellular system for evaluating PA-induced cytotoxicity. The relative high concentration (mM) of retrorsine needed to induce the toxic effects indicates that it is the metabolite, not the prodrug itself that causes the cytotoxicity. Based on the toxic potency of cisplatin found in section 2.1.3.1, there should be a balance in the cell number between producing enough toxic metabolite of PA and exhibiting detectable cytotoxic response to PA. In addition, some factors that may influence the cytotoxicity, including incubation period, vehicle control, and protein binding were also investigated to find optimal incubation conditions for eliciting a greater cytotoicity of PAs on HepG2 cells.

Since multiple and different early measurements of toxicity mechanisms are critical for the detection of toxic potential (Gerets et al., 2009), there is a need for measurement of multiple, independent and early mechanisms of cytotoxicity. In the present study, six cytotoxicity methods which measure different endpoints were appraised for their application in detection of PA-induced human hepatotoxicity in HepG2 cells. Cell viability was assayed by MTT and the ability to uptake of neutral red into lysosomes. Bio-reduction of resazurin by viable cells and the binding of cellular protein to sulforhodamine B (SRB) were also investigated for the evaluation of cell survival. Cell proliferation was assayed by quantification of incorporated bromodeoxyuridine (BrdU) in the newly synthesized DNA of replicating cells (Gage

et al., 1995). Cell death was evaluated by assessment of LDH which only leaked through the ruptured cell membrane. These six assays were selected to be appraised because they are easily adaptable to 96-well plates and able to accommodate a large number of samples, and are representative of several mechanisms.

2.3.2 Materials and Methods

2.3.2.1 Materials

Neutral red, resazurine and SRB were purchased from Sigma-Aldrich Corporation (St. Louis, MO, USA). Cell proliferation ELISA, BrdU kit, was purchased from Roche Applied Science (Germany).

2.3.2.2 Cell Culture

The details are described in section 2.1.2.2.

2.3.2.3 Optimization of Incubation Conditions

2.3.2.3.1 Investigation of the Course of Onset of Cytotoxicity of Retrorsine

In most cases, long time incubation will increase the toxicity of toxic drugs. In a preliminary experiment with retrorsine the optimal time for treatment of cells was determined. Cells (5000 cells/well for 96-well plate) were incubated with 0.5 or 1.0 mM retrorsine for 24 or 48 h in the presence of 10% FBS before MTT assay.

2.3.2.3.2 Test of the Influence of DMSO Percentage on Cell Viability

Most PAs were insoluble in aqueous environment, DMSO was used as the alternative solvent and the maximal concentration of retrorsine in DMSO was 200 mM. To rule out the toxic effect of DMSO on cell viability, 0%, 0.5%, 0.75% and 1.0% were tested as controls.

2.3.2.3.3 Determination of Optimal Cell Density

The seeding densities of the cell, 2000, 3000, 4000 and 5000 cells per well, were set to grow to 80 to 90 percent of confluence for analysis. The cells were allowed to attach overnight and then incubated with 0.5 mM retrorsine for 24 h before MTT assay. For positive control, 16 μM cisplatin with known effect were added in triplicate to each plate to confirm quality of testing for the plate.

2.3.2.3.4 Test of the Influence of FBS Percentage on the Cytotoxicity of Retrorsine

Since most PAs exert their toxicity by binding to proteins, FBS, with large amounts of proteins, has been generally suggested not to be used in the drug treatment of PA *in vitro*. To gauge the influence of the FBS on the cytotoxicity assay of retrorsine, FBS with different percentages, ranging from 0% to 10%, were tested.

2.3.2.3.5 MTT assay

The details are same as that described in 2.1.2.5.

2.3.2.4 Selection of Cell Viability Assays on HepG2 Cell

2.3.2.4.1 Cell Culture

HepG2 cells were seeded in 96-well assay plates with 2000, 4000 and 8000 cells/well in 100 μl DMEM containing 10% FBS and cultured overnight at 37°C in a humidified 5% CO_2 and 95% air atmosphere. After another 24 h of incubation with FBS free DMEM, The cell viability was assessed by MTT, neutral red, resazurin and SRB assays and calculated as percentage of 8000 cells/well.

2.3.2.4.2 MTT assay

Colorimetric assays of cell viability, activation and proliferation based on the use of the tetrazolium salt MTT have proven to be extremely useful (Ferrari et al., 1990). The MTT is a means of measuring the activity of living cells by assessing the activity of mitochondrial dehydrogenases. As the cell loses viability (metabolic activity) and decreases mitochondrial function, its ability to perform the conversion decreases. However, it is not uncommon for some chemicals to increase metabolic activity in a cell, which would result in increased mitochondrial succinate dehydrogenase activity. In addition, succinate dehydrogenase is an enzyme in the mitochondrial inner membrane and sensitive to local changes in ion concentration and ion flux. Therefore, the activity of this enzyme can be increased with the appropriate ionic conditions. The procedure for performing MTT assay is same as that described in section 2.1.2.5.

2.3.2.4.3 Neutral Red Assay

The use of neutral red, a cytotoxic indicator, is an assay modified from a viral cytopathogenicity test (Zhang et al., 1990). Neutral red is a weak cationic dye which is believed to enter the cell by non-ionic diffusion through the cell membrane. The dye then accumulates in the lysosomes of living cells. Whether this step is due to an active or passive mechanism is not clear (Werner et al., 1999). The standardized test can be used to score cell injury as well as to determine the number of remaining cells after toxic insult. Chemicals that damage plasma and/or lysosomal membranes or interfere with the normal energy-requiring endocytosis process will decrease the ability of the cell to take up neutral red (Kull and Cuatrecasas, 1983). The linearity of neutral red uptake and cultures ranging from 1×10^3 to 4×10^4 cells per well for 96-well plate has been demonstrated in a previous study (Borenfreund and Puerner, 1985).

The preparation of the dye solution was modified according to a previous report (Borenfreund and Puerner, 1985). Briefly, ten times (10×) aqueous stock solution of the dye was prepared and then diluted with DMEM to a final concentration of 0.033%. The dye-containing DMEM was incubated overnight at 37°C and centrifuged at 1500 g for 10 min before use. The cell medium was replaced by 100 µl of dye-containing DMEM. Another 3 h of incubation at 37°C in a humidified 5% CO_2/95% air atmosphere was performed to allow neutral red to be incorporated by the live cells. Then the dye-containing DMEM was carefully aspirated and the cells were quickly rinsed with PBS to remove unincorporated dye. The incorporated dyes were then dissolved in 100 µl of a mixture of 1% acetic acid-50% ethanol. The plates were shaken for 10 min and then the absorbance was measured at 540 nm with 690 nm as reference wavelength using the microplate reader.

2.3.2.4.4 Resazurin Assay

The resazurin system measures the metabolic activity of living cells. Solutions of resazurin are dark blue in color. Bioreduction of the dye by viable cells reduces the amount of its oxidized form (blue) and concomitantly increases the amount of its fluorescent intermediate (red), indicating the degree of cytotoxicity caused by the test agent (Perrot et al., 2003). To perform resazurin assay, 10 µl of 0.5 mg/ml resazurin dye solution were added to the culture medium. Cells were incubated for another 3 h at 37°C in a humidified 5% CO_2/95% air atmosphere to allow resazurin to be reduced by the vital cells before measurement. The plate was shaken for 10 min and then the absorbance was measured at 600 nm with 690 nm as reference wavelength.

2.3.2.4.5 Sulforhodamine B (SRB) Assay

SRB assay determines total cell number by measuring cellular protein (Skehan et al., 1990). The protein binds to the dye, SRB, and is then extracted from the cells in a Tris base solution. The SRB colorimetric assay was optimized based on the method reported in a previous study (Papazisis et al., 1998; Pinmai et al., 2008). In brief, the cells were fixed by gently layering 25 µl of cold 50% trichloroacetic acids (TCA) on top of the growth medium. Cells were kept at 4°C for 1 h and then rinsed with water twice to remove TCA. To stain the cells, 50 µl of 0.4% SRB solution was added into the wells and incubated with cells for 30 min after the plate was air dried. Then the SRB solution was removed and the cells were rinsed quickly with 1% acetic acid to remove unincorporated dye. The rinsed cultures were left to air dry and then 100 µl of 10 mM Tris were added to dissolve the incorporated dye. The absorbance of multi-well plates was measured at 565 nm with 690 nm as reference wavelength.

2.3.2.5 Selection of Cytotoxicity Assays for Retrorsine on HepG2 Cells

2.3.2.5.1 Cell viability Assays

Retrorsine was first dissolved in DMSO and further diluted with FBS-free DMEM to the desired final concentrations. Cells in 96-well plate with 3000 cells/well were incubated for 24 h with different concentrations (0.125, 0.25 and 0.5 mM) of retrorsine before cytotoxicity assay. After incubation with retrorsine, the cell viability was assessed by selected assays as described above and was calculated as percentage of vehicle control.

2.3.2.5.2 Cell Proliferation Assay

BrdU uses nucleotide substitution to replace thymidine with uridine in the DNA structure of dividing cells both *in vitro* and *in vivo* (Gage et al., 2000). Cell proliferation is thus measured by quantitating BrdU incorporated into the newly

synthesized DNA of replicating cells. They offer a nonradioactive alternative to the [3H]-thymidine-based cell proliferation assay with comparable sensitivity. To perform BrdU assay, the BrdU labeling reagents were added into the cells together with retrorsine. After incubation with retrorsine together with the process of BrdU incorporation, the culture medium containing BrdU labeling reagent was removed and cultures were rinsed off with PBS, pH 7.4, and fixed with fixation solution (100 μl/well, 30 min, RT). After the fixation solution was thoroughly removed, the cells were then incubated with 50 μl/well blocking buffer (2% BSA in PBS) (1 h, 37 °C). Cells were then rinsed twice with PBS and incubated with anti-BrdU-POD working solution (100 μl/well, 90 min, 37 °C). The solutions were removed and then cells were washed for three times (200 μl/well, 5 min, RT). Wells were then incubated with substrate solution (100 μl/well) for 30 min (37 °C). The reaction was stopped by addition of 1 M H_2SO_4 (25 μl/well) and 5 min shaking was followed afterwards. The absorbance at 450 nm with the reference of 690 nm was measured using the microplate reader.

2.3.2.5.3 LDH Release Assay

The details are described in section 2.1.2.7.

2.3.2.6 Cell Morphology

After being incubated with 0.5 mM retrorsine, the cells were observed and taken images under the microscope equipped with a digital camera (Nikon DS-5Mc) before being rinsed with fresh DMEM for subsequent staining. Giemsa's solution was added into cells after the cells were fixed with 10% formalin for 30 min and rinsed twice with PBS. After 15 min staining, the Giemsa's solution was removed.

The cells were observed and taken images again under the digital camera-equipped light microscope.

2.3.2.7 Statistical Analysis

All data are represented as mean values ± SD and the mean values were obtained from 9 data points from triplicate wells in triplicate cultures unless otherwise stated. Data curves were generated using least-squares fitting routines using a log scale for the cell density or drug concentration on the horizontal axis and a linear scale for the toxic response on the vertical axis. The regression and correlation analysis were carried out using the statistical package GraphPad Prism 5.0 for the selection of suitable assays for model development. For the comparison of different treatments in two or more than two groups, the data were analyzed by student's *t*-test or one-way analysis of variance (ANOVA) followed by Bonferroni's multiple comparison post hoc test using GraphPad Prism 5.0, respectively. For the comparison of various treatment groups with different time periods, two-way ANOVA was used followed by Bonferroni's post-tests. Differences were considered statistically significant at $P < 0.05$.

2.3.3 Results and Discussion

2.3.3.1 Optimal Incubation Conditions

Fig.2.15A shows the cytotoxicity of retrorsine when incubated with HepG2 cells for 24 or 48 h. When compared the cell viability between two time points, there was no significant difference observed at 1 mM retrorsine treatment. Hence, the time point of 24 h was thus selected for our study.

Fig.2.15B shows the cytotoxic effect of different concentrations of DMSO on HepG2 cells. Only 0.5% DMSO did not lead to a significant decrease in the cell viability and was thus selected for further experiments.

Fig.2.15C shows the cytotoxicity of retrorsine influenced by cell density. The selected density of cells per well was 2000–4000 cells in a total volume of 100 µl of medium. Under these conditions, the cell viabilities treated by 16 µM cisplatin or 0.5 mM retrorsine were relatively stable and maintained at around 15% and 55% respectively.

Fig.2.15D shows the effect of FBS percentage on the cytotoxicity of retrorsine. The selected condition was serum free medium because only under these condition, 1 mM retrorsine showed a significant cytotoxicity on cells ($P < 0.05$).

Taken together, 24 h incubation, 0.5% DMSO as vehicle control, cell density of 2000–4000 cells per well and drug treatment in the serum free medium are the optimal experimental conditions. And they were consistently employed in all further experiments.
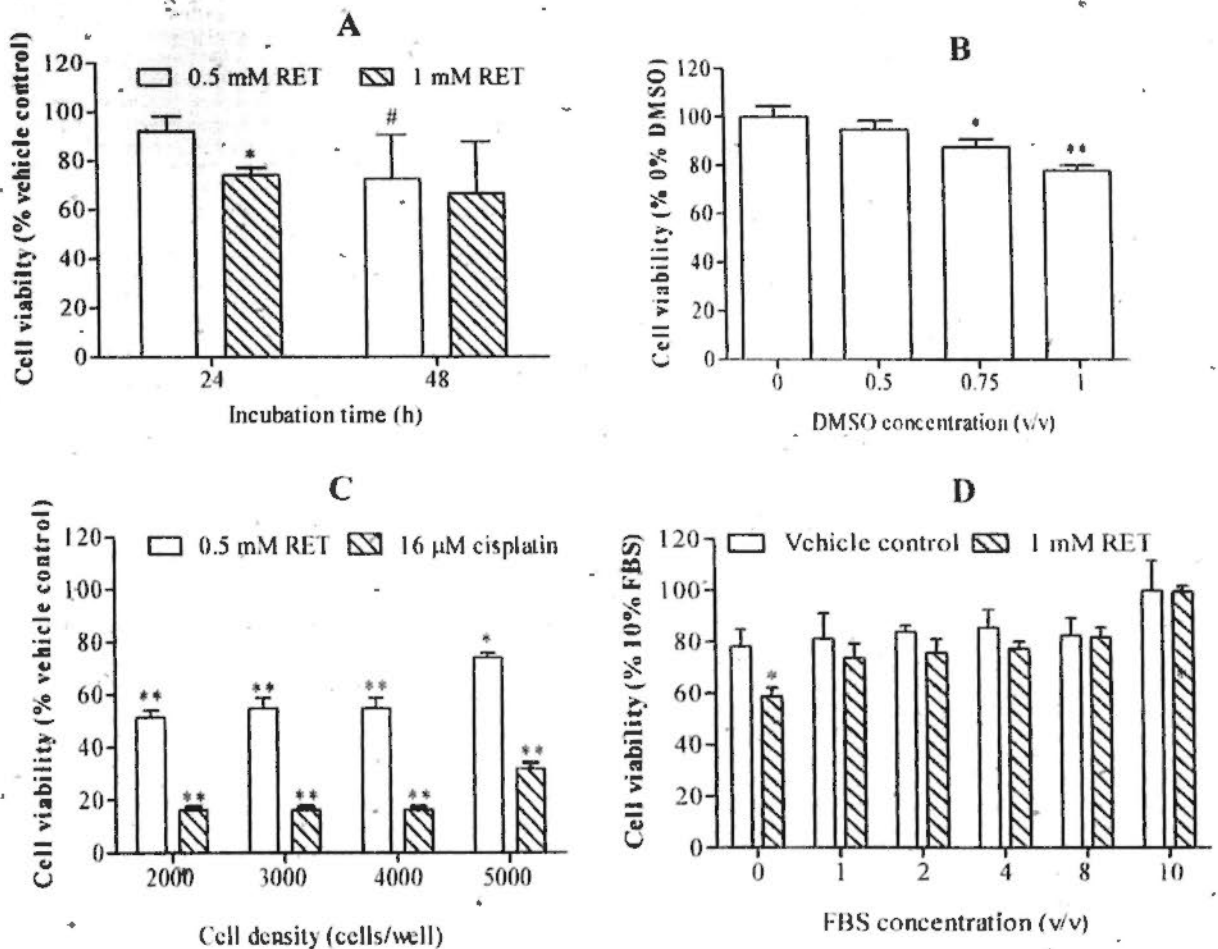
Fig.2.15.Optimal incubation conditions for cytotoxicity assessment of retrorsine determined by MTT assay. (A) Effect of different incubation times on the cytotoxicity of retrorsine. (B) Effect of different concentrations of DMSO on HepG2 cells. (C) Effect of different cell densities on the cytotoxicity of retrorsine. (D) Effect of different FBS concentrations on the cytotoxicity of retrorsine. RET: retrorsine. $*P < 0.05$ and $**P < 0.01$ comparing with vehicle control; $^{\#}P < 0.05$ comparing with 24 h.

2.3.3.2 Selected Cell Viability Assays for HepG2 Cells

With the increase of cell density, cell viability of HepG2 cells determined with four assays increased accordingly (Fig.2.16). In order to compare the sensitivity, linear regression analysis was performed and the parameters were shown in Table

2.7. With high R^2 value (> 0.95), four cell viability assays showed good linear relationships with cell density under the fixed optimal culture conditions. MTT and neutral red assays had the two highest R^2 value (R^2 = 0.9903 and 0.9876 respectively). Correlation coefficients appraising the linear association between two assays were shown in Table 2.7. The significant correlation was only observed between MTT and neutral red assays ($P < 0.01$) despite all the other paired assays also appeared well-correlated with each other with a Pearson r value larger than 0.92.

By investigating the linearity of cell viability and cell density, all of the selected cell viability assays, MTT, neutral red, resazurin and SRB were able to present an accurate prediction for HepG2 cells at the density of 2000-8000 cells/well in 96-well plate. This result suggested that these four assays were adaptable for the prediction of drug-induced effect on HepG2 cells. The good correlations between them indicated that a high accordance would be obtained by these assays, that is to say, these four assays should produce similar result. In order to facilitate further study, MTT and neutral red assays with higher sensitivity and better correlation were selected.
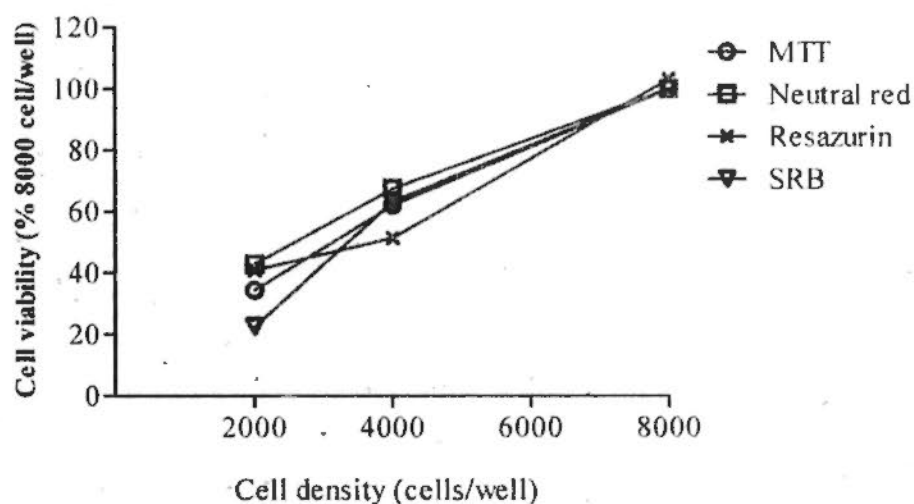
Fig.2.16.Effect of cell density on cell viability of HepG2 cells determined by MTT, neutral red, resazurin and SRB assays.

2.3.3.3 Selected Cytotoxicity Assays for Retrorsine on HepG2 Cells

As shown in Fig.2.17, 0.5 mM retrorsine induced a significant decrease in cell viability and cell proliferation ($P < 0.01$ comparing with vehicle control), whereas no obvious increase of LDH release was observed ($P > 0.05$ comparing with vehicle control), suggesting that not cell death, but cell proliferation might be involved in retrorsine-induced cytotoxicity. In addition, two cell viability assays and BrdU assay showed acceptable linear relationships with drug concentration with a R^2 value larger than 0.9 as shown in Table.2.7. Furthermore, significant correlations were observed between MTT and neutral red, neutral red and BrdU assays ($P < 0.05$) as shown in Table 2.7, confirming that inhibition of cell proliferation was the main atribution of cell viability decrease induced by retrorsine. Thus, MTT, neutral red and BrdU assays combined were selected to evaluate the PAs-induced cytotoxicity in HepG2 cells.

Cellular proliferation requires the replication of genomic DNA. BrdU assay is able to reflect the numbers of newly proliferated cells because it is based on the detection of BrdU incorporated in place of thymidine into the genomic DNA of proliferating cells. These two selected cell viability assays and BrdU assay could complementarily reveal the toxicity of retrorsine, implying that the inhibition of cell proliferation was the main atribution of the cytotocivity of retrorsine. The possible mechanism of the toxicity is that the metabolites of retrorsine cause the formation of DNA-adducts and thereafter interfere with DNA replication or transcription. Thus, three developed assays including MTT, neutral red and BrdU assays under optimized culture conditions in HepG2 cells are effective for the assessment of the cytotoxicity of PAs.
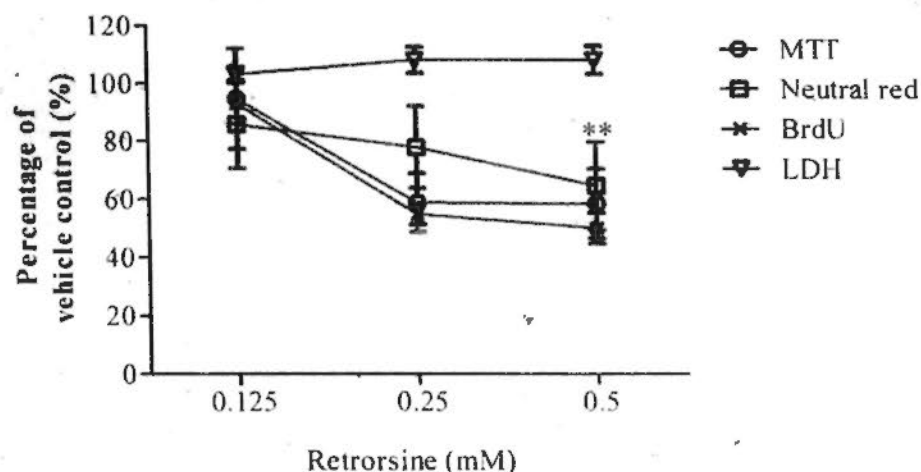
Fig.2.17. Cytotoxic effects of retrorsine on HepG2 cells determined by MTT, neutral red, BrdU and LDH assays. ** $P < 0.01$ comparing with corresponding vehicle control.

Table 2.7 Linear regression and correlation analysis

		Cell viability assays on HepG2 cells			
Assay	R^2 (linear regression)	r (correlation)			
		MTT	Neutral red	Resazurin	SRB
MTT	0.9903	1	0.9999**	0.9623	0.9926
Neutral red	0.9876		1	0.9587	0.9941
Resazurin	0.9690			1	0.9221
SRB	0.9522				1
		Cytotoxicity assays for retrorsine on HepG2 cells			
Assay	R^2 (linear regression)	r (correlation)			
		MTT	Neutral red	BrdU	LDH
MTT	0.9042	1	0.9631*	0.9979*	-0.9214
Neutral red	0.9982		1	0.9787*	-0.7829
BrdU	0.9392			1	-0.8940
LDH	0.5714				1

*$P < 0.05$ and **$P < 0.01$ meant the correlation was statistically significant.

2.3.3.4 Effect of Retrorsine on Cell Morphology

To confirm our observation that inhibition of cell proliferation unleashed retrorsine-induced cytotoxicity, retrorsine-treated cells were observed under light microscope. Similar amounts of cells were found rounded and detached in the medium after 24 h incubation of vehicle control or 0.5 mM retrorsine (indicated by white arrow in Fig.2.18A and A'). The normal basal cell death should be the reason behind this. After the detached cells were rinsed off, the numbers of remaining cells with normal morphology in retrorsine treatment group were approximately half of that in vehicle control group after Giemsa's staining (indicated by black arrow in Fig.2.18B and B'). This morphology observation confirmed that retrorsine-induced decrease of cell number was mainly caused by inhibition of cell proliferation, but not by direct killing the cell.
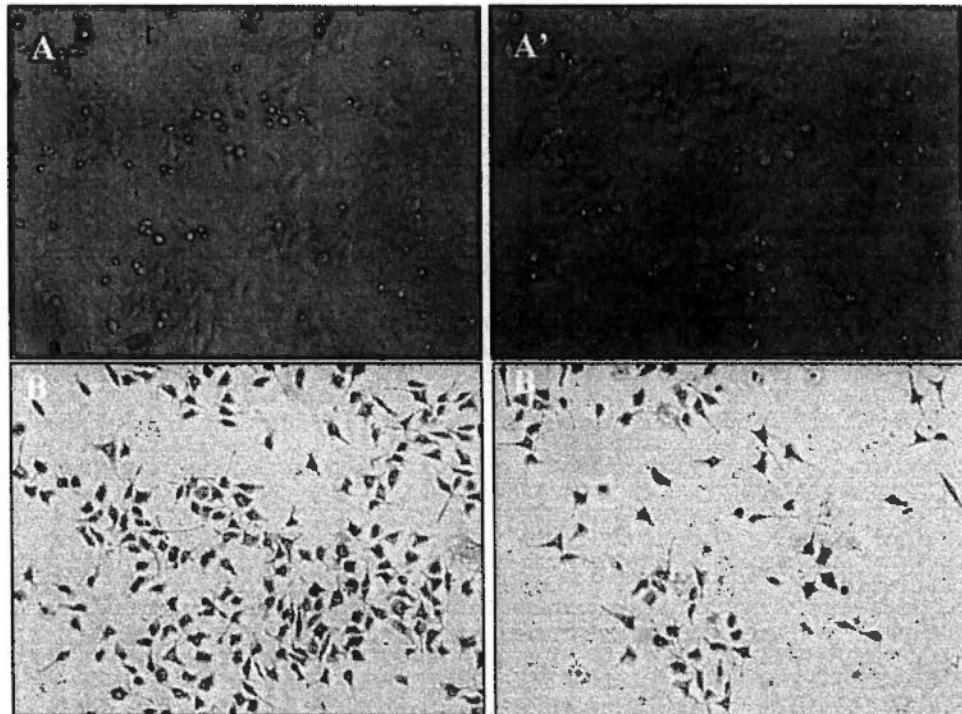
Fig.2.18.Toxic effects of retrorsine on morphology of HepG2 cells prior to (A and A') and (B and B') after Giemsa's staining. Dead cells which were round and detached and the remaining cells with normal morphology are indicated by black white arrow respetively. A and B: Vehicle control. A' and B': 0.5 mM retrorsine. (200× magnification)

2.3.4 Summary

Each kind of chemical has its unique property of cytotoxicity on different type of cell cultures. As a specific type of compound, PAs should also have its own particular characteristic cytotoxicity on HepG2 cells. To achieve an accurate prediction for PA intoxication, it is necessary to develop an optimized HepG2 cell model based on present knowledge about PA intoxication. For this purpose, the incubation time, vehicle control, cell density and FBS percentage were investigated to obtain an optimal incubation conditions for eliciting a maximal cytotoxicity of PA.

Furthermore, as different cytotoxicity assays evaluate different aspects of the endpoint, a combinational usage of several assays could help both complimentarily predict the toxicity and illustrate the toxic mechanism. As discussed earlier, the high agreement between MTT and BrdU assay as well as the discrepancy between these two assays with LDH assay suggested that it was inhibition of cell proliferation, but not direct cell death that contributed to the loss of cell viability. Interestingly, the combinational usage of more cytotoxicity assays have been seen in many other studies (Grant et al., 1992; Putnam et al., 2002; Spielmann et al., 1993; Yang and Acosta, 1994). In these studies, different assays may produce similar, comparable or totally different results. However, each endpoint by the cytotoxicity assays plays an important role in understanding the mechanisms.

In conclusion, the developed *in vitro* model has been proved to be successful in detecting the cytotoxicity of retrorsine, a representative PAs. Cytotoxicity test results for retrorsine reported here are quite consistent with the literature. This model was then used to assess the cytotoxicity of different PAs and at the same time, its reliability and reproducibility was tested.

Chapter 3 Assessment of the Hepatocytotoxicity of PAs Using Developed *in vitro* Model

3.1 Introduction

As discussed in chapter 1, PAs are a group of heterocyclic compounds including more than 660 identified structures that are classified into three types, namely otonecine-, retronecine- and platyphylline-type (Fu et al., 2004; Mattock, 1986). PA-containing plants are extensively distributed with accounting for about 3% of the world flowering plant (Roeder, 2000; Stegelmeier et al., 1999). Some of these PA-containing plants are considered beneficial and are being used for medicinal purposes or as herbal teas (Joosten et al., 2011; Joosten and van Veen, 2011; Kumana et al., 1983; McGee et al., 1976).

However, several outbreaks of PA-poisoning cases reported in African and Middle East make people notice its hazard in early 1970's (Mohabbat et al., 1976; Stillman et al., 1977a; Stillman et al., 1977b). Since then, more attentions have been paid to PAs and now over half of the identified PAs are found to be toxic (Stegelmeier et al., 1999). However, till now, no effective strategy has been established for the treatment of PA-induced hepatotoxicity and thereafter HSOS (Chen and Huo, 2010; Gao et al., 2009). To restrict the exposure to PA-containing medicinal herbs is thus believed to be a suitable option for putting PA-poisoning under control. To achieve this, several countries have established regulations (Roeder, 2000). For example, the Federal Health Department of Germany stipulates that manufacture and use of PAs should be under limit of internal exposure less than 1 μg/day for less than six weeks (Roeder, 1995). Medicines and Healthcare Products Regulatory Agency of the UK restricts the internal use of Qianbai Biyan Pian, a PA-containing Chinese medicine proprietary product, not more than 1 mg/day for 2 weeks or 0.1 mg/day for longer

periods (Roeder, 2000). Obviously, these regulations are all established based on the case studies; they cannot be considered as general rules and applied universally to all PA-containing products.

In addition, due to the worldwide distribution, PA-containing plants often easily contaminate prepared grains which are then readily taken by human and/or animals (Mohabbat et al., 1976). Therefore, human poisonings most often are a result of food contamination. Furthermore, as we demonstrated in a recently reported study (Lin et al., 2011), erroneous ingestion of PA-containing natural products may account in part for the high prevalence of global PA-poisonings when they are misused for medicinal purpose. Thus, plant-derived PAs may represent the most poisonous compounds affecting livestock, wildlife, and humans without any effective prevention, which urge a scientific understanding for their intoxication.

As the plant-derived PAs are a diverse class of alkaloids with considerable structure differences, the toxicity of them are assumed to be different (Culvenor et al., 1976). The structure-toxicity relationship of PAs has been described and the structural characteristics of the various PAs are supposed to determine their variable degrees of toxicity to livestock and humans (Frei et al., 1992; Kim et al., 1993; Wiedenfeld et al, 2008). For example, for the induction of hepatotoxicity, PA should contain a 1, 2 unsaturated necine base, which is usually esterified to necic acid (Fig.1.1 and 1.2) (Mattocks, 1986). The toxicity of a PA is increased if the hydroxyl groups are esterified in positions 7 and 9, if the necic acids have branched chains or are unsaturated, or if the necic acid forms a cyclic diester ring (Mattocks, 1968), as observed in senecionine and monocrotaline. Non-cyclic diesters are generally less toxic and monoesters display even a lower toxicity (Mattocks, 1986). However, as structure is only one of the factors that determine the toxic property of a chemical,

only using above structure-based rule as the reference will not allow us to make an accurate prediction on the severity of toxicity of each PA.

For idiosyncratic toxicity, a more important determinant is the biological response of the human/animal body (Tujios and Fontana, 2011). For example, species differences in activities of CYP3A may explain their variable susceptibility to PA (Huan et al., 1998a, b; Yan and Huxtable, 1995). Under experimental conditions, several retronecine-type PAs have been shown to induce a variety of acute and chronic pathological lesions in the livers of animals (Gordon et al., 2000). In *in vitro* systems, retronecine-type and otonecine-type PAs exhibit different profiles of cytotoxicity (Copple et al., 2004; DeLeve et al., 1996; Ji et al., 2010; Ji et al., 2008; Ji et al., 2005). Although it is generally recognized that the potency of cytotoxicity and acute toxicity varies remarkably among PAs (Mattocks, 1986), till now, no systematical study has been done to compare the toxicity profiles of different types of PAs. In order to understand the diversity of PAs-induced hepatocytotoxicity, it is necessary to systemically assess the cytotoxicity of all types of PAs.

In order to accurately predict the hepatotoxicity of PA on human, a species-relative biological system is needed. Thus in the present study, the hepatocytotoxicity of seven PAs and one PA-containing herb were evaluated using our developed reliable assessment model, optimized HepG2 cell model, as demonstrated in chapter 2.

3.2 Materials and Methods

3.2.1 Materials

Platyphylline was a gift from Prof. Hai Shen Chen from the Department of Phytochemistry, The Secondary Military Medical University, China. Isatidine

(retrorsine *N*-oxide) was purchased from Aldrich Chemical Co. (P.O.Box 355, USA). Riddelliine was a gift from Dr. Po-Chuen Chan from the National Toxicology Program. Senecionine and seniciphylline were purchased from Extrasynthese Corporation. Alkaloid extract of *G. segetum* was prepared using herbal part tuberous roots according to the protocol previously reported (Lin et al, 2009) and 83% of the content was senecionine and seneciphylline. All other drugs and chemicals were purchased from Sigma-Aldrich unless stated otherwise, and were of the highest possible content.

3.2.2 Cell Culture

The protocol is same as that described in section 2.1.2.2.

3.2.3 PA Treatment

The structures of seven PAs tested were shown in Fig.1.2. To prepare the stock solution, retrorsine, isatidine, riddelliine and platyphylline were first dissolved in DMSO and further diluted with FBS-free DMEM to final concentration. Senecionine and seneciphylline were dissolved in PBS acidified by 1.0 M HCl. The pH was then raised to 7.0 by titrating with 0.5 M NaOH, and the volume was adjusted with FBS-free DMEM to the appropriate final concentration. Clivorine and alkaloid extract of *G. segetum* were directly dissolved in FBS-free DMEM. When DMSO was used to dissolve PAs, it was added to the final concentration of 0.5% (volume/volume) for all wells used for determining the drug response. Final concentrations of PAs in the plate were 0.0625, 0.125, 0.25, 0.5 and 1.0 mM. The concentration of *G. segetum* extract was determined based on its content of two PAs, senecionine and seneciphylline. For BrdU assay, the labeling reagent was added together with PAs. After addition of the different concentration of PAs, the plates

were incubated at 37°C in the CO_2-incubator for 24 h before MTT, neutral red and BrdU assays.

3.2.4 Cytotoxicity Assays

After incubation with different concentrations of PAs, the cell viability was assessed by MTT and neutral red assays, and cell proliferation by BrdU assay as described previously and was calculated as percentage of vehicle.

3.2.5 Statistical Analysis

All data are represented as mean values ± SD unless otherwise stated. The mean values were obtained from 9 data points from triplicate wells in triplicate cultures. The concentration-response relationship for each assay was quantified where possible using the IC_{20}, the concentration causing 20% reduction of cell viability or inhibition of cell proliferation. Curves were generated using least-squares fitting routines with IC_{20} valued determined using variable-slope, sigmoidal, curve-fitting routines, using a log scale for the drug concentration on the horizontal axis and a linear scale for the toxic response on the vertical axis. For the comparison of different treatments in two or more than two groups, the data were analyzed by student's t-test or one-way analysis of variance followed by Bonferroni's multiple comparison post hoc test using GraphPad Prism 5.0, respectively. Differences were considered statistically significant at $P < 0.05$.

3.3 Results and Discussion

3.3.1 Cytotoxicity of Retrorsine, Clivorine and Platyphylline

HepG2 cells were treated with the concentration range (0.0625-1 mM) of three PAs for 24 h, thereafter cytotoxicity was determined by MTT reduction, neutral red

uptake and BrdU labeling. Fig.3.1 shows that retrorsine and clivorine, but not platyphylline, induced a significant cytotoxicity in a concentration-dependent manner determined by three assays ($P < 0.05$ or $P < 0.01$ comparing with vehicle control). As shown in Table 3.1, the hepatotoxic potency (MTT: IC_{20}, mM) of clivorine (0.01 ± 0.01) was significantly greater than that of retrorsine (0.27 ± 0.07) ($P < 0.01$). This difference between these two PAs was confirmed by neutral red and BrdU assays ($P < 0.05$ comparing with retrorsine) (Table 3.1). The toxic potency (IC_{20}) of clivorine assessed by BrdU assay was significantly smaller than that assessed by MTT or neutral red assays ($P < 0.05$ and $P < 0.01$, respactively), whereas similar results were obtained for retrorsine and platyphylline ($P > 0.05$ comparing with MTT or neutral red assay).

Our present findings that retrorsine and clivorine, but not platyphylline, were toxic is consistent with a previous report by Chen et al (1939), which showed that no hepatic damage was observed in mice, rats and guinea pigs treated with sub-lethal dosages of platyphylline. Thus, these two studies can provide scientific support for the generally accepted view that for the induction of hepatotoxicity, PA should contain a 1, 2 unsaturated necine base (Mattocks, 1986). The lack of hepatotoxicity of PAs with saturated necine base is assumed to be due to their in ability to convert to toxic metabolites (Fu et al, 2004).

The toxicities of retrorsine and clivorine found in the present study are comparable to those reported in two previous studies (DeLeve et al, 1996; Ji et al, 2009). In addition to these two studies, the cytotoxicity and/or mechanism of retronecine-type and otonecine-type PAs have been investigated by several other *in vitro* models (Kim et al, 1993; DeLeve et al, 1996; Copple et al, 2004; Ji et al, 2005, 2008a, 2008b). However, no study has ever been done to simultaneously investigate the cytotoxicity of both types. We are the first group to compare their cytotoxicity and

find that an otonecine-type PA is more toxic than a retronecine-type one. It's generally accepted that all PAs exert their toxicity by forming highly reactive pyrroles through the oxidative metabolic process, whereas hydrolysis and N-oxidation process are considered as detoxification pathways. Therefore, the metabolic dynamics between the pyrrolic ester formation and the detoxification pathways appears to be crucial in determining the toxicity of PAs (Fu et al, 2004). In the present study, clivorine had a higher toxic potency than retrorsine, which may result from two aspects: one is the different biological reaction upon two types of PAs, the other is the different metabolic rate including toxic and detoxication.
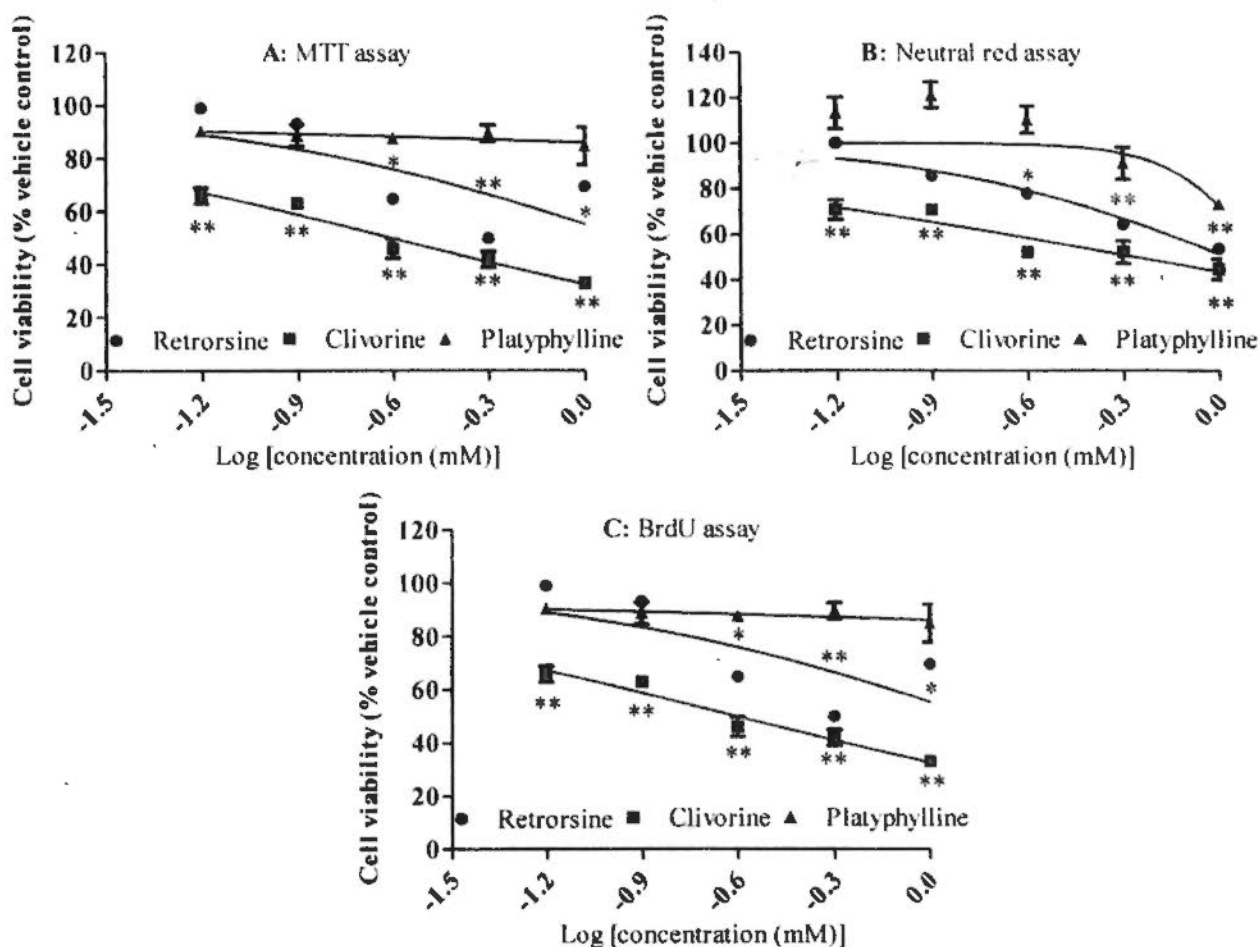
Fig.3.1. Cytotoxicity of retrorsine, clivorine and platyphylline determined by MTT (A), neutral red (B) and BrdU (C) assays. *$P < 0.05$ and **$P < 0.01$ comparing with the corresponding vehicle control.

3.3.2 Cytotoxicity of Retrornecine-Type PAs

The other four tested retrornecine-type PAs concentration-dependently induced cytotoxicity as assessed by all assays and exhibited similar hepatotoxic potency to that of retrorsine ($P > 0.05$) as shown in Fig.3.2 and Table 3.4. The rank orders of hepatotoxic potency were retrorsine $\geq$ riddelliine $\geq$ senecionine $\geq$ isatidine $\geq$ seneciphylline by MTT assay; retrorsine $\geq$ riddelliine $\geq$ isatidine by neutral red assay; and retrorsine $\geq$ senecionine $\geq$ riddelliine $\geq$ seneciphylline $\geq$ isatidine by BrdU assay. The data for senecionine and seneciphylline assayed by neutral red were not applicable as the dilution effect of adding these two PAs to the cells obscured the assay system. Thus, this assay was suggested to be not suitable for screening all PAs cytotoxicity. With BrdU assay, all retronecine-type PAs exhibited similar toxicity to that with MTT and neutral red assays ($P > 0.05$).

The similar toxic potency observed with tested five PAs belonging to one type confirms the view that chemical structure is one of the key determinants of PAs toxicity (Kim al, 1993). Interestingly, there are slight variations of toxicity among tested five retrorsine-type PAs, and four rank orders of their toxic potency: 1) retrorsine $\geq$ riddelliine $\geq$ isatidine; 2) senecionine $\geq$ seneciphylline; 3) retrorsine $\geq$ senecionine; and 4) riddelliine $\geq$ seneciphylline were consistently proved by all assays, which may be due to the slight differences in their structures (Yan, et al, 1995). To exert toxicity, PA N-oxide must be firstly reduced to the corresponding PA mainly in the gut before being activated in liver cells (Kim et al, 1993; Mattocks, 1971). Accordingly, as found in the present study, the retrorsine N-oxide, isatidine, exhibited a milder cytoxicity when compared to retrorsine, which could be linked to the lack of enzymatic reduction of N-oxide *in vitro*. This finding is accordant to that of several previous studies, in which, N-oxides were demonstrated less toxic than

their bases as they cannot be converted to toxic pyrroles by liver microsomal enzymes either in cell system, or when given intravenously to rats (Mattocks, 1971; Mattocks and White, 1971). A lower cytotoxicity of riddelliine than that of retrorsine are presumably attributed to the double bond that riddelliine contains, which is the only difference in the structure between retrorsine and riddelliine as shown in Fig.1.2. Similarly, the double bond that seneciphylline contains also resulted in a higher toxic potency than that of senecionine. Accordingly, the additional hydroxyl group may be responsible for the higher cytotoxicity of retrorsine than that of senecionine, and riddelliine than that of seneciphylline, but further studies are needed for confirmation.
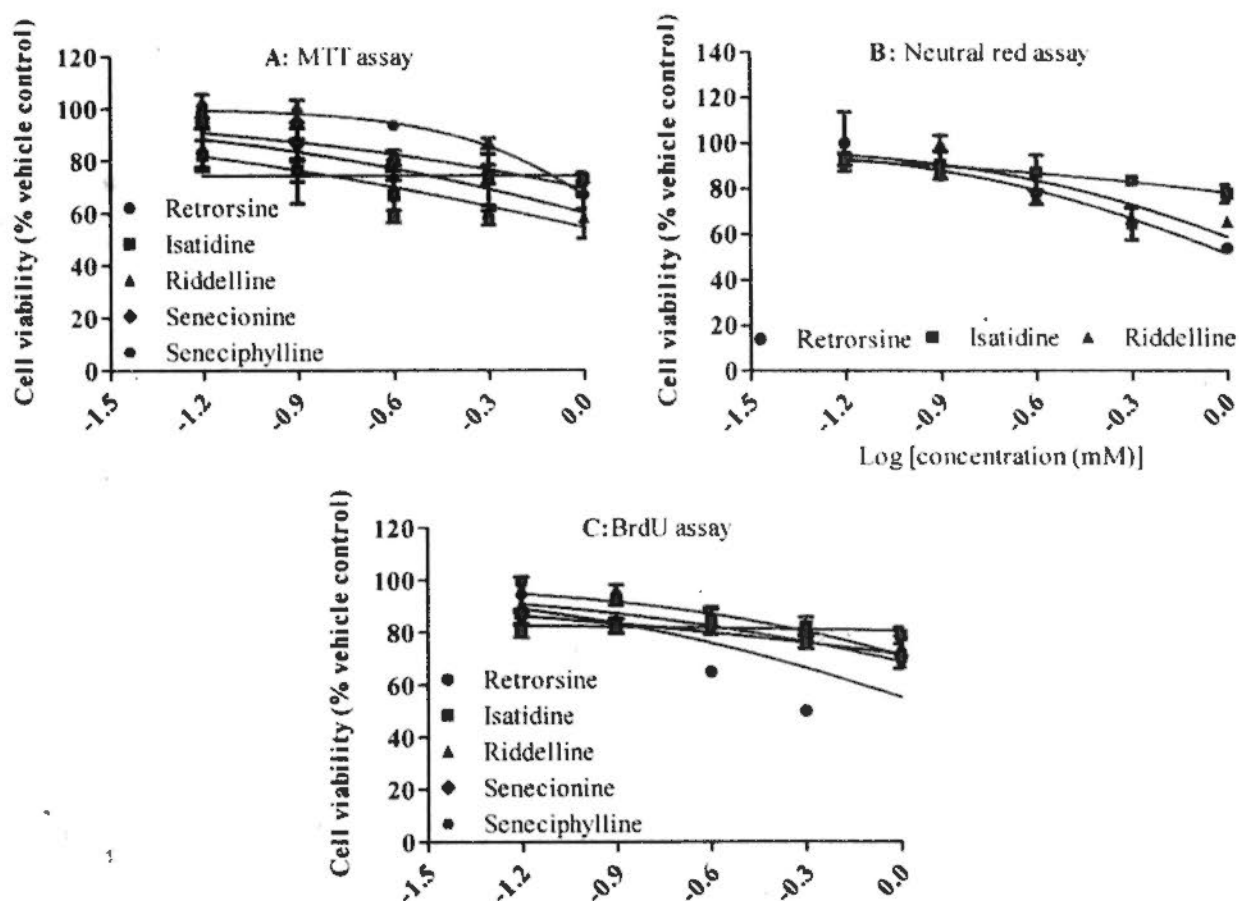
Fig.3.2. Cytotoxicity of 5 retronecine-type PAs determined by MTT (A), neutral red (B) and BrdU (C) assays.

3.3.3 Cytotoxicity of Alkaloids Extract of *Gynura segetum*, a PA-Containing Herb

The cytotoxicity induced by alkaloid extracts of *G. segetum* which contains pure senecionine and seneciphylline is shown in Fig.3.3 and Table 3.1. *G. segetum* extract exhibited a significant cytotoxicity to HepG2 cells in a concentration-dependent manner. The rank order of their cytotoxicity was senecionine ≥ *G. segetum* extract ≥ seneciphylline, suggesting that its cytotoxicity was similar to that of senecionine and seneciphylline. The toxicity of *G. segetum* extract obtained from BrdU assay was similar to that obtained from MTT assay ($P > 0.05$). Considering the contents (83%) of these two PAs in the herb, *G. segetum* extract-induced cytotoxicity was comparable to that of senecionine and seneciphylline tested in the developed model.

A strong evidence for PA-induced HSOS resulting from intake of PA-containing *G. segetum*, an erroneous substitute of non-PA-containing *Sedum aizoon*, has been recently reported in one Chinese patient by our group (Lin et al, 2010). Serum pyrrole-protein adducts were detected in the patient and two PAs, senecionine and seneciphylline, contained in the herb collected from the patient's home were quantified. To provide clear evidence that the liver injury is induced by *G. segetum*, an animal model was used for the assessment of *G. segetum* extracts-induced hepatotoxicity. To further test the cytotoxicity of these extracts, they were applied to our developed *in vitro* model. The demonstrated hepatocytoxicity in the present model suggested an accordance of toxicity to that demonstrated by the animal study, which implies a potential usage of the present model in the assessment of PA-containing herb-induced hepatotoxicity.
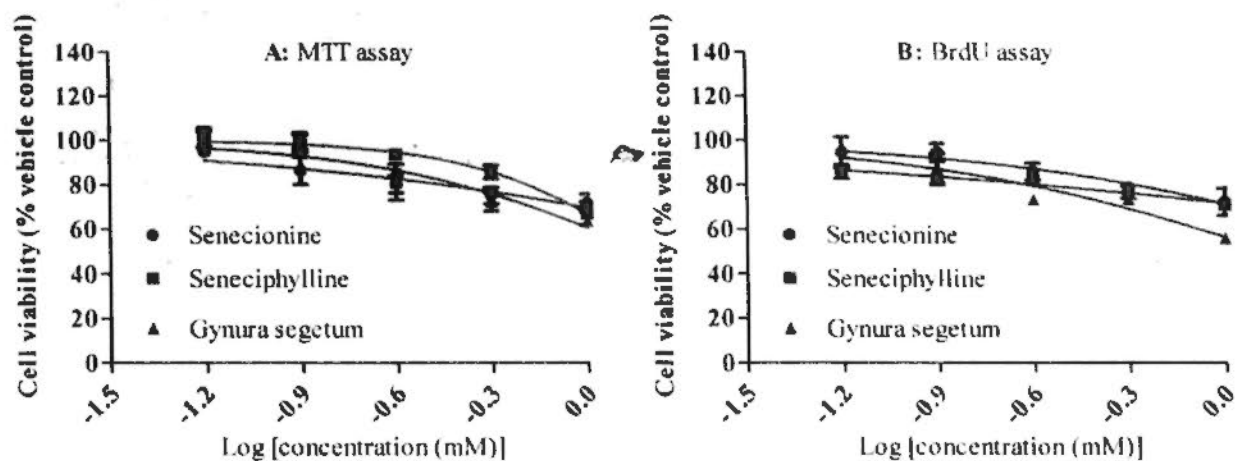
Fig.3.3. Cytotoxicity of alkaloid extract of *G. segetum* determined by MTT (A) and BrdU (B) assays. The concentration of *G. segetum* was estimated from the content of two PAs it contained.

Table 3.1 Effect of different PAs on cell viability and cell proliferation

PA	IC_{20} (mM)		
	MTT	Neutral red	BrdU
Retrorsine	0.27 ± 0.07	0.26 ± 0.09	0.19 ± 0.03
Clivorine	$0.01 \pm 0.01^{**}$	$0.03 \pm 0.00^{*}$	$0.08 \pm 0.06^{*\#\#\$}$
Platyphylline	$0.85 \pm 0.11^{*}$	$0.90 \pm 0.08^{**}$	$1.01 \pm 0.40^{\#}$
Isatidine	0.37 ± 0.15	0.54 ± 0.04	0.76 ± 0.17
Riddelliine	0.32 ± 0.08	0.34 ± 0.08	0.27 ± 0.08
Senecionine	0.34 ± 0.16	-	0.26 ± 0.05
Seneciphylline	0.66 ± 0.20	-	0.50 ± 0.25
G. segetum extract	0.39 ± 0.12	-	0.28 ± 0.04

$^{*}P < 0.05$ and $^{**}P < 0.01$ comparing with retrorsine; $^{\#}P < 0.05$ and $^{\#\#}P < 0.01$ comparing with MTT assay; $^{\$}P < 0.05$ comparing with neutral red assay.

3.4 Summary

The consumption of PAs through the intake of PA-containing herbal medicines, dietary supplements and other natural products as well as PA-contaminated food stuffs leads to serious health problems. However, the severity of hepatotoxicity of different PAs varies significantly, and thus makes it difficult to set up the regulation for a universal threshold of toxic dose of individual PAs. Our present study aims to develop a convenient and simple *in vitro* model for the rapid assessment of the severity of hepatotoxicity of different PAs using human hepatocellular carcinoma HepG2 cells. In this model, the developed combinational use of MTT and BrdU assays was able to discriminate the cytotoxicity of different PAs. The result demonstrated that among seven different types PAs tested, clivorine, a otonecine-type PA representative, was significantly more toxic than retrorsine, a retronecine-type one, while platyphylline, a platyphylline-type one, was not toxic, indicating that the developed model was able to distinguish the cytotoxicity of three types of PAs. Moreover, the cytotoxicity of *G. segetum* extract was comparable to that of the two pure PAs that it contained, senecionine and seneciphylline, demonstrating that the developed model was also suitable for the assessment of PA-containing herbs intoxication. In conclusion, we have developed, for the first time, a rapid and simple *in vitro* model for the detection of the severity of hepatic cytotoxicity of different types of PAs and also discrimination of toxic PAs from non-toxic one. This method has a potential to be used for the quick screening the toxicity of PA-containing natural products.

Chapter 4 Investigation of the Development of Hepatotoxicity Induced by

Retrorsine, a Representative PA, in Rats by Conventional Technologies

4.1 Introduction

HSOS has long been known as a serious human disease caused by ingestion of certain toxins with a series of common symptoms including abdominal pain, rapidly developing ascites and hepatomegaly (Wadleigh et al., 2003). Naturally occurring PAs are among the first identified toxins, which have caused sporadic or epidemic intoxication for HSOS through the consumption of contaminated grains and herbal medicines (Chen and Huo, 2010). The pathogenesis of hepatotoxicity or HSOS induced by pure PA administration to rats has been investigated by many studies (Chen et al., 2008; Copple et al., 2003; Copple et al., 2004; Copple et al., 2006; DeLeve, 2001; DeLeve et al., 1999; DeLeve et al., 2002; Deleve et al., 2003; Wang et al., 2000). Although these studies have defined some underlying mechanisms, the detailed events leading to the development of HSOS is still unknown (Boppre, 2011). The structural diversity among different PAs coupled with the uncertainties about their hepatotoxic targets and mechanisms make it difficult for generalizing the nature of the injury. Many new PAs poisoning cases are still reported (Bensaude et al., 1998; Ka et al., 2006; Rasenack et al., 2003).

PA poisoning is now only diagnosed based on HSOS symptoms and simultaneous detection of PA in the body or food of the patient by excluding other causes. The methods used for detection of PAs include LC-MS (Gao et al., 2009) or developed enzyme-linked immunoassay (ELISA) (Langer et al., 1996; Roeder and Pflueger, 1995; Roseman et al., 1996; Schnitzius et al., 2001). Recently, serum pyrrole-protein adducts are shown to have the potential to be used as a new biomarker for the assessment the severity of PA-induced HSOS (Lin et al., 2011). Regarding the

treatment, no specific methods have been developed other than supportive and symptomatic care (Chen and Huo, 2010; Gao et al., 2009). Furthermore, none of any mechanism-based biomarkers have been developed with the specificity and sensitivity to be used for identifying PA intoxication *in vivo*. Additional work is needed to define a representative model to better identify risks and better prognose the outcome for exposed animals. Thus ongoing work, including development of a suitable animal model and investigation of specific toxic targets are needed to help understand the pathogenesis and enable us to develop effective therapeutic or preventive options.

As discussed earlier, PAs could induce a variety of acute and chronic pathological lesions in the livers of animals, even after administration of a single sublethal dose (Mattocks, 1986). The lesions of PA-induced toxicities are proved to be dose-dependent and are histologically characterized as acute and chronic courses (Stegelmeier et al., 1999). The quick and general changes caused by high doses of PA ingestion are recognized as acute intoxication and animals develop panlobular hepatocellular damage characterized by acute extensive necrosis with hemorrhage and minimal inflammation (Stegelmeier et al., 1999). Some animals exposed to low doses of PA may not develop liver disease. The progressive nature of chronic PA intoxication suggests that low, chronic PA exposure has cumulative effects. Currently, little is known about what doses or durations will ultimately lead to damage. More information is thus needed to identify these 'safe' exposure limits. Also whether there is a strict dose-dependent character is needed to be delineated. Additionally, more work is needed to better define its progression and to identify markers to predict how animals will progress after exposure.

Therefore, in the starting part of the *in vivo* study, a reliable and reproducible animal model was developed to form a solid foundation for further mechanism

study. Retrorsine, a retronecine-type PA, was used as the representative to induce an acute hepatotoicity in rats. The dose-dependent response and the progress of hepatotoxicity were defined by investigating the extent of hepatotoxicity at different doses using conventional technologies.

4.2 Materials and Methods

4.2.1 Materials

Peroxidase, N, N-dimethylformamide, 3, 3', 5, 5' - tetramethyl benzydine (TMB), hydrogen peroxide (H_2O_2), bilirubin, sulfanilic acid, and sodium nitrite were purchased from Sigma-Aldrich Corporation (St. Louis, MO, USA).

4.2.2 Animals

Male Sprague-Dawley rats weighting 240–260 g were supplied by the Laboratory Animal Services Centre at the Chinese University of Hong Kong. Animals were allowed food and water *ad libitum*. They were housed no more than 3 to a cage on chip bedding. The animals were maintained on a 12-h dark/light cycle in a controlled temperature (18–25 °C) and humidity (55 ± 5 %) environment for a period of 3 days before use. All procedures on animals as detailed below were conducted under the license provided by the Government of Hong Kong and followed the guidance for animal treatments set by the Animal Experimental Ethics Committee, The Chinese University of Hong Kong.

4.2.3 Treatment Protocol

Retrorsine was dissolved in sterile saline acidified by 2.0 M HCl. The pH was then raised to 7.0 by titrating with 1.0 M NaOH and the volume was adjusted with sterile saline to the appropriate final concentration. Rats in treatment groups were

orally treated with a single low, medium or high dose of retrorsine (35, 70 or 140 mg/kg, $n = 6$), while the ones in vehicle control group were administered with sterile saline ($n = 6$) correspondingly. The three doses of retrorsine used were corresponding to 0.7, 1.4 and 2.8 fold of its median lethal dose (LD_{50}) respectively. The gavage volume for all groups was 1 ml/kg of rat. The rats were then fasted for 24 h before being sacrificed.

4.2.4 Sample Collection

At 24 h after treatment, rats were weighted and anesthetized with 20% urethane (5 ml/kg, ip). Blood was collected from the descending aorta into a syringe. Half of them were added to tubes containing trisodium citrate (0.38% final concentration) to obtain plasma for measurement of ALT, LDH, GSH and MPO. The remaining was transferred into a glass tube and put in the room temperature for 2 h to prepare serum for the measurement of TB level. Liver was weighted for calculating relative liver weight (RLW) [RLW = liver weight (LW)/body weight (BW) × 100%]. One transverse section from the central region of the left lateral live lobe and one transverse section from the left lung were fixed in 4% formalin solution before being processed for H&E staining. The remaining liver was snap-frozen in liquid nitrogen for GSH, ratio of GSSG to GSH (GSSG/GSH), and glutathione reductase (GR) analysis as described below.

4.2.5 ALT Activity in Plasma

Hepatocytes damaged by necrosis release intracellular ALT into the circulation and is detected by increase in levels of plasma ALT, which is used as the standard but not specific clinical and experimental indicator of hepatotoxicity (Amacher, 1998). ALT activity in plasma was measured by a standard spectrophotometric

method (Reitman and Frankel, 1957). Briefly, 100 µl of freshly collected plasma or different concentrations of sodium pyruvate (used to make standard curve) were added to 0.5 ml ALT substrate solution (the mixture of 0.2 M L-alanine and 1.8 mM α-ketoglutaric acid prepared in PBS) and left in a water bath at 37°C for 30 min. Then 0.5 ml of 1 mM DNP color reagent was added to the reaction system and incubated for 20 min. And 5 ml of 0.4 M NaOH was added and the absorbance of the mixture was detected on a spectrophotometer at 505 nm. The value of ALT activity was calculated according to the formula of standard curve.

4.2.6 TB Level in Serum

TB has been recommended as a better indicator of disease severity compared to ALT in acute human hepatic injury (Dufour et al., 2000a, b). The principle of TB assay is that bilirubin reacts with diazotized sulfanilic acid to produce azobilirubin, which has an absorbance maximum at 560 nm in DMSO. The intensity of the color produced is directly proportional to the amount of TB concentration (Fossati et al., 1989). In brief, TB reagent (16 mM sulfanilic acid, 164 mM HCl, 4.4 M DMSO) and sodium nitrite reagent (0.6 M sodium nitrite) as well as calibrator solution (5 mg/dl bilirubin) were freshly prepared before assay. Then 20 µl of freshly collected serum or 5mg/dl bilirubin were added to 303 µl of bilirubin working reagent (the mixture of 300 µl TB reagent and 3 µl sodium nitrite reagent) and left at room temperature for 5 min. Then the absorbance of the mixture was detected at 550 nm. The following formula, bilirubin (mg/dl) = A/Ac × bilirubin value of calibrator (A = absorbance of testing sample, Ac = absorbance of calibrator) was used to calculate the bilirubin concentration.

4.2.7 LDH Release in Plasma

The release of cytoplasmic LDH into extracellular environment only occurs in dead cells (for example, liver parenchyma cells) or cells that have lost their membrane integrity such as in hemolysis. LDH release may thus indicate liver damage (Abraham, 2006). The assay was performed according to the protocol of the commercially-available kit. Briefly, 100 μl of the reaction mixture (provided in the kit) were added to 50 μl freshly collected plasma and incubated for 30 min at room temperature. The absorbance of the solution was measured at 490 nm, with background subtraction at 620 nm. LDH release in the treatment group was expressed as a percentage of the vehicle control.

4.2.8 H&E Staining of Liver Section and Lung Section

The liver and lung tissues were processed through dehydration from 70%, 80%, and 95% ethanol solutions twice, 5 min each and xylene twice, 3 min each, before being incubated in paraffin wax twice, each for 10 min, and then embedded in paraffin. The paraffin-embedded tissues were cut at 5 μm and collected on positively charged microslides (Superfrost® Plus slide, Menzel-Glaser). For H&E staining, the sections were dried overnight for adherence and then were rehydrated by series of xylene and gradient ethonal immersion (xylene 3 times each for 5 min, 95%, 80% and 70% ethanol, each for 5 min). After rehydration, slides were immersed in haemetoxylin for 1.5 min, and then rinsed with tap water. Then, the slides were immersed in acidified alcohol for 1 min, followed by being rinsed with tap water. After being rinsed with Scott's Tap water for 10-20 s, the slides were viewed under bright field microscope to check the status of nuclei staining. Then the slides were immersed in eosin for 5 min, quickly rinsed with tap water and viewed under bright field microscope to check the status of cytoplasm staining. Then, the slides were

subjected to dehydration by a series of gradient ethanol solutions (70%, 80%, 95% and 100%) each for 5 min and then xylene twice for 5 min. The sections were mounted with Permount (Fisher Scientific) and covered with coverslips. Then the photomicrographs of the sections were taken under a light microscope (Zeiss, AXIOSKOP 2 PLUS) connected with a Spot cooled CCD camera (Spot Diagnostic instrument) under the control of a Metamorph imaging system (University Imaging Corporation, Downington, PA, USA).

4.2.9 Immunostaining of RECA-1

For liver EC immunostaining, rats ($n = 3$) were anesthetized with 20% urethane (5 ml/kg, ip) and transcardially perfused with 0.9% saline followed by 4% paraformaldehyde (PFA). A 1 cm^3 block of liver cut from the central and perhipheral region of the live lobe were post-fixed overnight in 4% PFA and then were dehydrated through a graded series of (10%, 20% and 30%) sucrose solution. The blocks were frozen in Tissue-Tek® O.C.T.™ Compound for 8 min in isopentane immersed in liquid nitrogen. For immunostaining, 10 μm thick sections of frozen liver were incubated with blocking solution (PBS containing 10% goat serum, VC-S-1000-L020, Vector laboratories, CA, USA) for 1 h, then with mouse anti-rat endothelial cell antigen-1 (RECA-1, ab 9774, Abcam, Cambridge, MA, USA), diluted (1:100) in blocking solution overnight at 4 °C. In the liver, this antibody binds to rat endothelium but not other cell types (Duijvestijn, et al, 1992). In the liver, this antibody stains both SECs and central vein endothelial cells (CVECs). After incubation with the RECA-1 antibody, sections were incubated for 1 h with biotinylated goat anti-mouse secondary antibody (Vector Laboratories, Burlingame, CA), and then with Streptavidin Alexa Fluor 488 conjugate (Invitrogen, USA) in blocking solution. Sections were washed 3 times, 5 min each, with PBS and

counterstained with mounting medium containing DAPI (VC-H-1200-L010, Vector laboratories, CA, USA) to exhibit the nucleus. The slides were examined and visualized using a confocal microscope system (Olympics Fluoview FV-1000). All treatment groups and the negative controls without primary or secondary antibody were stained in parallel at the same time.

4.2.10 GSH Level in Plasma and Liver Homogenate

GSH concentration was determined by the method of Tietze (1969). Briefly, liver homogenates were prepared by suspending 100 mg liver tissue in 0.9 ml of potassium dihydrogenphosphate/EDTA/ethanol solution, and homogenized at $4^{\circ}C$. The tissue homogenates were centrifuged at 10,000 g for 15 min at $4^{\circ}C$, and clear supernatant was obtained. Then 30 µl freshly collected plasma, supernatant of liver homogenate or different concentrations of GSH (used to make standard curve) were mixed with 150 µl of 1.5 mg/ml DTNB and 2820 µl of 0.1 M PBS. The tube was shaken and left at room temperature for 20 min and then the absorbance was detected at 412 nm. The GSH concentration of each sample was calculated according to the standard curve with a R^2 equaling to 0.9949. GSH level in the treatment groups was expressed as a percentage of the vehicle control.

4.2.11 GR Activity in Liver Homogenate

GR activity was determined using Cayman's GSH assay kit (703002, Cayman Chemical Co) by measuring the rate of NADPH oxidation. The oxidation of NADPH to $NADP^+$ is accompanied by a decrease in absorbance at 340 nm (A340). Since GR is present at rate limiting concentrations, the rate of decrease in the A340 is directly proportional to the GR activity in the sample (Carlberg and Mannervik, 1985). Briefly, 20 µl supernatant of liver homogenate and 20 µl of GSSG were added into

100 µl assay buffer. The reaction was initiated by adding 50 µl NADPH to the system and the absorbance was read once every minute at 340 nm. For background and positive control, the sample supernatant was replaced by assay buffer and diluted GR respectively. One unit of enzyme activity yields the reduction of 1 µ mol GSH disulfide/min. Results were expressed as µ mol /min·mg liver.

4.2.12 Ratio of GSSG/GSH in Liver Homogenate

The accurate measurement of GSSG levels has proved to be difficult due to the low amount of GSSG in tissues as well as the absence of effective methods to prevent oxidation of GSH to GSSG during sample preparation. The GSSG level was thus indirectly obtained by subtracting the value of reduced GSH from total GSH, which was obtained by the addition of GR and NADPH to deoxidize GSSG (Pastore et al., 2003). The ratio of GSSG/GSH was calculated by the formula of GSSG/GSH = (total GSH-reduced GSH)/reduced GSH.

4.2.13 MPO Activity in Plasma

MPO is a peroxidase enzyme most abundantly present in neutrophil granulocytes and has been used as a biomarker of neutrophil accumulation and represents oxidative stress process (Heinecke et al., 1993a; Heinecke et al., 1993b). MPO activity in the plasma was measured by a modified method as described previously (Ko and Cho, 2005) using H_2O_2 and TMB. In brief, the reaction was started at 25°C for 5 min in a tube by adding 50 µl plasma or horseradish peroxidase, 150 µl of 2 mM TMB solution (in 8% N, N-dimethylformamide), and 250 µl of 80 mM PBS (pH 5.4). Next, 50 µl of 0.3 M H_2O_2 was added and the mixture was incubated at 25°C for another 25 min. The reaction was stopped by the addition of 2.5 ml of 0.5 M H_2SO_4 and quantified at 450 nm. Horseradish peroxidase was used as standard

(ranging from 0–40 mU/ml). One unit of horseradish peroxidase (from plasma samples or standard solutions) will oxidize 1 µmole of the reaction product 2, 2'-azino-bis 3-ethylbenzthiazoline-6-sulfonic acid per min at 25°C under pH 5.0. One unit of MPO activity is defined as degradation of 1 µmol H_2O_2/min at 25 °C. Results were expressed as mU/ml plasma.

4.2.14 Statistical Analysis

All data are represented as mean values ± SEM unless otherwise stated. For the comparison of different treatments in two or more than two groups, the data were analyzed by student's t-test or ANOVA followed by Bonferroni's multiple comparison post hoc test using GraphPad Prism 5.0, respectively. Differences were considered statistically significant at $P < 0.05$.

4.3 Results and Discussion

4.3.1 Elevation of Liver Weight Induced by Retrorsine

As shown in Table 4.1, no significant differences in body weight were observed upon retrorsine treatment among all groups. To estimate the general status of rats, the net decrease of body weight was measured by calculating the difference between pre-treatment and 24 h post treatment. The results showed that no significant difference was detected in net body weight decrease and body weight of post treatment among all groups. The results suggested that at the doses tested, retrorsine did not exhibit a deleterious effect on the general status of animal, which implied that the injury maybe limited within the liver. However, liver weight and relative liver weight were dose-dependently increased by retrorsine treatment, which was significant at high dose treatment ($P < 0.05$ comparing with vehicle control), indicating the development of hepatomegaly. For hepatomegaly, there are three

possible reasons: 1) more parenchyma formation caused by liver regeneration, 2) the enlargement of individual liver cells and 3) the retention of blood or/and fluid within the liver. But when considering the stage of pathogenesis, a 24 h exposure is believed to be insufficient for eliciting liver regeneration. The latter two causes were then investigated by further histological and biochemical studies. No spontaneous death was observed at any of the doses examined, which confirmed that the present dose range did not influence the general status of animal. This result is also accordant to previous studies indicating that the acute death occurred most frequently between 3 and 7 days after the animal received a single dose of PA (Mattocks, 1986). The relatively limited damage to rat induced by a 24 h exposure may ensure that the further mechanism studies shall be controlling.

Table 4.1 Effects of low, medium and high dose (35, 70 and 140 mg/kg) of retrorsine treatment on body weight and liver weight of rat

Group	BW (g) Pre-treatment	24 h BW (g) Post treatment	Net BW decrease (g)	LW (g) Post treatment	RLW (%) Post treatment
Vehicle	258.2 ± 8.0	236.0 ± 10.1	21.8 ± 3.3	7.5 ± 0.6	3.20 ± 0.32
Low	253.8 ± 8.3	231.8 ± 9.8	22.0 ± 3.0	7.9 ± 0.3	3.40 ± 0.14
Medium	247.6 ± 6.7	227.1 ± 5.8	20.4 ± 4.2	7.9 ± 0.2	3.48 ± 0.13*
High	262.3 ± 9.2	240.0 ± 3.3	25.2 ± 3.9	9.0 ± 0.9*	3.74 ± 0.33*

BW: body weight; LW: liver weight; RLW: relative liver weight. Data are presented as Mean ± SD ($n = 6$). *$P < 0.05$ comparing with vehicle control.

4.3.2 Parenchymal Cell Damage Induced by Retrorsine

Blood ALT activity level is the most frequently used laboratory indicator of hepatotoxic effects and is considered as a gold standard clinical chemistry marker of liver injury (Ozer et al., 2008). As shown in Fig.4.1A, retrorsine dose-dependently

produced hepatic parenchymal cell injury in rats as measured by a statistically significant elevation of ALT release into the plasma. The elevation of ALT activites is thought to be caused by enzyme leakage associated with hepatic parenchyma cell damage. Damaged hepatocytes release their contents including ALT into the extracellular compartment. The released enzymes ultimately enter into circulation and thereby increase the plasma levels of ALT compared to control subjects.

ALT plays an important role in amino acid metabolism and gluconeogenesis. It catalyzes the reductive transfer of an amino group from alanine to alpha-ketoglutarate, to yield glutamate and pyruvate. Recently, two ALT isozymes, ALT_1 and ALT_2, have been identified based on molecular structure and tissue specificity pancreas (Lindblom et al., 2007) and only a small part of ALT_1 are localized in human hepatocytes. Importantly, ALT activity is proved to be a composite of ALT_1 and ALT_2 isozyme activities because ALT_2 also catalyzes alanine transamination like ALT1 (Yang et al., 2002). Thus, the increase in plasma ALT activity induced by retrorsine treatment may also arise from some unknown extra-hepatic injuries. For example, ALT_2 isozymes are also detected n renal tubular epithelial cells, salivary gland epithelial cells and cardiac myocytes (Lindblom et al., 2007). Accordingly, an assay that can discriminate between these two isozymes can therefore be expected to aid in differentiating the tissue source of ALT activity and may help determine whether other tissues are involved in the process of PA intoxication.

Although the overall clinical utility of plasma ALT measurements is authorized and common, it does not always correlate well with preclinical histomorphologic data. Thus, additional markers are sought to add information to plasma ALT enzymatic signals. Some markers with greater specificity to liver could be used in conjunction with ALT for the safety evaluation. In human, TB and LDH are conventional

markers of liver function that have complementary advantages when used together with plasma ALT activity, especially with regard to the differential diagnosis of biliary function. Thus, the assessment of TB and LDH release were used to confirm the retrorsine-induced liver injury.

As shown in Fig.4.1B and C, a significant elevation of serum TB level and LDH release were only observed after high dose treatment, suggesting that a severe toxicity only occurred after high dose treatment. TB is composed of direct (hepatic) and indirect (non-hepatic) bilirubin, which elevates when there is excessive destruction of hepatocyte as well as hemolysis. Interestingly, we assumed earlier that the hepatomegaly induced by high dose retrorsine treatment might be caused by blood retention in the liver. Similarly, the detected remarkable elevation of TB level and LDH release at high dose treatment might be due to hemolysis as a result of blood retention.
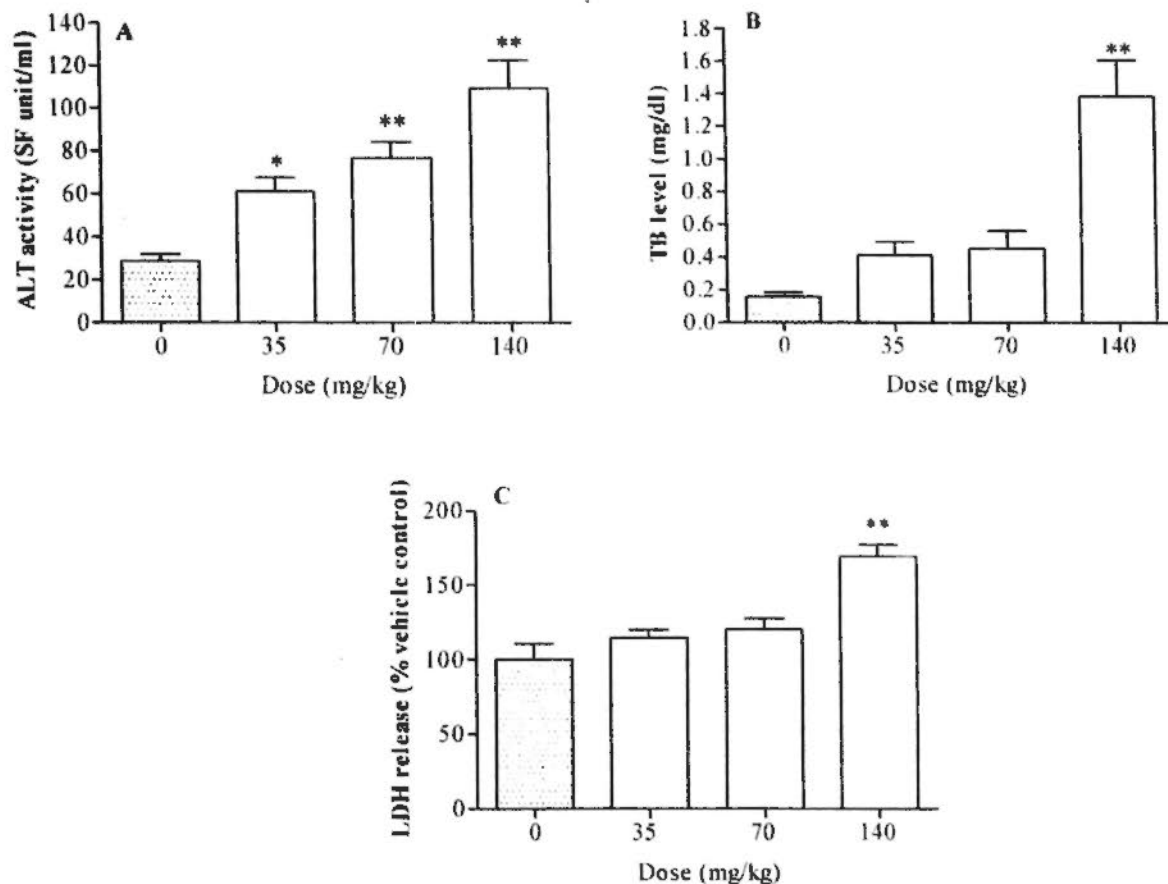
Fig.4.1. Effects of retrorsine on liver injury in rats after 24 h administration as demonstrated by A) ALT activity in plasma, B) TB level in serum and C) LDH release in plasma. *$P < 0.05$ and **$P < 0.01$ comparing with vehicle control.

4.3.3 Histological Changes of Liver Produced by Retrorsine

Livers obtained from rats treated with vehicle control showed normal lobule, central vein and sinusoid morphology as indicated in Fig.4.2A, A' and A''. Central regions of liver lobe isolated from rats treated with high dose retrorsine exhibited extensive lesions including sinusoid hemorrhage and lobule disarray (Fig.4.2D, D' and D''). As shown in Table 4.2, 4 out of 6 and 5 out of 6 rats treated with high dose retrorsine exhibited both lesions and sinusoid hemorrhage respectively; whereas only 2 out of 6 rats treated with medium dose exhibited sinusoid hemorrhage, which indicated a large variations of the liver in response to this dose. None of the rats treated with low dose exhibited obvious histological lesions.

The occurrence of extensive sinusoid hemorrhage and lobule disarray with severe parenchymal cell damage confirmed that severe liver lesions were developed at high dosage as supported by a notable elevation of TB level and LDH release. The presence of enlarged hepatocytes containing large, hyper-chromatic nuclei, termed megalocytosis, is a characteristic feature of PA-induced chronic hepatotoxicity in experimental animals, which occurs through the potent antimiotic action of the pyrrole metabolite of PAs (Mattocks, 1986). However, this change was not observed in the present acute rat model, implying that the pathogenesis of PA-induced acute hepatotoxicity is different from that of chronic process. This result also excludes the possibility that the observed hepatomegaly is caused by enlargement of the individual cells as discussed earlier. It could be affirmed that the hepatomegaly should be caused by blood retention in the liver due to the extensive sinusoid hemorrhage because they were simultaneously observed at high dose treatment. Similarly, the remarkably elevated TB level and LDH release induced by high dose treatment may also be due to hemolysis and extensive hepatocyte injury caused by severe hemorrhage. Since no biliary occlusion was observed during histological examination, the increase in TB levels was most likely due to the hemorrhage.
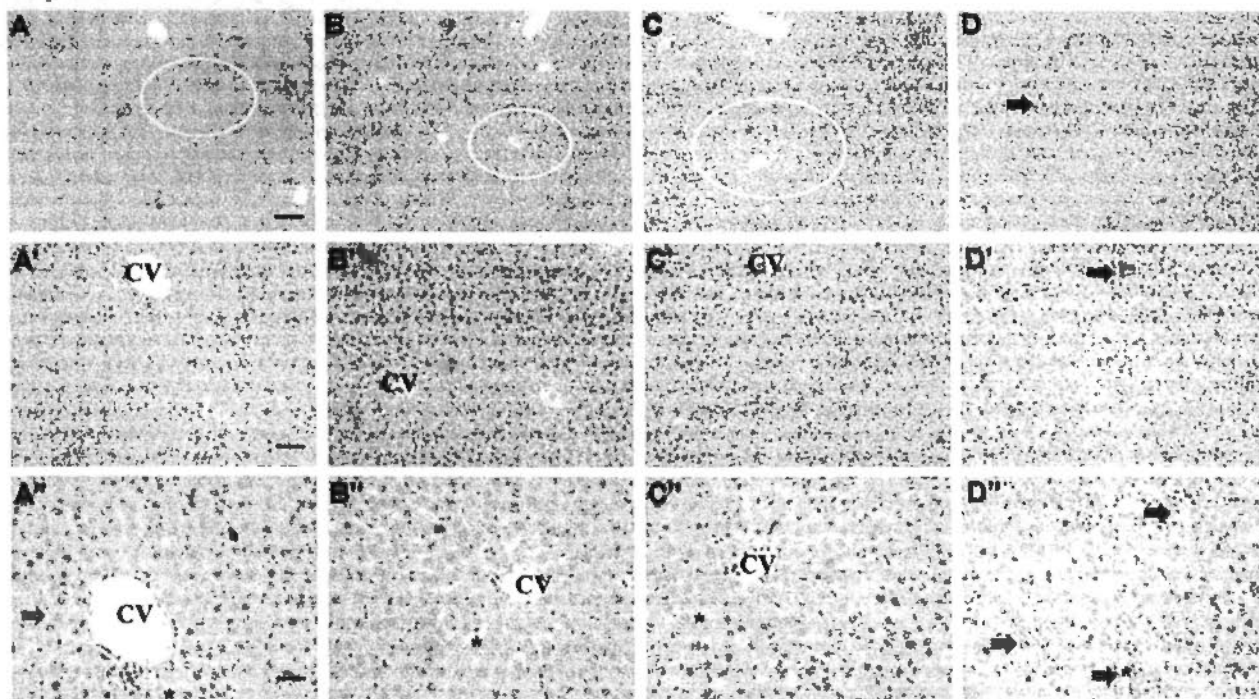
Fig.4.2. Effects of retrorsine on the histology of liver. Representative hematoxylin and eosin staining images of the middle regions of liver section obtained from rats treated with A), A'), A'') saline, B), B') and B'') 35 mg/kg retrorsine, C), C') and C'') 70 mg/kg retrorsine and D), D') and D'') 140 mg/kg retrorsine. Scale bar in (A-D) = 100 μm; (A'-D') = 50 μm; (A''-D'') = 25 μm. The central vein is abbreviated as CV and sinusoid is indicated in asterisk. Sinusoid hemorrhage and lobule disarray are indicated by black arrow and no appearance of a circled area respectively.

Table 4.2 Histological changes in the middle regions of liver of rats treated with low, medium and high dose (35, 70 and 140 mg/kg) of retrorsine

Histological change	Number of rats		
	Low	Medium	High
Sinusoids hemorrhage	0	2	5
Lobular disarray	0	0	4

4.3.4 Histological Changes of Lung Produced by Retrorsine

As indicated in Fig.4.3A, A' and A'', the alveolar sac, the surrounding alveoli and blood capillaries were normally present in the section of lungs obtained from rats treated with vehicle control. No obvious lesions were observed in the lung sections of retrorsine-treated rats as shown in Fig.4.3B-D, B'-D', B''-D''. The absence of lesions in the lung indicated that the toxicity of retrorsine might be limited within the liver, which was in partial agreement with a previous study that gastric intubation of retrorsine produced severe liver lesions but minimal lung lesions in Vervet Monkeys (Mattocks, 1986). However, monocrotaline, a very often used representative PA in model development, has been proved to be more potent to elicit toxicity in lung (Mattocks, 1986). The discrepancy of toxicity of PAs to different organs is determined by the stability and clearance of the intermediate metabolite in the liver. A higher stability as well as slower clearance allows the toxic metabolite to attain extra-hepatic organ for exerting its toxicity (Mattocks, 1986). Regarding model development, a limited or localized drug response within specific organ should be better for simplifying the illustration and elucidation of underlying specific mechanisms. Thus, due to no involvement of pulmonary toxicity, the use of retrorsine as the representative PA to develop the hepatotoxicity model is more suitable than the use of monocrotaline.
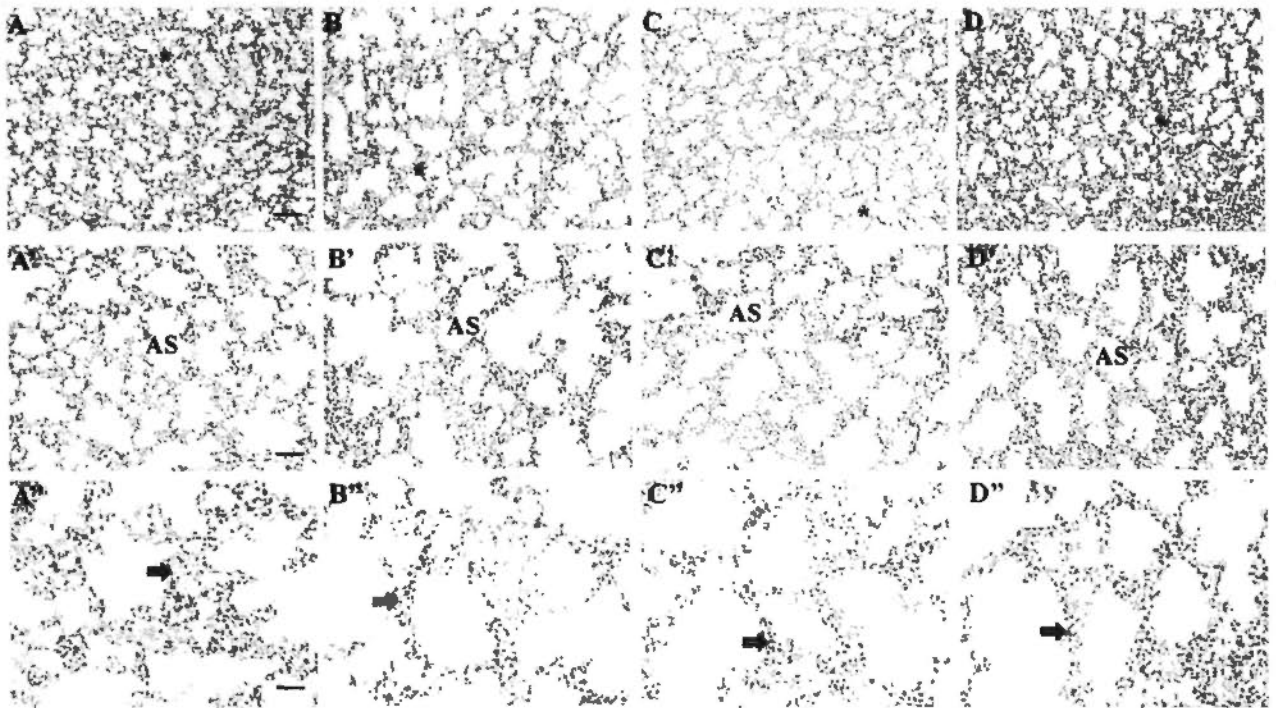
Fig.4.3. Effects of retrorsine on the histology of lung. Representative hematoxylin and eosin staining images of the lung section obtained from rats treated with A), A'), A'') saline, B), B') and B'') 35 mg/kg retrorsine, C), C') and C'') 70 mg/kg retrorsine and D), D') and D'') 140 mg/kg retrorsine. Scale bar in (A-D) = 100 μm; (A'-D') = 50 μm; (A''-D'') = 25 μm. The blood capillary, alveolar sac and surrounding alveoli are indicated as asterisks, AS and black arrows, respectively.

4.3.5 RECA-1 Staining of Central Regions of the Liver Lobe

Since SECs cannot be observed under light microscope, the possible damage to them may be easily overlooked by H&E staining. To make the cells visible, liver sections were immunohistochemically stained with RECA-1 antibody. Sections of the central regions of the liver lobe from rats treated with saline showed continuous RECA-1 staining along the sinusoids and lining of CV of the liver (Fig.4.4A, A' and A''), suggesting that RECA-1 antibody recognizes both SECs and CVECs in the liver. However, in livers obtained from rats treated with retrorsine, RECA-1 staining density within the sinusoids and CV decreased, indicating the loss of ECs

(Fig.4.4B-D, B'-D' and B"-D"). When the percentage of EC loss was less than 50%, the degree of damage was indicated as slight (+), between 50–80% as mild (++), and over 80% as severe (+++). Approximate 40% (+) of the ECs were lost after low dose (Fig.4.4B, B' and B", Table.4.3), 70% (++) lost and staining in the CV became discontinuous (+) after medium dose (Fig.4.4C, C' and C", Table.4.3), and no sinusoids (+++) were detected and the CV was severely discontinuous (++) after high dose treatment (Fig.4.4D, D' and D", Table 4.3). No staining was observed in the negative controls in which the primary or secondary antibody was not added.

It has been suggested that PA-induced damage to SECs in rats results in microcirculatory disturbances that lead to hypoperfusion of the liver and consequently parenchymal cell injury (DeLeve et al., 1999). Observations presented herein support this hypothesis because the dose onset of destructions of SECs and CVECs preceded the parenchymal cell damage. A previous study showed that retrorsine could inhibit hepatic protein and RNA synthesis (Aston et al., 1996). Thus, the damage of retrorsine to SECs was supposed to be caused by a possible inhibition of SECs regeneration by inhibiting their constituent proteins.
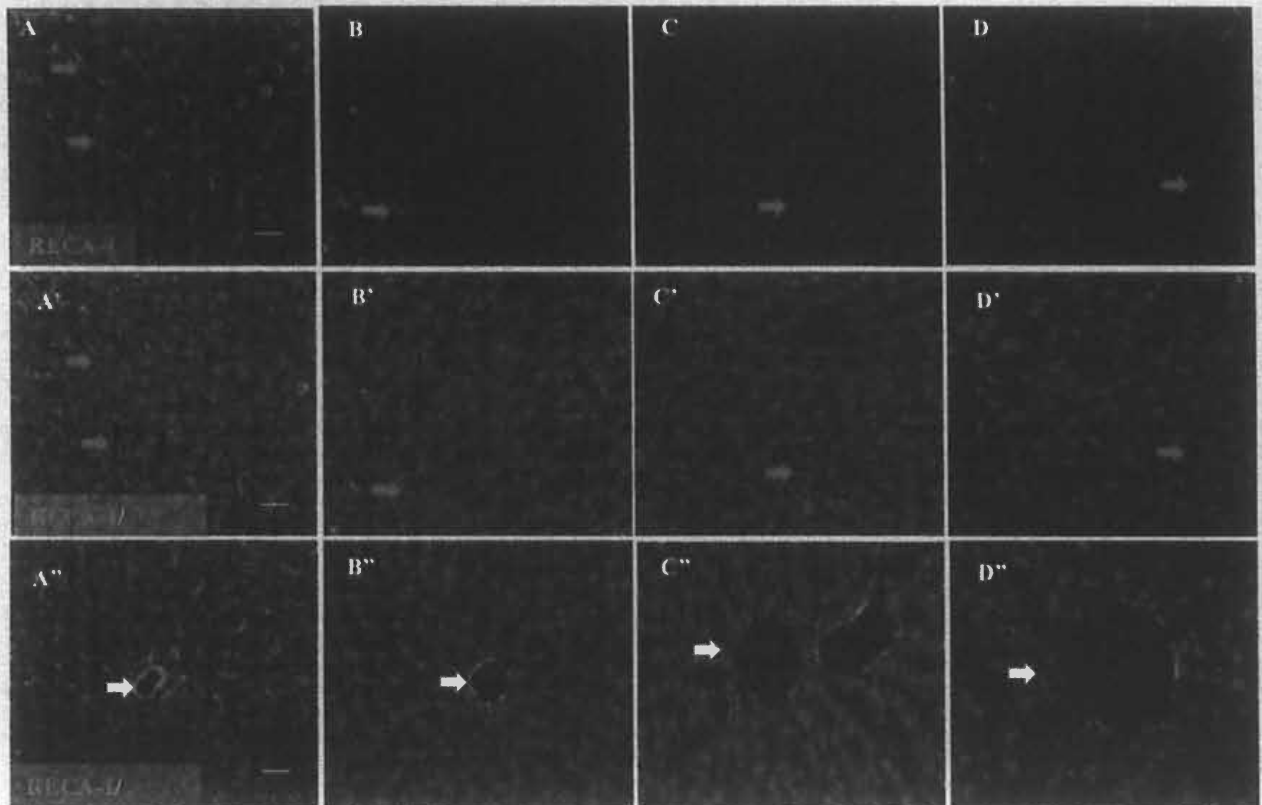
Fig.4.4. Effects of retrorsine on RECA-1 immunostaining in middle regions of the rat liver. Liver sections were obtained from rats treated with A), A'), A'') saline, B), B') and B'') 35 mg/kg retrorsine, C), C') and C'') 70 mg/kg retrorsine and D), D') and D'') 140 mg/kg retrorsine. The sinusoids are shown by green staining and indicated with red arrows. A'-D' and A''-D'': Double immunostaining with RECA-1 and DAPI (shown in blue) for sinusoids and central vein (CV, indicated with white arrow) respectively. Scale bar in (A-D, A'-D' and A''-D'') = 25 μm.

4.3.6 RECA-1 Staining of Peripheral Regions of the Liver Lobe

Similarly, in the peripheral regions of the liver lobe from rats treated with saline, RECA-1 staining was obvious and continuously present along the sinusoids (Fig.4.5A, A' and A''). However, in livers from rats treated with medium or high dose retrorsine, RECA-1 staining within the sinusoids was reduced (Fig.4.5C, C' and D, D'). There was no obvious loss of ECs in the liver after low dose (Fig.4.5B, B' and Table 4.3), whereas about 30% (+) of the ECs disappeared in medium dose

(Fig.4-5C, 5C' and Table 4.3) and 50% (++) disappeared in high dose of retrorsine treatment (Fig.4.5D, D' and Table 4.3). RECA-1 staining was present continuously along the lining of the CVs of the liver in all doses treatment groups (Fig.4.5A", B", C", D" and Table 4.3).

A progressive injury from the central to peripheral regions of rat liver lobe was revealed by comparing the RECA-1 staining between these two regions. The underlying mechanism is presumably attributed to the differences in the extent of metabolic activation and/or detoxification of PA in these two regions (DeLeve et al., 2002). Bioactivation by CYP3A4 has been proved to be required for PAs to produce liver injury (Schultze and Roth, 1998; Wilson *et al.*, 1992). Thus, we hypothesize that a higher expression of CYP3A4 in liver cells in the central regions may contribute to a greater toxicity observed when compared to peripheral region. However, CYP3A4 is expressed in both parenchymal cells and SECs (Lester *et al.*, 1993) and it is still unclear which one or whether both kinds of cells are involved in metabolic activation of PAs. The regional distribution of CYP on both cell types needs to be investigated as CYP3A4 has been shown to have zonal distribution in parenchymal cells (Oinonen and Lindros, 1998) and possibly also in SECs (Scoazec *et al.*, 1994). Alternatively, the greater toxicity of PA observed in the central regions may be attributed to a lower level of detoxification. In livers of humans exposed to PAs, damage to SECs occurred in all regions of the liver lobule (Brooks *et al.*, 1970) and no difference was observed between central and peripheral regions.

McLean (1970) demonstrated, through transillumination studies on rats, that the outlet end of the sinusoids is blocked by stationary columns of red blood cells, 16–24 h following administration of PAs. The reaction is typically patchy and results in stasis and extravasation of red cells spreading backwards from the centre of the lobule. Portal pressure is significantly raised 3 days after administration, notably

before the first appearance of collagenous venous occlusion at 7 days. McLean (1970) observed that 6–10 days after PA administration, a new irregular pattern of vascular flow, contrasting with the uniform radial pattern of flow in the normal liver lobule, develops, which corresponds to the bypass channels represented by dilated paraseptal sinusoids, as observed in human liver biopsies. Segments of central vein into which the blocked sinusoids open, are gradually abandoned in favour of such by-pass routes and undergo occlusion first by oedematous connective tissue and then by fibrosis. The mechanism of closure of the sinusoids is not clear. A toxic action on the sinusoidal or venous endothelium, which swells and occludes the lumen, seems possible, as suggested by electron microscopic studies on the monkey, and studies on children. The endothelial lining of the vessels is denuded and replaced by a fibrinous and proteinaceous precipitate, which, together with the oedematous wall of the vessel, becomes organized and slowly replaced by fibrous connective tissues. The occlusion of sinusoids is further contributed by the discharge of cellular debris into the space of Disse. The lumen of the sinusoids becomes occluded simultaneously with the fibrosis occurring in the central vein. Collagen fibres extend into the space of Disse and sinusoids leading to a fibrosis.
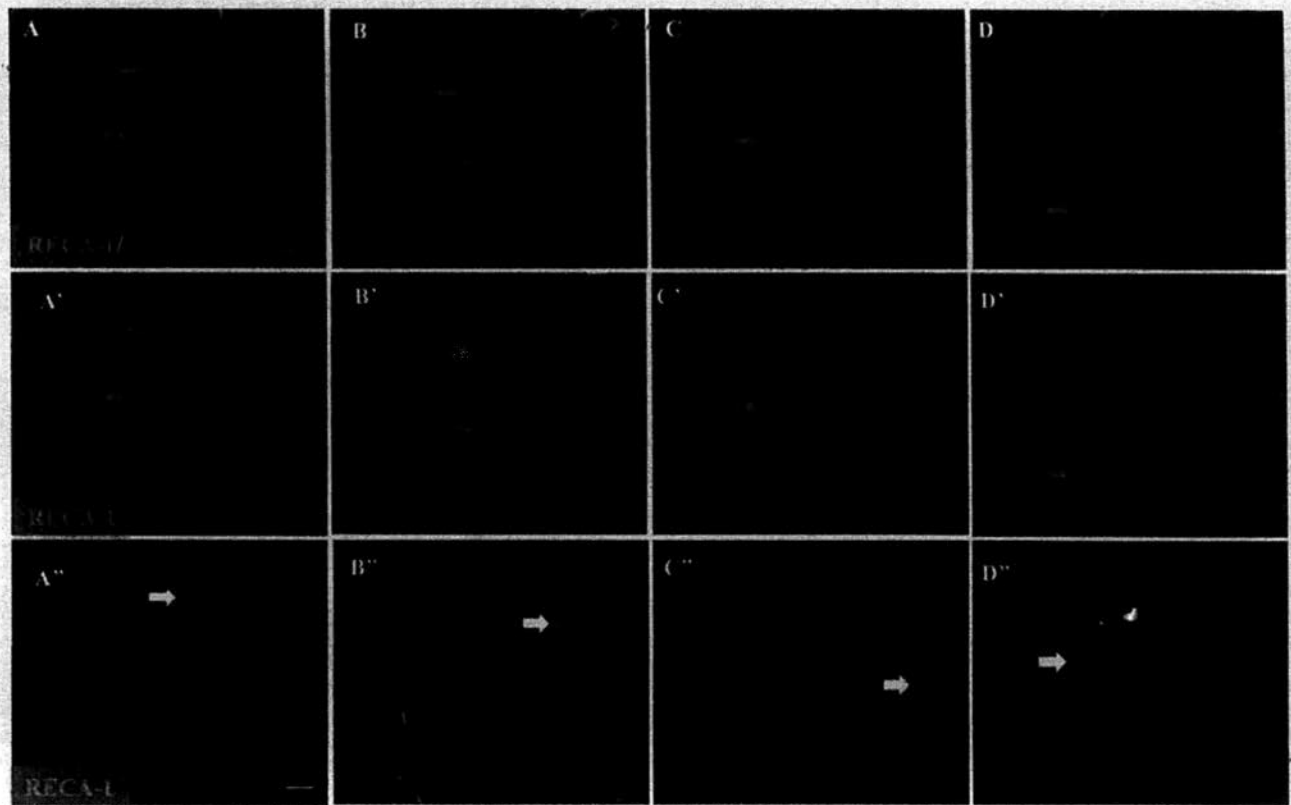
Fig.4.5. Effects of retrorsine on RECA-1 immunostaining in perhipheral regions of the rat liver. Liver sections obtained from rats treated with A), A'), A'') saline, B), B') and B'') 35 mg/kg retrorsine, C), C') and C'') 70 mg/kg retrorsine and D), D') and D'') 140 mg/kg retrorsine. The sinusoids are shown by green staining and indicated with red arrows. A'-D' and A''-D'': Double immunostaining with RECA-1 and DAPI (shown in blue) for sinusoids and central vein (CV, indicated with white arrow) respectively. Scale bar in (A-D and A'-D') = 25 µm; (A''-D'') = 50 µm.

Table 4.3 Loss of SECs and CVECs induced by low, medium and high dose (35, 70 and 140 mg/kg) of retrorsine treatment

Region of liver	Cell type	Severity		
		Low	Medium	High
Central	SEC	-	+	++
	CVEC	-	-	-
Peripheral	EC	+	++	+++
	CVEC	-	+	++

−: Absent; +: slight, ++: mild; +++: severe.

112

4.3.7 GSH Disturbance Induced by Retrorsine

Intracellular GSH functions as the major anti-oxidant and provides a first line of defense against oxidative and chemical injury (Wu et al., 2004). As shown in Fig.4.6A, no significant difference in plasma GSH levels was observed after rats were treated with low or medium dose of retrorsine when compared with vehicle control group. However, high dose retrorsine induced a significant increase og GSH levels in plasma, suggesting an increased release of GSH into systemic circulation caused by the destruction of cells, which was in accordance with previous results obtained from assays of ALT, TB, LDH and histological examination. These findings consistently suggested that the liver injury induced by high dose treatment was severe. In addition, hepatic GSH concentration and GR activity were increased by retrorsine in a dose-dependent manner. This increase was significant starting from medium dose treatment as shown in Fig.4.6B and C. As discussed earlier, PA is detoxified by forming a conjugation with GSH. Thus, the increased level of hepatic GSH may indicate a motivating of GSH to detoxify more toxic pyrroles produced by medium or high dose of retrorsine, that is, the conjugation of GSH was probably increased. Furthermore, GSH exists in both reduced (GSH) and oxidized (GSSG) form and GR is the enzyme responsible for the conversion of GSSG to GSH (Pastore et al, 2003). Thus, the simultaneously observed increase of GR activity may indicate that the increased level of GSH come from the GSSG reduced by GR. Other than being the conjugate to many active metabolite of drugs or toxins, GSH is also essential for scavenging ROS by being converted to GSSG during oxidative stress (Sakurai et al., 2005; Dukhande et al., 2006; Park and Park, 2007; Yadav et al., 2008). Since GSH and GR were regulated by retrorsine treatment, GSH disturbance

and thereafter oxidative stress were thought to be involved in the early stage of retrorsine intoxication.
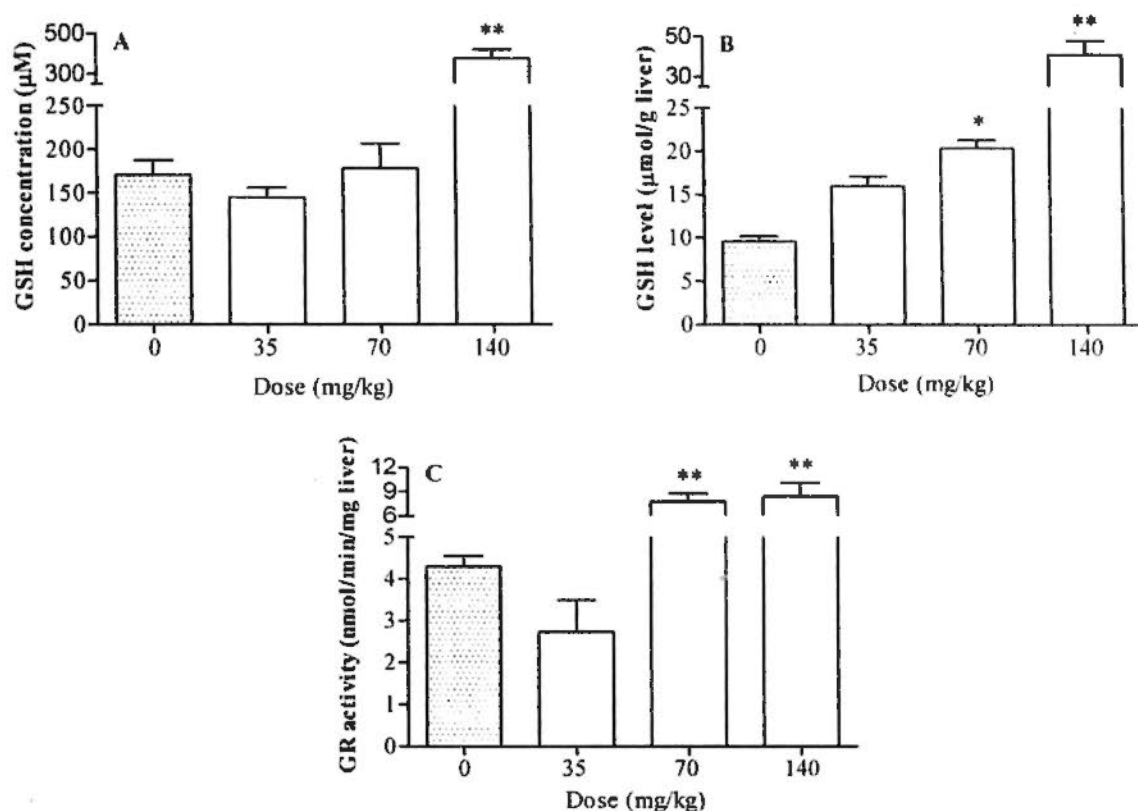
Fig.4.6. Effects of retrorsine on A) plasma GSH concentration, B) hepatic GSH concentration and C) hepatic GR activity. *$P < 0.05$ or **$P < 0.01$ comparing with vehicle control.

4.3.8 Oxidative Stress Induced by Retrorsine

To confirm whether oxidative stress was involved in retrorsine intoxication, hepatic ratio of GSSG/GSH was measured. As shown in Fig.4.7A, the hepatic GSSG/GSH ratio significantly increased after rats were treated with low or medium dose of retrorsine. As this ratio is determined by the relative level of GSSG and GSH, the increase of GSSG/GSH in the face of increased GSH (demonstrated in Fig.4.6B) means a net increase of GSSG, which may originate from the increased turnover of GSH. However, this ratio did not increase with increasing dose.

Conversely, it was decreased upon high dose treatment when compared to medium dose treatment, which was presumed to be due to the deficiency of GSH turnover by the depletion of the ability of liver to synthesis more GSH. This hypothesis is rational because a high level of PA exposure had been proved to be able to deplete all avaible GSH and destroy such detoxification system leading to severe liver (Yan, 1995; Huan J, Miranda, 1998).

At the same time, the increased ratio of GSSG/GSH implied that the oxidative stress occurred even at low dose treatment, which was confirmed by the assessment of another indicator of oxidative stress, MPO. As shown in Fig.4.6B, plasma MPO activity significantly increased after rats were treated with low or medium dose retrorsine ($P < 0.01$ comparing with vehicle control). MPO is a peroxidase enzyme most abundantly present in neutrophil granulocytes and it can be used as a biomarker of neutrophil accumulation and inflammation. MPO accounts for 5% of the total neutrophil protein and is responsible for the production of HOCl oxidant. The release of HOCl by neutrophils will cause oxidative damage to numerous biomolecules, such as proteins, carbohydrates, lipids, and nucleic acids, and can enhance inflammatory response, the latter acts a protective reaction of the body. Therefore, the increase of plasma MPO activity suggested a massive activation of neutrophil and thereafter oxidative stress caused by low and medium dose treatment. However, the plasma MPO activity was decreased to some extent (not significant when compared with vehicle control) by high dose treatment, which may imply that the protective effect of neutrophil and their anti-inflammation action was suppressed by a relative high level of PA exposure.
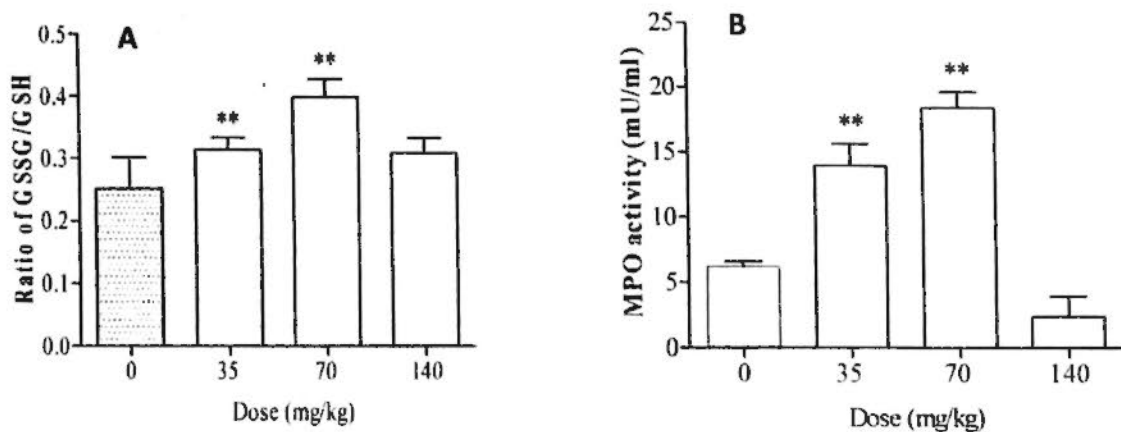
Fig.4.7. Effects of retrorsine on A) ratio of GSSG/GSH in liver homogenate and B) enzymatic activity of MPO in plasma. **$P < 0.01$ comparing with vehicle control.

4.4 Summary

PA-induced HSOS is an under-recognized cause of severe liver injury worldwide due to the difficulties in establishing a reliable diagnosis, which is based on the exclusion of other conditions (Sgro et al, 2002). Accordingly, the lack of an objective diagnostic biomarker makes it difficult to study the etiopathogenesis of this condition (Boppre et al, 2011). Thus, developing biomarker that predict HSOS risk and developing a better understanding of the mechanism have been put forward as two important strategies for decreasing the risk (Uetrecht, 2007). In fact, these two strategies have cause-effect relationship and they can be achieved in one whole study. For example, we are now attempting to develop specific biomarkers for the early prediction of PA-induced acute hepatotoxicity by elucidating the underlying mechanisms/pathways involved. To achieve this, a reproducible and reliable animal model is urgently needed.

Although several studies have used monocrotaline, another retronecine-type PA, to develop model, the treatment protocols used in these studies varied widely in the dose regimen (DeLeve et al, 1999; Copper et al, 2002; Chen et al, 2008).

116

Accordingly, the liver injury developed in these studies is highly variable, which makes it difficult to study the toxicological mechanism. Furthermore, as oral administration is the only practical route of exposure to PAs outside the laboratory, there is a surprising omission for previous studies considering that the majority toxicity data for PA relating to administration is via i.p. route or i.v. route (Mattocks, 1986). To study the development of liver injury after PA treatment, a protocol should be chosen that produced consistent, reproducible hepatotoxicity with a predictable dose-response and minimal lethality. A single oral administration of doses corresponding to 0.7, 1.4 and 2.8 fold of LD_{50} retrorsine to rats meet these criteria. This range doses produced liver injury with low intra- and inter-experimental variability and a predictable dose-response. In addition, the histopathological characteristics of the liver lesions were similar to these described previously (DeLeve et al, 1999; Copper et al, 2002; Chen et al, 2008). Therefore, retrorsine-induced hepatotoxicity may represent a better model of PA intoxication.

In addition, the damage to vascular ECs has been proved to be the specific target of PA-induced HSOS. Thus, a visualization of damages on sinusoilds and CV is crucial for the accurate illustration of the pathogenesis of PA toxicity. As SECs cannot be observed under light microscope, the possible damage to them may be easily overlooked by H&E staining. By using immunostaining stained with RECA-1 antibody, the SECs and CVECs are simultaneous visible, this is important for the determination of which cells are primarily or firstly referred to. As demonstrated in the Results and Discussion part, SECs loss were found occurring with low dose of retrorsine whereas CVECs loss with medium dose exposure. Thus the present study proves for the first time that SECs are more apt to being injured than CVECs after PA administration. This finding could directly explain why the term of HVOD has been switched into HSOS to illustrate the pathogenesis of PA intoxication.

117

Furthermore, a definite dose-dependent hepatotoxicity has been elicited by the single oral administration of dose corresponding to 0.7, 1.4 and 2.8 fold of LD_{50} retrorsine: low dose induced a slight injury with an elevation of ALT, GSSG/GSH, MPO, and slight loss of SECs in central region of the liver lobe; medium dose caused a mild injury referring to more damages including the elevation of RLW, GSH, GR, occasionally occurred sinusoid hemorrhage, damage in SECs and CVEC with more pronounced in central region of the liver lobe; whereas high dose resulted in severe damage referring to all above data, plus 1) significant increase in TB and LDH, 2) significant increase in GSH but no change in GSSG/GSH indicating the initiation of GSH depletion, 3) slight decrease in MPO supports the results of GSSG/GSH, 4) sinusoid hemorrhage (5/6) and lobular disarray (4/6) and 5) severe damage in SECs and CVEC in both central and peripheral regions of liver lobe. According to this character, we may hypothesize that a low dose exposure results in a sub-toxic effect involving oxidative stress and inflammation process, high dose represents a severe toxicity referring to cell necrosis and GSH depletion and reaction to medium dose is in intergrade. This dose-dependent liver damage should be due to the formation of different amounts of toxic pyrroles and it is thus the first systematic and comprehensive assessment of this dose-dependent response of PA.

The above findings formed a solid foundation for the further proteomic study. It would be helpful in understanding and illustrating the proteomic data in developing potential biomarkers and investigating pathway signatures of PA-induced hepatotoxicity. Thus, this developed animal model is useful for further studies.

Chapter 5 Proteomic Study of Retrorsine-Induced Acute Hepatotoxicity in Rats

5.1 Introduction

As discussed in chapter 1, the mechanisms underlying PA-induced hepatotoxicity are largely unknown. It has so far been established that the hepatotoxicity of PAs depends on their metabolic activation by hepatic CYP3A4 to become chemically reactive pyrroles that form covalent adducts with cellular nucleophiles including DNA and proteins (Xia et al., 2008). The subsequent formation of protein adducts led to the hypothesis that covalent binding to liver protein might be involved in PA-induced toxicity (Fu et al., 2004). Besides the alkylation of liver proteins, other process such as GSH disturbance (Yan and Huxtable, 1995a, b, c, d), inflammation activation (Copple et al., 2003), disrupted coagulation system (Copple et al., 2006) and DNA fragmentation (Gordon et al., 2000) are also suggested to be involved in. Nevertheless, arguments have been put forward to support that above process observed after exposure to PA are involved in the progression of toxicity rather than in its initiation (Guo et al., 2007; Mei et al., 2007). Since that the alkylation of hepatic proteins occurs shortly after PA administration, it is conceivable that specific proteins are responsible for the initiation of PA toxicity. Thus, the identification of possible target proteins for PA intoxication might provide important information regarding the mechanism. In addition, no standard approaches in preclinical toxicity assessments are available for the detection of the potential of PAs to produce HSOS. Therefore, some sensitive and reliable endpoints such as molecularly responsible biomarkers were required for setting the high throughput screening system of hepatotoxicity in the early stage of PA intoxication.

Recently, novel 'omics' techniques such as genomics using DNA microarray (De Backer et al., 2002), proteomics (Tyers and Mann, 2003) using two-dimensional gel

electrophoresis (2-DE) and mass spectrometry (MS), as well as metabonomics using both MS and nuclear magnetic resonance (NMR) (Nicholson et al., 2002) are promising tools for the elucidation of molecular mechanisms of toxicity and developments of novel biomarkers which may contribute to high throughput safety screening in the future (Bandara and Kennedy, 2002; Hayes and Bradfield, 2005; Kleno et al., 2004; Macgregor, 2003). Particularly proteomics, which allows the investigation on mechanisms of drug action at protein level in the cells enables us to identify pharmacologically responsible proteins, and thus plays a very important role in uncovering new biomarkers (Bandara and Kennedy, 2002; Gorg et al., 2000; Wetmore and Merrick, 2004; Pennington et al., 2004).

The technology used in proteomic analysis is main 2-DE, which is an effective method for the separation of proteins in complex mixtures and quantification of differential expression of individual proteins in treated and control samples. It offers a unique possibility to simultaneously identify and quantify a relatively large number of proteins. The application of proteomics has been proved to be able to conveniently simplify the identification of target proteins by comparing the protein expression levels in the tissues/body fluids of control and treated animals (Andringa et al., 2010; Low et al., 2004). This approach has been used to create 2-D databases of rat liver proteins and employed to identify proteins modified with disease (Fountoulakis et al., 2000; Fountoulakis and Suter, 2002). Furthermore, 2-DE offers opportunities to characterize complex patterns of tissue protein expressions responding to the administration of xenobiotics. These protein pattern profiles may potentially represent signatures of specific host/organ responses or offer insights into pathogenic processes and/or potential surrogate markers for specific toxicity or pathogenesis process (Newsholme et al., 2000). The work of development of a rudimentary database of rat liver and 2-DE characterization of some xenobiotic responses has

been initiated (Stephen et al, 2000). Profiling the proteome of xenobiotic-damaged rodent livers has the long-term objectives in assisting investigations of molecular mechanisms of hepatotoxicity, and establishing signature patterns and specific biomarkers of liver toxicity.

Till now, the proteomic evaluation of PA-induced toxicity has not been reported. The aim of the present study is to investigate the expression changes of hepatic protein induced by PA using proteomic approach. Moreover, through analyzing and comparing the 2-D snapshots of protein expression from different doses, a signature pattern of protein expression and specific biomarkers of liver toxicity were established for the determination of PA intoxication in rats.

5.2 Materials and Methods

5.2.1 Materials

Acrylamide mix and siLenfect were purchased from Bio-Rad. Dithiothreitol (DTT), 3-((3-cholamidopropyl)-dimethyl-ammonio)-1-propane sulfonate (CHAPS), sodium dodecyl sulphate (SDS) and immobilized pH gradient (IPG) buffer were purchased from Amersham Biosciences.

5.2.2 Animals

The details are described in section 4.2.2.

5.2.3 Treatment Protocol

This protocol is described in detail in section 4.2.3.

5.2.4 2-DE

Frozen liver tissues were ground in liquid nitrogen with apestle and mortar until fine and powdery. Lysis buffer consisting of 9 M urea, 65 mM DTT, 2% CHAPS, 40 mM Tris, 1 mM PMSF, 0.5 mg/mL DNase, and 0.5 mg/mL RNase were then added. The mixture was again ground to a fine powder in liquid nitrogen and left to thaw at 10°C for 30 min. The thawed tissue lysate was then carefully transferred to a microfuge tube and subjected to ultracentrifugation at 100,000 g in Optima™ XL-80XP ultracentrifuge for 1 h at 10 °C. The supernatants were collected and stored at −80 °C prior to the proteomic experiments. Protein concentration was determined by 2-D Quant Kit (GE Healthcare). One hundred and twenty µg of protein was solubilized in 250 µl rehydration buffer (8 M urea, 2% CHAPS, 2% DTT, 0.5% IPG buffer pH 4–7 and 1% bromophenol blue). IPG strips (GE Healthcare, pH 4–7, 13 cm) were rehydrated with sample-containing rehydration buffer for 17 h. Isoelectric focusing (IEF) was carried out in an Ettan IPGphor 3 IEF System (GE Healthcare) for 80,000 Vh. The isoelectric-focused IPG strips were equilibrated twice in SDS equilibration buffer (2% SDS, 75 mM Tris-HCl pH 8.8, 6 M urea, 30% (v/v) glycerol), 1% DTT or 2.5% IAA was included in the first and second equilibration step, respectively. Proteins were separated in 12.5% resolving SDS polyacrylamide gels using Hoefer SE 600 Unit (GE Healthcare). After electrophoresis, the gels were fixed overnight and the protein spots were visualized using silver stain. Briefly, the gels were sensitized in silver stain sensitizing solution. Gels were washed in de-ionized water and stained in silver staining solution. After washing in water, the gels were incubated in developing solution. Reactions were stopped with 1.46 % EDTA solution and the gels were washed and stored in water. Each group of experiment (control and treatment) was repeated in triplicate.

5.2.5 Image Analysis

Gel images were scanned on a gel scanner ImageScanner III (GE Healthcare). Proteins spots were detected, matched among groups, quantified and normalized using the Progenesis SameSpots software (Nonlinear Dynamics). Their normalized spots volumes (percentage of total spot volume on 2-D gel) were compared between control and retrorsine-treated groups. Spots volumes with differences equal to or greater than 1.5 fold or 0.5 fold ($P < 0.05$) compared with the control were selected for subsequent protein identification.

5.2.6 In-gel Tryptic Digestion

Excised spots were washed 3 times with de-ionized water and dehydrated with ACN. The gels were then reduced by DTT solution and alkylated by iodoacetamide solution. After dehydration with ACN, the gel pieces were digested at 37 °C overnight with trypsin (Promega). Digestion was stopped by the addition of 1% TFA, peptides were then extracted with ACN solution. The extracted peptides were vacuum-dried and stored at −20 °C prior to MS analysis.

5.2.7 MALDI-TOF MS and Protein Identification

Protein identification was performed using a Autoflex III MALDI-TOF/TOF MS (Bruker, Germany) equipped with a 200 Hz N_2 laser operating at 337nm. Data were acquired in the positive ion reflector mode over a mass range of 800–4000 m/z. Bruker calibration mixture were used as external standard and consisted of the following peptides (monoisotopic mass of the singly protonated ion is given in parenthesis in Da): bradykinin (757.3992), angiotensin II (1046.5420), angiotensin I (1296.6853), substance P (1347.7361), bombesin (1619.8230), renin substrate (1758.9326), ACTH clip 1-17 (2093.0868), ACTH clip 18-39 (2465.1990), and

somatostatin 28 (3147.4714). Keratin contamination peaks, matrix ion peaks and trypsin ion peaks were excluded from spectra. Typically 400 shots were accumulated per spectrum in MS mode and 2000 shots in MS/MS mode. The spectra were processed using the FlexAnalysis 3.0 and BioTools 3.1 software tools (Bruker, Germany). Peptide masses were matched with the theoretical peptides of all proteins in the IPI database using the Mascot search program (2.2.04, http://www.matrixscience.com). The following parameters were used for database searches: monoisotopic mass accuracy < 100 ppm, missed cleavages 1, carbamidomethylation of cysteine as fixed modification, oxidation of methionine as variable modifications. In MS/MS mode, the fragment ion mass accuracy was set to < 0.5 Da.

5.2.8 Validation of Candidate Biomarkers by IHC Analysis

For IHC analysis, the major procedures are similar to that described in section 4.2.9. The primary antibodies used in the present study were rabbit anti-rat Cps1, rabbit anti-rat Hspa9, and mouse anti-rat Atp5b which were diluted in blocking solution at 1:500, 1:100 and 1:100 respectively. The corresponding secondary antibodies were Alexa Fluor 488 conjugate goat anti-rabbit or goat anti-mouse secondary antibody (Invitrogen, USA).

5.2.9 Validation of Candidate Biomarkers by Western Blot Analysis

Frozen liver tissues (100 mg) were lysed with RIPA buffer containing a cocktail of protease inhibitors for 15–20 min on ice. Supernatants of tissue lysates were collected by centrifugation at 15,000 g for 20 min at 4°C and protein content was quantified using Bio-Rad protein assay kit. Samples were diluted in saline with a starting dilution factor of 1250 and adjusted according to their absorbance values.

Samples were incubated at room temperature for 15 min after the addition of the dye and the absorbance readings of the standard and samples were measured at 595 nm. The absorbance values at 595 nm and corresponding protein concentrations were used to obtain the standard curve and to calculate the sample protein concentration according to the standard curve (R^2 = 0.9707). Tissue lysates were dissolved in 4× sample buffer and heated at 100°C for 5 min to denature proteins to their primary structure. Equal amounts of samples (10 µg protein/lane) were loaded and proteins were separated by 7.5% sodium dodecyl sulfate polyacrylamide gel electrophoresis in a Mini-PROTEAN Tetra Cell (BioRad) at constant 100 V until the target protein reached the desired level on the gel. Then, proteins on the gel were transferred to a nitrocellulose membrane by electrophoresis at 100 V for 1 h in a trans-blot electrophoresis transfer cell (BioRad). The membrane was blocked with 5% non-fat dry milk or 5% BSA in 1× Tris-buffered saline containing 0.1% Tween-20 (block solution) for 1 h at room temperature with shaking. Then, the membrane was incubated with the primary antibody suitable for probing the target protein diluted in corresponding block solution at 4°C with shaking. The primary antibodies used included: rabbit anti-rat Cps1 (150 kDa, 1:5000), rabbit anti-rat Hspa9 (74kDa, 1:1000), mouse anti-rat Atp5b (52kDa, 1:1000), and mouse anti-rat Gapdh (37 kDa, 1:2000). After overnight incubation, membranes were washed three times with washing buffer and incubated with horseradish peroxidase-conjugated anti-mouse or anti-rabbit secondary antibodies diluted at 1:2000 in block solution for 1 h at room temperature with shaking. The antibody-bound proteins were detected by chemiluminescence using ECL reagent and ChemiDoc XRS Molecular Imager system (BioRad). Band intensities were estimated by the Quantity One 1-D Analysis software (BioRad) and the relative expressions of hepatic Cps1, Hsap9 and Atp5b

were normalized using the following equation: normalized band intensity = (band intensity of target protein)/(band intensity of Gapdh)

5.2.10 Statistical Analysis

The methods are described in detail in section 4.2.14.

5.3 Results and Discussion

5.3.1 Differential Expression of Liver Proteins after Retrorsine Treatment

In order to elucidate the molecular basis of the toxic effect of retrorsine on rat, changes of liver proteomes in response to retrorsine administration were evaluated using a quantitative proteomic approach. Proteins extracted from the livers of vehicle control and retrorsine treated animals were separated by 2-D gel and stained with silver stain. Representative 2D IEF/SDS-PAGE gels from each treatment group are shown in Fig.5.1. In the gels, the proteins were separated in two dimensions: in first dimension or transverse dimension, proteins were separated due to their differences in charge by IEF; in second or vertical dimension, proteins were separated due to their differences in molecular weight by SDS page gel electrophoresis. Scanned gel images were analyzed and the spots with differences more than 1.5-fold with statistical significance ($P < 0.05$) between the vehicle controls *versus* low, medium or high dose group were considered as differentially expressed protein spots. Fig.5.2 shows the Venn diagram analysis of the differentially expressed protein spots in three doses of retrorsine treatment groups. Altogether 52, 30 and 15 differentially expressed protein spots were detected with low, medium and high dose treatment respectively, 4 of them were observed in all three doses, 2 in both low and medium and 2 in both low and high dose treatment. This result suggested that different doses of PA had an individual pattern of the differential expressed protein profile. Thus

these few consistently regulated proteins may reveal the underlying correlation among different doses and had tight connection with the pathogenesis of PA intoxication. Furthermore, 40 spots were found down-regulated and 12 up-regulated by low, 15 down-regulated and 15 up-regulated by medium, and 1 down-regulated and 14 up-regulated by high dose treatment. This finding indicated that the regulating protein expressions by PA varied among doses and most proteins were down-regulated at low dose, whereas almost all proteins were up-regulated at high dose treatment. Four down-regulated protein spots were simultaneously found in both low and medium dose and 1 in both low and high dose treatment. Additionally, 1 up-regulated spot was found in both low and high dose treatment. All these altered protein spots were picked out from the 2-D gels and subjected to in-gel digestion and MALDI-TOF/TOF MS analysis for protein identification. Table 5.1 shows the cellular localization of the differentially expressed proteins analyzed using the UniProt database. The results revealed that the majority of altered proteins in retrorsine treated were mitochondrial and cytosolic proteins. Considering the relative low amounts of proteins in mitochondria as compared that in cytoplasm, an equal or similar numbers of proteins in these two compartments altered by retrorsine treatment indicated that retrorsine might impair the mitochondria functions in liver cells, resulting in hepatotoxicity.
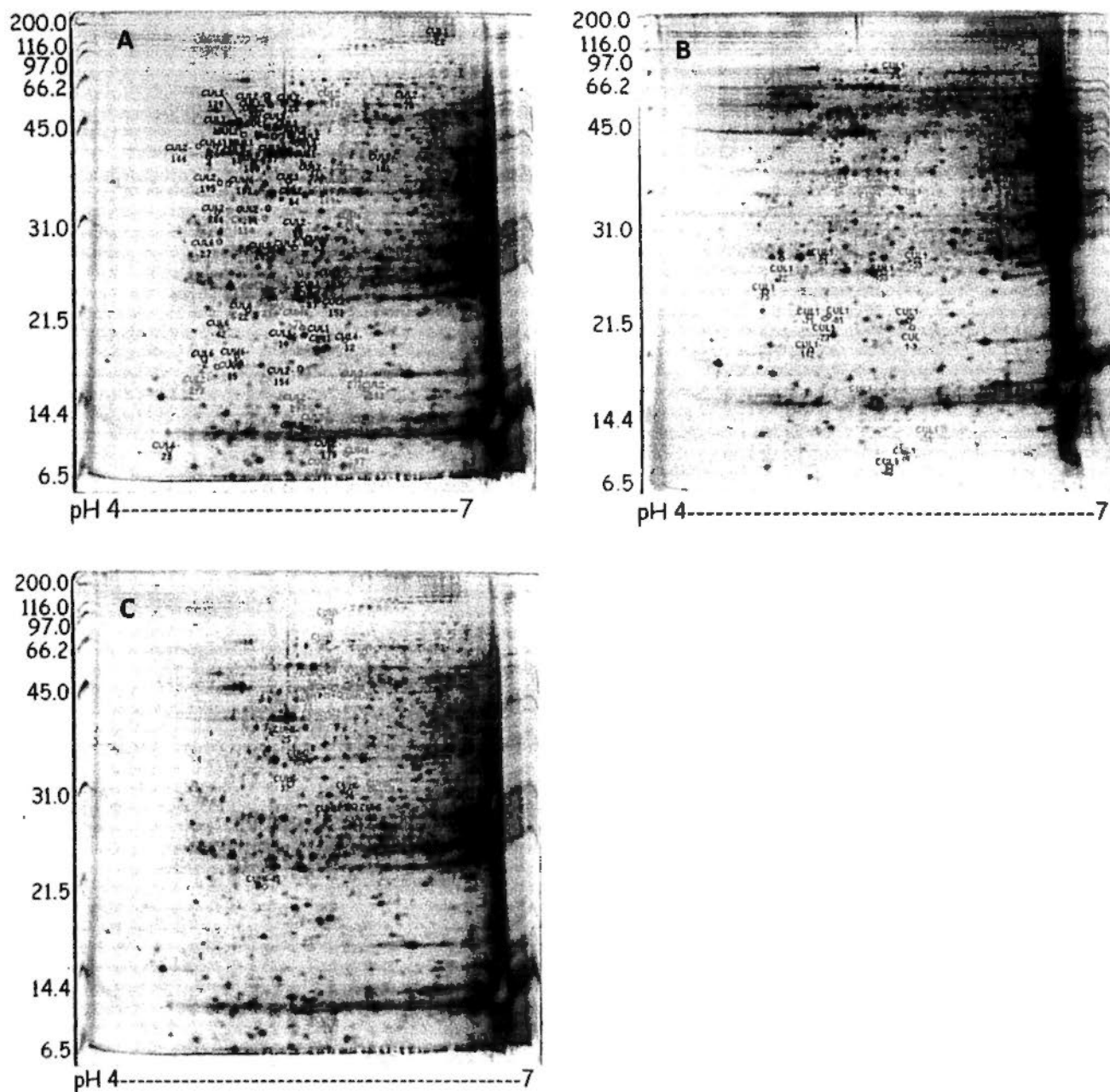
Fig.5.1. Representative 2-D gel of proteins in the liver of rat treated with low (A), medium (B) or high (C) dose of retrorsine. Significantly changed protein expressions are indicated by circles and respective ID code. Red: up-regulated; blue: down-regulated comparing with vehicle.
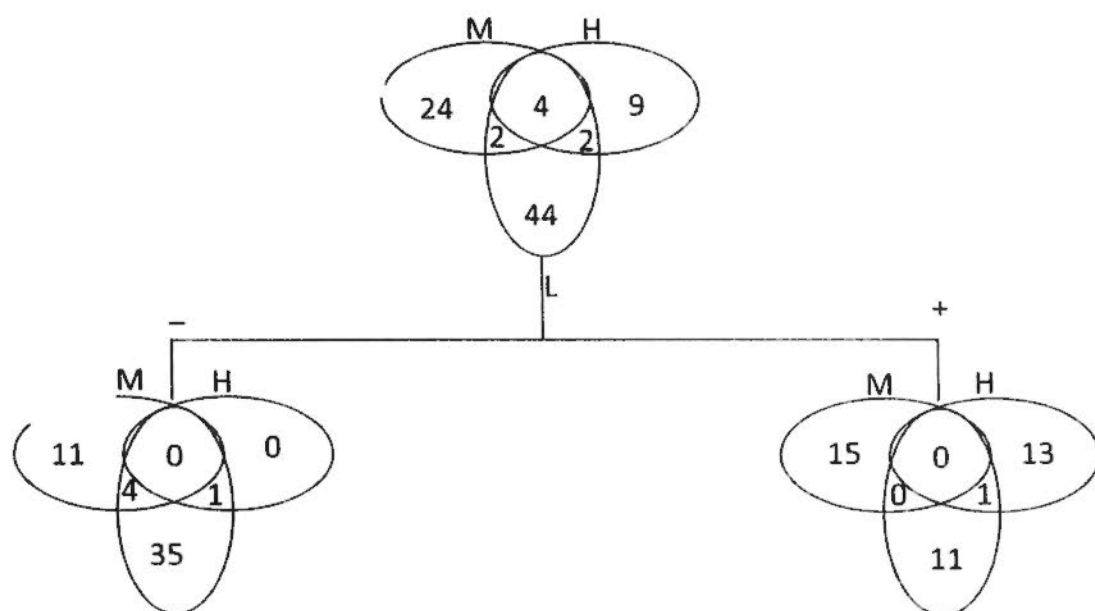
Fig.5.2. Venn diagram analysis of the differentially expressed proteins in three doses (L: low dose; M: medium dose; H: high dose) of retrorsine treatment groups. The numbers of differentially expressed spots (up- or down-regulated) in different groups are shown in the different segments.

Table 5.1 Cellular localization of the regulated proteins by retrorsine treatment

Cellular localization	Percentage of regulated proteins (%)		
	Low dose	Medium dose	High dose
Mitochondria	28	29	33
Cytoplasm	47	41	38
Endoplasmic reticulum	8	12	–
Membrane	2	–	5
Peroxisome	–	3	–
Unclassified	15	15	24

Low dose: 35, Medium dose: 70 and High dose: 140 mg/kg of retrorsine.

5.3.1.1 Effect of Low Dose

As shown in Table 5.2, at low dose of retrorsine treatment, altogether 24 down-regulated and 11 up-regulated proteins were identified. Among them, 14 were involved in energy and nutrients metabolism. These included carbamoylphosphate synthase (Cps1) in urea cycle, ATP synthase subunit beta (Atp5b), and malate dehydrogenase (Mdh1) in energy formation, *S*-adenosylmethionine synthetase isoform type-1 (Mat1a) and betaine-homocysteine *S*-methyltransferase (Bhmt) in amino-acid biosynthesis, hydroxymethylglutaryl-CoA synthase (Hmgcs2) and apolipoprotein A-I (Apoa1) in cholesterol metabolism, purine nucleoside phosphorylase (Np) in nucleoside metabolism and pyruvate carboxylase (Pc) in carbohydrate biosynthesis. Interestingly, most of these enzymes involved in biosynthesis of energy and nutrients were down regulated, indicating a possible decreased metabolic activity in liver tissues upon low dose retrorsine exposure. This hypothesis was partly confirmed by the up-regulation of the following two proteins: formimidoyltransferase-cyclodeaminase (Ftcd) involved in amino-acid degradation and urocanase domain containing 1 (Uroc1) responsible for amino-acid catabolic process. Besides, 5 proteins involved in cytoskeleton organization were also affected. Except for actin, cytoplasmic 2, 33 kDa protein (Actg1), other four proteins, actin, alpha skeletal muscle (Acta1), Actin, cytplasmic 1 (Actb), keratin, type I cytoskeletal 18 (Krt18) and keratin, type II cytoskeletal 8 (Krt8) were all down regulated. This result may propose a hypothesis that low dose of retrorsine induced a low level of cell organization process and thus resulting in a low level of regenerating rate. Interestingly, this hypothesis was partly confirmed · by the down-regulation of two proteins involved in cell proliferation: abhydrolase domain-containing protein 14B (Abhd14b) and up-regulation of ribonuclease UK114

(Hrsp12) which can inhibit protein biosynthesis. Additionally, three proteins involved in stress response were down-regulated. They were molecular chaperones stress-70 protein (Hspa9), 60 kDa heat shock protein (Hspd1) and 78 kDa glucose-regulated protein (Hspa5). The up-regulation of two proteins, ferritin light chain 1 (Ftl) and delta-1-pyrroline-5-carboxylate dehydrogenase (LOC641316) involved in oxidation reduction process confirmed that the oxidative stress occurred with low dose retrorsine exposure. Moreover, three proteins, phosphatidylethanolamine-binding protein 1 (Pebp1), isoform L-type of pyruvate kinase isozymes R/L (Pklr) and type I cytoskeletal 18 (Krt18) involved in thrombosis formation were also down-regulated. Pebp1 and Pklr can inhibit thrombin, whereas Krt18 plays a role in uptake of thrombin-antithrombin complexes. Thus the regulation of these three proteins by retrorsine may play an important role in the aggravation of hemorrhage induced by slight SEC loss as demonstrated in chapter 4. Finally, transthyretin (TTR) involved in signal transduction and serum albumin (Alb) which is produced by liver cells were also regulated.

Chapter 5 Proteomic Study of Retrorsine-Induce Hepatotoxicity

Table 5.2 Effect of low dose of retrorsine on protein expressions in rat liver

Protein ID	Fold change	Identity	Function
1) Metabolism proteins			
Cps1	-4.2	Carbamoyl-phosphate synthase [ammonia], mitochondrial	Urea cycle
Cps1	-4.2	Cps1 127 kDa protein	Urea cycle
Cps1	-3.4	Carbamoyl-phosphate synthase [ammonia], mitochondrial	Urea cycle
Cps1	-3.3	Carbamoyl-phosphate synthase [ammonia], mitochondrial	Urea cycle
Cps1	-3.2	Carbamoyl-phosphate synthase [ammonia], mitochondrial	Urea cycle
Cps1	-3.0	Carbamoyl-phosphate synthase [ammonia], mitochondrial	Urea cycle
Cps1	-2.8	Carbamoyl-phosphate synthase [ammonia], mitochondrial	Urea cycle
Cps1	-2.5	127 kDa	Urea cycle
Cps1	-2.3	127 kDa	Urea cycle
Cps1	-2.1	Carbamoyl-phosphate synthase [ammonia], mitochondrial	Urea cycle
Cps1	-1.9	Carbamoyl-phosphate synthase [ammonia], mitochondrial	Urea cycle
Atp5b	-2.2	ATP synthase subunit beta, mitochondrial	ATP synthesis
Atp5b	-2.1	ATP synthase subunit beta, mitochondrial	ATP synthesis
Atp5b	-3.6	ATP synthase subunit beta, mitochondrial	ATP synthesis
Mdh1	-2.0	Malate dehydrogenase, cytoplasmic	NADH metabolic process
Etfb	+1.6	Electron transfer flavoprotein subunit beta	Electron transport
Etfb	+1.5	Electron transfer flavoprotein subunit beta	Electron transport
Bhmt	-3.4	Betaine--homocysteine S-methyltransferase 1	Amino-acid biosynthesis
Mat1a	-3.0	S-adenosylmethionine synthetase isoform type-1	Amino-acid biosynthesis
Mat1a	-1.8	S-adenosylmethionine synthetase isoform type-1	Amino-acid biosynthesis
Ftcd	+1.7	Formimidoyltransferase-cyclodeaminase	Amino-acid degradation, One-carbon metabolism
Ahcy	+1.7	Adenosylhomocysteinase	One-carbon metabolism

To be continued

To be continued

Uroc1	+1.6	similar to urocanase domain containing 1	Histidine catabolic process
Pc	-2.9	Pyruvate carboxylase, mitochondrial	Carbohydrate biosynthesis, gluconeogenesis
Pc	-2.3	Pyruvate carboxylase, mitochondrial	Carbohydrate biosynthesis, gluconeogenesis
Apoa1	-2.3	Apolipoprotein A-I	Cholesterol metabolism, lipid metabolism
Hmgcs2	-1.5	Hydroxymethylglutaryl-CoA synthase	Cholesterol biosynthesis, lipid metabolism
Aldh2	+1.6	Aldehyde dehydrogenase, mitochondrial	Alcohol metabolism
Np	-2.0	Purine nucleoside phosphorylase	Purine nucleoside metabolic process

2) Cell organization

Acta1	-3.3	Actin, alpha skeletal muscle	Cell motion
Acta1	-2.5	Actin, alpha skeletal muscle	Cell motion
Actb	-2.6	Actin, cytplasmic 1	Cell motion
Actg1	+1.6	Actin, cytoplasmic 2, 33 kDa protein	Cell motion
Krt18	-2.5	Keratin, type I cytoskeletal 18	Filament reorganization
Krt8	-1.5	Keratin, type II cytoskeletal 8	Cytoskeleton organization

3) Cell proliferation

Abhd14b	-9.1	Abhydrolase domain-containing protein 14B	Cell proliferation
Hrsp12	+1.9	Ribonuclease UK114	Inhibits cell-free protein synthesis

4) Stress response

Hspa9	-3.1	Stress-70 protein, mitochondrial	Stress response
Hspa9	-2.6	Stress-70 protein, mitochondrial	Stress response
Hspa9	-2.3	Stress-70 protein, mitochondrial	Stress response
Hspa5	-1.9	78 kDa glucose-regulated protein	Stress response

To be continued

To be continued			
Hspa1a/1b	+1.5	Heat shock 70 kDa protein 1A/1B	Stress response
Hspd1	-3.1	60 kDa heat shock protein, mitochondrial	Stress response
Hspd1	-2.7	60 kDa heat shock protein, mitochondrial	Stress response
Ftl	+1.7	Ferritin light chain 1	Oxidation-reduction process
LOC641316	+1.5	Delta-1-pyrroline-5-carboxylate dehydrogenase	Oxidation-reduction process
5) Thrombosis			
Pklr	-3.4	Isoform L-type of Pyruvate kinase isozymes R/L	ATP binding
Pebp1	-2.4	Phosphatidylethanolamine-binding protein 1	Binds ATP, inhibits thrombin
Krt18	-2.9	Keratin, type I cytoskeletal 18	Uptake of thrombin-antithrombin complexes by hepatic cells
6) Other function			
IPI00189038	-2.1	12 kDa protein	
Alb	+1.5	Serum albumin	Regulate colloidal osmotic pressure of blood
Ttr	-2.5	Transthyretin	Thyroid hormone-binding protein

-: Down-regulated; +: Up-regulated comparing with vehicle control.

5.3.1.2 Effect of Medium Dose

When pretreated the rats with medium dose retrorsine, 29 proteins changed their expression level compared with rats treated with vehicle control (Table 5.3). Nearly half of these proteins (14 out of 29) were also metabolic enzymes. Different from the pattern changes induced by low dose, most of the proteins involved in energy metabolism were up-regulated by medium dose. For example, Cps1 in urea cycle, 3-mercaptopyruvate sulfurtransferase (Mpst), spermidine synthase (Srm), and ornithine aminotransferase (Oat) in amino acid metabolism, hydroxymethylglutaryl-CoA synthase (Hmgcs2), 3-hydroxybutyrate dehydrogenase I (Bdh1), acyl-CoA synthetase medium-chain family member 2 (Acsm2), butyryl coenzyme A synthase 1 (Bucs1) and fatty acid-binding protein (Fabp7) in lipid metabolism, 60S acidic ribosomal protein (Arbp) and purine nucleoside phosphorylase (Np) in nucleoside metabolism as well as Pc in carbohydrate biosynthesis. In addition, three proteins also involved in nutrition metabolism were down-regulated. They were Atp5b, ornithine aminotransferase (oat), and ureidopropionase beta (Upb1). This result implied that a large portion of the metabolic ability of liver might be activated upon medium dose treatment. Similarly, 2 proteins (Actb and Krt8) involved in cytoskeleton organization were also down-regulated by medium dose. However, cell proliferation was suggested to be activated due to the up-regulation of cathepsin B (Ctsb), a protein responsible for intracellular degradation and turnover of proteins. Additionally, two proteins, Hspa9 and heat shock protein beta-8 (Hspb8) which inhibit stress response were down-regulated. Moreover, spectrin alpha 2 (Spna2) regulating fibrinolysis and S100-A8 (S100-A8) which regulate thrombin were up-regulated. Different from that

of low dose exposure, medium dose treatment resulted in a down-regulation of Alb. Finally, six proteins were also regulated and they may possess unknown effect in the progress of PA-induced toxicity. For example, the down-regulation of proteasome subunit, beta type 9 (Psmb9), a protein involved in antigen processing to generate class I binding peptides, may represent an inhibitory effect of PA on antigen processing.

Table 5.3 Effect of medium dose of retrorsine on protein expressions in rat liver

Protein ID	Fold change	Identity	Function
1) Metabolism proteins			
Cps1	+2.3	Carbamoyl-phosphate synthetase 1, mitochondria	Urea cycle
Atp5b	-1.2	ATP synthase subunit beta, mitochondrial	ATP synthesis
Mpst	+1.8	3-mercaptopyruvate sulfurtransferase	Amino-acid metabolism, cysteine metabolism
Srm	+2.3	Spermidine synthase	Amino-acid metabolism, amine biosynthesis
Oat	-1.8	Ornithine aminotransferase, mitochondrial	Amino-acid metabolism, L-proline and L-glutamate 5-semialdehyde biosynthesis
Bdh1	+1.9	3-hydroxybutyrate dehydrogenase 1	Lipid metabolism
Acsm2	+1.9	Acyl-CoA synthetase medium-chain family member 2	Lipid metabolism
Bucs1	+1.5	Butyryl coenzyme A synthase 1	Lipid metabolism
Hmgcs2	+1.5	Hydroxymethylglutaryl-CoA synthase, mitochondria	Form HMG-CoA
Pc	+1.5	Pyruvate carboxylase protein	Catalyzes initial reactions of glucose and lipid synthesis from pyruvate
Akr1c14	-1.6	Aldo-keto reductase family 1, member C14	Reduction of aldehydes
Fabp7	+1.5	Fatty acid-binding protein	Carrier proteins for fatty acids and other lipophilic substances
Arbp	+1.7	60S acidic ribosomal protein	Ribonucleoprotein
Upb1	-1.7	Ureidopropionase beta	Pyrimidine and beta-alanine metabolism, pantothenate and coa biosynthesis
2) Cell organization			
Actb	-1.7	Actin, cytplasmic 1	Cell motion
Krt8	-1.6	Keratin type II	Cytoskeleton organization

To be continued

To be continued

3) Cell proliferation

Ctsb	+1.4	Cathepsin B	Intracellular degradation and turnover of proteins

4) Stress response

Hspa9	-1.4	Heat shock protein 70kDa protein 9	Inhibits apoptosis
Hspb8	-2.1	Heat shock protein beta-8	Inhibits apoptosis

5) Thrombosis

Spna2	+2.4	Spectrin alpha 2	Regulation of fibrinolysis
S100-A8	+2.3	S100-A8	Caicium binding protein

6) Other functions

Alb	-1.5	Albumin	Regulate colloidal osmotic pressure of blood
Coro1b	+2.0	Coronin, actin binding protein, 1B	Cytokinesis and signal transduction
Cnpy2	-1.5	Canopy 2	Positive regulator of neurite outgrowth
Cnpy2	-1.5	Canopy 2	Positivc regulator of neurite outgrowth
Psmb9	-1.5	Proteasome subunit, beta type 9	Antigen processing to generate class I binding peptides
Lactb2	+1.4	Beta-lactamaselike protein 2	Deactivating the molecule's antibacterial properties
Pgcl1	-2.1	Alpha 2μ globulin	Synthesis is inhibited by estrogens

-: Down-regulated; +: Up-regulated comparing with vehicle control.

5.3.1.3 Effect of High Dose

In high dose treatment, fewer proteins were regulated: altogether 9 proteins were up-regulated, whereas one was down-regulated, indicating that the expressions of hepatic proteins were not apt to be altered upon high dose comparing to low and medium dose treatment. As shown in Table 5.4, three proteins [Atp5b, acetyl-Coenzyme A dehydrogenase, short chain (Acads), and formimidoyltransferase-cyclodeaminase (Ftcd)] involved in metabolism and two proteins related to stress response (Hspa9 and Hspd1) were up-regulated. The up-regulation of cell organization related proteins (Acta1, Krt8, Cct5) implied that the liver might be undergoing regeneration. Besides, one down-regulated protein (Ttr) associated with signal transduction was also detected at high dose treatment.

Chapter 5 Proteomic Study of Retrorsine-Induce Hepatotoxicity

Table 5.4 Effect of high dose of retrorsine on protein expressions in rat liver

Protein ID	Fold change	Identity	Function
1) Metabolism proteins			
Cps1	+4.1	Carbamoyl-phosphate synthase [ammonia], mitochondrial	Urea cycle
Cps1	+2.1	Carbamoyl-phosphate synthase [ammonia], mitochondrial	Urea cycle
Cps1	+1.9	127 kDa	Urea cycle
Cps1	+1.7	Carbamoyl-phosphate synthase [ammonia], mitochondrial	Urea cycle
Cps1	+1.5	127 kDa	Urea cycle
Cps1	+1.5	Carbamoyl-phosphate synthase [ammonia], mitochondrial	Urea cycle
Atp5b	+2.5	ATP synthase subunit beta, mitochondrial	ATP synthesis
Acads	+2.1	Acetyl-Coenzyme A dehydrogenase, short chain	Butyrate catabolic process
Ftcd	+1.8	Formimidoyltransferase-cyclodeaminase	Amino-acid degradation, One-carbon metabolism
2) Cell organization			
Acta1	+3.3	Actin, alpha skeletal muscle	Cell motion
Krt8	+2.0	Keratin, type II cytoskeletal 8	Cytoskeleton organization
Cct5	+2.1	T-complex protein 1 subunit epsilon	Folding of actin and tubulin
3) Cell proliferation			
4) Stress response			
Hspa9	+2.2	Stress-70 protein, mitochondrial	Inhibits apoptosis
Hspd1	+2.0	60 kDa heat shock protein, mitochondrial	Stress response
5) Thrombosis			
6) Other functions			
Ttr	-1.6	Transthyretin	Thyroid hormone-binding protein

-: Down-regulated; +: Up-regulated comparing with vehicle control.

140

5.3.2 Protein Signature Pattern

These regulated proteins upon three doses of retrorsine treatment were loosely grouped into the following broad functional clusters (Table 5.2, 3 and 4), and their detailed information are described below.

5.3.2.1 Cluster 1: Metabolism Enzymes

Proteins in Cluster 1 were involved in energy and nutrients metabolisms such as urea cycle, ATP synthesis, amino acids metabolism, fatty acid b-oxidation, carbohydrate biosynthesis and lipid metabolism.

5.3.2.1.1 Urea Cycle and ATP synthesis

Cps1 is a ligase enzyme located in the mitochondria involved in the production of urea. It transfers ammonia from glutamine to a molecule of bicarbonate that has been phosphorylated by a molecule of ATP. The resulting carbamate is then phosphorylated with another molecule ATP. Cps1 was found down-regulated upon low, whereas up-regulated upon both medium and high dose treatment. Atp5b catalyzes the rate-limiting step of ATP formation which is essential for most of enzymatic reactions like in the urea cycle (Reyes and Izquierdo, 2007). The down-regulation of Atp5b observed at low and medium doses treatment in the present study gave a clue that the decreased expression of Atp5b may be a fundamental reason for the down-regulation of many metabolic enzymes of liver tissue, which need enough production of ATP to exert their metabolic activity. However, the expression of Atp5b was up-regulated upon a higher dose of PA treatment, which might be due to the preserving effect of liver tissue to produce more ATP to cope with an up-regulated metabolic rate upon high dose treatment. For example, the down-regulation of Cps1 should result in a low consumption of ATP,

whereas increased Cps1 need more ATP for exhibiting its catalyzing action. In addition, Mdh1 and Etfb, two proteins as the components of the respiratory chain, were only regulated at low dose treatment, implying that at sub-toxic stage, more proteins involved in the disturbance of energy metabolism were affected.

5.3.2.1.2 Amino Acid Metabolism

Several proteins such as Bhmt, Mat1a and Oat involved in amino acid synthesis were down-regulated by low or medium dose treatment. The possible reason is due to the DNA adduct formation by PA exposure, which interferes with their normal, often vital functions and results in less DNA being translated to corresponding proteins (Xia et al., 2006; Fu et al, 2004). In addition, the down-regulation of these hepatic enzymes is also presumed to be the homeostatic reaction of the body to PA exposure for conserving energy. The up-regulation of Ftcd and Ahcy, two enzymes taking part in amino acid degradation are supposed to be the body's way to compensate for the reduction of amino acid production. However, other two same kind enzymes, Mpst and Srm were up-regulated by medium dose treatment. Mpst is an enzyme responsible for cysteine formation which is important for GSH formation. As demonstrated in chapter 4, medium dose induced a significant increase in hepatic GSH level, the high expression of Mpst was thus supposed to be related to the production of cysteine for more GSH synthesis. Srm is responsible for spermidine synthesis. The up-regulation of Srm might result in a high level of spermidine production. As spermidine has an action of inhibition of neuronal NO synthase (Hu et al., 1994), the up-regulation of Srm was thus supposed to be involved in the possible decrease of NO production. In addition, Oat is a mitochondrial enzyme that reversibly converts ornithine and a-ketoglutarate to glutamic-g-semialdehyde and

glutamate, and acts in arginine metabolism, which may be also involved in the NO depletion induced by PA.

5.3.2.1.3 Cholesterol, Fatty Acid and Lipid Metabolism

Retrorsine treatment showed a profound effect on cholesterol biosynthesis. Hmgcs2 and Apoa1 were down-regulated after low dose treatment. Hmgcs2 is the key regulatory enzyme in the biosynthetic pathway for cholesterol and catalyzes the conversion of HMG-CoA to mevalonate. The inhibition of this enzyme results in both the down-regulation of cholesterol synthesis and the up-regulation of hepatic high affinity receptors for low density lipoproteins (LDL) followed by increased catabolism of LDL cholesterol (Goldstein and Brown, 1986). Apoa1 is synthesized in the liver and secreted into the blood, and is the major constituent of plasma high density lipoproteins (HDL). HDL mediates the reverse transport of cholesterol from tissues to the liver, the site of cholesterol metabolism and secretion. Thus, the decreased abundance of precursor Apoa1 suggests a down-regulation of HDL synthesis coupled with a decrease in cholesterol catabolism in the liver. In summary, the down-regulation of Hmgcs2 and Apoa1 complementarily reflects a decreased cholesterol metabolism, which should be ascribed to inhibition of the body's metabolic ability due to low dose exposure. The up-regulation of Aldh2 in the low dose retrorsine treated liver samples was presumed to play a role in eliminating toxic PA metabolite.

However, after medium dose treatment, five proteins (Hmgcs2, Acsm2, Bdh1, Pc and Bucs1) involved in cholesterol metabolism were all up-regulated. The data suggested that the up-regulation of the cholesterol synthesis pathway was a feedback reaction to the inhibition of amino acid synthesis and an attempt of the liver to compensate for the impaired pathway performance. The degree to which these

enzymes were induced seemed to link to the degree to which amino acid synthetase was inhibited and thus served as a measure of the toxic potency of PA. Expression increase was also found in Fabp7, a carrier protein for fatty acids and other lipophilic substances. The up-regulation of these enzymes might impair fatty acid b-oxidation and suggested an accumulation of fatty acid (fatty change) in the affected livers. Akr1c14 was also up-regulated. Like Aldh2 regulated in low dose treatment, Akr1c14 is also responsible for reduction of aldehydes and involved in numerous biochemical pathways including fatty acid metabolism and bile acid biosynthesis. In summary, the up-regulation of these aldehyde-metabolizing enzymes, as observed in low and medium dose treatment, was a strong indication of the presence of increased lipid peroxides.

Similarly, the up-regulation of Acads by high dose was in agreement with above observation referring to the lipid peroxides. As demonstrated in chapter 4, serum TB level, also an indicative of lipid peroxide was significantly elevated by high dose. How these two events correlated with each other await further investigation.

5.3.2.1.4 Carbohydrate and Nucleotide Acid Metabolism

Similarly, protein and lipid regulations induced by retrorsine included the interlinked carbohydrate metabolism. Pc, a key regulatory enzyme necessary for catalyzing initial reactions of glucose and lipid synthesis from pyruvate, and specific to, gluconeogenesis, was down-regulated by low dose while up-regulated by medium dose treatment. This pattern was in accordance with that of changes of other metabolism-related proteins, that was, down-regulated at low, whereas up-regulated at medium and high dose treatment. These findings confirmed the hypothesis that a relative low level of PA exposure may lead to a reduced metabolic rate of the liver, whereas higher level exposure may directly activate the repairing mechanism of the

liver tissue to produce more energy and materials for the rescue of liver from PA damage. Similarly, the regulation patterns of retrorsine to purine nucleoside phosphorylase (Np) involved in purine nucleoside metabolic process, ureidopropionase beta (Upb1) involved in pyrimidine metabolism and 60S acidic ribosomal protein (Arbp) were consistent with the trend to other nutrients.

5.3.4.2 Cluster 2: Cell Organization

Less is known about the character of the PA-induced DNA-protein cross-link. The involvement of actin in PA intoxication is a reasonable assumption due to the abundance of this protein in the nuclear matrix and its involvement as a target of cross-linker in cisplatin toxicity (Miller et al., 1991). Actin has been proved to be the major protein involved in PA-induced DNA-protein cross-link (Coulombe et al., 1999). As the megalocytic and antimitotic effects of PAs coincide with cross-linking potency (Kim et al., 1993), the antimitotic action of pyrrolic PAs may be explained, at least in part, by their ability to cross-link DNA with actin. Krt18 and Krt8, two components of the intermediate filament family were inhibited upon low dose treatment. Cytokeratin filaments are important components of the cytoskeletal structure and their alterations may reflect cellular stress. An inhibition was also observed in Acta1 and Actb, two proteins found in the thin filaments of muscle fibers. This down-regulation may also be explained as the depleting effect of low dose of PA on liver protein. As discussed earlier, PAs are found to crosslink DNA with actin (Kim et al, 1999), which may stop or interfere with the subsequent transcription and translation of above proteins. This effect was also observed in medium dose treatment with the down-regulation of Actb and Krt8. Conversely, in high dose treatment, Acta1, Krt8 and Cct5 were up-regulated, which might result from the breakdown of blood cells due to its large retention in the liver as

demonstrated in chapter 4. Changes in these sets of proteins are likely indicators of liver toxicity following different dose of retrorsine treatment. Hence, the degree to which these proteins are altered by specific doses may serve as a measure of toxicity associated with the treatment.

5.3.4.3 Cluster 3: Cell Proliferation

A very remarkable down-regulation of Abhd14b suggested that the cell proliferation process was severely inhibited after low dose treatment. However, this regulation was not observed at medium or high dose retrorsine treatment, indicating that this protein was especially important in sub-toxic stage of PA intoxication. The up-regulation of Hrsp12 was in agreement with this inhibited tendency on cell proliferation by inhibiting protein synthesis. This result was also accordant with above results of decreased synthesis of amino acid in low dose treatment. However, the turnover of proteins was suggested to be improved by the up-regulation of Ctsb induced by medium dose treatment, which suggested that the cell regeneration process was activated. This observation may explain why autophagy occurred with the *in vitro* PA exposure as demonstrated in chapter 1.

5.3.4.4 Cluster 4: Stress Response

Non-enzymatic antioxidants like GSH could prevent cellular damage from ROS (Klaunig et al., 1995). Gluthathione peroxidase (GP), most abundant in erythrocytes, catalyses the oxidation of hydrogen peroxide into water by converting GSH to GSSG. The regeneration of GSH is catalysed by GR. Thus, GSH, GP and GR work together and deficiency in any of those is believed to be associated with an increased sensitivity of the cell to oxidative stress (Klaunig et al. 1995). It has been established in chapter 4 that retrorsine even at low dose could induce a disturbance of GSH

system and result in the oxidative stress and inflammation process. Accordingly, several proteins associated with cellular stress were found being affected by retrorsine treatment in the present proteomic study. The expressions of Hspa9, Hspa5 and Hspd1 were down-regulated by low dose treatment; Hspa9 and Hspb8 were down-regulated by medium dose; whereas Hspa9 and Hspd1 were up-regulated by high dose of retrorsine treatment. Since most of these proteins are responsible for reducing the oxidative stress, the increase of them only occurred after high dose treatment suggested a more severe degree of oxidative stress which stimulated the induction of the anti-oxidative molecules. Ftl, the major form of tissue ferritin in liver, was up-regulated in the low dose treated rat livers. Ferritin was reported being degraded, with the release of iron, by autophagic vacuolar apparatus in macrophages during inflammation. Thus the up-regulation of Ftl implies that less free irons can act as a catalyst in the reactions generating free radicals, which may be also regarded as an index of oxidative stress caused by PA treatment.

5.3.4.5 Cluster 5: Thrombosis

A previous study demonstrated that the damage to SECs of liver resulting in disruption of vascular architecture and hemorrhage caused by PA was accompanied by activation of the coagulation system. This activation may advance the hepatic parenchymal cell injury through deposition of insoluble fibrin clots in the vasculature and ischemia and/or through other mechanisms, such as activation of a cellular receptor for thrombin (Copper et al, 2002). In addition, defibrotide, a single-stranded polydeoxyribonucleotide which is able to decrease thrombin generation (Zhou et al., 1994), has been proved to be a promising treatment of HSOS (Chopra et al., 2000; Richardson et al., 2002; Saviola et al., 2003). Thus, thrombosis is supposed to play an important role in the development of HSOS. However, how it

acts and the detail mechanisms remain largely unclear. In the present study, two ATP binding proteins, Pklr and Pebp1 which inhibit thrombin were down-regulated by low dose treatment (Table 5.2), which might be due to the reduced ability of the liver tissue for protein synthesis. Interestingly, as a slight loss of SECs occurred with the low dose retrorsine, which should result in a slight hemorrhage due to the intact lining of sinusoids. Thus an activated thrombin as the result of up-regulation of Pklr and Pebp1 should prevent or stop this slight hemorrhage. Accordingly, the ability of hepatic cells for uptake thrombin-antithrombin complexes was decreased because of the down-regulation of Krt18, which are also helpful in protecting the liver tissue from ischemia hemorrhage. Similarly, in medium dose treatment, Spna2 and S100-A8 were up-regulated, which represented an increased ability of release of thrombin and regulation of fibrinolysis respectively. This result was rational because most altered proteins began to be up-regulated at this dose and they should be responsible for reducing the degree of hemorrhage and clearing the formed fibrin.

5.3.4.6 Cluster 6: Other Functions

Several proteins taking part in cell signal transduction were regulated by retrorsine treatment. For example, Ttr was down-regulated by low and high and coronin, actin binding protein, 1B (Coro1b) was up-regulated by medium dose treatment. This result suggests that some inherent pathway such as insulin signaling pathway may act in the pathogenesis of PA intoxication. However, detailed information of the pathway are not available in these proteins profiles, hence, how they play a role in the pathogenesis of PA toxicity need to be studied further. In addition, an interesting finding was found with the alteration to Alb, an important constituent protein of the blood for maintaining the normal colloidal osmotic pressure of blood. As the largest amount of protein in the blood, Alb has been proved to form the main conjugates

with pyrroles by our group (data not shown). Thus a larger amount of pyrroles may conjugate more Alb. Alb is synthesized in liver hepatocyte and then released into the circulation, thus the up-regulation of Alb found with low dose exposure suggests an activation of Alb synthesis. Differently, the down-regulation of Alb upon high dose treatment was supposed to be due to more conjugation of Alb by more pyrroles produced.

5.3.3 Cellular Mechanism of PA by Integration of the Six Clusters

The six clusters can actually be integrated to form an "overview model" (Fig.5.3). At low dose exposure (Fig.5.3A), PA administration resulted in the decrease of enzymes involved in three of the primary metabolic pathways that are involved in the production of basic materials and energy of the liver tissue (Cluster 1). As a result, the biosynthesis of cell organization related proteins was reduced (Cluster 2) and this led to a reduction of cell proliferation (Cluster 3). Accordingly, most proteins involved in oxidative stress which need ATP were inhibited and the proteins responsible for reducing oxidative stress were up-regulated, which corresponds to the protective mechanism of the liver tissue to the reduce oxidative stress as demonstrated in chapter 4 (Cluster 4). Similarly, the proteins involved in the formation of thrombosis were also down-regulated, which may aggravate the potential hemorrhage resulting from the slight loss of SECs (Cluster 5). Besides, some proteins with other functions such as cell transduction were down-regulated by low dose exposure (Cluster 6). Therefore, the low dose of retrorsine exposure exhibited a definite down-regulation of protein patterns, which was believed to be the preserving mechanism of the body to a relative low amount of PA exposure. A previous study demonstrated that in the hepatocytes, the immediate action of PA resulted in a rapid fall in cytoplasmic protein synthesis reaching 30% of control

levels at 15 min and 6% at 1 h (Harris et al., 1969). This is manifested as disaggregation of polyribosomes and is followed by failure of pyruvate oxidation, loss of glycogen, structural damage to the mitochondria, lysosomal activity, failure of mitochondrial nicotine-adenine-dinucleotide (NAD) systems and nuclear NAD synthesis, and necrosis (McLean, 1970). We are the first group to identify these down-regulated proteins at cellular level.

However, for medium dose treatment, the pattern was a little different. Firstly, most of the metabolism proteins were up-regulated (Cluster 1), which were ascribed to the activation of the protective effect of body to synthesize more nutrients and energy to antagonize the detrimental effect of PA. The rate of cell reorganization (Cluster 2) and cell proliferation (Cluster 3) were still low. Due to the larger amount of pyrroles produced by the medium dose administration that directly broke down more cytoskeleton protein and cannot meet the repairing rate of the liver. Similarly, the repairing mechanism via anti-oxidants was still not fully activated (Cluster 4). However, the proteins involved in thrombosis inhibition were up-regulated, which should be the protective effect of the body to the increased hemorrhage by medium dose treatment as demonstrated in chapter 4 (Cluster 5). Similarly, some other proteins such as Coro1b playing a role in cell signaling pathway was activated (Cluster 6). In contrast to the previous studies, it is the first time to find that retrorsine can also activate the synthesis of hepatic proteins. Whether retrorsine acts as inhibitor or activator of protein synthesis is hypothesized to be determined by the exposure level. This hypothesis was partly confirmed by the regulation pattern of high dose treatment, in which, all of the involved clusters of proteins (Cluster 1, 2 and 3) were up-regulated. Thus, a dose-dependent manner of retrorsine on liver protein expression was established.
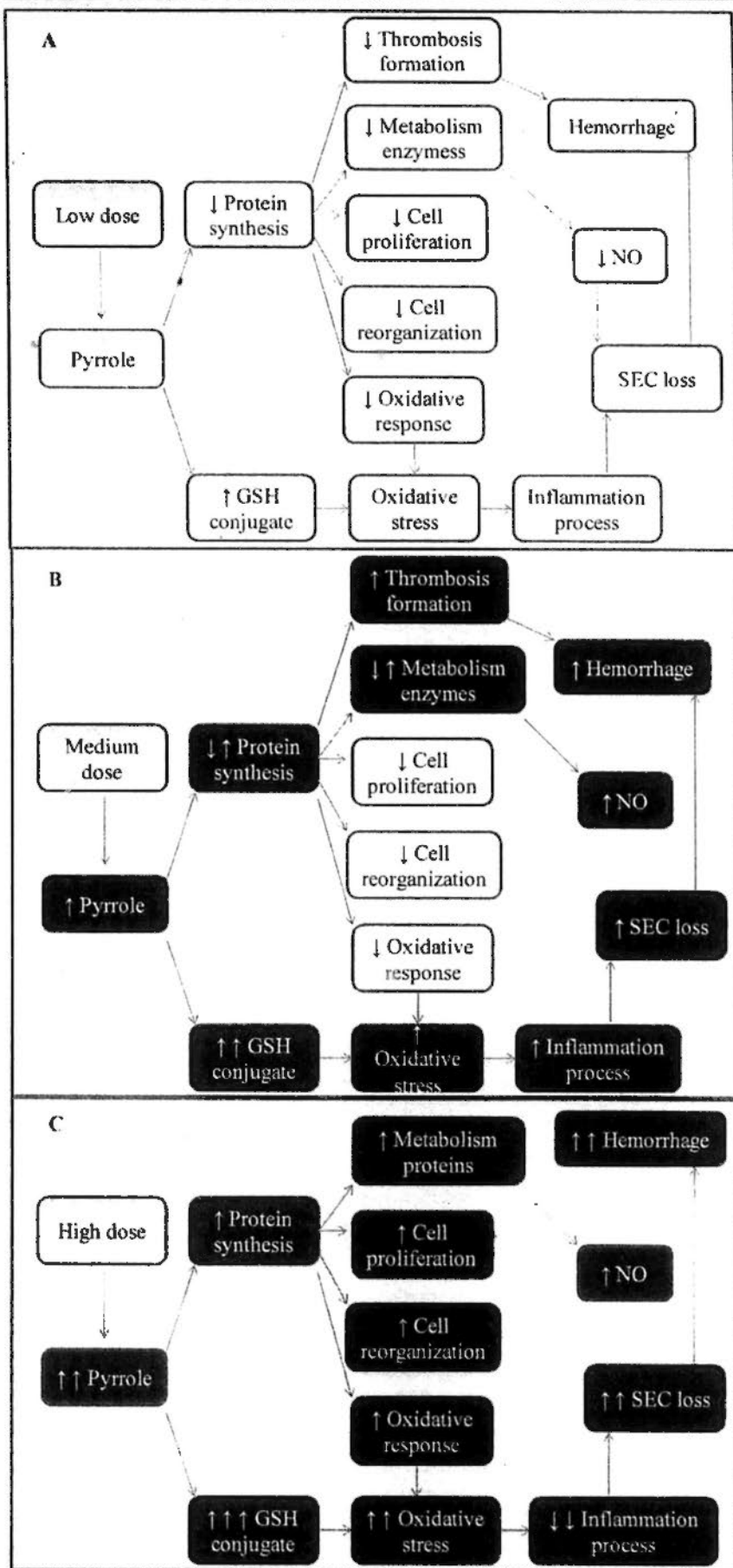
Fig.5.3. Mechanism models of acute hepatotoxicity induced by low A), medium B) and high C) dose of retrorsine treatment. ↑ and ↓ mean up- and down-regulation of process, respectively.

5.3.4 Selection of Candidate Biomarkers of Retrorsine-Induced Hepatotoxicity

As summarized in Table 5.5, there were 11 proteins involved in five clusters were consistently regulated by two or three doses of retrorsine exposure. As shown in Fig.5.4, a remarkable down-regulation (9.1 folds) of Abhd14b was found with low dose treatment, suggesting that it might have a great potential to be developed as a specific biomarker of PA intoxication. However, the regulation on Abhd14b was not observed in both medium and high dose treatment. Thus in the present study, it was not regarded as a consistent candidate proteins and did not obtain further confirmation studies. Conversely, the expressions of Cps1, Atp5b and Hspa9 which relate to urea cycle, energy metabolism and stress response respectively, were consistently altered by three doses of retrorsine treatment.

As demonstrated in Fig.5.5, urea cycle is the only non-dietary source of essential substrates (arginine or citrulline) for endothelial NO synthesis which occurs in the liver (Kallianpur et al., 2005). Cps1 catalyzes the rate-limiting step of the hepatic urea cycle, thereby controlling the availability of NO precursors. Impairment on both urea cycle function and NO production by intensive chemotherapy has been found to predispose patients to oxidative organ injury and HSOS (Pearson et al., 2001). Sustained endothelial NO production, which depends upon substrates generated by the urea cycle, may be important in limiting hepatocyte iron uptake and endothelial injury (Kim and Ponka, 2002, 2003; Moncada, 1993; Summar et al., 2004). Along with the decline in hepatic flow in HSOS, NO levels in the hepatic vein and sinusoids are shown to decrease (DeLeve et al., 1999). A sub-toxic dose of PA has been proved to be able to aggravate HSOS by inhibiting NO synthesis and the decrease of NO production contributes to the development of rat HSOS (DeLeve et

al, 2003). Thus, Cps1 regulated NO depletion is hypothesized to be vital for the development of clinic HSOS.

Atp5b is the major catalytic subunit of ATP synthase, which produces ATP from ADP in the presence of a proton gradient across the mitochondrial membrane. Regulated expression of hepatic Atp5b may explain ATP preserving effect of liver tissue toward drug-induced hepatotoxicity, an effect that was observed in recent studies but without detailed explanation. Cps1 and ATP5b may have an interaction in the regulation of NO production after PA exposure (Fig.5.5).

Hspa9, a heat-shock cognate protein, is primarily localized to the mitochondria but it is also found in the endoplasmic reticulum, plasma membrane and cytoplasmic vesicles. It plays a role in cell proliferation, stress response and maintenance of the mitochondria. However, detailed information of how it acts in any pathogenesis is absent. Since this protein was included in two cluster functions (stress response and cell proliferation) after PA treatment. We also used IHC and Western blot analysis to verify its expressions along with Cps1 and Atp5b.

Table 5.5 Potential biomarkers selected for retrorsine-induced hepatotoxicity in rat

	Protein ID	Fold change		
		Low dose	Medium dose	High dose
Cluster 1	Cps1	-4.2	+2.3	+4.1
	Atp5b	-3.6	-1.2	+2.5
	Ftcd	+1.7		+1.8
	Pebp1	-2.4	-1.8	
Cluster 2	Acta1	-3.3		+3.3
	Krt8	-1.5	-1.6	+2.0
	Ttr	-2.5		-1.6
Cluster 4	Hspa9	-3.1	-1.4	+2.2
	Hspd1	-3.1		+2.0
	Mdh1	-2.0		+1.3
Cluster 6	Alb	+1.5	-1.5	

Low dose: 35 mg/kg, Medium dose: 70 mg/kg and High dose: 140 mg/kg of retrorsine. -: Down-regulated; +: Up-regulated comparing with vehicle control group.
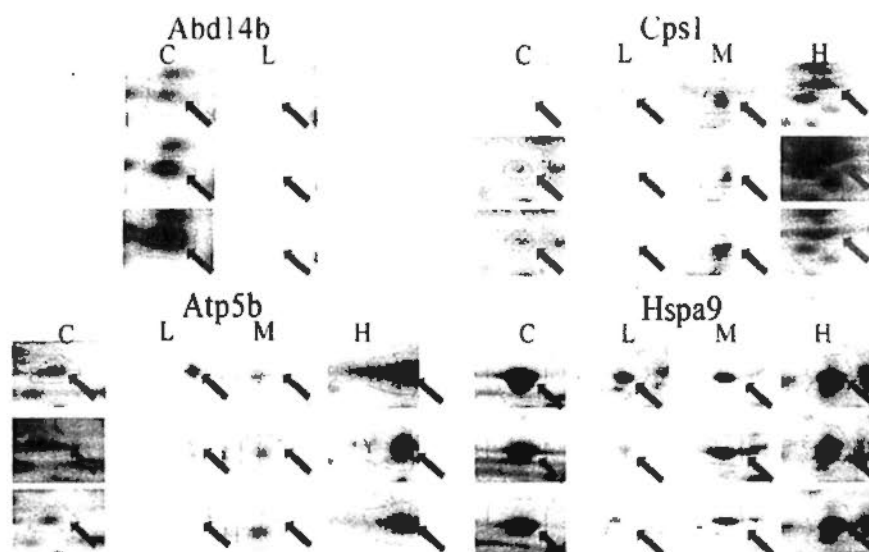
Fig.5.4. Sections of 2D-gel images showing remarkable down-regulation (9.1 folds) of Abhd14b by low-dose treatment, and consistent changes of Cps1, Atp5b and Hspa9 observed at all doses of retrorsine treatment (C: vehicle control; L: low dosage; M: medium dosage; H: high dosage).
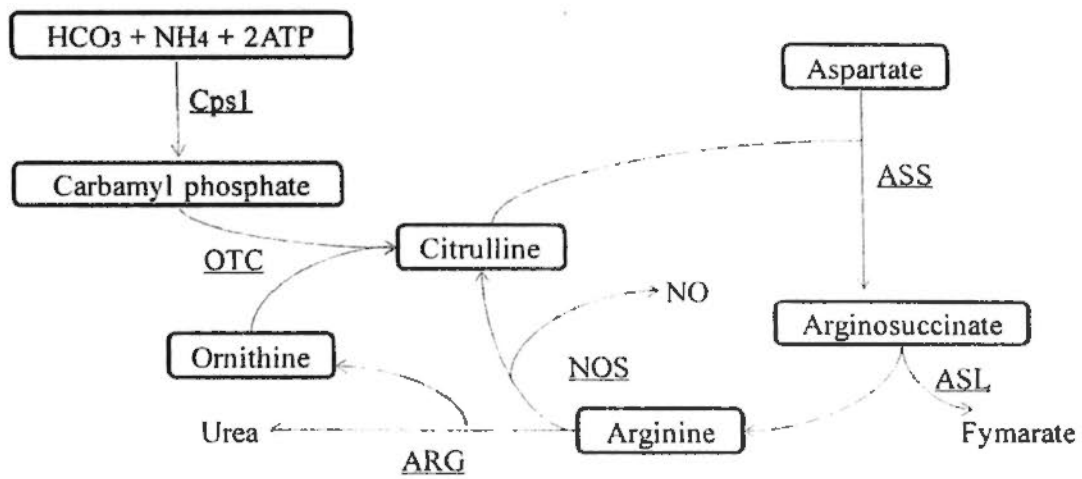
Fig.5.5. The hepatic urea cycle – dysfunction of Cps-1 results in a fall in citrulline and NO and a rise in ornithine levels. Cps-1: Carbamyl phosphate synthetase 1; OTC: Ornithine transcarbamylase; ASS: arginosuccinate synthetase; ASL: Arginosuccinate lyase; ARG: Arginase; NOS: Nitric oxide synthetase.

5.3.5 Verification of Cps1, Atp5b and Hspa9 as Potential Biomarkers

5.3.5.1 Expression of Hepatic Cps1

In the liver from rats treated with saline, Cps1 staining was obviously and predominantly cytoplasmic with no apparent nuclear staining (Fig.5.6A and A'), indicating that Cps1 antibody recognized Cps1 within the mitochondria of liver parenchymal cells. However, in livers obtained from rats treated with low or medium dose of retrorsine, Cps1 staining became less (Fig.5.6B, B'; C and C'), whereas slightly more with high dose treatment (Fig.5.6D and D'). In order to quantify the differential expression of Cps1, Western blot analysis was performed. As shown in Fig.5.9, in low and medium doses treatment groups, the hepatic expression of Cps1 was significantly down-regulated when compared with that of control group ($P < 0.01$ and $P < 0.05$, respectively), which was consistent with the identification made by 2-DE and with above qualified validation by IHC analysis. Accordingly, hepatic Cps1 expression was increased to some extent (not significant) by high dose

treatment, which was also in agreement with the result obtained from IHC analysis and proteomic approach. However, in medium dose treatment, the expression of Cps1 was down-regulated according to IHC and Western blot analysis, whereas up-regulated by proteomic analysis. The possible reason was supposed to be due to the significant individual variations in response to such dose as demonstrated in chapter 4. This regulation of Cps1 implied that the inherent production of endothelial NO was disturbed by PA treatment. The possible resultant NO reduction was hypothesized to be the underlying mechanism of slight SEC loss as found in chapter 4. However, the up-regulation of Cps1 upon a higher dose of retrorsine exposure should be a repairing effect of the liver against a severe toxicity.
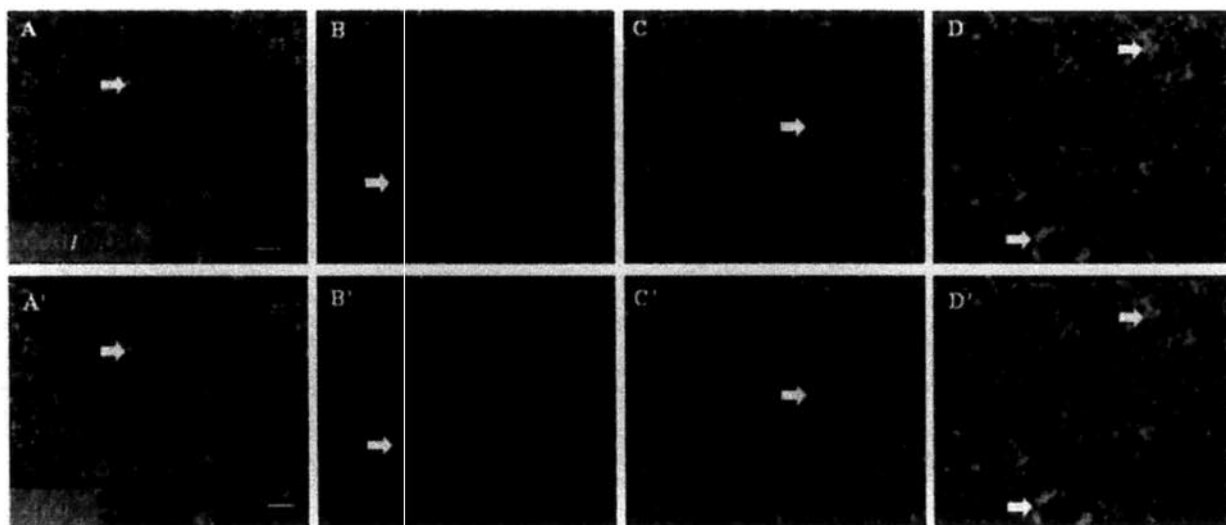
Fig.5.6. Effects of retrorsine on hepatic Cps1 expression assessed by immunostaining. Liver sections were obtained from rats treated with saline (A and A'), 35 mg/kg (B and B'), 70 mg/kg (C and C') and 140 mg/kg (D and D') retrorsine A-D: Double immunostaining with Cps1 (shown in red and indicated with white arrow) and DAPI (shown in blue). A'-D': Immunostaining of Cps1 (indicated with white arrows). Scale bar in (A-D and A'-D') = 25 μm.

5.3.5.2 Expression of Hepatic Atp5b

As shown in Fig.5.7, Atp5b staining was obviously present in the cytoplasm of hepatocyte of the liver. However, Atp5b staining became less in livers obtained from rats treated with low or medium dose (Fig. 5.7B, B'; C and C'), whereas a little more with high dose of retrorsine treatment (Fig. 5.7D and D'). Such expression pattern was in agreement with the proteomic results. Western blot analysis confirmed that the hepatic Atp5b was down-regulated in some extent ($P > 0.05$) by low, while up-regulated by high dose treatment ($P < 0.05$) (Fig.5.9). However, the up-regulation of Atp5b by medium dose revealed by the Western blot analysis was not consistent with that proved by either 2-DE or IHC analysis. The possible reason was also ascribed to the large individual variations as discussed earlier. The down-regulation of Atp5b observed at relative lower dose treatment suggested that the decreased expression of Atp5b may be an fundamental reason for the down-regulation of many metabolic enzymes of liver tissue, which need the ATP to exert their metabolic activity. However, the up-regulation of Atp5b was supposed to be caused by the preserving effect on ATP with more ATP production induced by the ischemic condition caused by a severe hemorrhage as demonstrated in chapter 4.
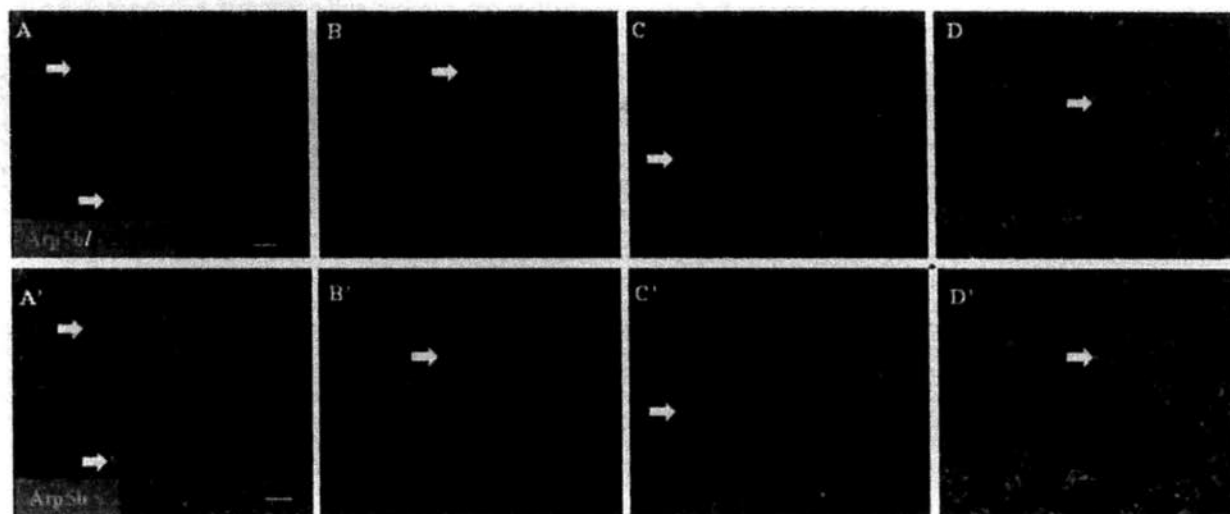
Fig.5.7. Effects of retrorsine on hepatic Atp5b expression assessed by immunostaining. Liver sections were obtained from rats treated with saline (A and A'), 35 mg/kg (B and B'), 70 mg/kg (C and C') and 140 mg/kg (D and D') retrorsine. A-D: Double immunostaining with Atp5b (shown in green and indicated with white arrow) and DAPI (shown in blue). A'-D': Immunostaining of Cps1 (indicated with white arrows). Scale bar in (A-D and A'-D') = 25 μm.

5.3.5.3 Expression of Hepatic Hspa9

As shown in Fig.5.8, the positive staining of Hspa9 was not seen in the livers obtained from control, which meant that Hsp9 was not evenly expressed in the normal liver section. Upon low dose treatment, a little amount of positive staining was seen along the sinusoids. However, the staining of the ECs of large vessels at medium dose became more concentrated to the lining of sinusoids at high dose treatment. This expression pattern was confirmed by Western blot analysis with a significant increase observed since low dose treatment ($P < 0.05$ comparing with vehicle control) (Fig.5.9). However, such expression pattern was not fully in agreement with the proteomic results, in which, Hspa9 was found down-regulated by retrorsine at both low and medium doses treatment. The lack of agreement in medium dose treatment can also be explained by the large individual variations in response to this dose as that demonstrated in Cps1 and Atp5b confirmation studies.

However, as demonstrated in chapter 1, the rats in response to low dose retrorsine show low individual variations in biochemical and histological changes. Thus, this discrepancy upon low dose treatment should not originate from the individual variation. By IHC analysis, the expression of Hspa9 was found to be locally which was different from that of Cps1 and Atp5b which showed an even staining through the section. Thus, some portion of tissue may present more Hspa9 expression, but other tissues may have none. As the proteomic study and Western blot analysis were performed in parallel and thus the samples for these two studies were different, which made it possible that the samples used in proteomic study with a lower Hspa9 expression, whereas used in Western blot and IHC analysis possessing a higher level of expression.
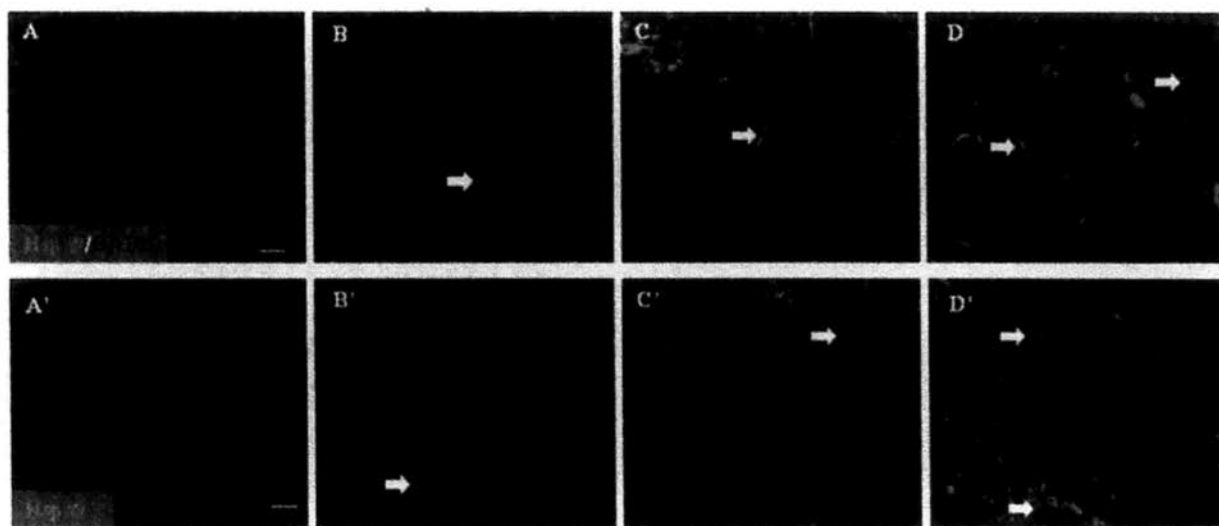
Fig.5.8. Effects of retrorsine on hepatic Hspa9 expression assessed by immunostaining. Liver sections were obtained from rats treated with saline (A and A'), 35 mg/kg (B and B'), 70 mg/kg (C and C') and 140 mg/kg (D and D') retrorsine. A-D: Double immunostaining with Hspa9 (shown in red and indicated with white arrow) and DAPI (shown in blue). A'-D': Immunostaining of Hspa9 (indicated with white arrows). Scale bar in (A-D) = 25 μm; scale bar in (A'-D') = 55 μm.
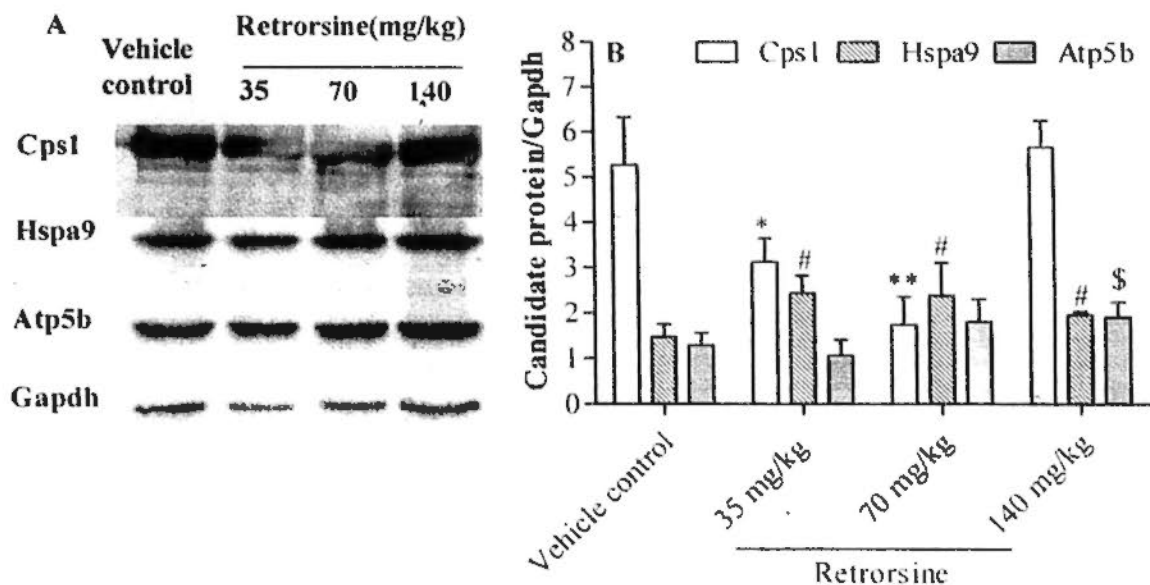
Fig.5.9. Effect of retrorsine on the hepatic Cps1, Hspa9 and Atp5b expression determined by Western blot analysis. The expressions of hepatic Cps1, Hspa9, Atp5b and Gapdh were analyzed using the intensities of separate bands, and the expressions of Cps1, Hspa9, Atp5b were normalized against that of Gapdh. $*P <$ 0.05 and $**P < 0.01$ comparing with the corresponding vehicle control.

5.3.5.4 Use of The Three Proteins as Candidate Biomarkers

When considering the regulation trend, both IHC and Western blot analysis demonstrated a similar pattern of changes in hepatic Cps1 and Atp5b expressions to the proteomic analysis upon low and high dose retrorsine treatment. Overall, the results supported that it is promising to use these proteins as potential biomarkers which warranted further development and should be evaluated against more PAs to characterize the specificity of these biomarkers for predicting PA-induced hepatotoxicity. While the exact mechanism of response of these proteins to the PA tested is not known, and therefore further deep studies are needed. In addition, to verify whether changes in protein expression correlated with transcript level, quantitative PCR is often used. However, low mRNA-protein correlations were

found in several other studies (Nie et al., 2006a, 2006b; Gygi et al., 1999) and one of the underlying reasons is proved to be the existence of posttranscriptional mechanisms which control the protein translation rate (Harford and Morris, 1997) and the half-lives of specific proteins or mRNAs (Varshavsky, 1996). Thus, in the present study, quantitative PCR was not applied for further verification of the selected candidate biomarkers.

5.4 Summary

The combinations of clinical pathology data and histopathological changes with findings of proteomic study offer new insights and understanding of the mechanisms of toxicity, and alterations relevant to toxicity that have not previously reported might be found (Kennedy, 2002). We have in previous chapter defined a characteristic rat model of hepatotoxicity induced by PA with a definite dose-dependence using several conventional technologies of biochemistry and histopathology. In this model, the low-dose effect with a slight regulation to hepatic biochemistry was regarded as a slight toxic response; whereas the high-dose effect is due to changes of circulatory biochemistry and liver histology, which was characterized as severe PA toxicity. The large variable injury caused by medium dose was believed to be a mild toxicity. The detected differential expressed proteins involved in different severity of PA intoxication were meaningful for predicting the toxicity prior to the appearance of morphological changes or analytic conventional biomarkers. When comparing the consistence and discrepancy of proteins profiles at different severity of the pathogenesis, the pathway that mainly contribute to the progression of PA intoxication can be identified. By integrating the proteomic study and conventional toxicological studies, an "overview model", a specific protein

signature pattern and candidate biomarkers which could be of value to future PA intoxication screening was generated.

In addition, identification of these altered proteins provides critical insight into the mechanisms responsible for PA-induced liver dysfunction and reveals multiple new molecular targets that can be exploited for therapeutic investigations. Specifically, it is the first time that PA was found to have profound interactions on chaperone proteins as well as the proteins related to cell proliferation and thrombosis. Novel observations of PA on pathways of urea cycle, stress response and ATP synthesis were reported and PA-mediated changes in several proteins, Cps1, Atp5b and Hspa9 were identified. These latter findings provide much needed insight into the precise molecular nature of the dose of PA that modulates liver function and structure. Retrorsine treatment also triggered alterations in key enzymes of amino acid and carbohydrate metabolism, and was associated with changes in a heterogeneous set of cellular stress proteins involved in cytoskeletal structure, calcium homeostasis and protease activity (Steiner et al., 2001). It is suggested that the degree to which cellular stress proteins are changed upon treatment may serve as a measure of toxicity induced by the PA. Toxicity protein markers selected in the present study may be used in the determination of PA intoxication. Future studies aimed at characterizing the urea cycle pathway needed to advance the concept that disrupted NO production contribute to the pathogenesis of PA intoxication in liver. Similarly, an understanding of how PA regulates mitochondrial function is required to advance our knowledge of the mechanism of PA-induced hepatotoxicity.

However, the current limited knowledge regarding liver protein identities, function, pathway interactions and ultimate biological outcomes (Abbott, 1999) constrained our interpretative ability; this protein data set provided little to further understanding the mechanisms or pathological consequences of this liver response.

Considerable challenges remain ahead in the definition of protein signatures and in the functional characterization of a broad assortment of proteins (Newsholme et al., 2000).

In summary, application of 2-DE to characterize the proteome of rat liver resulted in a successful characterization of a complex array of altered liver proteins. This study demonstrates that a systemic biology approach utilizing complementary proteomics technologies is a valuable tool that can be used to enhance ongoing mechanism studies aimed at elucidating the molecular events and pathways altered in HSOS. We have shown for the first time that our proteomics data can be readily correlated and integrated with the biochemical and pathological observations associated with PA-induced liver toxicity into an "overview model". This model can now provide us and other investigators with the framework for further experimental verification of the molecular basis of PA-induced hepatotoxicity.

Chapter 6 Comparative Proteomic Study of Cyclophosphomide-Induced

Hepatotoxicity in Rats

6.1 Introduction

Proteomics can be used to detect response to toxic drugs and have been integrated with conventional endpoints to obtain better understanding of key mechanism of toxicity and identify specific safety biomarkers (Suter et al., 2011). By providing mechanistic insight, protein profiles may be used to classify compounds with respect to pathological phenotypes they induce upon treatment. It can be expected that compounds which elicit similar pathologies are affecting the same or related mechanism of pathogenesis and are therefore likely to regulate similar sets of proteins in a comparable manner. These protein signatures may then be employed in a diagnostic or predictive reasoning.

PA-induced HSOS has perplexed human beings for more than 80 years, since it was first described in South Africa (Mattocks, 1986). So far, literature about PA-associated HSOS is only in the form of case reports, and the available reports do not provide sufficiently reliable data to be used in illustrating the accurate mechanism of this disease. At the same time, HSOS is becoming a major medical complication of chemotherapy after SCT and acts as the main cause of death (Chojkier, 2003; Poreddy and DeLeve, 2002).

Cyc is a commonly used chemotherapy drug and is the most hepatotoxic. It is a nitrogen mustard alkylating agent which attaches the alkyl group to the guanine base of DNA to form DNA cross-link between and within DNA strands. This linkage is irreversible and leads to cell death by slowing or stopping cell growth and has been proved to be able to elicit human HSOS (McDonald et al., 2005; McDonald et al., 2003). However, the detailed mechanism underlying Cyc-induced HSOS is also not

clear. A sublethal damage to SECs and/or depletion of reduced GSH in hepatocytes and SECs caused by Cyc metabolites are believed to be the possible mechanisms (DeLeve, 1996; Deleve et al., 2011; McDonald et al., 2005; McDonald et al., 2003). As demonstrated in chapter 4, the specific and early detectable damage to SECs is also involved in the pathogenesis of PA-induced hepatotoxicity. Thus, a comparable study of protein expression profile generated from rat liver after treatment with Cyc may provide mechanistic insight into the pathogenesis of HSOS.

In short, because of the similarity of HSOS produced after chemotherapy and PA exposure, a comparable proteomic study of the Cyc-induced acute hepatotoxicity is important for the understanding what factors contribute to the initiation and progression of this disease. To make a contribution, a 2-D protein map for rat liver was established to indentify the proteins whose expression level was changed by Cyc. In addition, a toxicity signature was constructed from the combination of altered proteome profiles and conventional toxicological parameters, which may offer potentially useful information in regard to signaling pathways mediating the toxicity.

6.2 Materials and Methods

6.2.1 Materials

Cyc was purchased from Sigma-Aldrich Corporation (St. Louis, MO, USA).

6.2.2 Animals

The details are described in section 4.2.2.

6.2.3 Treatment Protocol

Rats in treatment groups were orally treated with a single dose (56 mg/kg, $n = 6$) of Cyc, while the ones in vehicle control group were administered with normal saline

($n = 6$) correspondingly. The dose of Cyc used is corresponding to its LD_{50} in rats. The gavages volume for all drugs was 1 ml/kg of rat. Rats were fasted overnight after drug exposure.

6.2.4 Sample Collection

This protocol is same as that described in section 4.2.4.

6.2.5 Clinical Pathology and Liver Biochemistry

The protocols for measurements of enzymatic activities of ALT, LDH, MPO and GR, levels of GSH and GSSG/GSH ratio are described in detail in chapter 4.

6.2.6 Histological Examination

The protocols of H&E staining and RECR-1 immunostaining are described in detail in chapter 4.

6.2.7 Proteomic Study

The protocols include those described in section 5.2.5, 5.2.6. 5.2.7 and 5.2.8.

6.2.8 Validation of Candidate Proteins by IHC Analysis

The protocols include those described in section 5.2.9.

6.2.9 Statistical Analysis

The method is same as that described in section 4.2.14.

6.3 Results and Discussion

6.3.1 Toxic Effect of Cyc on Clinical Pathology and Liver Biochemistry

No death was observed during the period of drug exposure. As shown in Table 6.1, no significant differences were observed on percentage of body weight decrease

between Cyc and control group. However, the relative liver weight was significantly increased by Cyc treatment, which correlated well with the observed significant increases of plasma ALT activity, LDH release and TB level. As discussed previously in chapter 4, these changes may demonstrate a liver injury. Among four parameters involved in GSH system, only hepatic GSH level was significantly increased by Cyc treatment, implying a reflective response of the liver tissue to the consummation of GSH by conjugating with Cyc metabolite. The unchanged plasma GSH level and hepatic GR activity suggested that the GSH system was not seriously disturbed and thus the oxidative stress marker, GSSG/GSH ratio, was not significantly affected. However, MPO activity was significantly increased, suggesting that the inflammation process played a role in the pathogenesis of Cyc-induced hepatotoxicity.

As expected, an acute toxic effect of LD_{50} of Cyc was elicited on rat. When considering the changes of plasma ALT, LDH, serum TB and hepatic GSH, the degree of damage upon Cyc treatment was comparable to that induced by medium dose of retrorsine. Similarly, inflammation was also induced by Cyc treatment as that seen in low and medium doses retrorsine treatment. However, the lack of oxidative stress suggested that there might be some differences in the detailed mechanism between these two compounds (Cyc and retrorsine).

Table 6.1 Effects of Cyc on clinical pathology and liver biochemistry of rat

Biochemical parameter	Vehicle control	Cyc
24 BW post treatment (g)	236.0 ± 10.0	235.3 ± 10.1
Percentage of BWD (% BW)	8.2 ± 0.8	7.4 ± 1.2
Relative LW (% BW)	3.2 ± 0.3	3.5 ± 0.1*
Plasma ALT activity (SF unit/L)	28.6 ± 8.7	97.9 ± 10.5**
Serum TB (mg/mL)	0.17 ± 0.07	0.48 ± 0.33*
LDH release (% control)	100.0 ± 28.4	136.6 ± 25.2*
Plasma GSH level (µM)	. 170.5 ± 42.1	186.2 ± 30.4
Hepatic GSH level (µmol/g liver)	9.5 ± 1.7	14.7 ± 1.3**
Hepatic GR activity (mmol/min·g liver)	4.3 ± 0.6	3.6 ± 1.8
Hepatic GSSG/GSH ratio	0.25 ± 0.11	0.38 ± 0.14
Plasma MPO activity (mU/mL)	6.2 ± 1.0	22.1 ± 3.9**

Cyc: cyclophosphomide; BWD: body weight decrease, BW: body weight, LW: liver weight, ALT: alanine aminotransferase, TB: total bilirubin, LDH: lactate dehydrogenase, GSH: glutathione, GR: glutathione reductase, GSSG: oxidized GSH, MPO: myeloperoxidase. *$P < 0.05$ and **$P < 0.01$ comparing with vehicle control.

6.3.2 Toxic Effect of Cyc on Histopathology of Liver and Lung

As indicated in Fig.6.1, the normal structure of lobule, central vein and sinusoid were seen in liver sections obtained from rats treated with control or Cyc. No obvious necrosis was detected within the parenchymal cells after Cyc exposure. However, the sinusoids of liver in animals treated with Cyc were slightly broadened when compared with that of control (Fig.6.1B' and B''). These lesions were accompanied by a slight loss of SECs in liver sections exhibited by the decrease of immunostaining with RECA-1 antibody (Fig.6.2). These results implied that the increases of plasma ALT, LDH release and TB level should originate from the destruction of SECs, but not of parenchymal cells. No obvious lesions were observed in the lung after Cyc treatment (Fig.6.3), which was similar to that observed with retrorsine treatment. These histological changes of liver referring to hepatocyte and

SECs were similar as that developed with low dose of retrorsine treatment and comparable to that demonstrated in a previous study (Malhi et al., 2002). Taken together, a single oral LD_{50} of Cyc elicited a slight toxic effect on rat. The degree of toxicity was mostly similar to that elicited by low dose of retrorsine treatment.
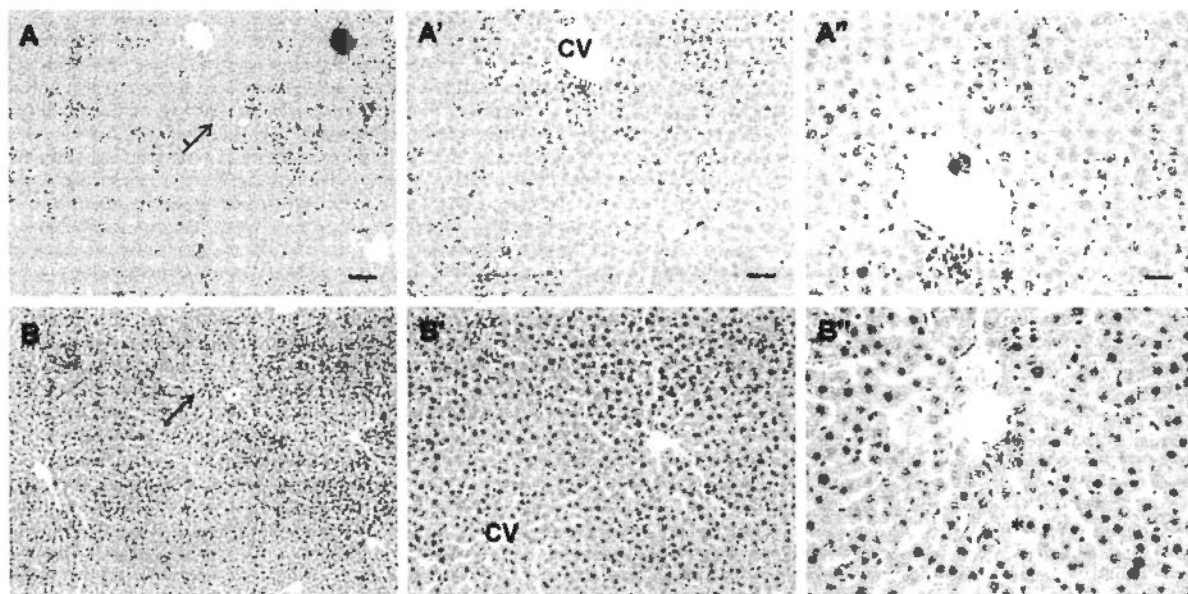
Fig.6.1. Effects of Cyc on the histology of liver. Representative hematoxylin and eosin staining images of the middle regions of liver section obtained from rats treated with saline (A, A' and A'') and 56 mg/kg Cyc (B, B' and B''). Scale bar in (A and B) = 100 μm; (A' and B') = 50 μm; (A'' and B'') = 25 μm. The central vein is abbreviated as CV and sinusoid is indicated in asterisk.
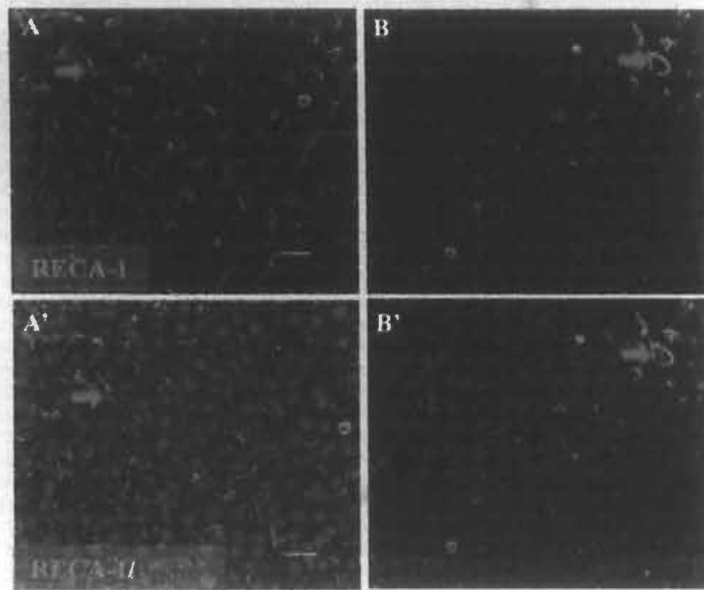
Fig.6.2. Effects of Cyc on RECA-1 immunostaining of liver section. Liver sections were obtained from rats treated with saline (A, A' and A'') and 56 mg/kg Cyc (B, B' and B''). The sinusoids are shown by green staining and indicated with red arrows. A and B: Immunostaining of RECA-1 (shown in green) for sinusoids. A' and B': Double immunostaining with RECA-1 and DAPI (shown in blue) for sinusoids. Scale bar in (A-B and A'-B') = 25 μm.
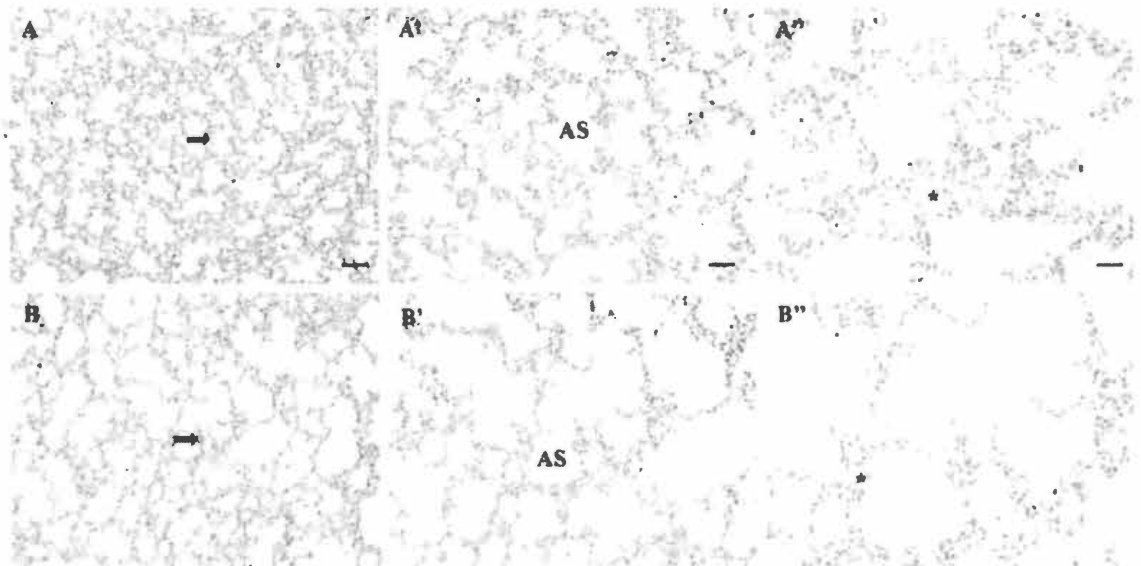
Fig.6.3. Effects of retrorsine on the histology of lung. Representative H&E staining images of the lung section obtained from rats treated with saline (A, A' and A'') and 56 mg/kg Cyc (B, B' and B''). Scale bar in (A-D) = 100 μm; (A'-D') = 50 μm; (A''-D'') = 25 μm. The blood capillary, alveolar sac and surrounding alveoli are indicated as asterisks, AS and black arrows, respectively.

6.3.3 Differential Expression of Liver Proteins after Cyc Treatment

Fig.6.4 shows a representative image of protein 2-D gels of liver obtained from rat treated with Cyc. Based on the results of the image analysis using PDQuest software, and according to Student's t-tests, 65 protein spots were found to exhibit more than 1.5-fold difference with statistical significance between the vehicle control and Cyc group ($P < 0.05$). Identification analysis revealed that 19 proteins were down-regulated and 26 were up-regulated upon Cyc treatment. The majority of the identified proteins are enzymes or enzymatic subunits (approximately 20) with a wide spectrum of catalytic activities. Other major classes included about 10 heat shock proteins. Also, approximate 6 different spots of structural proteins were represented on the gels. In addition, a high percentage of the identified proteins were localized in the mitochondria or mitochondria membrane (33%), a little more in cytoplasma (36%) and fewer in endoplasmic reticulum (9%) and peroxisome (2%). Based on the common properties and functions, these differentially expressed proteins were categorized into five clusters which were similar to that caused by PA retrorsine treatment except that no thrombosis related proteins were detected. These proteins, together with their expression levels and the pathways they involved in were summarized in Table 6.2.
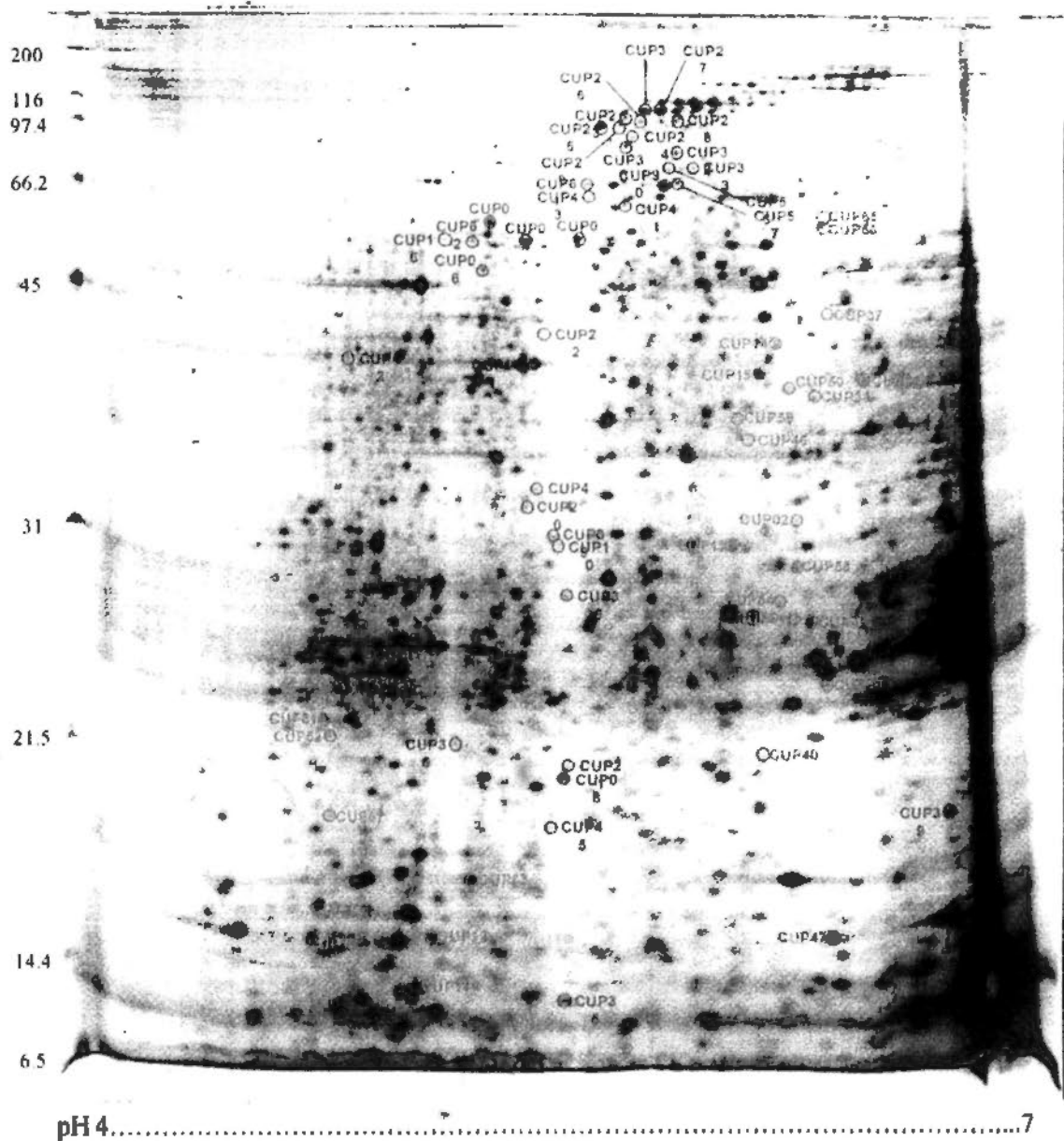
Fig.6.4. Representative 2-D gel of proteins in the liver of rat treated with 56 mg/kg

Cyc Significantly changed protein expressions are indicated by circles and respective

ID code. Red: up-regulated; blue: down-regulated comparing with vehicle.

Table 6.2 Effects of *Cyc* on protein expressions in rat liver

Protein ID	Fold change	Identity	Function
1) Metabolism proteins			
Cps1	-2.3	Carbamoyl-phosphate synthase [ammonia]	Mitochondria marker, Urea cycle
Cps1	-2.0	Carbamoyl-phosphate synthase [ammonia]	Mitochondria marker, Urea cycle
Cps1	-1.9	Carbamoyl-phosphate synthase [ammonia]	Mitochondria marker, Urea cycle
Cps1	-1.8	Carbamoyl-phosphate synthase [ammonia]	Mitochondria marker, Urea cycle
Cps1	-1.8	Carbamoyl-phosphate synthase [ammonia]	Mitochondria marker, Urea cycle
Cps1	-1.7	Carbamoyl-phosphate synthase [ammonia]	Mitochondria marker, Urea cycle
Cps1	-1.7	Carbamoyl-phosphate synthase [ammonia]	Mitochondria marker, Urea cycle
Cps1	-1.7	Carbamoyl-phosphate synthase [ammonia]	Mitochondria marker, Urea cycle
Cps1	-1.7	Carbamoyl-phosphate synthase [ammonia]	Mitochondria marker, Urea cycle
Cps1	-1.7	Carbamoyl-phosphate synthase [ammonia]	Mitochondria marker, Urea cycle
Cps1	-1.7	Carbamoyl-phosphate synthase [ammonia]	Mitochondria marker, Urea cycle
Cps1	-1.7	Carbamoyl-phosphate synthase [ammonia]	Mitochondria marker, Urea cycle
Cps1	-1.6	Carbamoyl-phosphate synthase [ammonia]	Mitochondria marker, Urea cycle
Atp5a1	+1.6	ATP synthase subunit alpha, mitochondrial	ATP synthesis
Atp5a1	+1.4	ATP synthase subunit alpha, mitochondrial	ATP synthesis
Atp5b	-1.5	ATP synthase subunit beta, mitochondrial	ATP synthesis
Cox5b	-1.5	Cytochrome c oxidase subunit 5B, mitochondrial	Mitochondrial electron transport
Ndufv1	+1.4	NADH dehydrogenase (Ubiquinone) flavoprotein 1, isoform CRA_a	Electron transport
Otc	+1.4	Otc protein	Citrulline biosynthetic process
Dlst	-1.7	Dihydrolipoyllysine-residue succinyltransferase component of 2-oxoglutarate dehydrogenase complex	Amino-acid degradation, tricarboxylic acid cycle
Pah	+1.5	Phenylalanine-4-hydroxylase	Amino-acid degradation
Hsp90b1	-1.5	Isoform 1 of Endoplasmin	ER-associated protein catabolic process
Aldh1l1	+1.6	10-formyltetrahydrofolate dehydrogenase	One-carbon metabolism
Shmt1	+1.4	Serine hydroxymethyltransferase	One-carbon metabolism

To be continued

To be continued			
Pc	-1.7	Pyruvate carboxylase, mitochondrial	Carbohydrate biosynthesis
Pc	-1.6	Pyruvate carboxylase, mitochondrial	Carbohydrate biosynthesis
Pc	-1.6	Pyruvate carboxylase, mitochondrial	Carbohydrate biosynthesis
Fbp1	-2.4	Fructose-1,6-bisphosphatase 1	Carbohydrate biosynthesis
Gapdh	-1.7	Glyceraldehyde-3-phosphate dehydrogenase	Carbohydrate biosynthesis
Pgk1	+1.4	Phosphoglycerate kinase 1	Carbohydrate degradation; glycolysis
Eno1	+1.4	Alpha-enolase	Gluconeogenesis, Plasminogen activation
Mpst	+1.5	3-mercaptopyruvate sulfurtransferase	Sulfate transport
Acaa2	+1.4	42 kDa protein (Acetyl-CoA acyltransferase)	Lipid metabolism; fatty acid metabolism.
Aldh2	+1.6	Aldehyde dehydrogenase, mitochondrial	Ethanol degradation
Dpys	+1.4	Dihydropyrimidinase	Thymine catabolic process
2) Cell organization/ cell motility			
Actb	-2.3	Actin, cytoplasmic 1	Cell motion
Actb	-2.0	Actin, cytoplasmic 1	Cell motion
Actb	-1.6	Actin, cytoplasmic 1	Cell motion
LOC100361457	+1.4	Actin, gamma 1 propeptide-like	Cell motion
Actn4	-1.9	Alpha-actinin-4	Cell motion
Actb	-1.7	Beta-actin FE-3 (Fragment)	Filament reorganization
Krt10	-1.5	Keratin, type I cytoskeletal 10	Cytoskeleton organization
Krt18	-1.5	Keratin, type I cytoskeletal 18	Thyroid hormone-binding protein
3) Cell proliferation			
Abhd14b	-2.5	Abhydrolase domain-containing protein 14B	Cell proliferation
Phb	+1.7	Prohibitin	Prohibitin inhibits DNA synthesis. It has a role in regulating proliferation
To be continued			

To be continued

4) Stress response		
Hspa9	-1.7	Stress-70 protein, mitochondrial
Hspa9	-1.6	Stress-70 protein, mitochondrial
LOC100363133	-1.8	heat shock cognate 71 kDa protein-like
Sod1	+1.4	Superoxide dismutase [Cu-Zn]
Hspd1	-1.9	60 kDa heat shock protein, mitochondrial
Hspd1	-1.7	60 kDa heat shock protein, mitochondrial
Hspd1	-1.4	60 kDa heat shock protein, mitochondrial
Hspa5	-1.7	78 kDa glucose-regulated protein
Cat	+1.4	Catalase
Mdh1	-1.7	Malate dehydrogenase, cytoplasmic
Prdx4	+1.5	Peroxiredoxin-4
P4hb	+1.4	Protein disulfide-isomerase
Pdia3	+1.6	Protein disulfide-isomerase A3
5) Thrombosis		
Alb	+1.5	Serum albumin
Alb	+1.4	Serum albumin
6) Other functions		
Psmb9	+1.6	Proteasome subunit beta type-9
Gnb2l1	+1.4	Guanine nucleotide-binding protein subunit beta-2-like 1

Stress response	
Stress response	
Stress response	
Stress response	
Stress response	
Stress response	
Stress response	
Oxidation-reduction process	
Protect cells from the toxic effects of hydrogen peroxide	
Oxidation-reduction process	
Oxidation-reduction process	
Catalyzes the rearrangement of -S-S- bonds in proteins, cell redox homeostasis	
Catalyzes the rearrangement of -S-S- bonds in proteins, cell redox homeostasis	
Regulate colloidal osmotic pressure of blood	
Regulate colloidal osmotic pressure of blood	
ATP-dependent proteolytic activity and involved in antigen processing	
Activation of protein kinase C activity by G-protein coupled receptor protein signaling pathway	

-: down-regulated; +: up-regulated comparing with vehicle control.

6.3.3.1 Proteins Involved in Energy and Substance Metabolism

Among these regulated proteins, most are involved in the metabolism of energy and substances. For example, down-regulated Cps1 is involved in urea cycle to eliminate extra ammonia. Up-regulated ATP synthase subunit alpha (Atp5a1) and down-regulated Atp5b are essential for ATP synthesis. Cytochrome c oxidase subunit 5B (Cox5b) and NADH dehydrogenase (Ubiquinone) flavoprotein 1, isoform CRA_a (Ndufv1) play important role in mitochondrial electron transport. Up-regulated serine hydroxymethyltransferase (Shmt1) and 10-formyltetrahydrofolate dehydrogenase (Aldh1l1) are involved in one-carbon metabolism. Dihydrolipoyllysine-residue succinyltransferase component of 2-oxoglutarate dehydrogenase complex (Dlst) and phenylalanine-4-hydroxylase (Pah) act in the process of amino-acid degradation as well as tricarboxylic acid cycle. Up-regulated Otc protein (Otc) is involved in citrulline biosynthetic process. Two proteins, serine hydroxymethyltransferase (Pc) and fructose-1, 6-bisphosphatase 1 (Fbp1), playing a role in carbohydrate biosynthesis were down-regulated, whereas phosphoglycerate kinase 1 (Pgk1), an important enzyme for carbohydrate degradation and glycolysis was up-regulated. Alpha-enolase (Eno1) was also be up-regulated which is involved in gluconeogenesis and plays a role in plasminogen activation. Three up-regulated proteins, 3-mercaptopyruvate sulfurtransferase (Mpst) is involved in lipid metabolism and fatty acid metabolism; ldehyde dehydrogenase (Aldh2) is essential for ethanol degradation, and dihydropyrimidinase (Dpys) is responsible for thymine catabolic process. Interestingly, most of these enzymes involved in biosynthesis of energy and nutrients were down-regulated, indicating a decreased metabolic activity in liver tissues upon Cyc exposure, which was confirmed by the upregulation of Pgk1, Mpst, Aldh2 and Dpys and similar to

isoform 1 of endoplasmin (Hsp90b1), which is involved in ER-associated protein catabolic process.

6.3.3.2 Proteins Involved in Cell Organization

Six proteins involved in cytoskeleton organization and/or cell motility were affected. Except for actin, gamma 1 propeptide-like (LOC100361457), other five proteins, Actb, Krt10, Alpha-actinin-4 (Actn4), Beta-actin FE-3 (Fragment) (Actb), type II cytoskeletal 10 (Krt10) were down-regulated. These down-regulations may come from two aspects: 1) the inhibition of syntheses of amino acids and 2) the destruction of SECs.

6.3.3.3 Proteins Involved in Cell Proliferation

Abhd14b was down-regulated, which was similar to that induced by low dose of retrorsine treatment. Additionally, prohibitin (Phb), which inhibits DNA synthesis and thus has a role in regulating cell proliferation, was up-regulated, confirming that an inhibition of cell proliferation was elicited by Cyc treatment.

6.3.3.4 Proteins Involved in Stress Response

Besides, five proteins involved in stress response were down-regulated, including Hspa9, Hspd1, Hspa5, heat shock cognate 71 kDa protein-like (LOC100363133) and Malate dehydrogenase, cytoplasmic (Mdh1). This change pattern was similar to that of low dose retrorsine treatment. However, superoxide dismutase [Cu-Zn] (Sod1), catalase (Cat), and peroxiredoxin-4 (Prdx4) involved in oxidation-reduction were up-regulated. Two proteins catalyze the rearrangement of -S-S-bonds in proteins, protein disulfide-isomerase (P4hb) and protein disulfide-isomerase A3 (Pdia3) were also up-regulated and play a role in cell redox homeostasis. These simultaneously occurring down- and up-regulations of oxidative stress related proteins imply that

there was a balance between the oxidative stress and anti-oxidative mechanism in the pathogenesis of Cyc toxicity, which may explain why the oxidative biomarker, ratio of GSSG/GSH was not significantly elevated as demonstrated earlier.

6.3.3.5 Proteins Involved in Other Functions

Alb was also up-regulated as that observed at low dose of retrorsine treatment. Up-regulated guanine nucleotide-binding protein subunit beta-2-like 1 (Gnb2l1) plays a role in activation of protein kinase C by G-protein coupled receptor protein signaling pathway and proteasome subunit beta type-9 (Psmb9) possesses ATP-dependent proteolytic activity and is involved in antigen processing. Finally, four uncharacterized proteins were also found up-regulated by Cyc treatment.

6.3.4 Proteins Consistently Regulated by Cyc and Retrorsine

There were ten proteins belonging to four clusters were consistently regulated by both Cyc and retrorsine treatment (Table 6.3), which implied that these four pathways, metabolism, cell organization, cell proliferation and oxidative stress may play a role in the common pathogenesis of HSOS induced by both PA and Cyc. Especially Cps1, Atp5b and Hspa9, they were consistently regulated by three doses of retrorsine as well as Cyc treatment (Fig.6.5). In addition, similar to that observed at low dose of retrorsine treatment, Abhd14b was also down-regulated by Cyc treatment (Fig.6.5), indicating that Abhd14b had a potential to be used for the detection of a slight toxic response during HSOS development. In summary, as both Cyc and PA are able to induce HSOS, the common regulations of proteins by the two compounds lead to a hypothesis that these three proteins may be specific biomarkers of HSOS and the pathways they are involved in maybe be responsible for the progression of HSOS.
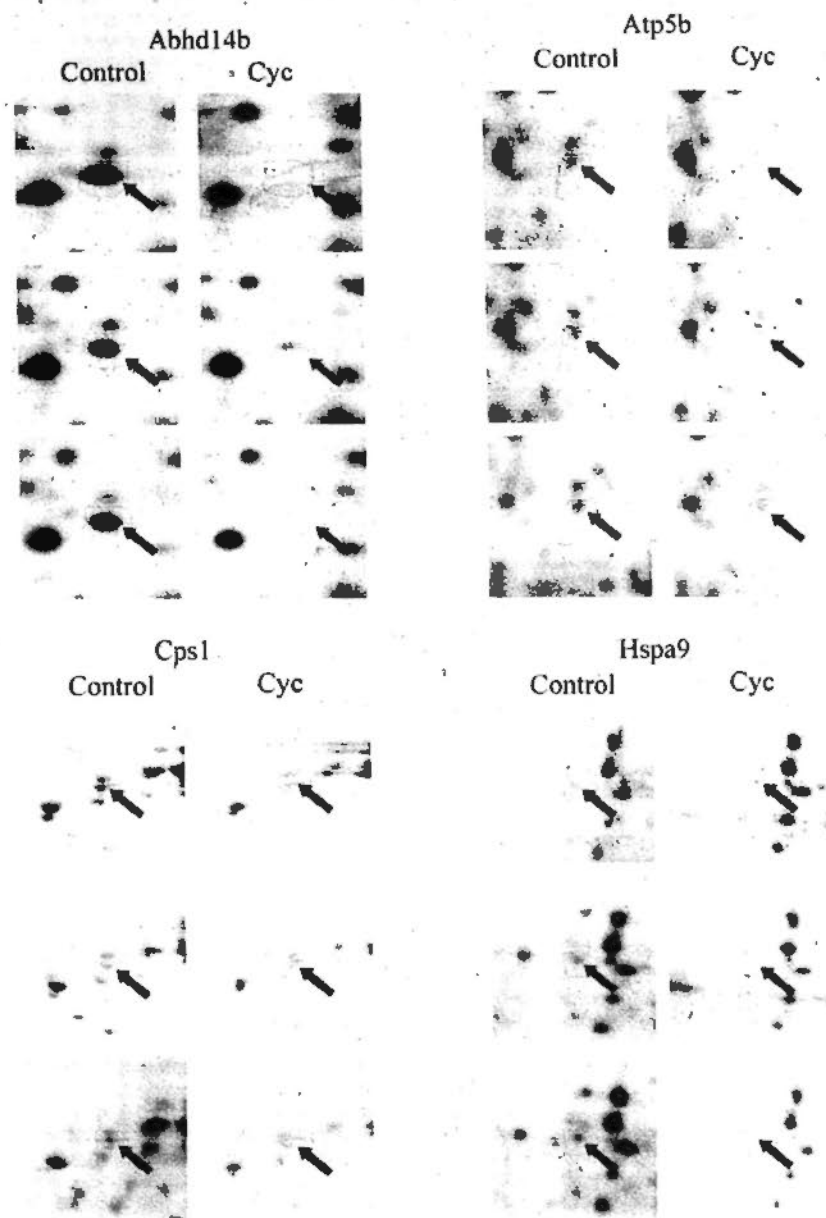
Fig.6.5. Sections of 2D-gel images showing down-regulation of Abhd14b, Cps1, Atp5b and Hspa9 observed at Cyc treatment.

Table 6.3 Proteins regulated by both retrorsine and Cyc treatment

Protein name		Fold change			
		Retrorsine			Cyc
		Low dose	Medium dose	High dose	
Cluster 1	Cps1	-4.2	+2.3	+4.1	-2.3
	Atp5b	-3.6	-1.2	+2.5	-1.5
	Pc		+1.5		-1.7
Cluster 2	Actb		-1.7		-2.3
	Abhd14b	-9.1			-2.5
Cluster 4	Hspa9	-3.1	-1.4	+2.2	-1.7
	Hspd1	-3.1		+2.0	-1.9
	Hspa5	-1.9			-1.7
	Mdh1	-2.0		+1.3	-1.7
Cluster 6	Alb	+1.5	-1.5		+1.5

Low dose: 35 mg/kg, Medium dose: 70 mg/kg and High dose: 140 mg/kg of retrorsine. Cyc: 56 mg/kg cyclophosphomide. -: Down-regulated; +: Up-regulated comparing with vehicle control group.

6.3.5 Cps1 and Atp5b Expression of the Liver

As demonstrated in chapter 5, the proteomics study revealed regulation patterns to Cps1 and Atp5b, but not Hspa9, were consistently verified, IHC and Western blot analysis after retrorsine treatment. Thus in the present study, only Cps1 and Atp5b were selected as potential biomarkers to be further verified by IHC analysis. As shown in Fig.6.6 and Fig.6.7, the strength of staining showed that an apparent decrease of Cps1, while slight decrease of Atp5b were induced by Cyc treatment, which was in agreement with the 2-D pattern. Interestingly, as demonstrated in chapter 5, down-regulation of these two proteins was also observed at low level of PA exposure. This consistency integrated with the similar degree of toxicity elicited by both kinds of compounds suggested that the down-regulation of Cps1 and Atp5b

should be characteristic of slight hepatotoxicity upon either low level of PA or Cyc treatment. In fact, in the cases of human HSOS, a low level as well as chronic exposure to the toxin is mostly common. Thus, the biomarkers and pathways contributed to the sub-toxic response may have potential to be used as specific biomarkers of early phase of pathogenesis before HSOS is developed.
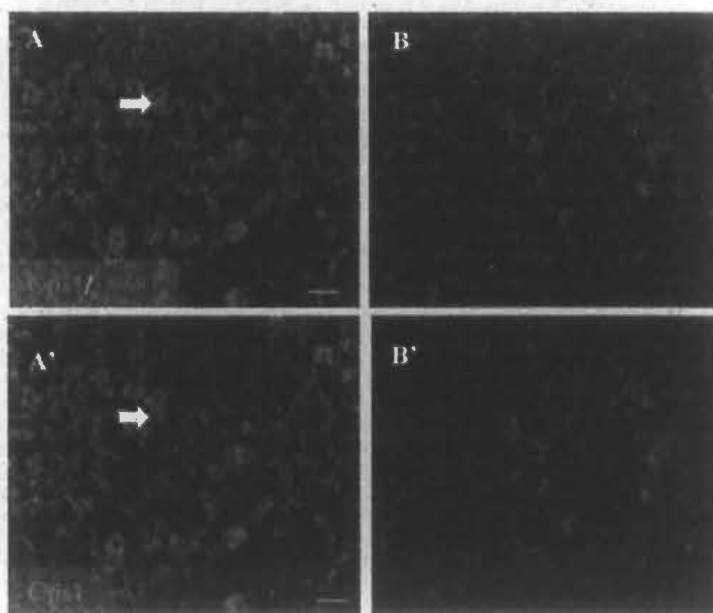
Fig.6.6. Effects of Cyc on liver Cps1 expression assessed by immunostaining. Liver sections were obtained from rats treated with saline (A, A' and A'') and 56 mg/kg Cyc (B, B' and B''). A and B: Double immunostaining with Cps1 (shown in red and indicated with white arrow) and DAPI (shown in blue). A' and B': Immunostaining of Cps1 (indicated with white arrows). Scale bar in (A-D and A'-D') = 25 μm.
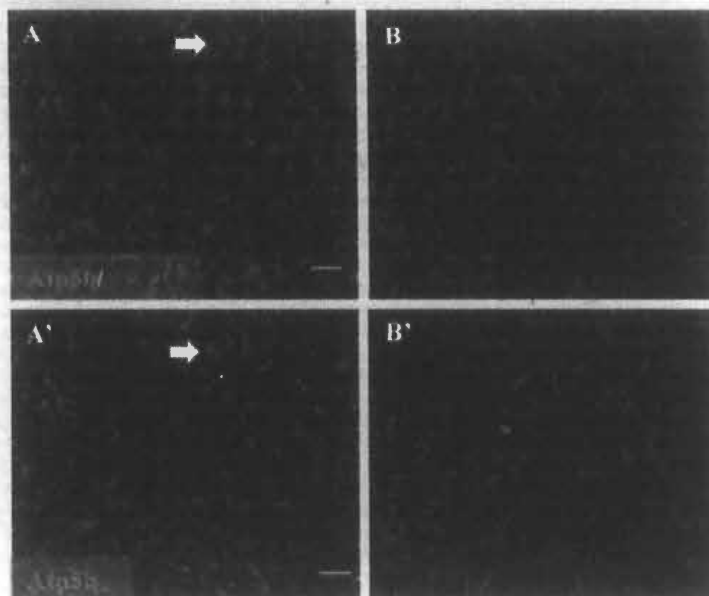
Fig.6.7. Effects of Cyc on hepatic Atp5b expression assessed by immunostaining. Liver sections were obtained from rats treated with saline (A, A' and A'') and 56 mg/kg Cyc (B, B' and B''). A and B: Double immunostaining with Atp5b (shown in green and indicated with white arrow) and DAPI (shown in blue). A' and B': Immunostaining of Atp5b (indicated with white arrow). Scale bar in (A-D and A'-D') = 25 μm.

6.4 Summary

The proteomic analysis revealed that Cyc exposure resulted in the alternation of metabolic enzymes, cellular organization, cell proliferation and stress response processes, which was also observed in retrosine treatment as demonstrated in chapter 5. Among the differential expressed proteins, over half of them were found to be enzymatic proteins which are involved in amino acid, nucleotide or fatty acid metabolism and ATP synthesis. Heat shock proteins were another cluster of regulated proteins related to oxidative stress. Most of the affected proteins appeared decreased at 24 h after dosing with low dose of retrorsine or Cyc. This can be due to

the decreased protein synthesis resulting in the reduced capacity of liver to generate and maintain sufficient levels of nutrition and ATP. The resultant decrease in bioenergetic capacity is thought to contribute to the decreased SEC viability and ultimately the pathological changes that occur before the development of HSOS. Especially, Cps1 and Atp5b were confirmed be consistently down-regulated by low dose of retrorsine and Cyc treatment. Identification of these altered proteins provides critical insight into the mechanisms of HSOS. Specifically, we show for the first time that both PA and Cyc have profound interactions with mitochondrial proteins, as well as metabolism enzymes. The novel observations of them on pathways of urea cycle and ATP synthesis suggest that these two pathways may contribute to the development of HSOS.

Four distinct stages for the protein biomarker development process are identified as discovery, qualification, verification, and validation with verification being the rate-limiting step (Berna and Ackermann, 2009). By a series of discovery, qualification and verification studies, Cps1 and Atp5b were proved to have the potential to be used as specific biomarkers for the detection of pathogenesis of HSOS. Subsequently, validations need to be achieved by knockdown or knockout of these two proteins to appraise their contribution and involvement in the development of HSOS in the future study.

Chapter 7 General Conclusions

7.1 *In Vitro* Study

Hepatotoxic PAs present in a wide variety of plant species and can easily intoxicate human beings by contaminating food stuffs such as cereal, honey, eggs, and meats. In addition, with the rapidly-growing interest worldwide in the use of natural products as medical remedies and dietary supplements, PAs are becoming one of the most important reasons for natural products poisoning. Till now, more than 8000 cases of HSOS induced by PA consumption have been reported over the world (Lin et al., 2010). However, due to a limited knowledge about the mechanism, no effective methods have been developed for the treatment of PA-induced HSOS. Under these conditions, prevention and restriction of PA exposure become a key strategy for controlling PA poisonings. Nowadays many Western countries have established some regulations for the use of PA-containing herb products. However, these regulations are based on case study and cannot be applied universally for all PAs due to the severities of toxicity of different PAs vary significantly. The different severity of toxicity as well as the diversity of PA types makes it difficult to set up the regulation for a universal threshold of toxic dose of individual PAs. Thus it is timely and important to develop an effective method to systematically and rapidly assess the severity of toxicity of different PAs.

By *in vitro* study, a convenient and simple model has been developed to screen the cytotoxicities of PAs using HepG2 cells. In this model, the developed combinational use of MTT and BrdU assays were able to discriminate the cytotoxicity of different PAs. Among different types PAs tested, an otonecine-type PA representative is significantly more toxic than a retronecine-type one, while a platyphylline-type one is non-toxic. Moreover, by successfully detecting the cytotoxicity of a PA-containing

herb, the developed model appears to be also suitable for the assessment of PA-containing herbs intoxication. In conclusion, we have developed, for the first time, a rapid and simple *in vitro* model for the detection of the severity of hepatic cytotoxicity of different types of PAs and also for the discrimination of toxic PAs from non-toxic one. This method has the potential to be used for the quick screening the toxicity of PA-containing natural products.

7.2 *In Vivo* Study

The toxicity of PAs is from the metabolic formation of pyrroles being catalyzed by hepatic CYP3A and CYP2B (Omiecinski et al., 1999; Yang et al., 2001a). Because of its limited metabolizing capacity as well as a lack of cell communication, the developed *in vitro* model cannot mimic the real pathogenesis of PA intoxication. Developing a reliable and reproducible animal model is thus fundamental for the delineation of underlying mechanisms of PA intoxication. In addition, the detailed events in the development of HSOS after PA exposure are largely unknown, resulting in the lack of specific methods for its diagnosis. Therefore, the aim of our *in vivo* study include two aspects: one is to develop a rat hepatotoxicity model and the other is to investigate the mechanisms of PA intoxication upon this developed model. Through the mechanism study, a signature pattern of protein expression and several specific mechanism-based biomarkers are proposed by using the integrated conventional toxicological studies and proteomic approach.

7.2.1 Model Development

By using retrorsine as the PA representative, we have developed a rat model that produces consistent and reproducible hepatotoxicity with minimal lethality. Furthermore, a definite dose-dependent toxic response has been elicited by the single oral administration of dose corresponding to 0.7, 1.4 and 2.8 fold of LD_{50} of

retrorsine: low dose induced a slight injury with an elevation of ALT, GSSG/GSH and MPO; medium dose caused a mild injury referring to more damage including the elevation of RLW, GSH and GR; whereas high dose resulted in severe damage referring to an elevation of ALT, RLW, GSH, GR, TB and LDH, but a slight decrease of GSSG/GSH and MPO. Thus the response to low dose retrorsine treatment can be characterized as a sub-toxic effect involving oxidative stress and inflammation activation; high dose represents a severe toxicity showing hepatocyte necrosis and the beginning of possible GSH depletion; whereas the degree of toxicity induced by medium dose showed significant specimen variations. This dose-dependent response was ascribed to the formation of different amounts of toxic metabolite of retrorsine.

In addition, by using RECA-1 immunostaing, we have, for the first time, made the SECs and CVECs simultaneously visible, which is crucial for the accurate determination of which kind of cells, either SECs or CVECS, are primarily affected first. Till now, there is only one study reporting the use of this method to visualize SECs (Deleve et al, 2002). However, no dose-dependent and region distribution of damages to SECs has been reported. In the present study, we find, for the first time, that the severity of EC damage between the central and peripheral regions of liver lobe was largely different accompanying with an obvious dose-dependent character: a slight loss of SECs in central region of the liver lobe was caused by low dose; a mild loss of SECs as well a slight loss of CVECs in central region, whereas slight loss of SECs in peripheral regions were caused by medium dose; and a severe loss of SECs and mild loss of CVECs in central region while mild loss of SECs and no obvious damage to CVECs in peripheral region were caused by high dose of retrorsine treatment. Thus the present study, for the first time, directly proves that SECs are more easily to being injured than CVECs by PA administration. More

importantly, it is the first time to find that the central region of liver lobe is firstly affected, then the peripheral region, which may provide useful information for the biopsy in collecting specimen for early diagnosis. In addition, as oxidative stress and inflammation activation also occurred with low dose of retrorsine expose, they may be the underlying mechanisms of ECs damage. Similarly, the sinusoid hemorrhage and lobule disarray observed at high dose treatment are believed to be resulted from the severe damage of SCEs and CVECs.

The above findings formed a solid foundation for the further proteomic study. It would be helpful in understanding and illustrating the proteomic data for investigating potential biomarkers and pathways of PA-induced hepatotoxicity.

7.2.2 Proteomic Study

7.2.2.1 Proteomic Study on PA-Induced Acute Hepatotoxicity

Proteomic study allows the investigation on mechanisms of drug action at protein levels. It plays a very important role in the elucidation of molecular mechanisms of toxicity and developments of novel biomarkers which may contribute to high throughput safety screening. As the toxicity mechanism of PA is not clear and the formation of protein-adduct is generally considered as one consequence of PA exposure, specific proteins are thus believed to be involved in the initiation or/and progression of PA-induced hepatotoxicity. The present study thus aims to investigate the expression changes of hepatic protein induced by PA using proteomic approach. Moreover, through analyzing and comparing the 2-D snapshots of protein expression from different doses, a signature pattern of protein expression and specific biomarkers of liver toxicity were established.

Proteomic study revealed that the regulated proteins were mostly down-regulated by low, half down-regulated by medium and mainly up-regulated by high dose of

retrorsine treatment. These regulated proteins are involved in six classified functions: metabolism enzymes, cell organization, cell proliferation, stress response, thrombosis and other functions. By integrating above clusters with the conventional toxicological assessments, an "overview model" of PA intoxication is constructed. Low dose of PA exposure resulted in the decrease of enzymes involved in three of the primary metabolic pathways, which led to the decrease of the production of basic materials and energy of the liver tissue. As a result, the biosynthesis of cell organization related proteins were also reduced, which was accompanied by the inhibition of cell proliferation. Similarly, proteins acting in ATP-dependent oxidative stress response and formation of thrombosis were inhibited, resulting in an oxidative stress and potentially aggravated hemorrhage resulting from the slight loss of SECs. In summary, a low level of PA exposure resulted in a definite down-regulation of protein patterns. There are two possible reasons: one is due to the formation of DNA- or protein-adducts which interfere with the expression of proteins; the other possibility is due to a preserving mechanism of the body to a slight injury caused by a relative little amount of PA exposure.

With medium dose of retrorsine treatment, most of the metabolism proteins were up-regulated, which were ascribed to the activation of the protective effect or feedback of the body to synthesize more nutrients and energy for antagonizing the damage effect of PA. However, the rates of cell reorganization and cell proliferation were still low. A possible explanation is that a larger amount of pyrrolic ester metabolite produced by the administration of medium dose of retrorsine directly bind and destroy more cytoskeleton proteins, which fail to overwhelm the repairing rate of the liver. Similarly, the repairing mechanism via anti-oxidants was also not fully activated. Interestingly, proteins for thrombosis inhibition were up-regulated, confirming that a repairing effect of the body has been activated to fix the increased

degree of hemorrhage. In contrast to a previous report (Mattocks, 1986), PA was, for the first time, found to increase the expression of hepatic proteins. Whether it acts as an inhibitor or activator of protein expression was hypothesized to be determined by the exposure level. This hypothesis is confirmed partly by the regulation pattern of high dose treatment, in which, all of the involved proteins were up-regulated.

Furthermore, three proteins, Cps1, Atp5b and Hspa9 related to urea cycle, energy metabolism and stress response respectively were consistently altered by three doses of PA treatment. The confirmation studies consistently proved that Cps1 and Atp5b were actually down-regulated by low dose, whereas up-regulated upon high dose of PA exposure. However, the regulating patterns of medium dose treatment to Cps1 and Atp5b were not fully consistent between two confirmation studies and proteomic analysis, which can be explained by the large individual variation upon this dose of retrorsine exposure as found with the conventional toxicological parameters. However, the expression pattern of Hspa9 revealed by confirmation studies was not in agreement with the proteomic results, which could be explained by the uneven distribution of Hspa9 in the livers. Thus, we believe that Hspa9 cannot act as a suitable biomarker of PA intoxication.

In conclusion, Cps1 and Atp5b could be further developed as specific biomarkers of PA intoxication. Down-regulation of these two proteins may indicate a slight hepatotoxicity upon a low level of PA exposure; up-regulation of them suggested a severe toxicity occurred with a higher dose of PA exposure. Overall, the results support that these two biomarkers are warranted further development and should be evaluated against more PAs to characterize their specificity for predicting the severity of PA-induced hepatotoxicity. Since the detailed mechanism of response of these proteins to the PA tested is not known, and therefore further in-depth studies are needed.

7.2.2.2 Comparative Proteomic Study on Cyc-Induced Acute Hepatotoxicity

A same class of compounds is expected to affect the same or related mechanism by eliciting similar pathologies and is therefore likely to affect similar sets of proteins in a comparable manner. These protein signatures may then be employed in a diagnostic or predictive way.

Because both chemotherapy and PA exposure can cause HSOS with a specific pathogenesis, a comparable proteomic study of the Cyc-induced acute hepatotoxicity was thus believed to be helpful in understanding the mechanism of this disease. Hence, we established a 2-D protein map for rat liver to identify the proteins which were regulated by Cyc and to construct a pathway signature from a combination of altered proteome profiles and conventional toxicological parameters.

As expected, Cyc at the dose corresponding to its LD_{50} elicited an acute toxic effect on rat. When considering all the changes in clinical pathology, liver biochemistry and histology, the degree of damage induced by Cyc is similar to that upon low dose of PA exposure. However, in these two hepatotoxicity processes, there were also some discrepancies such as a lack of oxidative stress in Cyc-induced hepatotoxicity, which suggests that the underlying mechanisms of these two kinds of compounds were not entirely the same.

Proteomic study indicated that 19 proteins were down-regulated and 26 were up-regulated upon Cyc treatment. Similar to PA treatment, except for thrombosis related proteins, these altered proteins could be categorized into the same five clusters: enzymes or enzymatic subunits, proteins related to cell organization, cell proliferation and oxidative stress related proteins, as well the proteins with other functions. This result indicated that these four pathways, metabolism, cell organization, cell proliferation and oxidative stress, may take part in the common

pathogenesis of HSOS induced by both PA and Cyc. Specifically, Cps1 and Atp5b were consistently confirmed to be down-regulated upon low level of PA and Cyc exposure. This consistency integrated with the similar degree of toxicity elicited by two exposures, suggested that the down-regulation of Cps1 and Atp5b might be a character of the slight toxic response prior to the development of HSOS. In fact, a low level as well as chronic exposure to the toxins is mostly common seen in the cases of human HSOS. Thus, the biomarkers and pathways contributed to the slight toxic response may be useful for the diagnosis of HSOS at the very beginning. In addition, the consistent involvement of the pathways of urea cycle and ATP synthesis suggested that these two pathways may contribute to the development of HSOS.

In conclusion, Cps1 and Atp5b have the potential to be developed as useful biomarkers for the diagnosis of HSOS. A further study with the aim to assess the specificity of these two biomarkers is needed.

References

Abraham N, Carty R, DuFour D, Pincus M. (2006). Clinical enzymology. In: McPherson R, Pincus M, eds. Henry's Clinical Diagnosis and Management by Laboratory Methods. 21st ed. Philadelphia, Pa: Saunders Elsevier, chap 20.

Abbott, A. (1999). A post-genomic challenge: learning to read patterns of protein synthesis. Nature 402, 715-720.

Amacher, D.E. (1998). Serum transaminase elevations as indicators of hepatic injury following the administration of drugs. Regul Toxicol Pharmacol 27, 119-130.

Andringa, K.K., King, A.L., Eccleston, H.B., Mantena, S.K., Landar, A., Jhala, N.C., Dickinson, D.A., Squadrito, G.L., and Bailey, S.M. (2010). Analysis of the liver mitochondrial proteome in response to ethanol and S-adenosylmethionine treatments: novel molecular targets of disease and hepatoprotection. Am J Physiol Gastrointest Liver Physiol 298, G732-745.

Aston, N., Morris, P., and Tanner, S. (1996). Retrorsine in breast milk influences copper hanling in suckling rat pups. J Hepatol 25, 748-755.

Bandara, L.R., and Kennedy, S. (2002). Toxicoproteomics -- a new preclinical tool. Drug Discov Today 7, 411-418.

Bazarbachi, A., Scrobohaci, M.L., Gisselbrecht, C., Marolleau, J.P., Mansi, A., Brice, P., Gorra, P., and Drouet, L. (1993). Changes in protein C, factor VII and endothelial markers after autologous bone marrow transplantation: possible implications in the pathogenesis of veno-occlusive disease. Nouv Rev Fr Hematol 35, 135-140.

Beales, K.A., Betteridge, K., Colegate, S.M., and Edgar, J.A. (2004). Solid-phase extraction and LC-MS analysis of pyrrolizidine alkaloids in honeys. J Agric Food Chem 52, 6664-6672.

Bearman, S.I. (2000). Veno-occlusive disease of the liver. Curr Opin Oncol 12, 103-109.

Bensaude, R.J., Monegier du Sorbier, C., Jonville-Bera, A.P., Autret, E., Ouyahya, F., and Metman, E.H. (1998). [Veno-occlusive disease after prolonged treatment with senecionine (Hemoluol)]. Gastroenterol Clin Biol 22, 363-364.

Berna, M., and Ackermann, B. (2009). Increased throughput for low-abundance protein biomarker verification by liquid chromatography/tandem mass spectrometry. Anal Chem 81, 3950-3956.

Betteridge, K., Cao, Y., and Colegate, S.M. (2005). Improved method for extraction and LC-MS analysis of pyrrolizidine alkaloids and their N-oxides in honey: application to Echium vulgare honeys. J Agric Food Chem *53*, 1894-1902.

Boppre, M. (2011). The ecological context of pyrrolizidine alkaloids in food, feed and forage: an overview. Food Addit Contam Part A Chem Anal Control Expo Risk Assess *28*, 260-281.

Boppre, M., Colegate, S.M., Edgar, J.A., and Fischer, O.W. (2008). Hepatotoxic pyrrolizidine alkaloids in pollen and drying-related implications for commercial processing of bee pollen. J Agric Food Chem *56*, 5662-5672.

Cesaro, S., Spiller, M., Sartori, M.T., Alaggio, R., Peruzzo, M., Saggiorato, G., and Bisogno, G. (2011). Veno-occlusive disease in pediatric patients affected by Wilms tumor. Pediatr Blood Cancer *57*, 258-261.

Chen, I.L., Yang, S.N., Hsiao, C.C., Wu, K.S., and Sheen, J.M. (2008a). Treatment with high-dose methylprednisolone for hepatic veno-occlusive disease in a child with rhabdomyosarcoma. Pediatr Neonatol *49*, 141-144.

Chen K. K., Paul N. H., Charles L. R.(1939). The action and toxicity of platyphylline and seneciphylline. J. Pharmacol. Exp. Ther. 68,130-140

Chen, M.J., Chiang, L.Y., and Lai, Y.L. (2001). Reactive oxygen species and substance P in monocrotaline-induced pulmonary hypertension. Toxicol Appl Pharmacol *171*, 165-173.

Chen, M.Y., Cai, J.T., Du, Q., Wang, L.J., Chen, J.M., and Shao, L.M. (2008b). Reliable experimental model of hepatic veno-occlusive disease caused by monocrotaline. Hepatobiliary Pancreat Dis Int *7*, 395-400.

Chen, Z., and Huo, J.R. (2010). Hepatic veno-occlusive disease associated with toxicity of pyrrolizidine alkaloids in herbal preparations. Neth J Med *68*, 252-260.

Cheng, J., Ma, X., Krausz, K.W., Idle, J.R., and Gonzalez, F.J. (2009). Rifampicin-activated human pregnane X receptor and CYP3A4 induction enhance acetaminophen-induced toxicity. Drug Metab Dispos *37*, 1611-1621.

Cheng, W., Oike, M., Hirakawa, M., Ohnaka, K., Koyama, T., and Ito, Y. (2005). Excess l-arginine restores endothelium-dependent relaxation impaired by monocrotaline pyrrole. Toxicol Appl Pharmacol *207*, 187-194.

Chojkier, M. (2003). Hepatic sinusoidal-obstruction syndrome: toxicity of pyrrolizidine alkaloids. J Hepatol *39*, 437-446.

Chopra, R., Eaton, J.D., Grassi, A., Potter, M., Shaw, B., Salat, C., Neumeister, P., Finazzi, G., Iacobelli, M., Bowyer, K., *et al.* (2000). Defibrotide for the treatment of hepatic veno-occlusive disease: results of the European compassionate-use study. Br J Haematol *111*, 1122-1129.

Chu, P.S., Lame, M.W., and Segall, H.J. (1993). In vivo metabolism of retrorsine and retrorsine-N-oxide. Arch Toxicol *67*, 39-43.

Copple, B.L., Banes, A., Ganey, P.E., and Roth, R.A. (2002). Endothelial cell injury and fibrin deposition in rat liver after monocrotaline exposure. Toxicol Sci *65*, 309-318.

Copple, B.L., Ganey, P.E., and Roth, R.A. (2003). Liver inflammation during monocrotaline hepatotoxicity. Toxicology *190*, 155-169.

Copple, B.L., Rondelli, C.M., Maddox, J.F., Hoglen, N.C., Ganey, P.E., and Roth, R.A. (2004). Modes of cell death in rat liver after monocrotaline exposure. Toxicol Sci *77*, 172-182.

Copple, B.L., Roth, R.A., and Ganey, P.E. (2006). Anticoagulation and inhibition of nitric oxide synthase influence hepatic hypoxia after monocrotaline exposure. Toxicology *225*, 128-137.

Coulombe, R.A., Jr. (2003). Pyrrolizidine alkaloids in foods. Adv Food Nutr Res *45*, 61-99.

Coulombe, R.A., Jr., Drew, G.L., and Stermitz, F.R. (1999). Pyrrolizidine alkaloids crosslink DNA with actin. Toxicol Appl Pharmacol *154*, 198-202.

Crews, C., Startin, J.R., and Clarke, P.A. (1997). Determination of pyrrolizidine alkaloids in honey from selected sites by solid phase extraction and HPLC-MS. Food Addit Contam *14*, 419-428.

Culvenor, C.C. (1983). Estimated intakes of pyrrolizidine alkaloids by humans. A comparison with dose rates causing tumors in rats. J Toxicol Environ Health *11*, 625-635.

Culvenor, C.C., Clarke, M., Edgar, J.A., Frahn, J.L., Jago, M.V., Peterson, J.E., and Smith, L.W. (1980). Structure and toxicity of the alkaloids of Russian comfrey (symphytum x uplandicum Nyman), a medicinal herb and item of human diet. Experientia *36*, 377-379.

Culvenor, C.C., Edgar, J.A., Jago, M.V., Qutteridge, A., Peterson, J.E., and Smith, L.W. (1976). Hepato- and pneumotoxicity of pyrrolizidine alkaloids and derivatives in relation to molecular structure. Chem Biol Interact *12*, 299-324.

Dai, N., Yu, Y.C., Ren, T.H., Wu, J.G., Jiang, Y., Shen, L.G., and Zhang, J. (2007). Gynura root induces hepatic veno-occlusive disease: a case report and review of the literature. World J Gastroenterol *13*, 1628-1631.

Dambach, D.M., Andrews, B.A., and Moulin, F. (2005). New technologies and screening strategies for hepatotoxicity: use of in vitro models. Toxicol Pathol *33*, 17-26.

De Backer, M.D., Thurmond, R.L., Carmen, A.A., and Luyten, W.H. (2002). Gene-Expression - Based Responses to Drug Treatment. Drug News Perspect *15*, 155-165.

Deeg, K.H., Glockel, U., Richter, R., and Beck, J. (1993). Diagnosis of veno-occlusive disease of the liver by color-coded Doppler sonography. Pediatr Radiol *23*, 134-136.

DeLeve, L.D. (1996). Cellular target of cyclophosphamide toxicity in the murine liver: role of glutathione and site of metabolic activation. Hepatology *24*, 830-837.

DeLeve, L.D. (2001). Hepatic venoocclusive disease: a major complication of hematopoietic stem cell transplantation in cancer patients. Tumori *87*, S27-29.

DeLeve, L.D. (2007). Hepatic microvasculature in liver injury. Semin Liver Dis *27*, 390-400.

Deleve, L.D., Jaeschke, H., Kalra, V.K., Asahina, K., Brenner, D.A., and Tsukamoto, H. (2011). 15th International Symposium on Cells of the Hepatic Sinusoid, 2010. Liver Int *31*, 764-774.

DeLeve, L.D., McCuskey, R.S., Wang, X., Hu, L., McCuskey, M.K., Epstein, R.B., and Kanel, G.C. (1999). Characterization of a reproducible rat model of hepatic veno-occlusive disease. Hepatology *29*, 1779-1791.

DeLeve, L.D., Shulman, H.M., and McDonald, G.B. (2002). Toxic injury to hepatic sinusoids: sinusoidal obstruction syndrome (veno-occlusive disease). Semin Liver Dis *22*, 27-42.

DeLeve, L.D., Wang, X., Kaplowitz, N., Shulman, H.M., Bart, J.A., and van der Hoek, A. (1997). Sinusoidal endothelial cells as a target for acetaminophen toxicity.

Direct action versus requirement for hepatocyte activation in different mouse strains. Biochem Pharmacol *53*, 1339-1345.

DeLeve, L.D., Wang, X., Kuhlenkamp, J.F., and Kaplowitz, N. (1996). Toxicity of azathioprine and monocrotaline in murine sinusoidal endothelial cells and hepatocytes: the role of glutathione and relevance to hepatic venoocclusive disease. Hepatology *23*, 589-599.

Deleve, L.D., Wang, X., Tsai, J., Kanel, G., Strasberg, S., and Tokes, Z.A. (2003). Sinusoidal obstruction syndrome (veno-occlusive disease) in the rat is prevented by matrix metalloproteinase inhibition. Gastroenterology *125*, 882-890.

Dufour, D.R., Lott, J.A., Nolte, F.S., Gretch, D.R., Koff, R.S., and Seeff, L.B. (2000a). Diagnosis and monitoring of hepatic injury. I. Performance characteristics of laboratory tests. Clin Chem *46*, 2027-2049.

Dufour, D.R., Lott, J.A., Nolte, F.S., Gretch, D.R., Koff, R.S., and Seeff, L.B. (2000b). Diagnosis and monitoring of hepatic injury. II. Recommendations for use of laboratory tests in screening, diagnosis, and monitoring. Clin Chem *46*, 2050-2068.

Edgar, J.A., Colegate, S.M., Boppre, M., and Molyneux, R.J. (2011). Pyrrolizidine alkaloids in food: a spectrum of potential health consequences. Food Addit Contam Part A Chem Anal Control Expo Risk Assess *28*, 308-324.

Edgar, J.A., Roeder, E., and Molyneux, R.J. (2002). Honey from plants containing pyrrolizidine alkaloids: a potential threat to health. J Agric Food Chem *50*, 2719-2730.

El Golli Bennour, E., Bouaziz, C., Ladjimi, M., Renaud, F., and Bacha, H. (2009). Comparative mechanisms of zearalenone and ochratoxin A toxicities on cultured HepG2 cells: is oxidative stress a common process? Environ Toxicol *24*, 538-548.

Fossati, P., Ponti, M., Prencipe, L., and Tarenghi, G. (1989). One-step protocol for assays of total and direct bilirubin with stable combined reagents. Clin Chem *35*, 173-176.

Fountoulakis, M., Berndt, P., Boelsterli, U.A., Crameri, F., Winter, M., Albertini, S., and Suter, L. (2000). Two-dimensional database of mouse liver proteins: changes in hepatic protein levels following treatment with acetaminophen or its nontoxic regioisomer 3-acetamidophenol. Electrophoresis *21*, 2148-2161.

Fountoulakis, M., and Suter, L. (2002). Proteomic analysis of the rat liver. J Chromatogr B Analyt Technol Biomed Life Sci *782*, 197-218.

Frei, H., Luthy, J., Brauchli, J., Zweifel, U., Wurgler, F.E., and Schlatter, C. (1992). Structure/activity relationships of the genotoxic potencies of sixteen pyrrolizidine alkaloids assayed for the induction of somatic mutation and recombination in wing cells of Drosophila melanogaster. Chem Biol Interact 83, 1-22.

Fu, P.P., Xia, Q., Lin, G., and Chou, M.W. (2004). Pyrrolizidine alkaloids--genotoxicity, metabolism enzymes, metabolic activation, and mechanisms. Drug Metab Rev 36, 1-55.

Fuhr, U. (2000). Induction of drug metabolising enzymes: pharmacokinetic and toxicological consequences in humans. Clin Pharmacokinet 38, 493-504.

Gao, J., Wang, C., Li, Y., and Wang, Z. (2009). [Advance on pharmacologic actions, toxicity and pharmacokinetics of pyrrolizidine alkaloids]. Zhongguo Zhong Yao Za Zhi 34, 506-511.

Gibson, J.D., Pumford, N.R., Samokyszyn, V.M., and Hinson, J.A. (1996). Mechanism of acetaminophen-induced hepatotoxicity: covalent binding versus oxidative stress. Chem Res Toxicol 9, 580-585.

Goldstein, J.L., and Brown, M.S. (1986). Atherosclerosis and its complications: contributions from the Association of American Physicians, 1886-1986. Trans Assoc Am Physicians 99, ccxxxi-ccxlvii.

Gomez-Quiroz, L.E., Factor, V.M., Kaposi-Novak, P., Coulouarn, C., Conner, E.A., and Thorgeirsson, S.S. (2008). Hepatocyte-specific c-Met deletion disrupts redox homeostasis and sensitizes to Fas-mediated apoptosis. J Biol Chem 283, 14581-14589.

Gordon, G.J., Coleman, W.B., and Grisham, J.W. (2000a). Bax-mediated apoptosis in the livers of rats after partial hepatectomy in the retrorsine model of hepatocellular injury. Hepatology 32, 312-320.

Gordon, G.J., Coleman, W.B., and Grisham, J.W. (2000b). Induction of cytochrome P450 enzymes in the livers of rats treated with the pyrrolizidine alkaloid retrorsine. Exp Mol Pathol 69, 17-26.

Gordon, G.J., Coleman, W.B., Hixson, D.C., and Grisham, J.W. (2000c). Liver regeneration in rats with retrorsine-induced hepatocellular injury proceeds through a novel cellular response. Am J Pathol 156, 607-619.

Gorg, A., Obermaier, C., Boguth, G., Harder, A., Scheibe, B., Wildgruber, R., and Weiss, W. (2000). The current state of two-dimensional electrophoresis with immobilized pH gradients. Electrophoresis *21*, 1037-1053.

Groneberg, D.A., Grosse-Siestrup, C., and Fischer, A. (2002). In vitro models to study hepatotoxicity. Toxicol Pathol *30*, 394-399.

Gruss, E., Bernis, C., Tomas, J.F., Garcia-Canton, C., Figuera, A., Motellon, J.L., Paraiso, V., Traver, J.A., and Fernandez-Ranada, J.M. (1995). Acute renal failure in patients following bone marrow transplantation: prevalence, risk factors and outcome. Am J Nephrol *15*, 473-479.

Guillouzo, A., Morel, F., Fardel, O., and Meunier, B. (1993). Use of human hepatocyte cultures for drug metabolism studies. Toxicology *82*, 209-219.

Guillouzo, A., Morel, F., Langouet, S., Maheo, K., and Rissel, M. (1997). Use of hepatocyte cultures for the study of hepatotoxic compounds. J Hepatol *26 Suppl 2*, 73-80.

Guo, D., Fu, T., Nelson, J.A., Superina, R.A., and Soriano, H.E. (2002). Liver repopulation after cell transplantation in mice treated with retrorsine and carbon tetrachloride. Transplantation *73*, 1818-1824.

Guo, L., Mei, N., Dial, S., Fuscoe, J., and Chen, T. (2007). Comparison of gene expression profiles altered by comfrey and riddelliine in rat liver. BMC bioinformatics *8 Suppl 7*, S22.

Gygi S.P., Rochon Y., Franza B.R., Aebersold R. (1999). Correlation between protein and mRNA abundance in yeast. Mol Cell Biol *19*, 1720-1730.

Hahn, T., Rondeau, C., Shaukat, A., Jupudy, V., Miller, A., Alam, A.R., Baer, M.R., Bambach, B., Bernstein, Z., Chanan-Khan, A.A., *et al.* (2003). Acute renal failure requiring dialysis after allogeneic blood and marrow transplantation identifies very poor prognosis patients. Bone Marrow Transplant *32*, 405-410.

Hall, T.J., James, P.R., and Cambridge, G. (1993). Development of an in vitro hepatotoxicity assay for assessing the effects of chronic drug exposure. Res Commun Chem Pathol Pharmacol *79*, 249-256.

Hanumegowda, U.M., Copple, B.L., Shibuya, M., Malle, E., Ganey, P.E., and Roth, R.A. (2003). Basement membrane and matrix metalloproteinases in monocrotaline-induced liver injury. Toxicol Sci *76*, 237-246.

Harris, C.L., Titchener, E.B., and Cline, A.L. (1969). Sulfur-deficient transfer ribonucleic acid in a cysteine-requiring, "relaxed" mutant of Escherichia coli. J Bacteriol *100*, 1322-1327.

Hayes, K.R., and Bradfield, C.A. (2005). Advances in toxicogenomics. Chem Res Toxicol *18*, 403-414.

Heinecke, J.W., Li, W., Daehnke, H.L., 3rd, and Goldstein, J.A. (1993a). Dityrosine, a specific marker of oxidation, is synthesized by the myeloperoxidase-hydrogen peroxide system of human neutrophils and macrophages. J Biol Chem *268*, 4069-4077.

Heinecke, J.W., Li, W., Francis, G.A., and Goldstein, J.A. (1993b). Tyrosyl radical generated by myeloperoxidase catalyzes the oxidative cross-linking of proteins. J Clin Invest *91*, 2866-2872.

Helmy, A. (2006). Review article: updates in the pathogenesis and therapy of hepatic sinusoidal obstruction syndrome. Aliment Pharmacol Ther *23*, 11-25.

Helmy, A.H., Abdel-Hady, A.A., el-Shanawany, F., Hammam, O., and Abdel-Hady, A. (2005). The pharmacological approach to reverse portal hypertention and hepatic schistosomal fibrosis in Egypt, control experimental study. J Egypt Soc Parasitol *35*, 731-750.

Hewitt, N.J., and Hewitt, P. (2004). Phase I and II enzyme characterization of two sources of HepG2 cell lines. Xenobiotica *34*, 243-256.

Hill, B.D., Gaul, K.L., and Noble, J.W. (1997). Poisoning of feedlot cattle by seeds of Heliotropium europaeum. Aust Vet J *75*, 360-361.

Ho, V., Momtaz, P., Didas, C., Wadleigh, M., and Richardson, P. (2004). Post-transplant hepatic veno-occlusive disease: pathogenesis, diagnosis and treatment. Rev Clin Exp Hematol *8*, E3.

Hristova, M., Heuvelmans, S., and van der Vliet, A. (2007). GSH-dependent regulation of Fas-mediated caspase-8 activation by acrolein. FEBS Lett *581*, 361-367.

Hu, J., Mahmoud, M.I., and el-Fakahany, E.E. (1994). Polyamines inhibit nitric oxide synthase in rat cerebellum. Neurosci Lett *175*, 41-45.

Huan, J.Y., Miranda, C.L., Buhler, D.R., and Cheeke, P.R. (1998a). The roles of CYP3A and CYP2B isoforms in hepatic bioactivation and detoxification of the

pyrrolizidine alkaloid senecionine in sheep and hamsters. Toxicol Appl Pharmacol *151*, 229-235.

Huan, J.Y., Miranda, C.L., Buhler, D.R., and Cheeke, P.R. (1998b). Species differences in the hepatic microsomal enzyme metabolism of the pyrrolizidine alkaloids. Toxicol Lett *99*, 127-137.

Huxtable, R.J. (1989). Human embryotoxicity of pyrrolizidine-containing drugs. Hepatology *9*, 510-511.

Ibrahim, R.B., Peres, E., Dansey, R., Abidi, M.H., Abella, E.M., and Klein, J. (2004). Anti-thrombin III in the management of hematopoietic stem-cell transplantation-associated toxicity. Ann Pharmacother *38*, 1053-1059.

International Program on Chemical Safety (IPCS), International programme on chemical safety. 1988. Geneva: World Health Organization; p. 1–19.

International Program on Chemical Safety (IPCS), International programme on chemical safety. 1989. Geneva: World Health Organization; p. 1–232.

Ji, L., Chen, Y., and Wang, Z. (2008a). Intracellular glutathione plays important roles in pyrrolizidine alkaloid clivorine-induced toxicity on L-02 hepatocytes. Toxicol Mech Methods *18*, 661-664.

Ji, L., Liu, T., Chen, Y., and Wang, Z. (2009). Protective mechanisms of N-acetyl-cysteine against pyrrolizidine alkaloid clivorine-induced hepatotoxicity. J Cell Biochem *108*, 424-432.

Ji, L., Liu, T., and Wang, Z. (2010). Pyrrolizidine alkaloid clivorine induced oxidative injury on primary cultured rat hepatocytes. Hum Exp Toxicol *29*, 303-309.

Ji, L.L., Chen, Y., and Wang, Z.T. (2008b). The toxic effect of pyrrolizidine alkaloid clivorine on the human embryonic kidney 293 cells and its primary mechanism. Exp Toxicol Pathol *60*, 87-93.

Ji, L.L., Zhang, M., Sheng, Y.C., and Wang, Z.T. (2005). Pyrrolizidine alkaloid clivorine induces apoptosis in human normal liver L-02 cells and reduces the expression of p53 protein. Toxicol In Vitro *19*, 41-46.

Joosten, L., Cheng, D., Mulder, P.P., Vrieling, K., van Veen, J.A., and Klinkhamer, P.G. (2011). The genotype dependent presence of pyrrolizidine alkaloids as tertiary amine in Jacobaea vulgaris. Phytochemistry *72*, 214-222.

Joosten, L., and van Veen, J.A. (2011). Defensive properties of pyrrolizidine alkaloids against microorganisms. Phytochem Rev *10*, 127-136.

Ka, A.S., Michel, G., Imbert, P., Diakhate, I., and Seye, M.N. (2006). [Hepatic veno-occlusive disease due to dietary toxins in a five-year-old child in Senegal]. Med Trop (Mars) *66*, 514-515.

Kallianpur, A.R., Hall, L.D., Yadav, M., Byrne, D.W., Speroff, T., Dittus, R.S., Haines, J.L., Christman, B.W., and Summar, M.L. (2005). The hemochromatosis C282Y allele: a risk factor for hepatic veno-occlusive disease after hematopoietic stem cell transplantation. Bone Marrow Transplant *35*, 1155-1164.

Kempf, M., Heil, S., Hasslauer, I., Schmidt, L., von der Ohe, K., Theuring, C., Reinhard, A., Schreier, P., and Beuerle, T. (2010). Pyrrolizidine alkaloids in pollen and pollen products. Mol Nutr Food Res *54*, 292-300.

Kennedy, S. (2002). The role of proteomics in toxicology: identification of biomarkers of toxicity by protein expression analysis. Biomarkers *7*, 269-290.

Khamaisi, M., Kavel, O., Rosenstock, M., Porat, M., Yuli, M., Kaiser, N., and Rudich, A. (2000). Effect of inhibition of glutathione synthesis on insulin action: in vivo and in vitro studies using buthionine sulfoximine. Biochem J *349*, 579-586.

Kim, H.Y., Stermitz, F.R., Li, J.K., and Coulombe, R.A., Jr. (1999). Comparative DNA cross-linking by activated pyrrolizidine alkaloids. Food Chem Toxicol *37*, 619-625.

Kim, H.Y., Stermitz, F.R., Molyneux, R.J., Wilson, D.W., Taylor, D., and Coulombe, R.A., Jr. (1993a). Structural influences on pyrrolizidine alkaloid-induced cytopathology. Toxicol Appl Pharmacol *122*, 61-69.

Kim, S., and Ponka, P. (2002). Nitric oxide-mediated modulation of iron regulatory proteins: implication for cellular iron homeostasis. Blood Cells Mol Dis *29*, 400-410.

Kim, S., and Ponka, P. (2003). Role of nitric oxide in cellular iron metabolism. Biometals *16*, 125-135.

Kim, S.R., Kim, Y., and An, G. (1993b). Molecular cloning and characterization of anther-preferential cDNA encoding a putative actin-depolymerizing factor. Plant Mol Biol *21*, 39-45.

Klaunig, J.E., Xu, Y., Bachowski, S., Ketcham, C.A., Isenberg, J.S., Kolaja, K.L., Baker, T.K., Walborg, E.F., Jr., and Stevenson, D.E. (1995). Oxidative stress in nongenotoxic carcinogenesis. Toxicol Lett *82-83*, 683-691.

Kleno, T.G., Kiehr, B., Baunsgaard, D., and Sidelmann, U.G. (2004). Combination of 'omics' data to investigate the mechanism(s) of hydrazine-induced hepatotoxicity in rats and to identify potential biomarkers. Biomarkers 9, 116-138.

Klionsky, D.J., Abeliovich, H., Agostinis, P., Agrawal, D.K., Aliev, G., Askew, D.S., Baba, M., Baehrecke, E.H., Bahr, B.A., Ballabio, A., et al. (2008). Guidelines for the use and interpretation of assays for monitoring autophagy in higher eukaryotes. Autophagy 4, 151-175.

Ko, J.K., and Cho, C.H. (2005). The diverse actions of nicotine and different extracted fractions from tobacco smoke against hapten-induced colitis in rats. Toxicol Sci 87, 285-295.

Kumana, C.R., Ng, M., Lin, H.J., Ko, W., Wu, P.C., and Todd, D. (1983). Hepatic veno-occlusive disease due to toxic alkaloid herbal tea. Lancet 2, 1360-1361.

Lame, M.W., Jones, A.D., Morin, D., Segall, H.J., and Wilson, D.W. (1995). Biliary excretion of pyrrolic metabolites of [14C]monocrotaline in the rat. Drug Metab Dispos 23, 422-429.

Langer, T., Mostl, E., Chizzola, R., and Gutleb, R. (1996). A competitive enzyme immunoassay for the pyrrolizidine alkaloids of the senecionine type. Planta Med 62, 267-271.

LeCluyse, E.L. (2001). Human hepatocyte culture systems for the in vitro evaluation of cytochrome P450 expression and regulation. Eur J Pharm Sci 13, 343-368.

Lee, J.H., Lee, K.H., Kim, S., Lee, J.S., Kim, W.K., Park, C.J., Chi, H.S., and Kim, S.H. (1998). Relevance of proteins C and S, antithrombin III, von Willebrand factor, and factor VIII for the development of hepatic veno-occlusive disease in patients undergoing allogeneic bone marrow transplantation: a prospective study. Bone Marrow Transplant 22, 883-888.

Levine, B., and Yuan, J. (2005). Autophagy in cell death: an innocent convict? J Clin Invest 115, 2679-2688.

Li, A.P., and Jurima-Romet, M. (1997). Applications of primary human hepatocytes in the evaluation of pharmacokinetic drug-drug interactions: evaluation of model drugs terfenadine and rifampin. Cell Biol Toxicol 13, 365-374.

Li, A.P., and Kedderis, G.L. (1997). Primary hepatocyte culture as an experimental model for the evaluation of interactions between xenobiotics and drug-metabolizing enzymes. Chem Biol Interact 107, 1-3.

Lin, G., Cui, Y.Y., and Hawes, E.M. (2000a). Characterization of rat liver microsomal metabolites of clivorine, an hepatotoxic otonecine-type pyrrolizidine alkaloid. Drug Metab Dispos 28, 1475-1483.

Lin, G., Cui, Y.Y., and Liu, X.Q. (2003). Gender differences in microsomal metabolic activation of hepatotoxic clivorine in rat. Chem Res Toxicol 16, 768-774.

Lin, G., Cui, Y.Y., Liu, X.Q., and Wang, Z.T. (2002). Species differences in the in vitro metabolic activation of the hepatotoxic pyrrolizidine alkaloid clivorine. Chem Res Toxicol 15, 1421-1428.

Lin, G., Rose, P., Chatson, K.B., Hawes, E.M., Zhao, X.G., and Wang, Z.T. (2000b). Characterization of two structural forms of otonecine-type pyrrolizidine alkaloids from Ligularia hodgsonii by NMR spectroscopy. J Nat Prod 63, 857-860.

Lin, G., Tang, J., Liu, X.Q., Jiang, Y., and Zheng, J. (2007). Deacetylclivorine: a gender-selective metabolite of clivorine formed in female Sprague-Dawley rat liver microsomes. Drug Metab Dispos 35, 607-613.

Lin, G., Wang, J.Y., Li, N., Li, M., Gao, H., Ji, Y., Zhang, F., Wang, H., Zhou, Y., Ye, Y., et al. (2011). Hepatic sinusoidal obstruction syndrome associated with consumption of Gynura segetum. J Hepatol 54, 666-673.

Lindblom, P., Rafter, I., Copley, C., Andersson, U., Hedberg, J.J., Berg, A.L., Samuelsson, A., Hellmold, H., Cotgreave, I., and Glinghammar, B. (2007). Isoforms of alanine aminotransferases in human tissues and serum--differential tissue expression using novel antibodies. Arch Biochem Biophys 466, 66-77.

Low, T.Y., Leow, C.K., Salto-Tellez, M., and Chung, M.C. (2004). A proteomic analysis of thioacetamide-induced hepatotoxicity and cirrhosis in rat livers. Proteomics 4, 3960-3974.

Lowry, O.H., Rosebrough, N.J., Farr, A.L., and Randall, R.J. (1951). Protein measurement with the Folin phenol reagent. J Biol Chem 193, 265-275.

Macgregor, P.F. (2003). Gene expression in cancer: the application of microarrays. Expert Rev Mol Diagn 3, 185-200.

Malhi, H., Annamaneni, P., Slehria, S., Joseph, B., Bhargava, K.K., Palestro, C.J., Novikoff, P.M., and Gupta, S. (2002). Cyclophosphamide disrupts hepatic sinusoidal endothelium and improves transplanted cell engraftment in rat liver. Hepatology 36, 112-121.

Matsuda, H., Kinoshita, K., Sumida, A., Takahashi, K., Fukuen, S., Fukuda, T., Yamamoto, I., and Azuma, J. (2002). Taurine modulates induction of cytochrome P450 3A4 mRNA by rifampicin in the HepG2 cell line. Biochim Biophys Acta *1593*, 93-98.

Matsumoto, Y., Horiike, S., Sakagami, J., Fujimoto, Y., Taniguchi, K., Shimizu, D., Shimura, K., Uchiyama, H., Kuroda, J., Nomura, K., *et al.* (2009). Early ultrasonographic diagnosis and clinical follow-up of hepatic veno-occlusive disease after allogeneic bone marrow transplantation in a patient with acute lymphoblastic leukemia. Intern Med *48*, 831-835.

Mattocks, A.R. (1968). Toxicity of pyrrolizidine alkaloids. Nature *217*, 723-728.

Mattocks A.R. (1986).Chemistry and toxicology of pyrrolizidine alkaloids. London: Academic Press.

Mattocks, A.R., Driver, H.E., Barbour, R.H., and Robins, D.J. (1986). Metabolism and toxicity of synthetic analogues of macrocyclic diester pyrrolizidine alkaloids. Chem Biol Interact *58*, 95-108.

McCaughan, G.W., Huynh, J.C., Feller, R., Painter, D., Waugh, R., and Sheil, A.G. (1995). Fulminant hepatic failure post liver transplantation: clinical syndromes, correlations and outcomes. Transpl Int *8*, 20-26.

McDonald, G.B., McCune, J.S., Batchelder, A., Cole, S., Phillips, B., Ren, A.G., Vicini, P., Witherspoon, R., Kalhorn, T.F., and Slattery, J.T. (2005). Metabolism-based cyclophosphamide dosing for hematopoietic cell transplant. Clin Pharmacol Ther *78*, 298-308.

McDonald, G.B., Slattery, J.T., Bouvier, M.E., Ren, S., Batchelder, A.L., Kalhorn, T.F., Schoch, H.G., Anasetti, C., and Gooley, T. (2003). Cyclophosphamide metabolism, liver toxicity, and mortality following hematopoietic stem cell transplantation. Blood *101*, 2043-2048.

McGee, J., Patrick, R.S., Wood, C.B., and Blumgart, L.H. (1976). A case of veno-occlusive disease of the liver in Britain associated with herbal tea consumption. J Clin Pathol *29*, 788-794.

McLean, A.E. (1970). The effect of protein deficiency and microsomal enzyme induction by DDT and phenobarbitone on the acute toxicity of chloroform and a pyrrolizidine alkaloid, retrorsine. Br J Exp Pathol *51*, 317-321.

Mei, N., Guo, L., Liu, R., Fuscoe, J.C., and Chen, T. (2007). Gene expression changes induced by the tumorigenic pyrrolizidine alkaloid riddelliine in liver of Big Blue rats. BMC Bioinformatics *8 Suppl 7*, S4.

Mendel, V.E., Witt, M.R., Gitchell, B.S., Gribble, D.N., Rogers, Q.R., Segall, H.J., and Knight, H.D. (1988). Pyrrolizidine alkaloid-induced liver disease in horses: an early diagnosis. Am J Vet Res *49*, 572-578.

Miller, K.G., Field, C.M., Alberts, B.M., and Kellogg, D.R. (1991). Use of actin filament and microtubule affinity chromatography to identify proteins that bind to the cytoskeleton. Methods Enzymol *196*, 303-319.

Mohabbat, O., Younos, M.S., Merzad, A.A., Srivastava, R.N., Sediq, G.G., and Aram, G.N. (1976). An outbreak of hepatic veno-occlusive disease in north-western Afghanistan. Lancet *2*, 269-271.

Molyneux, R.J., Gardner, D.L., Colegate, S.M., and Edgar, J.A. (2011). Pyrrolizidine alkaloid toxicity in livestock: a paradigm for human poisoning? Food Addit Contam Part A Chem Anal Control Expo Risk Assess *28*, 293-307.

Molyneux, R.J., and James, L.F. (1990). Pyrrolizidine alkaloids in milk: thresholds of intoxication. Vet Hum Toxicol *32 Suppl*, 94-103.

Moncada, S. (1993). [Significance of endogenous nitric oxide production for the effect of nitrates and in septic shock]. Schweiz Rundsch Med Prax *82*, 1154-1160.

Mortele, K.J., Van Vlierberghe, H., Wiesner, W., and Ros, P.R. (2002). Hepatic veno-occlusive disease: MRI findings. Abdom Imaging *27*, 523-526.

Neuman, M.G., Jia, A.Y., and Steenkamp, V. (2007). Senecio latifolius induces in vitro hepatocytotoxicity in a human cell line. Can J Physiol Pharmacol *85*, 1063-1075.

Newsholme S.J., Maleeff B.F., Steiner S., Anderson N.L., Schwartz L.W. (2000). Two-dimensional electrophoresis of liver proteins: characterization of a drug-induced hepatomegaly in rats. Electrophoresis *21*, 2122-2128.

Nicholson, J.K., Connelly, J., Lindon, J.C., and Holmes, E. (2002). Metabonomics: a platform for studying drug toxicity and gene function. Nat Rev Drug Discov *1*, 153-161.

Nie L., Wu G., Zhang W. (2006a). Correlation between mRNA and protein abundance in Desulfovibrio vulgaris: a multiple regression to identify sources of variations. Biochem Biophys Res Commun *339*, 603-610.

Nie L., Wu G., Zhang W. (2006b). Correlation of mRNA expression and protein abundance affected by multiple sequence features related to translational efficiency in Desulfovibrio vulgaris: a quantitative analysis. Genetics *174*, 2229-2243.

Nyska, A., Moomaw, C.R., Foley, J.F., Maronpot, R.R., Malarkey, D.E., Cummings, C.A., Peddada, S., Moyer, C.F., Allen, D.G., Travlos, G., *et al.* (2002). The hepatic endothelial carcinogen riddelliine induces endothelial apoptosis, mitosis, S phase, and p53 and hepatocytic vascular endothelial growth factor expression after short-term exposure. Toxicol Appl Pharmacol *184*, 153-164.

O'Brien, P.J., Irwin, W., Diaz, D., Howard-Cofield, E., Krejsa, C.M., Slaughter, M.R., Gao, B., Kaludercic, N., Angeline, A., Bernardi, P., *et al.* (2006). High concordance of drug-induced human hepatotoxicity with in vitro cytotoxicity measured in a novel cell-based model using high content screening. Arch Toxicol *80*, 580-604.

Omiecinski, C.J., Remmel, R.P., and Hosagrahara, V.P. (1999). Concise review of the cytochrome P450s and their roles in toxicology. Toxicol Sci *48*, 151-156.

Ozer, J., Ratner, M., Shaw, M., Bailey, W., and Schomaker, S. (2008). The current state of serum biomarkers of hepatotoxicity. Toxicology *245*, 194-205.

Paglin, S., Hollister, T., Delohery, T., Hackett, N., McMahill, M., Sphicas, E., Domingo, D., and Yahalom, J. (2001). A novel response of cancer cells to radiation involves autophagy and formation of acidic vesicles. Cancer Res *61*, 439-444.

Pastore, A., Federici, G., Bertini, E., and Piemonte, F. (2003). Analysis of glutathione: implication in redox and detoxification. Clin Chim Acta *333*, 19-39.

Pearson, D.L., Dawling, S., Walsh, W.F., Haines, J.L., Christman, B.W., Bazyk, A., Scott, N., and Summar, M.L. (2001). Neonatal pulmonary hypertension--urea-cycle intermediates, nitric oxide production, and carbamoyl-phosphate synthetase function. N Engl J Med *344*, 1832-1838.

Pennington, K., McGregor, E., Beasley, C.L., Everall, I., Cotter, D., and Dunn, M.J. (2004). Optimization of the first dimension for separation by two-dimensional gel electrophoresis of basic proteins from human brain tissue. Proteomics *4*, 27-30.

Pihusch, M., Wegner, H., Goehring, P., Salat, C., Pihusch, V., Hiller, E., Andreesen, R., Kolb, H.J., Holler, E., and Pihusch, R. (2005). Diagnosis of hepatic veno-occlusive disease by plasminogen activator inhibitor-1 plasma antigen levels: a prospective analysis in 350 allogeneic hematopoietic stem cell recipients. Transplantation *80*, 1376-1382.

Poreddy, V., and DeLeve, L.D. (2002). Hepatic circulatory diseases associated with chronic myeloid disorders. Clin Liver Dis *6*, 909-931.

Powis, G., Ames, M.M., and Kovach, J.S. (1979a). Metabolic conversion of indicine N-oxide to indicine in rabbits and humans. Cancer Res *39*, 3564-3570.

Powis, G., Ames, M.M., and Kovach, J.S. (1979b). Relationship of the reductive metabolism of indicine N-oxide to its antitumor activity. Res Commun Chem Pathol Pharmacol *24*, 559-569.

Prakash, A.S., Pereira, T.N., Reilly, P.E., and Seawright, A.A. (1999). Pyrrolizidine alkaloids in human diet. Mutat Res *443*, 53-67.

Putzke, H.P., and Persaud, T.V. (1976). Cytotoxicity of the pyrrolizidine alkaloid fulvine to pancreatic acinar cells in the rat. Light microscopic, histochemical and ultrastructural studies. Exp Pathol (Jena) *12*, 329-335.

Qian, W., Nishikawa, M., Haque, A.M., Hirose, M., Mashimo, M., Sato, E., and Inoue, M. (2005). Mitochondrial density determines the cellular sensitivity to cisplatin-induced cell death. Am J Physiol Cell Physiol *289*, C1466-1475.

Rasenack, R., Muller, C., Kleinschmidt, M., Rasenack, J., and Wiedenfeld, H. (2003). Veno-occlusive disease in a fetus caused by pyrrolizidine alkaloids of food origin. Fetal Diagn Ther *18*, 223-225.

Reitman, S., and Frankel, S. (1957). A colorimetric method for the determination of serum glutamic oxalacetic and glutamic pyruvic transaminases. Am J Clin Pathol *28*, 56-63.

Reyes, R., and Izquierdo, J.M. (2007). The RNA-binding protein PTB exerts translational control on 3'-untranslated region of the mRNA for the ATP synthase beta-subunit. Biochem Biophys Res Commun *357*, 1107-1112.

Richardson, P.G., Elias, A.D., Krishnan, A., Wheeler, C., Nath, R., Hoppensteadt, D., Kinchla, N.M., Neuberg, D., Waller, E.K., Antin, J.H., *et al.* (1998). Treatment of severe veno-occlusive disease with defibrotide: compassionate use results in response without significant toxicity in a high-risk population. Blood *92*, 737-744.

Richardson, P.G., Murakami, C., Jin, Z., Warren, D., Momtaz, P., Hoppensteadt, D., Elias, A.D., Antin, J.H., Soiffer, R., Spitzer, T., *et al.* (2002). Multi-institutional use of defibrotide in 88 patients after stem cell transplantation with severe veno-occlusive disease and multisystem organ failure: response without significant toxicity in a high-risk population and factors predictive of outcome. Blood *100*, 4337-4343.

Riley, L.G., Hirano, T., and Grau, E.G. (2004). Estradiol-17beta and dihydrotestosterone differentially regulate vitellogenin and insulin-like growth factor-I production in primary hepatocytes of the tilapia Oreochromis mossambicus. Comp Biochem Physiol C Toxicol Pharmacol *138*, 177-186.

Rio, B., Bauduer, F., Arrago, J.P., and Zittoun, R. (1993). N-terminal peptide of type III procollagen: a marker for the development of hepatic veno-occlusive disease after BMT and a basis for determining the timing of prophylactic heparin. Bone Marrow Transplant *11*, 471-472.

Roe, A.L., Snawder, J.E., Benson, R.W., Roberts, D.W., and Casciano, D.A. (1993). HepG2 cells: an in vitro model for P450-dependent metabolism of acetaminophen. Biochem Biophys Res Commun *190*, 15-19.

Roeder, E. (1995). Medicinal plants in Europe containing pyrrolizidine alkaloids. Pharmazie *50*, 83-98.

Roeder, E. (2000). Medicinal plants in China containing pyrrolizidine alkaloids. Pharmazie *55*, 711-726.

Roeder, E., and Pflueger, T. (1995). Analysis of pyrrolizidine alkaloids: a competitive enzyme-linked immunoassay (ELISA) for the quantitative determination of some toxic pyrrolizidine alkaloids. Nat Toxins *3*, 305-309; discussion 317.

Roeder, E., and Wiedenfeld, H. (2009). Pyrrolizidine alkaloids in medicinal plants of Mongolia, Nepal and Tibet. Pharmazie *64*, 699-716.

Roseman, D.M., Wu, X., and Kurth, M.J. (1996). Enzyme-linked immunosorbent assay detection of pyrrolizidine alkaloids: immunogens based on quaternary pyrrolizidinium salts. Bioconjug Chem *7*, 187-195.

Rudzok, S., Krejci, S., Graebsch, C., Herbarth, O., Mueller, A., and Bauer, M. (2011). Toxicity profiles of four metals and 17 xenobiotics in the human hepatoma cell line HepG2 and the protozoa Tetrahymena pyriformis--a comparison. Environ Toxicol *26*, 171-186.

Saviola, A., Luppi, M., Potenza, L., Morselli, M., Ferrari, A., Riva, G., and Torelli, G. (2003). Late occurrence of hepatic veno-occlusive disease following gemtuzumab ozogamicin: successful treatment with defibrotide. Br J Haematol *123*, 752-753.

Schnitzius, J.M., Hill, N.S., Thompson, C.S., and Craig, A.M. (2001). Semiquantitative determination of ergot alkaloids in seed, straw, and digesta samples using a competitive enzyme-linked immunosorbent assay. J Vet Diagn Invest *13*, 230-237.

Schoonen, W.G., de Roos, J.A., Westerink, W.M., and Debiton, E. (2005a). Cytotoxic effects of 110 reference compounds on HepG2 cells and for 60 compounds on HeLa, ECC-1 and CHO cells. II mechanistic assays on NAD(P)H, ATP and DNA contents. Toxicol In Vitro *19*, 491-503.

Schoonen, W.G., Westerink, W.M., de Roos, J.A., and Debiton, E. (2005b). Cytotoxic effects of 100 reference compounds on Hep G2 and HeLa cells and of 60 compounds on ECC-1 and CHO cells. I mechanistic assays on ROS, glutathione depletion and calcein uptake. Toxicol In Vitro *19*, 505-516.

Schultze, A.E., and Roth, R.A. (1998). Chronic pulmonary hypertension--the monocrotaline model and involvement of the hemostatic system. J Toxicol Environ Health B Crit Rev *1*, 271-346.

Shirai, M., Nagashima, K., Iwasaki, S., and Mori, W. (1987). A light and scanning electron microscopic study of hepatic veno-occlusive disease. Acta Pathol Jpn *37*, 1961-1971.

Shulman, H.M., and Hinterberger, W. (1992). Hepatic veno-occlusive disease--liver toxicity syndrome after bone marrow transplantation. Bone Marrow Transplant *10*, 197-214.

Smith, L.W., and Culvenor, C.C. (1981). Plant sources of hepatotoxic pyrrolizidine alkaloids. J Nat Prod *44*, 129-152.

Stegelmeier, B.L. (2011). Pyrrolizidine alkaloid-containing toxic plants (Senecio, Crotalaria, Cynoglossum, Amsinckia, Heliotropium, and Echium spp.). Vet Clin North Am Food Anim Pract *27*, 419-428, ix.

Stegelmeier, B.L., Edgar, J.A., Colegate, S.M., Gardner, D.R., Schoch, T.K., Coulombe, R.A., and Molyneux, R.J. (1999). Pyrrolizidine alkaloid plants, metabolism and toxicity. J Nat Toxins *8*, 95-116.

Steiner, S., Gatlin, C.L., Lennon, J.J., McGrath, A.M., Seonarain, M.D., Makusky, A.J., Aponte, A.M., Esquer-Blasco, R., and Anderson, N.L. (2001). Cholesterol biosynthesis regulation and protein changes in rat liver following treatment with fluvastatin. Toxicol Lett *120*, 369-377.

Stillman, A.E., Huxtable, R.J., Fox, D., Hart, M., and Bergeson, P. (1977a). Pyrrolizidine (Senecio) poisoning in Arizona: severe liver damage due to herbal teas. Ariz Med *34*, 545-546.

Stillman, A.S., Huxtable, R., Consroe, P., Kohnen, P., and Smith, S. (1977b). Hepatic veno-occlusive disease due to pyrrolizidine (Senecio) poisoning in Arizona. Gastroenterology *73*, 349-352.

Summar, M.L., Gainer, J.V., Pretorius, M., Malave, H., Harris, S., Hall, L.D., Weisberg, A., Vaughan, D.E., Christman, B.W., and Brown, N.J. (2004). Relationship between carbamoyl-phosphate synthetase genotype and systemic vascular function. Hypertension *43*, 186-191.

Suter, L., Schroeder, S., Meyer, K., Gautier, J.C., Amberg, A., Wendt, M., Gmuender, H., Mally, A., Boitier, E., Ellinger-Ziegelbauer, H., *et al.* (2011). EU framework 6 project: predictive toxicology (PredTox)--overview and outcome. Toxicol Appl Pharmacol *252*, 73-84.

Taylor, D.W., Wilson, D.W., Lame, M.W., Dunston, S.D., Jones, A.D., and Segall, H.J. (1997). Comparative cytotoxicity of monocrotaline and its metabolites in cultured pulmonary artery endothelial cells. Toxicol Appl Pharmacol *143*, 196-204.

Tietze, F. (1969). Enzymic method for quantitative determination of nanogram amounts of total and oxidized glutathione: applications to mammalian blood and other tissues. Anal Biochem *27*, 502-522.

Tujios, S., and Fontana, R.J. (2011). Mechanisms of drug-induced liver injury: from bedside to bench. Nature Reviews Gastroenterology & Hepatology *8*, 202-211.

Tuschl, H., and Schwab, C.E. (2004). Flow cytometric methods used as screening tests for basal toxicity of chemicals. Toxicol In Vitro *18*, 483-491.

Tyers, M., and Mann, M. (2003). From genomics to proteomics. Nature *422*, 193-197.

Valla, D.C. (2008). Vascular diseases of the liver. Semin Liver Dis *28*, 233.

Varshavsky, A. (1996). The N-end rule: functions, mysteries, uses. Proc Natl Acad Sci U S A *93*, 12142-12149.

Venkatakrishnan, K., Schmider, J., Harmatz, J.S., Ehrenberg, B.L., von Moltke, L.L., Graf, J.A., Mertzanis, P., Corbett, K.E., Rodriguez, M.C., Shader, R.I., *et al.* (2001a). Relative contribution of CYP3A to amitriptyline clearance in humans: in vitro and in vivo studies. J Clin Pharmacol *41*, 1043-1054.

Venkatakrishnan, K., Von Moltke, L.L., and Greenblatt, D.J. (2001b). Human drug metabolism and the cytochromes P450: application and relevance of in vitro models. J Clin Pharmacol *41*, 1149-1179.

Wadleigh, M., Ho, V., Momtaz, P., and Richardson, P. (2003). Hepatic veno-occlusive disease: pathogenesis, diagnosis and treatment. Curr Opin Hematol *10*, 451-462.

Wang, S., Ma, H., Li, J., Chen, X., Bao, Z., and Sun, S. (2006). Direct determination of reduced glutathione in biological fluids by Ce(IV)-quinine chemiluminescence. Talanta *70*, 518-521.

Wang, X., Kanel, G.C., and DeLeve, L.D. (2000). Support of sinusoidal endothelial cell glutathione prevents hepatic veno-occlusive disease in the rat. Hepatology *31*, 428-434.

Wetmore, B.A., and Merrick, B.A. (2004). Toxicoproteomics: proteomics applied to toxicology and pathology. Toxicol Pathol *32*, 619-642.

Wiedenfeld H, Roeder E, Bourauel T, Edgar J, 2008. Pyrrolidine alkaloids: structure and toxicity. Bonn University Press

Winter, H., Seawright, A.A., Hrdlicka, J., Mattocks, A.R., Jukes, R., Wangdi, K., and Gurung, K.B. (1993). Pyrrolizidine alkaloid poisoning of yaks: diagnosis of pyrrolizidine alkaloid exposure by the demonstration of sulphur-conjugated pyrrolic metabolites of the alkaloid in circulating haemoglobin. Aust Vet J *70*, 312-313.

Winter, H., Seawright, A.A., Noltie, H.J., Mattocks, A.R., Jukes, R., Wangdi, K., and Gurung, J.B. (1994). Pyrrolizidine alkaloid poisoning of yaks: identification of the plants involved. Vet Rec *134*, 135-139.

Xia, Q., Chou, M.W., Edgar, J.A., Doerge, D.R., and Fu, P.P. (2006). Formation of DHP-derived DNA adducts from metabolic activation of the prototype heliotridine-type pyrrolizidine alkaloid, lasiocarpine. Cancer Lett *231*, 138-145.

Xia, Q., Yan, J., Chou, M.W., and Fu, P.P. (2008). Formation of DHP-derived DNA adducts from metabolic activation of the prototype heliotridine-type pyrrolizidine alkaloid, heliotrine. Toxicol Lett *178*, 77-82.

Yan, C.C., and Huxtable, R.J. (1994). Release of an alkylating metabolite, dehydromonocrotaline, from the isolated liver perfused with the pyrrolizidine alkaloid, monocrotaline. Proc West Pharmacol Soc *37*, 107-108.

Yan, C.C., and Huxtable, R.J. (1995a). Effect of the pyrrolizidine alkaloid, monocrotaline, on bile composition of the isolated, perfused rat liver. Life Sci *57*, 617-626.

Yan, C.C., and Huxtable, R.J. (1995b). Effects of the pyrrolizidine alkaloid, retrorsine, on sulfur metabolism, in the liver. Proc West Pharmacol Soc *38*, 37-40.

Yan, C.C., and Huxtable, R.J. (1995c). Relationship between glutathione concentration and metabolism of the pyrrolizidine alkaloid, monocrotaline, in the isolated, perfused liver. Toxicol Appl Pharmacol *130*, 132-139.

Yan, C.C., and Huxtable, R.J. (1995d). The relationship between the concentration of the pyrrolizidine alkaloid monocrotaline and the pattern of metabolites released from the isolated liver. Toxicol Appl Pharmacol *130*, 1-8.

Yan, C.C., and Huxtable, R.J. (1996). Effects of monocrotaline, a pyrrolizidine alkaloid, on glutathione metabolism in the rat. Biochem Pharmacol *51*, 375-379.

Yan, J., Xia, Q., Chou, M.W., and Fu, P.P. (2008). Metabolic activation of retronecine and retronecine N-oxide - formation of DHP-derived DNA adducts. Toxicol Ind Health *24*, 181-188.

Yang, C.S., Chhabra, S.K., Hong, J.Y., and Smith, T.J. (2001a). Mechanisms of inhibition of chemical toxicity and carcinogenesis by diallyl sulfide (DAS) and related compounds from garlic. J Nutr *131*, 1041S-1045S.

Yang, R.Z., Blaileanu, G., Hansen, B.C., Shuldiner, A.R., and Gong, D.W. (2002). cDNA cloning, genomic structure, chromosomal mapping, and functional expression of a novel human alanine aminotransferase. Genomics *79*, 445-450.

Yang, Y.C., Yan, J., Doerge, D.R., Chan, P.C., Fu, P.P., and Chou, M.W. (2001b). Metabolic activation of the tumorigenic pyrrolizidine alkaloid, riddelliine, leading to DNA adduct formation in vivo. Chem Res Toxicol *14*, 101-109.

Yasutomo, K., and Himeno, K. (1993). Monitoring of veno-occlusive disease after bone-marrow transplantation by serum aminopropeptide of type III procollagen. Lancet *342*, 1062.

Zhou, Q., Chu, X., and Ruan, C. (1994). Defibrotide stimulates expression of thrombomodulin in human endothelial cells. Thromb Haemost *71*, 507-510.